DEPARTAMENTO DE BIOQUÍMICA

Y BIOLOGÍA MOLECULAR

TESIS DOCTORAL

Dinámica de SHP-1, SHP-2, PTP1B, LAMP-2 y estabilidad lisosómica en la pancreatitis aguda experimental

NANCY SARMIENTO SANDOVAL

Salamanca, 2015

DEPARTAMENTO DE BIOQUÍMICA Y BIOLOGÍA MOLECULAI
Campus Miguel de Unamuno - Edificio Departamental Pza. Doctores de la Reina s/n 37007 Salamanca. Spain. Tel.+34-923 294 465 Fax:+34-923 294 579

D. JESÚS SÁNCHEZ YAGÜE y Dña. Mª DEL CARMEN SÁNCHEZ BERNAL, Profesores Titulares de Universidad del Departamento de Bioquímica y Biología Molecular de la Universidad de Salamanca,

CERTIFICA:

Que la presente Memoria de Tesis Doctoral titulada "**Dinámica de SHP-1, SHP-2, PTP1B, LAMP-2 y estabilidad lisosómica en la pancreatitis aguda experimental.**", que para optar al Grado de Doctor en Biología presenta Dña. Nancy Sarmiento Sandoval, ha sido realizada bajo mi dirección en el Departamento de Bioquímica y Biología Molecular de la Universidad de Salamanca.

Considerando que la Tesis Doctoral se halla concluida, autorizo su presentación para que sea juzgada por el Tribunal correspondiente.

Y para que así conste, firmo el presente documento en Salamanca, a veintiuno de diciembre de dos mil quince.

Fdo: Jesús Sánchez Yagüe y Mª del Carmen Sánchez Bernal

DEPARTAMENTO DE BIOQUÍMICA Y BIOLOGÍA MOLECULAR
Campus Miguel de Unamuno - Edificio Departamental

NANCY SARMIENTO SANDOVAL, Licenciada en Biología por la Universidad de Salamanca,

DECLARO:

Que soy la Autora de esta Tesis Doctoral titulada, "**Dinámica de SHP-1, SHP-2, PTP1B, LAMP-2 y estabilidad lisosómica en la pancreatitis aguda experimental.**", realizada en el Departamento de Bioquímica y Biología Molecular de la Universidad de Salamanca bajo la dirección de los Drs. D. Jesús Sánchez Yagüe y Dña. Mª del Carmen Sánchez Bernal.

Y para que así conste, firmo el presente documento en Salamanca a veintiuno de diciembre de dos mil quince.

Fdo: Nancy Sarmiento Sandoval

NOTA PRELIMINAR

Este trabajo de investigación ha sido financiado con cargo a los proyectos subvencionados por el Ministerio de Ciencia y Tecnología (BFU2006-103627BMC), el Instituto de Salud Carlos III (FIS-FEDER**,** PS09/01075) y la Junta de Castilla y León (SA033A05, SA126A07, Biomedicina SAN673/SA10/08).

El autor de la Memoria ha disfrutado de una beca de colaboración USAL-Banco Santander para estudiantes Iberoamericanos (octubre 2008-octubre 2011).

Los resultados recogidos en esta Memoria han sido en parte publicados en tres artículos y presentados en cuatro congresos:

Artículos:

Nancy Sarmiento, Carmen Sánchez-Bernal, Manuel Ayra, Nieves Pérez, Angel Hernández-Hernández, José J. Calvo, Jesús Sánchez-Yagüe. Changes in the expression and dynamics of SHP-1 and SHP-2 during cerulein-induced acute pancreatitis in rats. Biochim. Biophys. Acta. (Mol. Bas. Dis.) (2008) 1782, 271-279.

Nancy Sarmiento, Carmen Sánchez-Bernal, Nieves Pérez, Arturo Mangas, José L. Sardina, José J. Calvo, Jesús Sánchez-Yagüe. Rolipram and SP600125 suppress the early increase in PTP1B expression during cerulein-induced pancreatitis in rats. Pancreas (2010) 39, 639-645.

Nancy Sarmiento, Jesús Sánchez-Yagüe, Pedro P.Juanes, Nieves Pérez, Laura Ferreira, Violeta García-Hernández, Arturo Mangas, José J. Calvo, Carmen Sánchez-Bernal. Changes in the morphology and lability of lysosomal

subpopulations in cerulein-induced acute pancreatitis. Digest. Liver Dis. (2011) 43, 132-138.

Congresos:

N Sarmiento, MC Sánchez Rodríguez, N Pérez-González, JJ Calvo, A Hernández-Hernández, J Sánchez-Yagüe. Dynamics of the protein tyrosine phosphatases PTP1B, PTP 1C and PTP 1D in experimental acute pancreatitis. Effect of Nitric Oxide. 9th Meeting of the Spanish Bilio-Pancreatic Club. Valencia, 25-26 de noviembre de 2005. Pancreatology, vol 6, pág 47, 2006.

N. Sarmiento Sandoval, M.C. Sánchez Bernal, M. Ayra Rivas, N. Pérez González, J.J. Calvo Andrés, A. Hernández Hernández y J. Sánchez Yagüe. Expresión de SH-PTP1 en la Pancreatitis Aguda Experimental. Efecto de la Inhibición de JNK y ERK1/2, o de la Fosfodiesterasa Tipo IV. X Reunión del Club Español Biliopancreático. Santander, 28-29 de septiembre de 2007. Gastroenterología y Hepatología, Vol 30, pág 437, 2007.

N. Sarmiento Sandoval, M.C. Sánchez Bernal, V. García Hernández, N. Pérez González , A. Mangas, J.J. Calvo Andrés, J. Sánchez Yagüe. Rolipram y SP600125 suprimen el aumento de la expresión de PTP1B durante la pancretitis aguda experimental. XI Reunión del Club Español Biliopancreático. Vitoria-Gasteiz, 22-24 de octubre de 2009. Gastroenterología y Hepatología, Vol 33(1) e8, 2010.

Nancy Sarmiento, Carmen Sánchez Bernal, Nieves Pérez González, Violeta García Hernández, Angel Hernández Hernández, José J calvo Andrés, Jesús Sánchez Yagüe. Dinámica de la expresión de LAMP-2 durante el desarrollo de la pancreatitis aguda experimental. XXXIII Congreso de la Sociedad Española de Bioquímica y Biología Molecular. Córdoba, 14-17 de septiembre de 2010. Libro de resúmenes, Grupo Bases Moleculares de la Patología, Abstract PO22.

Agradecimientos

Después de tantos años, ha llegado la hora de mirar hacia atrás y agradecer a todas las personas que de una u otra forma han colaborado en este trabajo:

A mis directores de Tesis, Jesús Sánchez Yagüe y Carmen Sánchez Bernal, a los que agradezco su imprescindible colaboración y labor docente. Sin vuestra ayuda, dedicación y mucha paciencia, probablemente yo no estaría escribiendo estas palabras.

A Nieves Pérez, porque siempre estaba dispuesta en compartir sus conocimientos y colaborar en todo lo necesario.

Al Dr. Jose J. Calvo, por su generoso apoyo y sus valiosas aportaciones científicas en el campo de la pancreatitis aguda.

A Violeta, gracias por tus consejos, por animarme, por poner a mi disposición tus nociones de informática, por ser ejemplo de compañerismo, empeño y por toda la ayuda que me has brindado. Te admiro muchísimo.

A Esther, que desde el primer momento me ofreciste tu amistad, a pesar de vernos poco, te recuerdo con mucho cariño.

A Guillermo y Nacho, por vuestra disposición en todo momento.

Mi último agradecimiento va para mi marido y mi hijo Javier, a quienes dedico esta Tesis. Sois todo para mi.

Abreviaturas

ADNc: Ácido desoxirribonucleico copia**.**

AMPc: Adenosina 3´,5´-monofosfatocíclico.

APS: Persulfato amónico.

ARN: Ácido ribonucleico.

ARNm: Ácido ribonucleico mensajero.

β-NPH: β-nafilamida.

CCK: Colecistoquinina.

Cer: Ceruleína.

DMSO: Dimetilsulfóxido.

dNTPs: Desoxirribonucleósidos trifosfato.

Dominio SH2: Dominios homólogos al dominio 2 de la proteína Src.

DTT: Ditiotreitol.

EDTA: Ácido etilendiaminotetraacético.

ERK: Quinasa reguladas por señales extracelulares.

F-Actina: Actina fibrilar.

HRP: Peroxidasa de rábano.

JAKs: Quinasas de la familia “Janus”.

JNK: Quinasa c-Jun N-terminal.

HRP: Peroxidasa de rábano.

KCL: Cloruro de potasio.

L+M: Fracción de lisosomas y mitocondrias.

LAMP: Proteína de membrana asociada al lisosoma.

LIMP: Proteína de membrana integral del lisosómica.

L-NAME: N-nitro-L-arginina- metiléster.

MAPK: Proteínas quinasas activadas por mitógenos.

$MgCl_2$: Cloruro de magnesio.

MPO: Mieloperoxidasa.

MU: Metilumbeliferona.

NAG: N-acetil-β-D-glucosaminidasa.

NaOH: Hidróxido de sodio.

NF-κB: Factor nuclear kappa B.

NOS: Óxido nítrico sintasa.

OCBP: Obstrucción del conducto biliopancreático.

OsO_4: Tetróxido de osmio.

PA: Pancreatitis aguda.

PAGE: Electroforesis en gel de poliacrilamida.

pb: Pares de bases.

PMSF: Fenilmetil-sulfonil fluoruro.

PSTI: Inhibidor de la tripsina.

PTPs: Proteína tirosina fosfatasas.

p/v: peso/volumen.

PVDF: Difluoruro de polivinilideno.

RE: Retículo endoplasmático.

ROS: Especies reactivas del oxígeno.

RPTPs: Proteína tirosina fosfatasas de tipo receptor.

RT-PCR: Transcripción reversa acoplada a la reacción en cadena de la polimerasa.

RTKs: Receptores tirosina quinasa.

SDH: Succinato deshidrogenasa.

SDS: Dodecil sulfato sódico.

SDS-PAGE: electroforesis en gel de poliacrilamida en presencia de SDS.

SNP: Nitroprusiato sódico.

STATs: Proteínas transductoras de señales y activadoras de la transcripción.

TAU: Taurocolato sódico.

TBS: Tampón Tris Salino.

TEMED*: N,N,N´,N´,*-tetrametil-etilendiamida.

TNF-α: factor de necrosis tumoral alfa.

Tris: Tris(hidroximetil)aminometano.

Tween 20: Polioxietileno 20 sorbitan monolaurato.

U: Unidades enzimáticas.

v/v: volumen/volumen.

Índice

I. Introducción

1. El páncreas

El páncreas es una glándula alargada situada en el retro-peritoneo ventral izquierdo, sobre la pared posterior del abdomen. Se localiza por detrás del estómago y por delante de la columna vertebral, estando también en contacto directo con el intestino delgado y el higado. En este órgano se distinguen tres zonas principalmente: cabeza (enmarcada en el duodeno), cuerpo y cola (en contacto con el bazo). Se encuentra rodeado de una capa de tejido conjuntivo y se divide en lóbulos separados por septos vascularizados e inervados de dicho tejido (*Geneser, 2000; Segarra, 2006*).

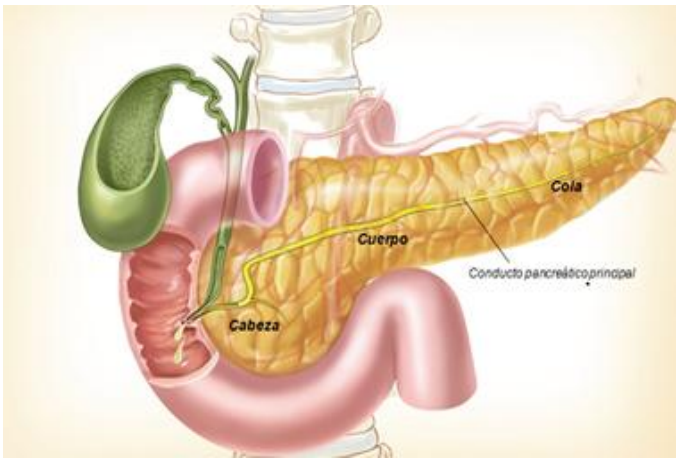

Figura 1. Representación esquemática de las partes del páncreas, sus conductos internos y estructuras asociadas.

Histológicamente, el páncreas está compuesto por dos tipos de tejido, endocrino y exocrino. La porción exocrina se divide en lóbulos, separados entre sí por septos de tejido conjuntivo que contienen vasos sanguíneos, linfáticos y nervios (*Sastre et al*., 2005), y constituye el 80-85% de todo el páncreas; los vasos sanguíneos y la matriz extracelular representan un 10-15%, y el 2% restante corresponde a la parte endocrina (*Klein et al., 1996; Longnecker, 2014*).

El tejido endocrino está constituido por los islotes de Langerhans, los cuales contienen principalmente células de tres tipos: las células alfa (producen glucagón), las células beta (producen insulina) y las células delta (producen somatostatina). La función de esta parte endocrina es producir y secretar hormonas directamente a la sangre (*Segarra, 2006*). El páncreas exocrino está

constituido por los acinos y el sistema ductal. En cada unidad funcional se pueden distinguir tres tipos de células: células acinares secretoras, las células centro o paraacinares y las células ductales (Fig. 2) (*Sastre et al., 2005*). Las células acinares son células cúbico-piramidales caracterizadas por tener ciertas formaciones intracitoplasmáticas en su parte apical denominadas gránulos de zimógeno (orgánulos que almacenan las enzimas digestivas inactivas en su interior), mientras que el resto de la célula está conformado por un extenso retículo endoplasmático, aparato de Golgi y mitocondrias (*Bockman et al*.,1998).

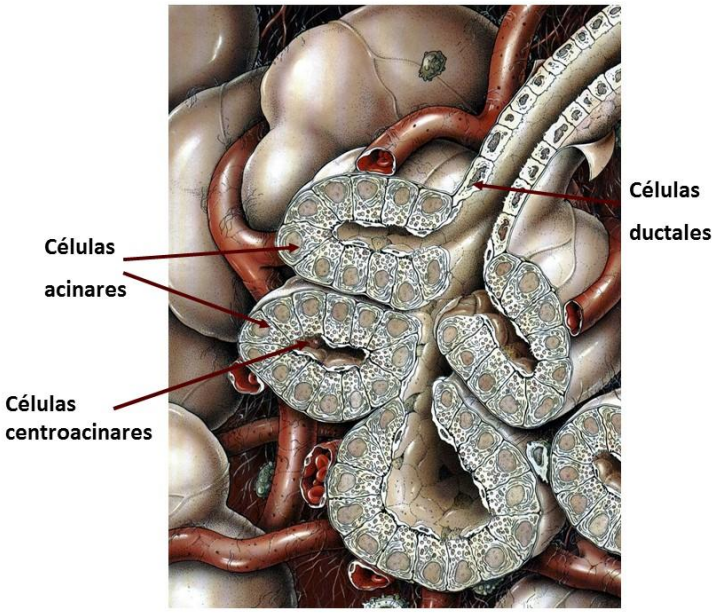

Figura 2. Corte histológico del páncreas donde se observan los acinos y el sistema ductal.

Las secreciones de este componente exocrino, que desembocan en el duodeno a través de los conductos pancreáticos, están formadas por un componente enzimático (procedente sobre todo de las células acinares) y una secreción hidroelectrolítica (procedente de las células ductales). La secreción hidroelectrolítica es una solución acuosa rica en iones, mayoritariamente sodio y bicarbonato, cuya función es neutralizar el quimo ácido procedente del estómago y proporcionar un medio neutro para que las enzimas digestivas actúen correctamente en el duodeno. El componente enzimático consta de numerosas enzimas cuya función es digerir el contenido del duodeno; éstas

son de diferentes tipos: proteolíticas (tripsina, quimotripsina, etc.), lipolíticas (fosfolipasa, esterasa, etc.), glucolíticas (amilasas) y nucleolíticas (nucleasas).

Las secreciones están reguladas por señales nerviosas y hormonales, originadas en respuesta a la acidez y los productos de la digestión en el duodeno. Entre las hormonas más importantes están la secretina, que estimula la secreción hidroelectrolítica, y la colecistoquinina (CCK), que estimula la secreción enzimática (*Sastre et al., 2005*).

1.1. Pancreatitis aguda (PA)

1.2. Concepto

La pancreatitis aguda es un proceso inflamatorio agudo producido por la activación prematura de las enzimas proteolíticas del páncreas dentro de los acinos pancreáticos, a consecuencia de diferentes estímulos de autodigestión de la glándula.

El proceso inflamatorio es de gravedad variable, presentándose desde una forma leve o edematosa hasta una forma grave o necrotizante asociada a daño multiorgánico producido por la dispersión de los productos inflamatorios activados (*Jha et al., 2009*). En el 80% de los pacientes la patología se resuelve sin una grave morbilidad, pero el 20% de casos restantes están complicados con una alta mortalidad y morbilidad, principalmente debido a las alteraciones multiorgánicas secundarias a la necrosis pancreática. Además, la incidencia de pancreatitis aguda se ha incrementado en las últimas décadas (*Frossard et al., 2008*).

1.2.1. Etiología y factores de riesgo

El origen de la pancreatitis aguda sigue siendo en la actualidad controvertido, ya que en realidad se debe a la implicación de un complejo rango de agentes genéticos y ambientales, que todavía no están esclarecidos completamente. Por ejemplo, se ha visto predisposición genética en mutaciones de algunos genes como el del tripsinógeno catiónico (PRSS1), el de la fibrosis quística (CFTR), o el del inhibidor de la serín-proteasa Kazal de tipo 1 (SPINK1), pero también se han caracterizado una amplia multitud de factores no genéticos como los cálculos biliares y la colestasis, el alcohol, las

infecciones, la hiperestimulación pancreática (por ejemplo, de hormonas como la colecistoquinina), las intervenciones quirúrgicas, la hipercalemia, la hipertrigliceridemia, las alteraciones en el parénquima y los conductos pancreáticos o la autoinmunidad (*Abela et al., 2010; Baddeley et al., 2010*).

De todos los casos de pancreatitis aguda, se detecta el agente desencadenante en el 75-85% de los pacientes. En los países desarrollados las principales causas son la obstrucción de los canales pancreáticos por cálculos biliares (38%) y el abuso de alcohol (36%), seguido a gran distancia por la hiperestimulación pancreática, algunas anomalías congénitas del tejido pancreático, tumores que obstruyen los conductos o el daño producido tras realizar una colangiopancreatografía retrógrada endoscópica (CPRE) (*Wang et al., 2009*).

1.2.2. Fisiopatología

Los mecanismos fisiopatológicos no se conocen en su totalidad, aunque prácticamente se sabe que la predisposición a un determinado estímulo, de los citados anteriormente, provoca la activación prematura y anormal de las enzimas pancreáticas en las células acinares, que lleva a un proceso de autodigestión e inflamación local de la glándula (*Frossard et al., 2008*).

El estadio inicial de la enfermedad se produce fundamentalmente por la activación del tripsinógeno (zimógeno) a tripsina (enzima activa), desencadenando una cascada de activación del resto de enzimas acinares y resultando en el daño celular y los procesos de autodigestión (*Braddeley et al., 2010*). Se ha comprobado la implicación del factor de necrosis tumoral (TNFα), producido por la activación de la Catepsina B, y fallos en la regulación de la concentración de calcio citosólico libre, como inductores de la activación del tripsinógeno intraacinar (*Sah & Saluja, 2012*).

Posteriormente se origina un proceso inflamatorio causado por la producción de citocinas y quimiocinas por las células acinares dañadas, que atraen a neutrófilos, macrófagos y linfocitos a la zona de la lesión. Esta respuesta sistémica está determinada por la concentración en sangre de mediadores pro-inflamatorios (que aumentan) y anti-inflamatorios (que

disminuyen) (*Frossard et al., 2008; Abela et al., 2010*). El origen del proceso inflamatorio en las células acinares también es un motivo de discusión, ya que también se ha propuesto que se debe a la activación del factor transcripcional NF-κB y este hecho sería independiente de la activación prematura de las enzimas acinares (*Sah & Saluja, 2012; Lankisch et al., 2015*). Además, la presencia de factores inflamatorios y el estrés sistémico provocan la activación de las células endoteliales de esta zona, permitiendo la migración de más células leucocitarias al tejido pancreático y provocando variaciones en otras enzimas implicadas. Esto provoca la disminución de los niveles de oxígeno en el órgano y el aumento de radicales libres, que contribuyen también al daño pancreático (*Frossard et al., 2008*).

La gravedad del proceso fisiopatológico de la pancreatitis aguda en el órgano, como ya se ha indicado, es variable. Se han descrito factores que pueden influir en el proceso: estrés oxidativo, alteración de la autofagia, disfunción mitocondrial, alteraciones del pH acinar, etc. Estos eventos provocan una variación en el balance de la muerte celular por apoptosis respecto a necrosis. La apoptosis se considera una muerte celular protectora mientras que la necrosis es destructiva. Por tanto, la gravedad dependerá del tipo de muerte celular que predomine (*Sah & Saluja, 2012*).

Finalmente, la pancreatitis aguda puede progresar a un síndrome de respuesta inflamatoria sistémica caracterizado por hipovolemia, reducción de fluido en el espacio intersticial y daño capilar. La presencia de factores pro-inflamatorios en la sangre lleva a procesos isquémicos en el páncreas, daño pulmonar agudo, fallo renal agudo, descompensación hepática o infecciones graves (sepsis) (*Baddeley et al., 2010*).

Para facilitar el desarrollo de nuevos tratamientos farmacológicos es necesario conocer aquellos mediadores y receptores involucrados en las rutas de señalización de la patología. Por este motivo es necesario el estudio de modelos experimentales que permitan explicar los mecanismos involucrados en la pancreatitis aguda, y que en humanos serían imposibles de estudiar. Entre los diferentes tipos de modelos experimentales que existen, los más mpleados, y utilizados en este trabajo, son los modelos animales (*Zhao et al., 2013*).

1.3. Pancreatitis aguda experimental

1.3.1. Modelos animales

Los modelos animales pueden facilitar la comprensión de la patogénesis de la pancreatitis aguda, siempre que sean comparables con la patología en el ser humano. De este modo, el desarrollo de diferentes modelos animales ha contribuido al conocimiento de los procesos celulares tempranos, la patogénesis y la fisiopatología de la enfermedad.

Cada modelo animal presenta una serie de ventajas e inconvenientes para el estudio de un determinado aspecto. Esto permite que, metodológicamente, se seleccione el modelo animal apropiado para el estudio que se quiere realizar (*Zhao et al., 2013*).

En general, el modelo animal ideal debe cumplir una serie de criterios: ser económico, reproducir la patología (seguir el curso básico que presenta la enfermedad), permitir la repetición de la misma patogenia y fisiopatología siempre que se realice, responder al mismo tratamiento que se utiliza en humanos, y que el proceso de desarrollo de la pancreatitis en el animal experimental sea sencillo para poder estandarizarlo (*Foitzik et al., 2000*).

A partir de esta premisa, existen numerosos modelos animales clasificados en base a diferentes criterios: la técnica empleada (invasivas o no invasivas), la causa de la patología (alcohólica, tóxica, obstructiva, isquémica, etc.), o la gravedad del daño (edematosa o necrotizante). El criterio de la gravedad es importante; por ejemplo, los modelos de pancreatitis aguda edematosa son oportunos para estudiar la patología cuando no hay procesos de necrosis y sepsis graves, es decir, cuando la enfermedad está en un estadio temprano (*Foitzik et al., 2000; Zhao et al., 2013*).

En base a estos criterios se han desarrollado varios modelos animales que tratan de reproducir y explicar los cambios bioquímicos y celulares que se producen en la pancreatitis aguda humana; como por ejemplo, el modelo de una dieta deficiente en colina y suplementada con etionina, el modelo del asa duodenal cerrada, el modelo de obstrucción del conducto biliopancreático o los ductos pancreáticos por infusión de sales biliares (como el taurocolato sódico)

o por ligadura quirúrgica (*Steer, 1992; Foitzik et al., 2000*), el modelo de la oclusión vascular pancreática, el modelo de pancreatitis alcohólica inducido por la ingesta abusiva de etanol o el modelo de inducción por hiperestimulación con colecistoquinina (CCK) o su análogo, la ceruleína (*Mansfield, 2012*).

En el presente trabajo se ha utilizado como modelo experimental la hiperestimulación con ceruleína.

1.3.2. Pancreatitis aguda inducida por hiperestimulación con ceruleína

La ceruleína es un análogo de la CCK. Tiene una acción farmacológica y una estructura similar, aunque es mucho más potente que esta hormona intestinal. Además, la administración de ceruleína, en dosis supramáximas en ratas, provoca la aparición de una pancreatitis aguda edematosa. Este modelo experimental reproduce los cambios y síntomas que experimenta el humano durante la fase temprana de esta enfermedad, por lo que es uno de los principales modelos para el estudio de los cambios celulares y moleculares en dicha fase de la pancreatitis aguda.

Respecto a los criterios que se mencionaron anteriormente, cabe destacar que el modelo de la hiperestimulación con ceruleína no es invasivo (administración subcutánea, inyección intraperitoneal o infusión intravenosa), no es mortal, presenta gravedad moderada y es altamente reproducible. Además, en función de la dosis y de las pautas de administración del compuesto, permite generar diferentes niveles de gravedad (*Willermer et al*., *1992*).

A altas dosis, la ceruleína actúa a través de los receptores de CCK, sobreestimulándolos y provocando el bloqueo de la secreción del contenido de los gránulos de zimógeno. Los gránulos interaccionan con los lisosomas formando vacuolas autofágicas, lo que provoca la activación de enzimas lisosómicas como la catepsina B. Esto lleva a la activación prematura del tripsinógeno a tripsina en las células acinares, lo que desencadena la cascada de activación de las enzimas digestivas (lipasa, fosfolipasa, proelastasa, quimotripsinógeno, etc.) (*Hofbauer et al., 1998; Lankisch et al., 2015*).

El patrón de cambios estructurales y moleculares que se produce en este modelo se da de forma progresiva: a los 15-30 minutos se puede observar una redistribución de enzimas lisosómicas y la citada activación temprana del tripsinógeno dentro de las células acinares; a los 60 minutos se produce una vacuolización dentro de las células acinares y la progresión de un edema en el espacio intersticial (*Grady et al., 1996*); en las primeras horas hay una invasión progresiva de células inflamatorias, fibroblastos y células inmunológicas en el espacio intersticial y, posteriormente, se observa la atrofia y destrucción de algunas células acinares (*Niederau et al., 1990; Mayerle et al., 2005*).

Durante la pancreatitis aguda tardía (a las doce horas de la inducción de la pancreatitis aguda) las células acinares sufren alteraciones morfológicas claras, como la alteración de la cromatina, la dilatación del retículo endoplasmático, la formación de grandes vacuolas y la pérdida del dominio apical. Finalmente, las células mueren por apoptosis o necrosis; aunque la glándula se puede recuperar completamente a los 12-24 días debido a su elevada tasa de división celular (*Ëlsaser et al., 1986*).

1.4. Estudio de la fase temprana de la pancreatitis aguda

Aunque se ha descrito el mecanismo general de la pancreatitis aguda, no se conoce la totalidad de los eventos implicados en las fases tempranas de la enfermedad. Esto dificulta el desarrollo de terapias específicas y efectivas contra esta patología. Hay diversos estudios que demuestran que durante sus primeras etapas se incrementa la expresión de determinados genes y proteínas. Por este motivo, se ha propuesto que la variación de dichas proteínas jugaría un papel importante en el desarrollo y la gravedad de la enfermedad (*Sarmiento et al., 2010; García-Hernández et al., 2014*).

Por otro lado, durante dicha fase temprana se produce un incremento de las especies reactivas de oxígeno (ROS), que ejercen un papel importante en la patología, dañando las células acinares y contribuyendo a su progresión. El estrés oxidativo provoca la oxidación de proteínas, hecho que interviene en el desarrollo de la patología. Además el proceso patológico se agrava por la pérdida de sustratos antioxidantes (como el glutatión) en el páncreas (*Dabrowski et al., 1999*).

Como se indicó anteriormente, uno de los acontecimientos más relevantes durante la fase temprana es el bloqueo de la secreción acinar de las enzimas digestivas, aunque los procesos de síntesis y transporte no están afectados en esta fase. Además de esto, se observa colocalización de las enzimas lisosómicas y los zimógenos, que lleva a la acidificación de las vacuolas autofágicas y la activación prematura del tripsinógeno comenzando la cascada y favoreciendo el desarrollo de la enfermedad (*Van Acker et al., 2006*). Otros procesos de la fase inicial de la PA son el aumento de la fragilidad de los lisosomas, la distribución basolateral de la F-actina subapical, la formación de vacuolas en el citoplasma, y la activación de factores de transcripción proinflamatorios y de mediadores inflamatorios (*Van Acker et al., 2007; Sarmiento et al., 2011*).

2. LISOSOMAS

Los lisosomas son orgánulos rodeados de membrana, que fueron descubiertos por Christian de Duve (*De Duve y Wattiaux, 1966*). Contienen enzimas hidrolíticas para degradar materiales intracelulares y extracelulares en su lumen, por lo que constituyen los principales orgánulos digestivos en las células eucariotas. La carga extracelular es vertida en los lisosomas por endocitosis o fagocitosis, mientras que los componentes intracelulares son dirigidos para la degradación lisosomal a través de autofagia (*Shen y Mizushima, 2014*). Hasta ahora se han descrito tres formas de autofagia, de las cuales la mejor conocida es la *macroautofagia*, donde el material a degradar es trasladado por otro orgánulo, el autofagosoma, el cual se fusiona con el lisosoma para degradar del material secuestrado. En la *microautofagia*, el material destinado para la degradación es directamente engullido por el lisosoma, mientras que en la *autofagia mediada por chaperones*, algunos chaperones moleculares tales como Hsp70 reconocen un motivo de aminoácidos en ciertas proteínas, que son introducidas en el lisosoma mediante la participación del receptor “proteína de membrana 2A asociada con el lisosoma” (*LAMP-2A*) (*Boya et al., 2013*).

Los lisosomas también participan en la transducción de señales, en el control de las respuestas celulares a nutrientes, en la exocitosis y reparación de la membrana plasmática, y en la muerte celular. Otra función esencial de los lisosomas (así como de orgánulos relacionados con los lisosomas) es su papel como almacenes de calcio. Actualmente, varios canales de Ca^{2+} se han asociado con la membrana lisosómica, siendo los de la familia TRP (potencial de receptor transitorio) los mejor caracterizados. Aunque el mecanismo de activación de estos canales TRP es desconocido, se ha propuesto que son activados por NAADP (dinucleótido fosfato adenina de ácido nicotínico), Ca^{2+} y especies reactivas de oxígeno (ROS) (*Zhang y Li, 2007; Faouzi y Penner, 2014*).

El rasgo más importante de los lisosomas es su lumen acídico (pH 4,5-5) y la presencia de más de 50 enzimas catabólicas, que incluyen proteasas, lipasas, fosfatasas, peptidasas y nucleasas, las cuales son generalmente activas a pH ácido. Otras proteínas integrales de la membrana de los lisosomas están implicadas en la homeostasis lisosómica. Entre ellas están las H^{+}-ATPasas de tipo vacuolar (v-ATPasas), que utilizan la energía metabólica del ATP para bombear protones en el lumen lisosómico y mantener el medio acídico (*Mindell, 2012*).

La formación de lisosomas requiere la integración de las vías endocítica y biosintética. Mientras que las proteínas luminales recién sintetizadas alcanzan el lisosoma vía el receptor de manosa-6-P y la acción de la proteasa S1P (*Marschner K et al. 2011*), el mecanismo por el que las proteínas de membrana son transportadas a los lisosomas se conoce peor.

Se han propuesto dos rutas diferentes para el transporte de las proteínas de la membrana lisosómica recién sintetizadas (*Hunziker y Geuze, 1996*). Una de ellas es la ruta intracelular, que vierte estas proteínas desde el *trans*-Golgi a los lisosomas vía endosomas. La otra es la ruta indirecta, en la cual las proteínas recién sintetizadas son transportadas desde el *trans*-Golgi a la membrana plasmática, y posteriormente dirigidas a los lisosomas por medio de la vía endocítica. En ambas rutas, directa e indirecta, distintos complejos adaptadores heterotetraméricos facilitan el tráfico y la clasificación de las

proteínas de membrana lisosómica. Se han descrito 4 complejos adaptadores, AP-1, AP-2, AP-3 y AP-4. En concreto, AP-3 participa en la clasificación de varias proteínas de la membrana lisosómica, incluyendo $LAMP_s$ y LIMP-2, hacia los lisosomas desde el *trans*-Golgi o desde endosomas, usando los motivos basados en tirosina y dileucina (*Le Borgne et al., 1998*).

Durante el proceso de la vía endocítica se forma un cuerpo multivesicular, un endosoma tardío, el cual después se funde directamente con los lisosomas (*Futter et al., 1996; Bright et al., 1997*). Experimentos tanto *in vivo* como *in vitro*, revelan que los endosomas tardíos y los lisosomas, en realidad, experimentan múltiples ciclos de fusión y fisión (*Luzio et al., 2000*). Esto implica que los endosomas tardíos y los lisosomas están en equilibrio dinámico, y podría explicar por qué todas las proteínas de la membrana lisosómica están en ambos tipos de orgánulos.

La expresión de muchas proteínas lisosómicas está regulada, ante todo, por el factor de transcripción EB (TFEB), el cual se transloca desde el citoplasma al núcleo donde se une a los promotores de una red de genes específicos conocida como CLEAR (expresión y regulación lisosómica coordinada) (*Sardiello et al., 2009*). La importancia de este red de genes para la proliferación celular es evidente en ciertos tipos de cáncer, como *cáncer de páncreas*, que son altamente dependientes de la actividad transcripcional de esta familia de factores de transcripción, la cual induce altos niveles de función catabólica lisosómica, permitiendo a las células cancerosas sobrevivir en condiciones de estrés metabólico (*Perera et al., 2015*).

Debido a que los lisosomas contienen muchas enzimas catabólicas, como se ha indicado anteriormente, la ruptura de estos orgánulos puede ser peligroso para la célula. La ruptura lisosómica masiva induce la liberación del contenido lisosómico desencadenando una cascada de hidrólisis del contenido citoplasmático, que conduce a una acidificación generalizada del citoplasma, con consecuencias letales para la célula. Sin embargo, la permeabilización parcial y selectiva de la membrana lisosómica (LMP) produce una liberación al citosol de enzimas lisosómicas que induce muerte celular regulada. Esta LMP se observa en muchas circunstancias y se piensa que ocurre tras

desestabilización de la membrana lisosómica (Fig 3) (*Serrano-Puebla & Boya, 2015*).

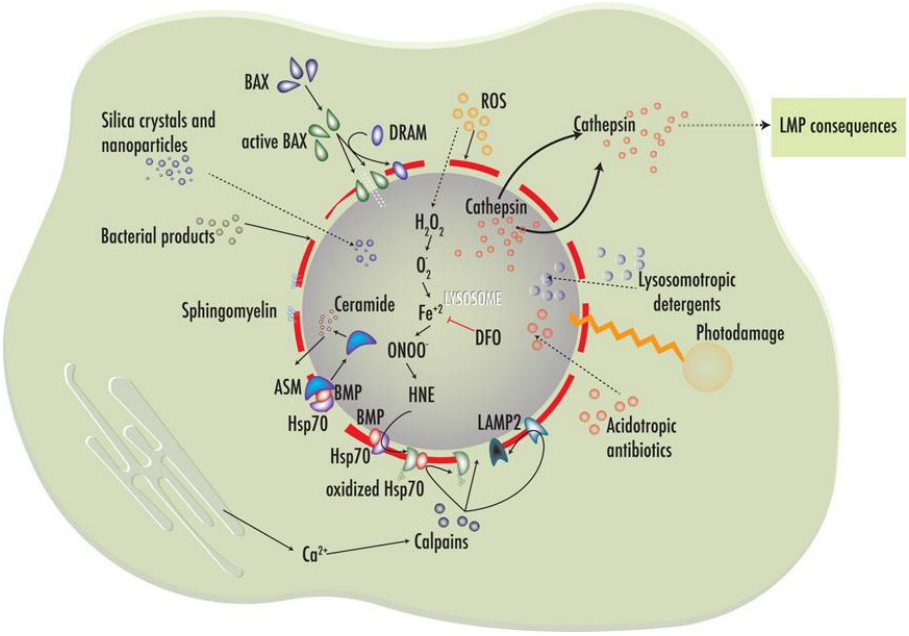

Figura 3. Inductores de permeabilización de la membrana lisosómica. Agentes, tales como Bax, que actúan sobre la membrana lisosómica inducen su ruptura y la translocación de hidrolasas lisosómicas al citosol (ej: catepsinas). Especies reactivas de oxígeno (ROS) pueden atravesar la membrana lisosómica y, en presencia de hierro libre catalizar reacciones de Fenton para producir intermediarios altamente tóxicos que dañan las proteínas lisosómicas. Calpaínas, activadas por incrementos in los niveles de calcio, actúan sobre varias proteínas lisosómicas, incluyendo LAMP 2 y Hsp 70. Este proceso está aumentado tras la oxidación de Hsp70 por 4-hidroxinonenal (HNE), el cual es un producto de las reacciones de Fenton intralisosómicas. Otros agentes, tales como productos de bacterias y virus, y nanopartículas, también inducen LMP.

2.1. Proteínas de la membrana lisosómica

Las proteínas de la membrana lisosómica tienen múltiples funciones, tales como la retención de las numerosas hidrolasas ácidas indicadas anteriormente, el mantenimiento de un medio ambiente ácido dentro del lisosoma (llevado a cabo por las v-ATPasas; el transporte de productos de degradación (aminoácidos y carbohidratos) desde el lumen lisosómico al citoplasma, y la interacción específica y fusión entre lisosomas y otros orgánulos (*Fukuda, 1991; Peters y von Figura, 1994; Hunzikery Geuze, 1996*).

La membrana de los lisosomas contiene un grupo característico de proteínas que atraviesan la membrana y que están altamente glicosiladas, tales como LAMP-1, LAMP-2, LAMP-3 (también llamada LIMP-I ó CD63), LIMP-2 (ó LIMP-II, LPG85, SCARB2), fosfatasa ácida lisosómica y sialina (Fig.2).

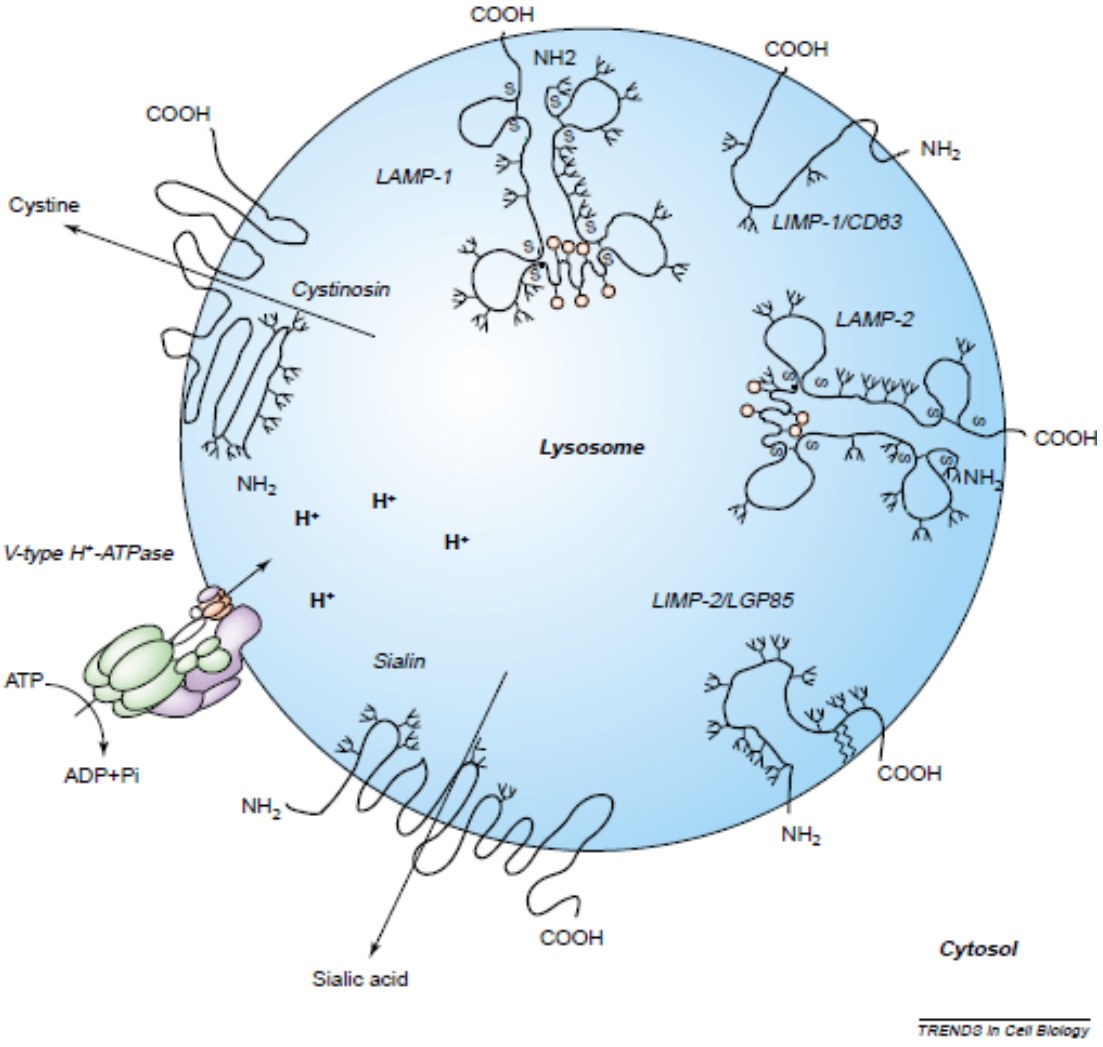

Figura 4. Principales proteínas de la membrana lisosómica. Las antenas indican posibles sitios de *N*-glicosilación y los círculos de *O*-glicosilación. LAMP: proteína de membrana asociada con el lisosoma LIMP: proteína integral de la membrana lisosómica; LGP: glicoproteína de la membrana lisosómica. Tomado de *Eskelinen et al., 2003*.

Entre ellas, LAMP-1 y LAMP-2 son las mejor caracterizadas; son proteínas de membrana tipo I que presentan un gran dominio luminal con cadenas de oligosacárido unidas a asparragina (*N*-unidas), un único segmento transmembrana y un corto dominio citoplasmático con un motivo de tirosina, que es necesario y suficiente para el movimiento de estas proteínas hacia los lisosomas. LAMP-2 ha sido descrita como un receptor para la toma selectiva y

degradación de proteínas citosólicas en el lisosoma, o en la autofagia mediada por chaperones moleculares (*Cuervo y Dice, 1998; Eskelinen et al.*, 2002).

La liberación patológica de enzimas lisosómicas puede deberse a mecanismos que afectan a su biosíntesis o a mecanismos que permitan que las enzimas, que ya han alcanzado los lisosomas, sean liberadas. Así, por ejemplo, si la membrana del lisosoma se altera, se produce la liberación de ciertas enzimas al citosol, como señalábamos en el apartado anterior, con la consiguiente digestión de los sustratos situados en su proximidad lo que, en ocasiones, provoca la muerte celular.

De forma considerable, la estabilidad de la membrana lisosómica se mantiene por la presencia de esas proteínas altamente glicosiladas, que previenen la ruptura del orgánulo por sus proteasas intraluminales. Otras moléculas, como Hsp70, también son esenciales para proteger a los lisosomas de dicha ruptura. Finalmente, la composición lipídica de la membrana lisosómica es también esencial para su estabilidad, ya que tiene más baja concentración de colesterol que otras membranas celulares (*Repnik et al., 2014*).

Se había propuesto que durante la pancreatitis aguda tiene lugar un incremento de la fragilidad de los lisosomas pancreáticos (*Saluja et al., 1987; Steer y Meldolesi, 1988; Guillaumes et al., 1996; Bragado et al., 1998*). *Fortunato et al.,* (*2009*) señalaron, asimismo, que la variación de proteínas lisosómicas juega un papel crítico en el inicio de esta enfermedad. En este sentido, nosotros hemos observado (*Sarmiento et al., 2011*) que, en la fracción citosólica de páncreas de ratas pancreatíticas, se produce un aumento de la actividad de algunas enzimas lisósomicas con respecto a la observada en ratas control. Estos datos, junto con los cambios que habíamos descrito acerca de la composición de las membranas de páncreas durante la pancreatitis aguda (*Ferreira et al., 2002*), sugieren una alteración en la membrana de los lisosomas.

2.2. LAMP-2

El gen que codifica LAMP-2 en humanos, o en ratas (LGP-B y LGP 110 respectivamente), presenta 9 exones. Los exones 1-8 y parte del 9 codifican para el dominio luminal. El resto del último exón se encarga de los otros dos dominios restantes. Por mecanismos de empalme alternativo en el exón 9 se forman tres isoformas: LAMP-2A, LAMP-2B y LAMP-2C. Estas tres isoformas son idénticas en su dominio luminal pero difieren en los dominios citosólico y transmembrana. Las proteínas destinadas a ser degradadas se unen al dominio citosólico de LAMP-2, en la membrana lisosómica y luego son trasportadas hacia el interior del lisosoma, para su degradación (*Cuervo y Dice et al., 1996*). LAMP-2A es un receptor para las proteínas sustrato de la autofagia mediada por chaperonas moleculares (*Cuervo y Dice, 1996*).

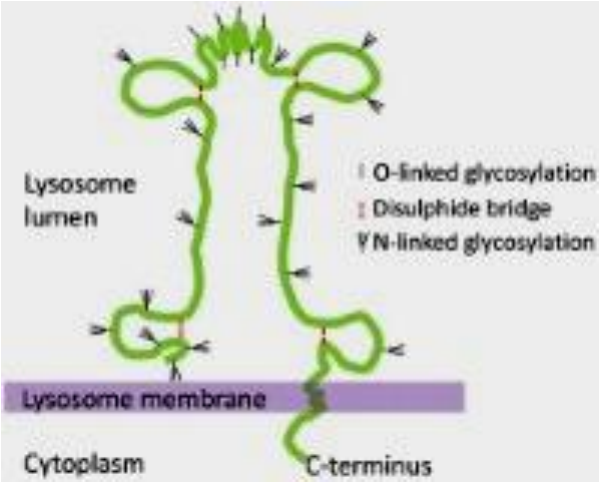

Figura 5. Esquema de la estructura de LAMP-2. Los cuatro bucles representan puentes disulfuro y la zona en zig-zag simboliza dominios ricos en prolina. Los tridentes presentes en la estructura constituyen lugares de unión de glúcidos N-unidos y los espirales de la parte superior representan glúcidos O-unidos (tomado de *Eskelinen et al., 2008*).

2.3. Autofagia en la pancreatitis aguda

Como se ha indicado anteriormente, en la autofagia se forman autofagosomas que se fusionan con los lisosomas provocando la degradación del material autofágico. Por consiguiente, LAMP-2 podría ser determinante en la fusión de estos orgánulos para formar autofagolisosomas (*Levine y Kroemer, 2008*).

A primera vista no parece lógico que un proceso de autodigestión pueda ser beneficioso, pero en caso de falta de nutrientes intracelulares y energía, la célula se ve obligada a utilizar sus propios recursos tales como el recambio de proteínas y orgánulos. Asímismo, diversos componentes celulares como el retículo endoplásmático, las mitocondrias y la membrana plasmática, podrían aportar membranas para la biogénesis de autofagosomas (*Weidberg et al., 2011*).

Aunque a menudo se detecta la autodigestión en células que mueren, no es fácil discernir su participación directa en la muerte celular (Kroemer y Levine,et al., 2008).

La pancreatitis tiene dos efectos en la autofagia: su activación y el impedimento o retardo de su flujo (*Gukovsky et al., 2011; Mareninova et al., 2009 et al; Gukovsky et al., 2010; Mareninova et al., 2010a, Mareninova et al., 2010b*). El impedimento de la autofagia se debe a un defecto en la degradación a nivel del lisosoma, una de cuyas manifestaciones principales es el dramático descenso de la actividad enzimática de las catepsinas lisosómicas, cuyo procesamiento está alterado en la pancreatitis, de modo que se forman y acumulan formas inmaduras, principalmente de las catepsinas B y L (*gukovsky et al., 2012*). Otro defecto en los lisosomas es el descenso de los niveles pancreáticos de LAMP-1 y LAMP-2, mediado por catepsinas (*Mareninova et al., 2010a; Mareninova et al., 2010b; Fortunato et al., 2009*). Se ha especulado que a causa del procesamiento anormal de las catepsinas, su interacción y localización en el lisosoma estaría alterado en la pancreatitis, de modo que las proteínas LAMP serían accesibles a la rotura proteolítica por las catepsinas, principalmente por la zona C-t, en un lugar próximo al dominio que atraviesa la membrana (*gukovsky et al., 2012*).

En muestras humanas, el estudio del tejido pancreático durante la pancreatitis, reveló la presencia de vacuolas citoplasmáticas (*Helin et al., 1980*), así como un descenso marcado de LAMP-1 y LAMP-2 (*Fortunato et al., 2009*). Del mismo modo, nuestro grupo de investigación ha observado en subpoblaciones enriquecidas de lisosomas de páncreas de ratas pancreatíticas, la aparición de grandes vacuolas (*Sarmiento et al., 2011*).

Recientemente, se ha evidenciado que dicha vacuolización refleja la acumulación de autofagosomas (*Hashimoto; Ohmuraya y Yamamura,et al., 2008*). En ratones knockout para LAMP-2 (*Eskelinen et al., 2002*), se ha comprobado que al mes de edad se aprecia una acumulación en las células acinares pancreáticas de grandes vacuolas auotofágicas con material degradado parcialmente. Este suceso se asocia a un aumento progresivo de la infiltración, principalmente por macrófagos, y por necrosis acinar. Por lo tanto, los ratones knockout LAMP-2 desarrollan espontáneamente una patología tipo pancreatitis.

3. FOSFORILACIÓN EN TIROSINAS: PROTEÍNA TIROSINA FOSFATASAS (PTPs)

Inicialmente, la mayoría de estudios consideraban a las PTPs como un componente poco sofisticado en las reacciones de fosforilación, incluso se pensaba que el único propósito de unas pocas tirosinas fosfatasas era terminar el trabajo de las numerosas proteína tirosina quinasas (PTKs). Sin embargo, los resultados de los últimos años han demostrado que los niveles de fosfotirosina estarían regulados por las PTKs y por las PTPs.

Las PTPs forman una gran familia de enzimas altamente específicas sometidas a una compleja regulación, que pueden intervenir en la activación e inhibición de múltiples rutas de señalización celular, dependiendo de su localización y de sus dianas moleculares (*Tonks et al., 2013*). Estas enzimas regulan una variedad de procesos celulares incluyendo la diferenciación, proliferación, adhesión, migración y secreción. También, han sido implicadas en un amplio rango de enfermedades adquiridas o heredadas, entre ellas el cáncer, la diabetes y procesos autoinmunes (*Hendriks et al., 2013*).

El análisis de estas fosfatasas en el genoma humano reveló la existencia de 107 genes, pero probablemente solo 81 de ellos codifican PTPs (*Alonso et al., 2004*)

3.1. Características estructurales y clasificación de las PTPs

Las PTPs se dividen en dos clases distintas: las tirosinas clásicas, PTPs, y las fosfatasa duales (DSPs), definidas por desfosforilar residuos de serina, treonina y tirosina aunque también, algunos lípidos y ARN mensajeros (*Tonks et al, 2006*)

Las PTPs "clásicas" son las más estudiadas y pueden subdividirse dependiendo de su localización celular: las PTPs de membrana o de tipo receptor (RPTPs), y las PTP no transmembrana, también llamadas citosólicas. El dominio catalítico característico de las PTPs clásicas está constituído por unos 280 aminoácidos que presentan un motivo conservado formado por 7 aminoácidos R-HC-(X5)-R esencial para la catálisis (*Tonks et al, 2013*). Las PTPs transmembrana presentan una estructura similar a la de un receptor típico de membrana, codificadas por 21 genes en humanos, y constan de un dominio extracelular de tamaño variable, un corto dominio hidrofílico que atraviesa la membrana, y normalmente presentan dos dominios catalíticos. El dominio extracelular puede interaccionar con ligandos que regulan la actividad de los dominios catalíticos. Estos dominios presentan una gran variabilidad estructural, posiblemente reflejo de sus diferentes funciones y ligandos fisiológicos. Las PTPs citosólicas son codificadas por 16 genes en humanos y se caracterizan por tener un solo dominio catalítico y en su extremo N-terminal o C-terminal aparecen diferentes dominios estructurales de longitud variable, que confieren distintos modos de compartimentación dentro de la célula y de regulación (*Alonso et al, 2004*).

La nomenclatura de las PTPs citosólicas se ha realizado en base a su estructura, secuencia y función. Esta nomenclatura se describe en la siguiente tabla:

Nombre del gen	**diferentes nombres de la proteína**
Ptpn1	PTPN1, PTP-1B
Ptpn2	PTPN2, TC-PTP, MPTP, PTP-S
Ptpn3	PTPN3, PTPH1
Ptpn4	PTPN4, PTP-MEG1, TEP
Ptpn5	PTPN5, STEP
Ptpn6	PTPN6, Shp1, PTP1C, SH-PTP1, HCP
Ptpn7	PTPN7, HePTP, LCPTP
Ptpn9	PTPN9, PTP-MEG2
Ptpn11	PTPN11, Shp2, SH-PTP2, Syp, PTP1D, PTP2C, SH-PTP3
Ptpn12	PTPN12, PTP-PEST, PTP-P19, PTPG1
Ptpn13	PTPN13, PTP-BAS, FAP-1, PTP1E, RIP, PTPL1, PTP-BL
Ptpn14	PTPN14, PTP36, PEZ, PTPD2
Ptpn18	PTPN18, PTP-HSCF, PTP20, BDP
Ptpn20	PTPN20, TypPTP
Ptpn21	PTPN21, PTPD1, PTP2E, PTP-RL10
Ptpn22	PTPN22, LYP, PEP

Tabla 3.1. Nomenclatura modificada de *Senis, 2013*.

3.1.1. SHP-1 y SHP-2 proteínas con dominios SH2

SHP-1 y SHP-2 son dos proteínas tirosina fosfatasas de tipo no receptor que contienen dominios homólogos a los SH2 de la familia tirosina quinasa del virus del sarcoma de Rouss (del inglés, Src Homology2) en el extremo N-terminal de la molécula. SHP-1 también llamada PTPN6, PTP1C, SH-PTP1 y HCP es codificada por el gen PTPN6. SHP-2 conocida como PTPN11, SH-PTP2, Syp, PTP1D, PTP 2C y SH-PTP3, está codificada por el gen PTPN11.

3.1.2. PTP1B

La proteína PTP1B se caracteriza por poseer un segmento carboxilo terminal hidrofóbico por el que se encuentra anclado a la membrana del retículo ensoplasmático. Cuando dicho anclaje es catalizado por calpaína resulta en una relocalización desde la membrana del RE hasta el citosol. (*Frangioni et al, 1992*).

3.1.3. Regulación de la actividad PTP

Como habíamos comentado anteriormente, la localización de las PTPs dentro de la célula es un aspecto relevante para la regulación de su actividad ya que determina el acceso de cada enzima a un determinado grupo de sustratos, originándose así una especificidad por el mismo (*Hernández et al., 1999*). Las PTPs citosólicas contienen secuencias o dominios no catalíticos en su extremo amino terminal que podrían modular la función de estas proteínas, dirigiéndolas a compartimentos subcelulares específicos o autoregulando su actividad mediante el bloqueo de su centro catalítico, como es el caso de los dominios SH2 de SHP-1 y SHP-2. Concretamente, la actividad SHP-1 y SHP-2 en la célula, podría estar regulada por diferentes mecanismos de un modo positivo o negativo (*Persson et al, 2004*): La fosforilación de residuos de tirosina podría aumentar su actividad de dos a cuatro veces; la traslocación a diferentes zonas puede limitar su capacidad para desfosforilar sustratos. Además, los dominios SH2 tienen un efecto inhibidor sobre la actividad PTP, de modo que cuando la enzima se une a una fosfoproteína ese efecto inhibitorio desaparece.

Aunque estructuralmente SHP-1 y SHP-2 son similares, sus funciones en las distintas vías de señalización celular no son coincidentes. Probablemente, esto se debe a diferencias en su dominio catalítico y a la especificidad que tienen los dominios SH2 de cada una de ellas para interaccionar con cierta clase de proteínas. Esta afinidad de los dominios SH2 por moléculas especificas, explicaría por qué estos dominios no son intercambiables (*Neel et al., 2003; Tenev et al., 1997*).

Es conocido que SHP-1, SHP-2 y PTP1B, actúan como reguladores de la señalización de diversos receptores ligados a PTK, incluyendo por ejemplo, los receptores de citoquinas y de factores de crecimiento o las integrinas (*Pao et al., 2007*). Generalmente, SHP-1 se considera un regulador negativo en la señalización intracelular, mientras que SHP-2 es considerado un regulador positivo, sin embargo, existen procesos en los que esto no ocurre. En el caso de SHP-2, varios estudios la sitúan como activador de Ras. Ras es una de las proteínas que participan en la activación de las MAPK.

Las MAPK desencadenan la activación de ERK en la señalización de receptores de citoquinas y factores de crecimiento (*Kontaridis et al., 2004*). Además, se ha descrito que SHP-1 y SHP-2 son reguladores negativos de la señalización mediada por citoquinas mediante desfosforilaciones en JAK y STAT. Por lo tanto, SHP-1 es capaz de desfosforilar a JAK1, JAK2, JAK3 y STAT5. Y SHP-2 desfosforila a JAK2, STAT1 y STAT2.

Finalmente, Se ha sugerido que las PTPs pueden estar reguladas por mecanismos de oxidación. El residuo de cisteína, sitio catalítico conservado, es esencial durante la catálisis. Las cisteínas catalíticas son susceptibles a la oxidación debido a su bajo pKa. La cadena lateral de la cisteína está formada por un grupo SH y, para que esta sea funcional, el azufre se debe encontrar en forma de tiol (S-) o de sulfhidrilo (SH). Sin embargo, cuando algunos oxidantes, por ejemplo el H_2O_2, reaccionan con ella, el grupo sulfhidrilo se oxida a ácido sulfénico (SOH), estado en el cual la cisteína no puede llevar a cabo la acción catalítica. Si las concentraciones de oxidante son altas, el estado del grupo sulfato de la cisteína puede llegar a ácido sulfínico (SO2H) o ácido sulfónico (SO3H). La oxidación de los residuos de cisteína a ácido sulfénico es reversible, mientras que la posterior oxidación a ácido sulfónico es irreversible. La oxidación inhibe la capacidad de las PTPs para desfosforilar sus sustratos, actuando así como sensores del estado redox de la célula (*Groen A. et al, 2004*).

Todas las rutas de señalización descritas anteriormente, en las cuales interviene SHP-1 y/o SHP-2 se han implicado en el dearrollo de la pancreatitis aguda

3.1.4. Papel biológico de las PTP

Las PTPs con dominios SH2: SHP-1 y SHP-2, estructuralmente son muy similares pero tienen diferentes funciones en la transducción de señales.

SHP-1 se expresa abundantemente en las células hematopoyéticas, donde juega un papel señalizador negativo y a menor nivel en muchos otros tipos celulares. De hecho, la deleción del gen que codifica esta enzima evidencia alteraciones hematopoyéticas que van desde inflamación crónica hasta alteraciones de tipo inmunológico y muerte. (*Kozlowski et al, 1998*).

SHP-2 puede actuar en múltiples lugares incluso dentro de una misma ruta de señalización y desempeña un papel importante en la regulación del crecimiento, proliferación y diferenciación celular (*Qu Cheng et al., 2000*).

La proteína tirosina fosfatasa 1B (PTP1B) desempeña un rol importante en la regulación de diversas vías de señalización. En este sentido, nuestro grupo demostró recientemente un aumento en la expresión de PTP1B en la fase temprana de la pancreatitis aguda inducida por ceruleína, aunque un aumento en los niveles de AMPc en las células inflamatorias, así como, la inhibición de JNK Y ERK ½ lo suprimen a nivel proteíco. (*N. Sarmiento et al., 2010*). Además, se ha implicado a la PTP1B, en la homeostasis de la glucosa, la masa corporal y en la regulación de diversas vías de señalización implicadas en el estrés del retículo (*Elchebly et al., 1999; Klaman et al., 2000*).

II. Objetivos

Sobre la base bibliográfica relativa a nuestro tema de estudio, nos hemos planteado como objetivo general estudiar, en pancreatitis aguda experimental edematosa, la dinámica de algunas proteínas pancreáticas implicadas en rutas de señalización alteradas en esta patología, así como los posibles cambios en la estabilidad lisosómica. Dicho objetivo general se concretó en los siguientes objetivos específicos:

1. Estudiar los cambios de expresión y dinámica de las PTPs con dominios SH2: SHP-1 y SHP-2, en la PA inducida por ceruleína.

1.1. Estudiar la especificidad de dichos cambios respecto a otros modelos de PA.

1.2. Estudiar la influencia de la infiltración por neutrófilos en dichos cambios.

1.3. Estudiar la influencia de la inhibición de las MAPKs: JNK y ERK ½ , así como de la fosfodiesterasa tipo IV, sobre los mismos.

1.4. Analizar la distribución subcelular de las dos PTPs durante el desarrollo de la PA inducida por ceruleína.

2. Investigar los cambios de expresión de la PTP PTP1B durante el desarrollo de la PA inducida por ceruleína.

2.1. Valorar la especificidad de dichos cambios respecto a otros modelos de PA.

2.2. Estudiar la influencia de la infiltración por neutrófilos en dichos cambios.

2.3. Estudiar la influencia de la inhibición de las MAPKs: JNK y ERK ½ , así como de la fosfodiesterasa tipo IV, sobre los mismos.

3. Desarrollar un método para el aislamiento de subpoblaciones de lisosomas de páncreas de rata que nos permita el estudio futuro de las proteínas lisosómicas

3.1. Analizar la estabilidad de la membrana lisosómica en la subpoblación de lisosomas primarios, determinando la dinámica de dos formas de la N-acetil-β-D-glucosaminidasa en la PA.

4. Investigar los cambios de expresión y dinámica de la proteína lisosómica LAMP-2 durante el desarrollo de la PA inducida por ceruleína.

III. Materiales y Métodos

1. MATERIAL Y APARATOS

1.1. Material

1. Filtros estériles de 0,2 µm de Pall Corporation.
2. Casete de revelado Hypercassete™ de Amersham Pharmacia Biotech.
3. Membrana de difluoruro de polivinilideno (PVDF) de GE Healthcare.
4. Película fotográfica Hyperfilm ECL High performance chemiluminescence film de Amersham Biosciences.
5. Papel Whatman estándar de Whatman®.
6. Placas de Petri.

Otro material de vidrio y plástico de uso corriente en el laboratorio.

1.2. Material informático

1. Adobe Photoshop: Procesamiento de imágenes.
2. Programa Kodak Digital Science v 3.0.
3. Programa analizador de imágenes MacBas 2.5.
4. Programa informático SPSS para MS Windows (versión 18.0).
5. Paquete Microsoft Office: Se empleó para la redacción del trabajo y elaboración de figuras.

1.3. Aparatos

- Agitador balancín BFR 25 de Grant Boekel.
- Agitador magnético Minimix de OVAN.
- Balanza analítica 40SM-200A de Precisa y granataria Electronic Scale de Want.
- Baño termostatado Retostat.
- Bomba de vacío.

- Cámara frigorífica a 4º C.
- Centrífugas.
- Congeladores de -20º C y -80º C.
- Escáner Hewlett-Packard, modelo Scanjet 3C.
- Espectrofotómetro GeneQuant pro RNA/DNA Calculator.
- Homogeneizador tipo Potter-Elvehjem.
- Lector de ELISA de Thermo Scientific y Varioskan Flash Thermo Electron Corporation.
- Material de disección.
- Máquina de revelado Medical X-ray Processor de Kodak.
- Microscopio Optico Zeiss.
- pH-metro Hanna Instruments.
- Sistema de electroforesis vertical Mini-Protean II y equipo para transferencia de *Western* Mini Trans-Blot cell, ambos de Bio-Rad.
- Unidad de corriente Power Pac 300 de Bio-Rad.
- Ultracentrífuga Beckman Optima^{TM} XL-100K.

Otros aparatos de uso frecuente en el laboratorio.

2. REACTIVOS

Todos los productos empleados en este trabajo fueron de calidad analítica:

- Los anticuerpos anti-SHP-1 (D11) y anti-PTP 1B (H-135) fueron adquiridos de Santa Cruz Biotechnology.
- El anticuerpo monoclonal anti-SHP-2 se adquirió de BD Biociences.
- El anticuerpo policlonal anti-Lamp-2 fue suministrado por Zymed.

- El anticuerpo anti-mouse Ig G conjugado con peroxidasa de rábano (HRP) y el sistema de revelado de transferencias de Western (ECL plus Western Blotting Detection System) fueron adquiridos en Amersham.

- El kit 2D Clean up fue obtenido de GE Healthcare.

- El kit Top-block fue adquirido en Fluka, Biochemica.

- La retrotranscriptasa "Revert Aid M-MULV RT, la Taq ADN polimerasa, los desoxinucleótidos trifosfato (dNTPs) y el marcador de tamaño de ADN (Gene ruler), se obtuvieron de Fermentas.

- Los oligonucleótidos se obtuvieron de Isogen.

- La acrilamida, la bisacrilamida (bis-N-N'-metileno-bis-acrilamida), el dodecil sulfato sódico (SDS), el persulfato amónico, el N,N,N´,N´,-tetrametil-etilendiamida (TEMED) fueron adquiridos en BioRad.

- El β-mercaptoetanol y el azul de bromofenol fueron suministrados por Merck.

- El cóctel inhibidor de proteasas (P 8340), el rolipram, el taurocolato sódico, el sulfato de vinblastina, el inhibidor de tripsina, el SP600125, el fluoruro de fenilmetilsulfonilo (PMSF), el ditiotreitol (DTT), el Percoll, la ceruleína sulfatada, el detergente IGEPAL CA-630, la DEAE- Celulosa y el anticuerpo monoclonal anti-β Tubulina se obtuvieron de Sigma.

3. ANIMALES DE EXPERIMENTACIÓN

Para la realización de este trabajo de investigación se han empleado ratas adultas Wistar machos, con un peso corporal medio de 250-300 gr, proporcionadas por el Servicio de Animalario de la Universidad de Salamanca, donde se mantuvieron a una temperatura ambiental de 20-22º C, con periodos de luz y oscuridad de 12 horas cada uno. En todo momento los animales tuvieron libre acceso a la comida y al agua de bebida.

Todos los estudios se realizaron cumpliendo con la normativa impuesta por el Consejo de la Comunidad Europea, en relación con la protección de

animales utilizados para experimentación y con otros fines científicos y los protocolos fueron aprobados por el Comité de Bioética Ético de la Universidad de Salamanca.

3.1. Grupos Experimentales

Tras 12 horas de ayuno, los animales se distribuyeron en dos grupos experimentales:

- **Grupo Control:** animales no sometidos a la pancreatitis.
- **Grupo Pancreatítico:** animales en los que se indujo una PA experimental.

3.2. Modelos de pancreatitis aguda experimental

3.2.1. Hiperestimulación con ceruleína

La inducción de la pancreatitis aguda se realizó por hiperestimulación con ceruleína, siguiendo el método descrito por *Lampel y Kern* (*1977*), tal como se expone a continuación. En primer lugar, la ceruleína se disolvió en suero fisiológico estéril y posteriormente se administró a las ratas en dos o cuatro inyecciones por vía subcutánea a intervalos de 1 hora. La dosis empleada fue 20 µg/kg/h. Dentro de este modelo, se establecieron también grupo control de animales que recibieron dosis similares de suero salino al 0,9%. Los animales se sacrificaron por dislocación cervical a las 2, 4 ó 9 horas de la primera inyección, tiempos que denominamos arbitrariamente como fases temprana, intermedia y final del desarrollo de la PA inducida por ceruleína **(esquema 1).**

- **Fase temprana:**

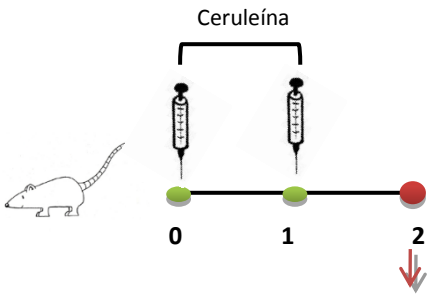

- **Fase intermedia:**

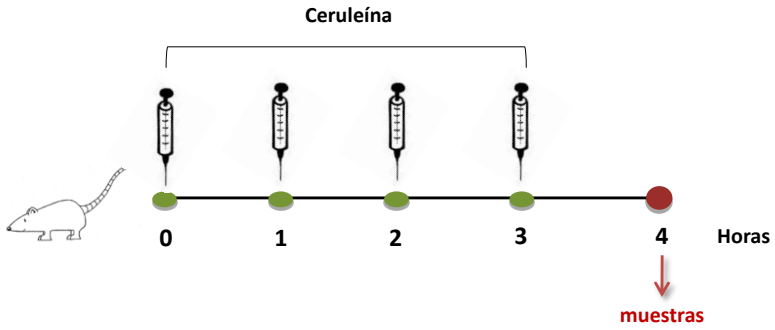

- **Fase final:**

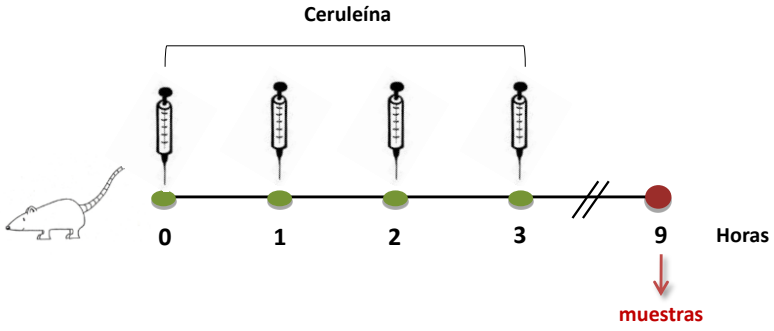

Esquema 1. Fases establecidas en el desarrollo de la pancreatitis aguda inducida por ceruleína.

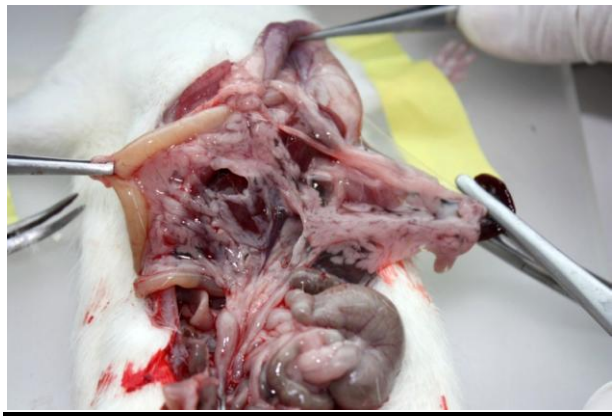

Figura 6. Fotografía del páncreas en la fase final del modelo de la PA inducida por ceruleína. Puede apreciarse el páncreas edematoso de una rata a las 9h de la primera inyección de ceruleína.

3.2.2. Ligadura del conducto bilio-pancreático (OCBP)

Este modelo experimental fue realizado en el Departamento de Fisiología y Farmacología con la ayuda del Dr. Manuel Manso.

Después de un ayuno de 12 horas con acceso libre al agua, los animales se anestesiaron y se colocaron en posición “decúbito supino”. Se practicó una laparotomía ventral media para acceder a la cavidad peritoneal y aislar el colédoco. Tras aislar este conducto, se realizó una ligadura en su extremo más distal, próximo a su desembocadura en el duodeno **(figura 7)**. Las muestras de páncreas se recogieron 12 horas después de inducir la PA **(esquema 2).**

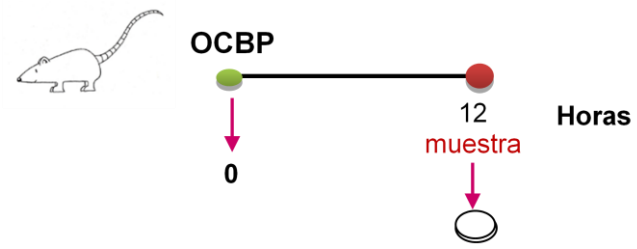

Esquema 2. Modelo de pancreatitis aguda por ligadura del conducto bilio-pancreático.

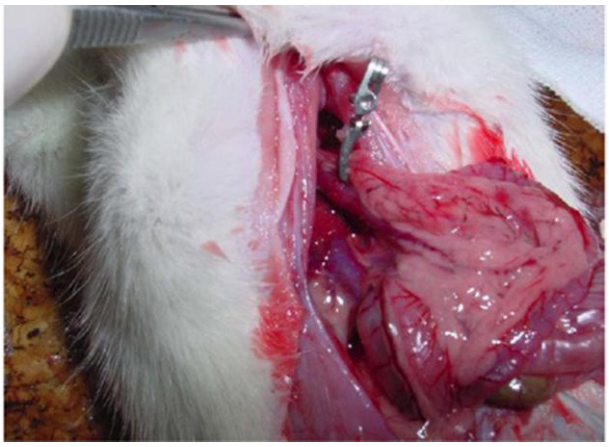

Figura 7. Fotografía del páncreas y aislamiento del colédoco en el modelo OCBP de PA.

3.2.3. Infusión retrógrada de taurocolato sódico (TcNa).

Este procedimiento se realizó con ayuda del Dr. José J. Calvo, en el Departamento de Fisiología y Farmacología.

La PA se generó siguiendo el método de *Aho y Nevalainen (1980)*. Los animales se sometieron a un procedimiento quirúrgico y, bajo anestesia general, se realizó una laparotomía transversa subcostal.

Tras cerrar momentáneamente el conducto hepático, se practicó una ligadura en la parte distal del colédoco y mediante una cánula de 0,6 mm de diámetro (Braun), se indujo la pancreatitis aguda con una inyección intraductal de sal biliar TcNa al 4% (0,1ml/100 g de peso), utilizando para ello una bomba peristáltica programada para flujo constante de 0,03 ml/min.

En este modelo, las muestras de páncreas se recogieron 3 horas después de inducir la PA (**Esquema 3).**

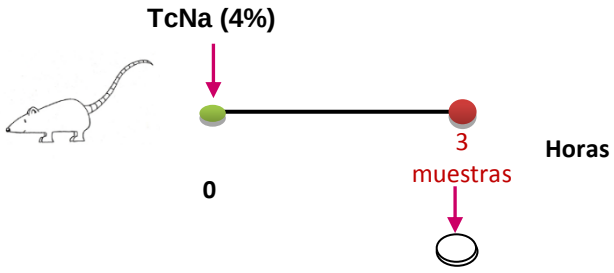

Esquema 3. Modelo de pancreatitis aguda por infusión retrograda de TcNa.

4. TRATAMIENTOS

4.1. Inhibición de MAPKs por SP600125

Para estudiar la participación de las principales MAPKs, JNK y ERK 1/2, en el desarrollo de la pancreatitis aguda inducida por ceruleína, se empleó el inhibidor SP600125, siguiendo el método descrito previamente por *Minutoli et al.*, (*2004*). Dos horas antes de la primera inyección de ceruleína y 30 minutos después de la misma, las ratas fueron inyectadas intraperitonealmente con 15 mg/kg de SP600125 disuelto en su vehículo (1 ml/kg de una solución de DMSO al 10% en NaCl al 0,9%). A su vez, dosis similares de dicho vehículo se inyectaron a un segundo grupo de ratas no tratadas con el inhibidor. Dos horas después de la primera inyección de SP600125 o del vehículo, y dependiendo de cada caso, se administraron 20 μg/kg de ceruleína o suero fisiológico por vía subcutánea a intervalos de una hora **(esquema 4).** Paralelamente a este tratamiento, dos grupos adicionales fueron inyectados con ceruleína o suero salino al 0,9%, siguiendo el mismo procedimiento que se indica en la sección 3.2.1 de Métodos. Los grupos resultantes se detallan a continuación:

- Ceruleína + SP600125
- Ceruleína + vehículo
- Suero salino + SP600125
- Suero salino + vehículo
- Suero salino
- Ceruleína

Por último, todos los animales se sacrificaron 2 horas después de la primera inyección de ceruleína, lo que representa la fase temprana del desarrollo de la pancreatitis aguda.

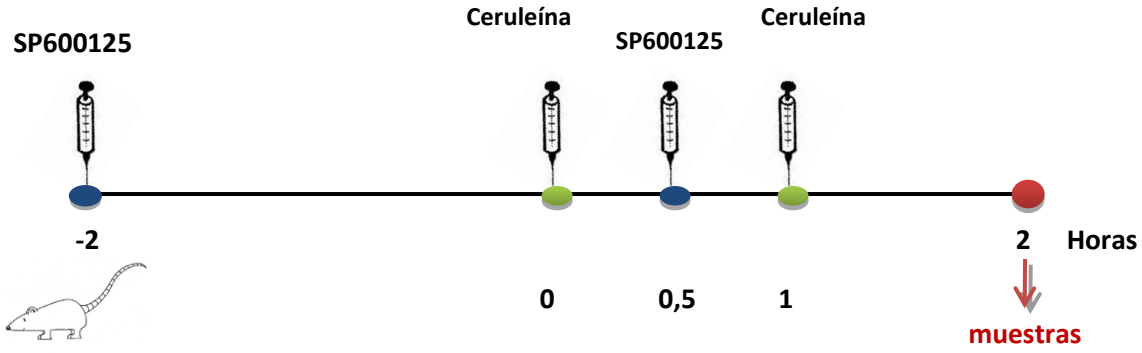

Esquema 4. Inhibición de JNK y ERK ½ por SP600125.

4.2. Inhibición de la fosfodiesterasa tipo IV por rolipram

Para inhibir la fosfodiesterasa tipo IV se ha empleado el inhibidor rolipram siguiendo el método descrito previamente *Sato et al.*, (*2006*). Treinta minutos antes de la primera inyección de ceruleína y 30 minutos después de la misma, las ratas fueron inyectadas intraperitonealmente con 5 mg/kg de rolipram disuelto en su vehículo (1 ml/kg de una solución de DMSO al 10% en NaCl al 0,9%). A su vez, dosis similares de dicho vehículo se inyectaron a un segundo grupo de ratas no tratadas con inhibidor. Treinta minutos después de la primera inyección de rolipram o del vehículo, y dependiendo de cada caso, se administraron 20 μg/kg de ceruleína o de suero fisiológico por vía subcutánea a intervalos de una hora **(esquema 5)** Paralelamente a este tratamiento, dos grupos adicionales fueron tratados con ceruleína o suero salino al 0,9%, siguiendo el mismo procedimiento que se indica en la sección 3.2.1 de Métodos

Los grupos resultantes fueron:

- Ceruleína + rolipram
- Ceruleína + vehículo
- Suero salino+ rolipram
- Suero salino + vehículo
- Suero salino
- Ceruleína

Todos los animales se sacrificaron 2 horas después de la primera inyección de ceruleína, lo que representa la fase temprana del desarrollo de la pancreatitis aguda.

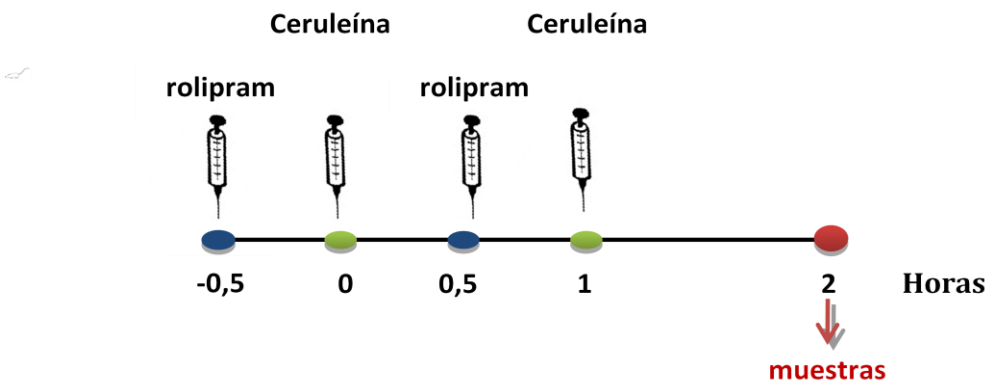

Esquema 5. Inhibición de la fosfodiesterasa tipo IV por rolipram.

4.3. Inducción de la neutropenia

Para estudiar el efecto de la neutropenia en la expresión proteica de distintas PTPs durante el desarrollo de la PA inducida con ceruleína, las ratas recibieron, por vía intravenosa, sulfato de vinblastina disuelto en su vehículo (tampón fosfato sódico 10 mM pH 7,4, que contenía NaCl 147 mM y KCl_2 7 mM) a una dosis de 0,75 mg/kg en el día 1, siguiendo el método descrito por *Clemons et al.,* (2002). Teniendo en cuenta la dosis administrada, los animales se vuelven neutropénicos entre los días 4 y 6 *Clemons et al.,* (2002). Al mismo tiempo, un segundo grupo de ratas no tratadas con dicho fármaco fueron inyectadas con solución salina estéril. Cinco días después de la administración del sulfato de vimblastina o de la solución salina estéril, los animales fueron inyectados con 4 dosis de ceruleína **(esquema 6)**, como se indica en la sección 3.2.1 de Métodos. El sacrificio de los animales se practicó 4 horas después de la primera inyección de ceruleína, lo que representa la fase intermedia del desarrollo de la pancreatitis aguda. La validación del tratamiento se realizó

mediante la valoración de la actividad mieloperoxidásica, según se describe en el apartado 10.1 de esta sección, y mediante el recuento total y diferencial de leucocitos.

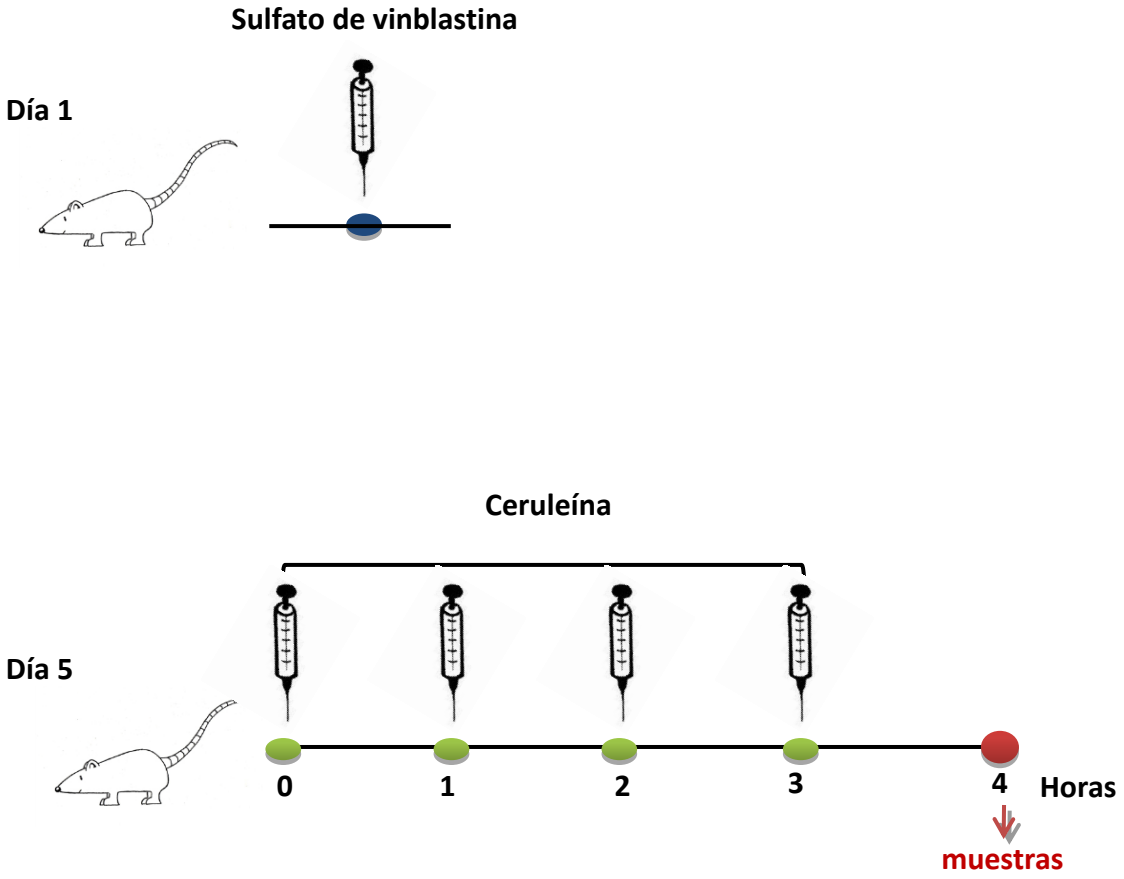

Esquema 6. Indución de un estado neutropénico.

Para el **recuento total** un volúmen de sangre total anticoagulada se mezcló con la solución de Turk (dilución 1:20), y empleando una cámara de Neubauer, se realizó el contaje de globulos blancos (el resultado se expresó por mm^3). El **recuento diferencial** incluye el contaje y clasificación de 100 leucocitos consecutivos en un frotis de sangre periférica teñido con el colorante de Wright (el resultado se indicó como % de los diferentes tipos de leucocitos).

5. RECOGIDA DE LAS MUESTRAS DE SANGRE Y DE PÁNCREAS

La sangre se obtuvo por punción cardíaca justo antes del sacrifico de los animales, e inmediatamente se centrifugó a 1.500×*g* durante 10 minutos. Pasado este tiempo, el suero sanguíneo se separó, transfiriéndose a un tubo de almacenamiento. Los sueros se congelaron inmediatamente en nieve

carbónica para su uso posterior en la valoración enzimática de amilasas séricas. A continuación, las ratas fueron sacrificadas por dislocación cervical y con la mayor rapidez posible se extrajeron los páncreas por laparotomía ventral media. Tras la extracción, los órganos se lavaron con suero fisiológico a 4ºC. Utilizando unas tijeras se retiró el tejido graso circundante, los ganglios linfáticos y los vasos sanguíneos. Una vez limpios los páncreas, se secaron y pesaron.

Finalmente, los páncreas se procesaron para obtener las distintas fracciones subcelulares tal como se expone en el esquema 7. En diversos experimentos, se separaron secciones de páncreas para llevar a cabo estudios enzimáticos e histológicos, así como para la valoración de ARNm por la técnica RT-PCR.

6. AISLAMIENTO DE LAS FRACCIONES SUBCELULARES DE PÁNCREAS

Los páncreas se homogeneizaron en tampón imidazol 3mM pH 7,4 que contenía sacarosa 0,25 M, EDTA 1 mM, ortovanadato sódico 2 mM, PMSF 1mM, inhibidor de tripsina (10^6 unidades BAEE) y cóctel de inhibidores de proteasas de Sigma (200 µl/100 ml de tampón) (tampón de homogeneización). La homogeneización se realizó con 20 volúmenes de tampón/gramo de tejido, con la ayuda de un homogeneizador tipo Potter-Elvehjem. El homogenado conseguido se centrifugó a 150×*g* durante 15 minutos, obteniéndose un precipitado y un sobrenadante (A) **(esquema 7)**. El precipitado se resuspendió en 1 ml del tampón de homogeneización y se volvió a centrifugar en las mismas condiciones, obteniéndose un nuevo sobrenadante (B) y un precipitado final, que se desechó. La mezcla de los dos sobrenadantes (A+B) se centrifugó a 1.300×*g* durante 15 minutos, lográndose así un precipitado que se resuspendió en el mismo tampón y que correspondía a la fracción subcelular de los zimógenos. El nuevo sobrenadante (C) fue entonces centrifugado a 20.000×*g* durante 30 minutos, obteniéndose un precipitado que se resuspendió en tampón de homogeneización, consiguiéndose así la fracción de lisosomas y mitocondrias (L+M). Por último, el sobrenadante (C) se centrifugó a 150.000×*g* durante 1 hora para obtener un sobrenadante final (D) que corresponde a la

fracción soluble del páncreas y un precipitado que se resuspendió con el mismo tampón, obteniéndose así una fracción de microsomas. Las muestras se mantuvieron entre hielo durante todo el aislamiento y después se almacenaron a -80º C, en atmósfera de N_2, hasta su utilización.

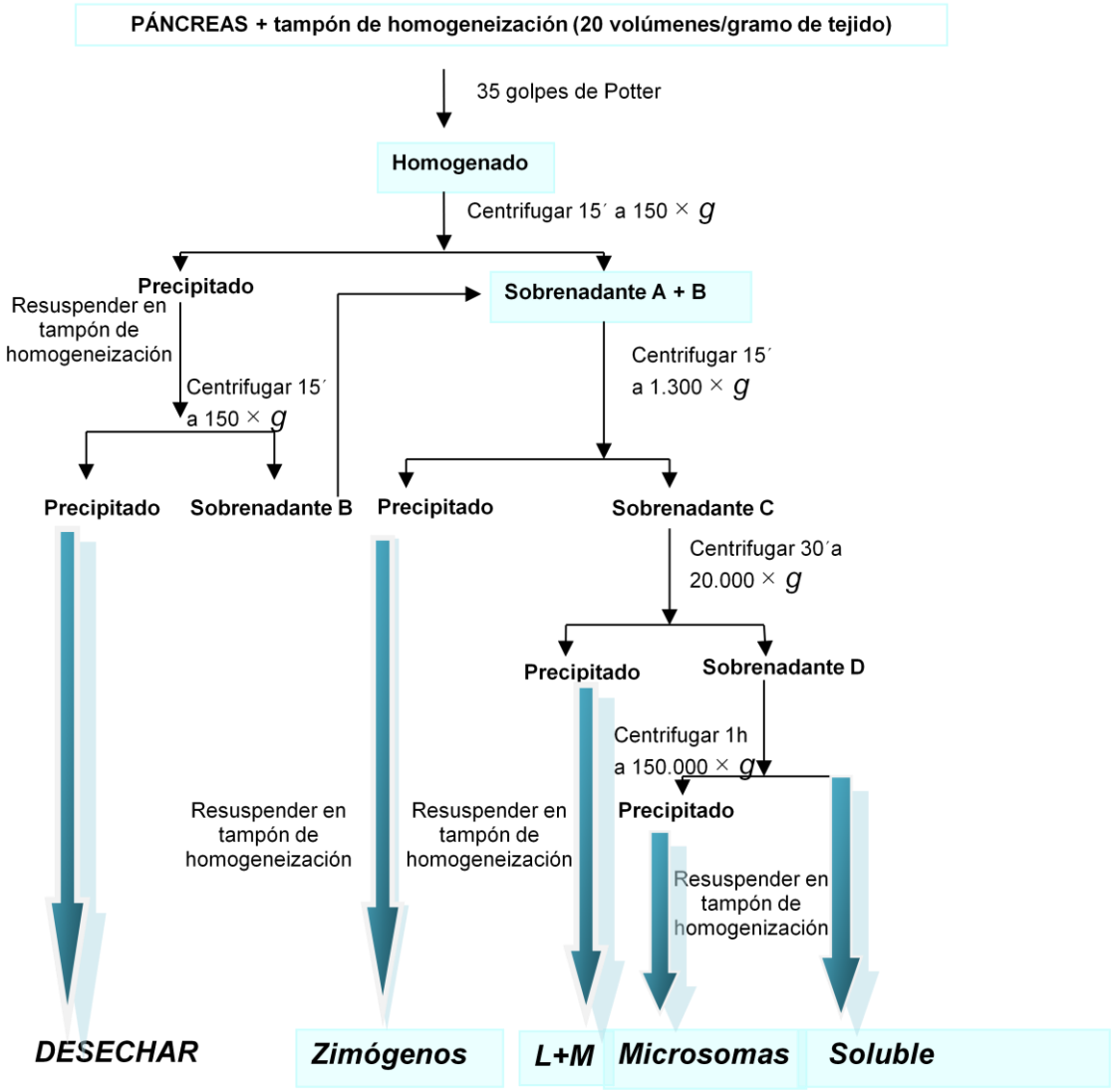

Esquema 7. Procesamiento de las fracciones subcelulares de páncreas.

6.1. Separación de lisosomas y mitocondrias. Gradiente discontinuo de Percoll

Con el fin de separar los distintos orgánulos de la fracción L+M obtenida en el fraccionamiento subcelular, ésta se sometió a un gradiente discontinuo de Percoll.

6.1.1. Gradiente discontinuo de Percoll

Se prepararon tres soluciones de Percoll a diferentes concentraciones (17%, 10%, 5%) en el mismo tampón de homogeneización de los páncreas. Utilizando una pipeta Pasteur, se adicionaron desde abajo hacia arriba 3,8 ml de cada solución a los tubos del gradiente, con lo que se consiguieron tres fases de mayor a menor concentración. Posteriormente, en la parte superior de estos tubos se añadieron 1,5 ml de la muestra (diluída tres veces en tampón de homogeneización) y se realizó una centrifugación a 50.500x*g* durante 30 minutos, en un rotor oscilante SW 40 (Beckman) **(esquema 8)**. Pasado este tiempo, se recogieron fracciones de 0,5 ml, desde la parte superior hacia el fondo del tubo, para valorar las enzimas marcadoras de lisosomas y mitocondrias en cada una de las fracciones.

Con objeto de hacer una estimación aproximada de la densidad de estos órganulos, se incluyeron perlas marcadoras de densidad (Pharmacia) en algunos tubos del gradiente.

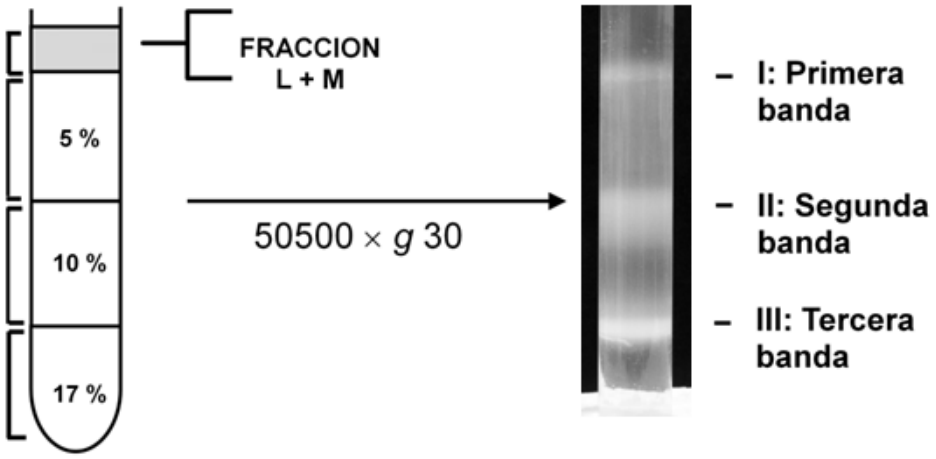

Esquema 8. Gradiente discontinuo de Percoll y bandas de lisosomas obtenidas después de la centrifugación.

En cada una de las fracciones obtenidas se realizó la valoración de la actividad N- actividad enzimática N-acetilglucosaminidásica (marcadora de lisosomas), de la actividad enzimática de las succinato deshidrogenasa (SDH) (marcadora de mitocondrias).

6.1.2. Lavado de las fracciones obtenidas en el gradiente discontinuo de Percoll

Las fracciones enriquecidas en lisosomas (bandas I, II y III del gradiente), se lavaron dos veces con tampón de homogeneización por centrifugación a 50.500×g durante 1 hora, en un rotor oscilante 70.1 Ti (Beckman). De este modo se consigue eliminar los restos de Percoll y concentrar la muestra. Las tres fracciones enriquecidas en lisosomas se analizaron por microscopía electrónica.

7. PCR SEMICUANTITATIVA

7.1. Obtención del ARN

Los niveles de expresión del ARNm de SHP-1, SHP-2, PTP1B y LAMP-2 se determinaron por RT-PCR semicuantitativa. El ARN total se obtuvo a partir de secciones de los páncreas y cerebros de ratas control y pancreatíticas representativas de la fase temprana de la pancreatitis aguda inducida por ceruleína. Se empleó el reactivo "TRI reagent" de SIGMA siguiendo las instrucciones de la casa comercial para la extracción. Se incubaron homogenados de las muestras a temperatura ambiente durante 5 minutos. A continuación, se añadieron 0,2 ml de cloroformo y se agitaron los tubos durante 15 segundos. Se incubaron de nuevo a temperatura ambiente durante 2-3 minutos y se centrifugaron a 12.000×*g* durante 15 minutos a 4º C. Tras la centrifugación, la fase acuosa superior se transfirió a un tubo limpio y se añadieron 0,5 ml de isopropanol, incubándose a temperatura ambiente durante 10 minutos. Se centrifugaron a 12.000×*g* durante 10 minutos a 4º C para precipitar el ARN. El ARN se sometió a un lavado con 1 ml de etanol al 75% y se volvió a centrifugar a 7.500×*g* durante 5 minutos a 4º C. Se dejó secar el precipitado y se resuspendió en tampón TE (Tris-HCl 10 mM y EDTA 1mM, pH 7,5). La concentración de ARN se calculó midiendo la absorbancia a 260 nm en un espectrofotómetro GeneQuant pro RNA/DNA Calculator. La integridad del ARN se comprobó corriendo 1 µg de ARN en geles de agarosa.

7.2. Síntesis del ADN copia (ADNc) y reacción de PCR

La síntesis del ADNc se llevó a cabo incubando 2 μg del ARN total con 0,5 μg de 18-mer oligo-dT a 42º C durante 1 hora, utilizando 200 U de la retrotranscriptasa (RevertAid M-MuLV Reverse Transcriptase) en una solución que contenía Tris-HCl 50 mM pH 8,3, KCl 50 mM, $MgCl_2$ 4 mM, DTT10 mM, dNTPs individuales1 mM y 20 U del inhibidor de Ribonucleasa en un volumen final de 20 µl. Se dejó transcurrir la reacción durante 1 hora a 37º C y se paró calentando la mezcla a 70º C durante 10 minutos. Después, 4 μl de esta reacción se utilizaron para la reacción de PCR, que se llevó a cabo en un volumen final de 40 µl, conteniendo 1 U de Taq polimerasa y 0,4 µM de los oligonucleótidos específicos. Para estar seguros de que trabajábamos en condiciones semicuantitativas, a partir del ADNc se realizó la reacción de PCR con distinto número de ciclos, comprobando que tanto el aumento de la cantidad de ARN como el aumento del número de ciclos reflejaba un aumento de la cantidad de ADN obtenido en la PCR. Se emplearon 25, 29, 32 y 35 ciclos y la temperatura de hibridación fue de 54º C. Se realizó la PCR a partir del mismo ADNc para cinco genes: SHP-1; SHP-2; PTP1B; LAMP-2 y β-actina (empleado como control de carga). Cada ciclo de la PCR consistió en un paso de desnaturalización (1 minuto a 95º C), un paso de hibridación y un paso de amplificación (1 minuto a 72º C).

Las secuencias de los oligos empleados fueron las siguientes:

- **SHP-1:**

  Oligo sentido: 5´-AGGCCGGCTTCTGGGAGGAGTT -3´

  Oligo antisentido: 5´-CCAGTGGGGAGATCTGCAATGTTC -3´

  Tamaño del amplicón: 400 pb.

- **SHP-2:**

  Oligo sentido: 5´-TGACCTCTATGGCGGGGAAAAGTT -3´

  Oligo antisentido: 5´-GCCACATAGCACAGCTTCTCCTTGA -3´

  Tamaño del amplicón: 486 pb.

- **PTP1B:**

  Oligo sentido: 5´-CTCACCCAGGGCCCTTTACCAA -3´

  Oligo antisentido: 5´-TGGATGAGCCCCATGCGGAACC -3´

  Tamaño del amplicón: 539 pb.

- **LAMP-2:**

  Oligo sentido: 5´-CCACCGCTATGGGCACAAGGAAGTT -3´

  Oligo antisentido: 5´-CAGCTGAACATCACCGAGGAGAAGG -3´

  Tamaño del amplicón: 427 pb.

- **β actina:**

  Oligo sentido: 5´-TCTGTGTGGATTGGTGGCTCTA -3´

  Oligo antisentido: 5´-CTGCTTGCTGATCCACATCTG -3´

8. ELECTROFORESIS EN GEL DE AGAROSA

Esta técnica consiste en separar los fragmentos de ADN en función de su tamaño. Para la preparación de los geles se realizó una disolución de agarosa al 1% en TAE (Tris-Acético-EDTA: Tris 40 mM, ácido acético glacial 20 mM y EDTA 2 mM) a la cual se añadieron 1-3 μl de bromuro de etidio (10 mg/ml) por cada 50 ml de gel, dejándose solidificar a temperatura ambiente. Las muestras se cargaron en los geles mezcladas con tampón de carga 10X. La electroforesis se realizó a 100 V (geles de 50 ml) usando el tampón TAE como tampón de electroforesis. Las imágenes de los geles se obtuvieron sobre un transiluminador de luz ultravioleta acoplado a una cámara "Kodak GL 100", y se procesaron mediante el programa “Kodak Digital Science" v 3.0.

9. DETERMINACIÓN DE LA CONCENTRACIÓN PROTEÍNAS

La concentración de proteínas de las diversas fracciones subcelulares se valoró por el método de *Bradford* (*1976*).

El patrón utilizado fue BSA a distintas concentraciones. Para realizar las mediciones de la absorbancia de las muestras se emplearon lectores de placa de ELISA: ELx800 de "BIO-TEK Instruments, Inc" o MultisKan FC de "Termo Scientific". Antes de las determinaciones se diluyeron tanto las muestras como el patrón con NaOH 0,5 N.

10. DETERMINACIONES ENZIMÁTICAS

10.1. Actividad mieloperoxidásica (MPO)

La mieloperoxidasa (MPO) es una enzima presente principalmente en los gránulos de los neutrófilos polimorfonucleares, que puede llegar a representar el 5% del peso de la célula y que se utiliza como marcador de la presencia de estas células en el tejido inflamado. La determinación enzimática se efectuó en páncreas de ratas que habían sido tratadas con ceruleína o suero salino. En primer lugar, los órganos conservados a -80º C se descongelaron para su posterior homogeneización. Tras obtener el homogenado, la actividad MPO se valoró empleando el kit comercial MPO Fluorometric Detection Kit (Assay Design, Stressgene, Enzo Life Sciences, Madrid, España) siguiendo exactamente las indicaciones del fabricante.

Los resultados se expresaron como veces de aumento de la actividad de la enzima con respecto a los valores obtenidos en muestras control.

10.2. Actividad amilásica sérica

La actividad amilásica sérica se valoró siguiendo el método descrito por *Lorentz*, en un analizador de Bioquímica Gernon Star, usando el kit comercial "Alfa Amilasa Liquicolor" (RAL, Técnica para el Laboratorio, S.A., Barcelona, España), en el Servicio de Bioquímica del Hospital Fundación Santísima Trinidad de Salamanca, con la colaboración del Dr. Jesús Hueso.

10.3. Actividad de la Catepsina B

Esta determinación se realizó con la colaboración del Dr. Pedro P Juanes, en nuestro laboratorio. La medición de la actividad de la Catepsina B se realizó según *Mc Donald y Ellis* (*1975*). Diez µl de la muestra problema se mezclaron

con 380 µl de tampón catepsina (EDTA 10 mM, DTT 10 mM, fosfato monosódico 50 mM, pH 6.5). Dicha mezcla se preincubó 5 minutos a 37º C, y después se añadió 10 µl del sustrato N-CBZ-Arg Arg-4-metoxi-β-naftilamida 20 mM en tampón catepsina. El tiempo máximo de incubación fue de 22 minutos. La reacción se paró con 2,6 ml de tampón carbonato/bicarbonato sódico 0,5 M, pH 10,7.

La longitud de onda de emisión fue 410 nm y la de excitación 338 nm. El estándar utilizado fue una solución de β-naftilamida (β-NPH) 3.5 µM en tampón carbonato/bicarbonato.

Se define la unidad de enzima como la cantidad de enzima necesaria para la transformación de 1nmol de sustrato por minuto.

10.4. Actividad de la succinato deshidrogenasa (SDH)

La actividad de la SDH fue valorada espectrofotométricamente siguiendo el método descrito por *Pennington* (1961). Una mezcla que contenía 50 µl de succinato sódico, 100 µl de INT, 50 µl de tampón fosfato sódico 0,5M pH 7,4, 50 µl de sacarosa 0,25 M, 200 µl de agua y 100 µl de muestra se incubó a 37 ºC durante 20 minutos. Al finalizar el tiempo de incubación, la reacción se paró con 500 µl de TCA al 10 % (p/v). A continuación, el desarrollo de color se llevó a cabo con la adición de 1,5 ml de acetato de etilo. La mezcla coloreada se centrifugó para poder leer la absorbancia del sobrenadante a 490 nm. La unidad de actividad enzimática se define como la cantidad de enzima necesaria para la liberación de 1 nmol de producto por hora.

10.5. Actividad N-acetil-β-D-glucosaminidásica (NAG)

Se valoró la actividad de la enzima NAG en las fracciones de lisosomas y en las bandas enriquecidas de lisosomas, siguiendo el método descrito por *Robinson et al.* (*1967*). En un baño termostatado a 37º C se mezclaron 50 µl de muestra y 100 µl de sustrato (4-metilumbeliferil-β-D glucosaminidósido 3 mM, en solución amortiguadora de ácido cítrico/citrato sódico 0.1 M, pH 4.0). Dicha mezcla se incubó durante 30 minutos para permitir que la enzima actúase sobre el sustrato 4-metilumberiferil derivado y se liberase metilumbeliferona (MU), altamente fluorescente. Transcurrido este tiempo, se paró la reacción con 2 ml de tampón glicina/NaOH 0.5M pH 10.4 y se midió la fluorescencia en un

espectrofluorímetro a 365 nm de excitación y 450 nm de emisión. La unidad de actividad enzimática (U) se define como la cantidad de enzima necesaria para la liberación de 1 nmol de metilumbeliferona por hora.

11. SOLUBILIZACIÓN DE LA ENZIMA NAG LIGADA A LA MEMBRANA LISOSÓMICA

Se trataron alícuotas de la fracción L+M del fraccionamiento subcelular con el detergente no iónico IGEPAL CA-630. Se estudió en primer lugar la concentración de detergente que producía la máxima solubilización de la enzima. Para ello, alícuotas de la fracción L+M se mantuvieron en contacto con el detergente a concentraciones desde 0.25% hasta 5% a 4º C, en agitación constante, durante 30 minutos. Después de cada uno de los tratamientos se valoró la actividad NAG en las muestras tratadas, así como en las muestras sin tratar. Una vez establecida la concentración óptima de detergente se analizó el efecto del tiempo sobre la solubilización de la enzima (5, 10, 30, 45, 60, 90 y 120 minutos).

12. CROMATOGRAFÍA DE INTERCAMBIO IÓNICO EN DEAE-CELULOSA

Las fracciones L+M y soluble obtenidas de los distintos fraccionamientos subcelulares de páncreas, así como las población de lisosomas ligeros recogidas del gradiente discontinuo de Percoll, fueron sometidas a cromatografía en DEAE celulosa para la separación de las formas isoenzimáticas de la enzima NAG. Las muestras se dializaron en solución amortiguadora de fosfato (monosódico/bisódico) 10mM pH 7.0, durante, al menos, 24 horas a 4º C y en agitación constante. Las columnas empleadas contenían 2 ml del intercambiador aniónico DEAE-celulosa. Previamente a su utilización, la resina empacada se equilibró con solución amortiguadora de fosfatos. A continuación se pasaron alícuotas de las muestras dializadas, que contenían 4,5 mg de proteínas, en el caso de las fracciones L+M y soluble, ó 2,5 mg en el caso de las población lisosómica libres de mitocondrias. Las enzimas retenidas por el intercambiador se eluyeron con un gradiente salino de

ClK (0-0.3 M) en el mismo tampón y las no retenidas fueron eluidas con tampón de cromatografía. La concentración de proteínas y la actividad enzimática se valoró en cada una de las fracciones recogidas. La actividad enzimática de la NAG presente en cada pico, se expresa como porcentaje relativo a la actividad recuperada en el total de picos.

13. ANÁLISIS DE LA EXPRESIÓN DE PROTEÍNAS MEDIANTE TRANSFERENCIA DE WESTERN

El análisis de proteínas tirosina fosfatasas (PTPs) y de la proteína lisosómica Lamp-2, se realizó en las distintas situaciones experimentales mediante transferencia de Western. Para ello, se utilizaron diversos anticuerpos primarios que se detallan a continuación:

- Anticuerpo monoclonal contra SHP-1 obtenido en ratón y con reactividad hacia la zona C terminal.
- Anticuerpo monoclonal contra SHP-2 obtenido en ratón y con reactividad hacia la zona N-terminal.
- Anticuerpo policlonal contra PTP1B obtenido en cabra y con reactividad hacia la zona N-terminal.
- Anticuerpo policlonal contra Lamp-2 obtenido en conejo y con reactividad hacia la zona C-terminal.

Como control de carga se utilizó el anticuerpo monoclonal anti- β-tubulina (Ref. SAP.4G5 de Sigma), con reactividad hacia la zona C-terminal.

13.1. Electroforesis en geles de poliacrilamida en presencia de SDS (SDS- PAGE)

Los extractos proteicos procedentes de las diferentes muestras se sometieron a electroforesis desnaturalizante en condiciones reductoras, siguiendo el método de *Laemmli* (1970). Las muestras se incubaron a 100º C durante 5 minutos en tampón de carga (Tris-HCl 125 mM, que contenía SDS al 2% (p/v), glicerol al 5% (v/v), azul de bromofenol 0,03% (p/v) y β-mercaptoetanol

al 1% (v/v) pH 6,8). Con el propósito de eliminar diversos contaminantes como sales, lípidos, acídos nucleícos y detergentes, algunas muestras fueron tratadas previamente con “2D Clean-Up kit” siguiendo las instrucciones del fabricante, obteniéndose un precipitado de proteínas que se resuspendió en tampón de rehidratación constituído por: Urea 7M, tiourea 2M y DTT 50 mM. Las electroforesis se efectuaron en una disolución amortiguadora (tampón de electroforesis), aplicándose un voltaje constante de 125 V a temperatura ambiente.

13.2. Transferencia de las proteínas a la membrana de difluoruro de polivinilideno (PVDF)

Tras la electroforesis se transfirieron las proteínas a una membrana de PVDF como se ha descrito previamente *Hernandez-Hernandez et al.*, (*1999*).Para ello se empleó un sistema de transferencia húmeda utilizando una disolución amortiguadora (tampón de transferencia) de Tris-HCl 25 mM, con glicina 190 mM y metanol al 20% (v/v), pH 8,1-8,4. La transferencia se efectuó aplicando un amperaje constante de 400 mA durante 4 horas a 4° C.

13.3. Incubación de la membrana con los anticuerpos

Una vez realizada la transferencia se bloqueó la membrana mediante inmersión de ésta en una disolución de bloqueo que contenía leche desnatada al 5% (p/v) en TBS (Tris-HCl 10 mM, ClNa 100 mM y Tween 20 al 0,05% (v/v), pH 7,5), durante 1 hora a temperatura ambiente con agitación constante. A continuación, se incubó la membrana con el anticuerpo primario convenientemente diluido durante toda la noche a 4º C y con agitación constante. Los anticuerpos fueron diluidos en la disolución de bloqueo en las siguientes proporciones (v/v): anti-SHP-1 (1/150), anti-SHP-2 (1/2500), anti-PTP1B (1/1.000), anti-Lamp-2 (1/1.000) y anti β-tubulina (1/1.000). Después de la incubación con el anticuerpo primario, la membrana se lavó con TBS (tres veces, durante 10 minutos cada vez) y se incubó con el correspondiente anticuerpo secundario conjugado con peroxidasa de rábano, diluido en la disolución de bloqueo: para SHP-1 y SHP-2 (anti-ratón 1:10.000), PTP1B (anti-cabra 1:5.000), Lamp-2 (anti conejo 1:15.000) y para

β-tubulina (anti-ratón 1:10.000), durante 1 hora a temperatura ambiente y con agitación constante.

13.4. Detección

Tras la incubación de la membrana con los anticuerpos, ésta se lavó de nuevo con TBS (tres veces, durante 10 minutos cada vez) y se sometió al revelado por el sistema de sustrato luminiscente para la peroxidasa de rábano mediante el kit comercial "ECL plus Western Blotting Detection System" de GE Healthcare, siguiendo las instrucciones de la casa comercial. Cuando la señal del anticuerpo primario era muy fuerte se empleó un sistema de revelado basado en el empleo de la solución de revelado AB [Solución A (Luminol 1mM, ácido cumárico 0,4 mM y Tris-HCl 100 mM pH 8,5) y solución B (H_2O_2 0,02% y Tris-HCl 100 mM, pH 8,5)]. Las membranas se incubaron durante dos minutos con esta solución de revelado AB. El tiempo de exposición de las películas a las membranas varió en función de la muestra. Tras la exposición, la película se reveló en una máquina de revelado para Western "Medical X-ray Processor" de Kodak.

Las películas reveladas se digitalizaron con un Escáner Hewlett-Packard, modelo Scanjet 3C y el posterior análisis de la imagen se hizo utilizando el programa Adobe Photoshop Macintosh versión 2.5.1. Las cuantificaciones de las bandas proteicas se llevaron a cabo en cada uno de los carriles, los cuales contenían la misma cantidad de proteínas de la correspondiente muestra.

14. DETERMINACIÓN DE PROTEÍNAS OXIDADAS (OXYBLOT) POR TRANSFERENCIA DE WESTERN

Los perfiles de las proteínas oxidadas con grupos carbonilo se obtuvieron por inmunodetección con el kit "Oxyblot, Protein Oxydation Detection Kit" (Intergen Parchase, NY USA), de acuerdo a las indicaciones del fabricante, tal y como describió previamente nuestro grupo de investigación *Hernández-Hernández, et al*., (2005).

Quince mg de proteínas de cada muestra se incubaron con 2,4-dinitrofenilhidrazina (DNPH) a temperatura ambiente durante 15 minutos, con lo que los grupos carbonilos de las cadenas laterales de las proteínas generan 2,4-dinitrofenilhidrazona. Tras neutralización, las muestras se redujeron con 2-mercaptoetanol y se sometieron a electroforesis desnaturalizante en un gel SDS-PAGE al 6% en condiciones reductoras. Los geles se transfirieron a membranas de PVDF, y las proteínas oxidadas se revelaron con un anticuerpo primario anti DN, visualizándose mediante el sistema quimioluminiscente ECL plus.

15. VALORACIÓN HISTOLÓGICA DEL PÁNCREAS

Las muestras fueron procesadas siguiendo la metodología estándar para ser observadas por microscopía óptica. Los páncreas analizados provenían de animales sacrificados a las 2, 4 y 9 horas de haber recibido la primera dosis de ceruleína o de suero salino. Inmediatamente después del sacrificio, pequeños trozos de páncreas se fijaron en una solución tamponada de paraformaldehído al 4% durante 48 horas a 4° C. Posteriormente, se deshidrataron en concentraciones ascendentes de etanol (50-100%), se lavaron con xileno y se incluyeron en parafina. Se montaron secciones de 10 μm de grosor en portas recubiertos de gelatina, que se desparafinaron, hidrataron y tiñeron con hematoxilina-eosina para su observación. Estas técnicas se llevaron a cabo con la colaboración del Dr. Arturo Mangas, en el Departamento de Biología Celular y Patología de nuestra Universidad, y el análisis histológico lo realizó el Dr. Rafael Coveñas, valorando la presencia de edema, inflamación, infiltración por neutrófilos y la posible necrosis de todas las muestras procesadas.

16. PERFUSIÓN Y OBTENCIÓN DE LAS SECCIONES DE TEJIDO PARA VALORACIÓN INMUNOCITOQUÍMICA

Cuando el objetivo experimental era la realización de técnicas inmunocitoquímicas en cortes de páncreas, los animales incluidos en los diferentes grupos experimentales (control y pancreatíticos) fueron anestesiados

con hidrato de cloral (0,3 gr/kg vía intraperitoneal), heparinizados y perfundidos a través de la aorta con 50 ml de solución salina (9 g/l de NaCl) y, a continuación, con 200 ml de paraformaldehido al 4 % en tampón Sörensen (pH 7,4) (solución fijadora).

Una vez finalizada la perfusión, se practicó una laparotomía ventral media a todos los animales, se extrajeron los páncreas, se etiquetaron y posteriormente se realizó la post-fijación durante 12 horas en la misma solución fijadora (paraformaldehido al 4 %). A continuación, el material se introdujo en una solución creciente de sacarosa comenzando al 5 % (lavado del excedente de fijador) hasta llegar al 30 % de sacarosa en tampón Sörensen. Como la sacarosa se introduce en el tejido cambiando la densidad del mismo, los baños se cambiaron tras el hundimiento del páncreas (5 %, 10 %, 15 %, 20 % 25 % y 30 %). Después de mantener el tejido durante un periodo de 3-4 días en la concentración superior (30 %) se consideró finalizada la crioprotección. Todo el proceso fue realizado a 4° C. Utilizando un criostato, se obtuvieron secciones seriadas de 10-12 µm. A las secciones obtenidas se les aplicó una técnica inmunocitoquímica indirecta.

16.1. Técnica Inmunocitoquímica

La inmunotinción se realizó mediante la técnica estreptavidina-peroxidasa, previamente descrita por *Mangas et al.,* (*2006*). Dos horas antes de la realización de la técnica, los portaobjetos que contenían las secciones seriadas se sacaron del congelador y se lavaron en PBS durante unos diez minutos con el fin de que las muestras de tejido no se despegasen de los portaobjetos. Posteriormente los pasos que se siguieron fueron:

1- Las secciones se trataron con una solución compuesta de 1/3 de peróxido de hidrógeno al 30% y 2/3 de metanol al 99,5% durante un periodo de treinta minutos en recipientes tapados (oscuridad). Este paso se realizó para inactivar las peroxidasas endógenas. A continuación, se lavaron las secciones en PBS durante diez minutos. Los lavados se repitieron tres veces.

2- El material se incubó en tampón PBS con 1% de suero normal de caballo y 0,3% de Triton X-100 (mezcla) durante veinte minutos en agitación y a temperatura ambiente. Este paso se realizó para facilitar la penetración de los anticuerpos.

3- Posteriormente se incubó durante una noche con el primer anticuerpo anti-PTP1B (Abcam) diluido 1/20-1/100 en la mezcla del paso 2. La primera parte de la incubación se efectuó con agitación, durante dos horas y la segunda parte en reposo, a 4 °C durante 15-18 h.

4- Las secciones se lavaron en PBS durante treinta minutos a temperatura ambiente y en agitación.

5- Se incubó durante una hora (agitación), a temperatura ambiente, con un anticuerpo biotinilado anti-inmunoglobulina G de conejo diluido 1/200 en la mezcla del paso 2.

6- Se realizó un lavado con PBS durante 30 minutos a temperatura ambiente y en agitación.

7- Las secciones se incubaron una hora con el complejo avidita-biotina peroxidasa (ABC) (Vectastain), diluido 1/100 a temperatura ambiente.

8- Se realizó un lavado, durante diez minutos (reposo) a temperatura ambiente en tampón Tris-ClH (pH 7,6).

9- Se llevó a cabo el revelado de la peroxidasa con 3, 3'-diaminobenzidina disuelta en 75 ml de Tris-ClH y 37,5 µl de peróxido de hidrógeno durante aproximadamente 5 minutos.

10- Las secciones fueron lavadas con PBS y montadas en portas y cubiertas con una mezcla de PBS/Glicerol (1/1).

Para garantizar la especificidad del anticuerpo primario, se incubaron varias secciones en ausencia de este anticuerpo o en presencia de un anticuerpo (inmunoglobulina Ig G) de conejo no inmunizado.

17. MICROSCOPÍA ELECTRÓNICA DE TRANSMISIÓN

Se realizó un estudio por microscopía electrónica correspondiente a las distintas poblaciones lisosómicas separadas en el gradiente de Percoll. Los pasos que se siguieron se resumen en los siguientes:

1- Alícuotas concentradas de las fracciones enriquecidas en lisosomas (bandas I, II y III del gradiente), se lavaron en tampón fosfato sódico 0,1 M pH 7,4, al que se le añade sacarosa al 6,8 % (p/v) y cloruro cálcico al 1 % (p/v) (Tampón A). Se centrifugaron dichas alícuotas durante 2 minutos a 10.000 $\times$ *g*.

2- Después de eliminar el sobrenadante, los precipitados se fijaron 3 h con glutaraldehido al 5 % (p/v) en tampón A.

3- Tras centrifugar, se eliminó el líquido sobrenadante y los orgánulos se recuperaron del fondo del tubo.

4- A continuación, la muestra se recubrió con agar (DIFCO) al 1,5% previamente fundido, que se enfrió posteriormente hasta 45-50 ºC y se centrifugó hasta su solidificación.

5- Tras solidificar el agar, se cortaron secciones que contenían orgánulos en trozos pequeños y se introdujeron posteriormente en tubos que contenían glutaraldehído al 3% (p/v), durante 30 min.

6- Transcurrido el tiempo de fijación, el glutaraldehído se eliminó con tampón A, mediante tres lavados sucesivos de 30 min cada uno.

7- La muestra se sometió a un tratamiento de post-fijación con tetróxido de osmio (OsO_4) al 1 % (p/v) en tampón A, durante 2 horas en oscuridad.

8- El OsO_4 se eliminó mediante tres lavados sucesivos, de 10 min cada uno, con tampón de lavado y posteriormente se realizaron cuatro lavados con agua destilada, 10 min cada vez.

9- Una vez fijadas y lavadas, las muestras se deshidrataron mediante inmersión en series de acetona de concentración creciente, desde 10% hasta acetona anhidra, durante 15 min en cada concentración de acetona.

10- Se procedió a la inclusión de los bloques en resina Durcupan (Fluka): La inclusión de las muestras se realizó, manteniéndolas durante 1 hora en series de concentración creciente de resina, empezando por la resina al 25% (p/v) en acetona anhidra y finalizando con la resina al 100% durante toda la noche. Para conseguir la dureza que requieren los cortes, las muestras se mantuvieron en una estufa a 70° C durante 8 horas.

11- Las secciones se cortaron con un ultramicrotomo y se tiñeron con acetato de uranilo al 2% y con citrato de plomo al 2%.

Las observaciones se realizaron en un microscopio electrónico de transmisión modelo EM900, de la casa comercial Zeiss.

El tamaño de los orgánulos de la primera y segunda bandas de lisosomas se determinó en 25-30 campos microscópicos escogidos al azar. El tamaño de los orgánulos de la tercera banda se determinó en 8 campos microscópicos también escogidos al azar. Se analizaron aproximadamente un total de 700 orgánulos. El aumento empleado para el análisis de imagen fue de 50.000 x. Los resultados se expresaron como porcentaje relativo al número total de orgánulos de cada banda, considerado como el 100%.

18. TRATAMIENTO CON LECTINAS

Diferentes alícuotas de la fracción de microsomas y de la fracción soluble, se trataron con el detergente no iónico NP40 al 0,5-1% (p/v), durante 60 minutos a 4ºC en agitación constante con objeto de solubilizar, en su caso, las proteínas asociadas a membranas. Las diferentes muestras de proteínas solubilizadas se adicionaron a tubos Ependorf que contenían 200 µl de lectinas (Aglutinina de germen de trigo (WGA) ó Concanavalina A (Con A)) inmobilizadas, resuspendidas en tampón imidazol 3mM, y NP40 al 0,5%. Las mezclas se mantuvieron en rotación durante 4 horas a 4° C, y, después, se centrifugaron a velocidad máxima durante 10 minutos en una centrífuga de mesa refrigerada. Estas condiciones se escogieron por conveniencia, y no representan las condiciones óptimas de unión de las lectinas. Después de centrifugar, se recogieron los sobrenadantes, donde quedaban las proteínas no unidas a lectinas (sobrenadante 1). Posteriormente, los geles se lavaron dos veces con tampón imidazol 3 mM, y se centrifugaron nuevamente. Las proteínas se eluyeron de las lectinas con 0.5 M *N*-acetil-glucosamina en el caso de (WGA) o 1M metil α-manopiranosido en el caso de (Con A) durante toda la noche a 4 ºC y con rotación constante. Los sobrenadantes de las centrifugaciones de estas mezclas contenían las proteínas unidadas a lectinas (sobrenadante 2).

19. TRATAMIENTO CON GLICOSIDASAS

Para los estudios relacionados con el contenido en glúcidos de LAMP-2, las diferentes muestras se incubaron en presencia de 2 µl/ml de cóctel de inhibidores de proteasas a 37 ºC y con agitación suave con: (i) sin ningún tipo de adiciones durante diferentes periodos de tiempo, (ii) con 100 mU/ml de neuraminidasa durante un máximo de 24 horas, (iii) con 10 U/ml de péptido *N*-glicosidasa-F (PGNase-F) durante 8 ó 24 horas, o (iv) con 100 mU/ml de endoglicosidasa-H (Endo-H) durante 24 horas.

Tratamiento con neuraminidasa: las muestras se dializaron previamente frente a un tampón acetato sódico 50 mM, pH 5,5 ó 6, que contenía 134 mM NaCl y 9 mM $CaCl_2$, después de lo cual se adicionó 2,5% NP-40 (concentración final) antes de la incubación con la glicosidasa. Se recogieron alícuotas a los distintos tiempos de incubación, las cuales fueron usadas en las transferencias de Western.

Tratamiento con PGNase-F: se añadió 1% NP-40 (concentración final) y las muestras se mantuvieron en hielo durante 1 hora con agitación ocasional. Después, se añadieron 0.1% SDS y 10mM β-mercaptoetanol (concentración final, disuelto in 3 mM tampón imidazol, pH 7.4), y las muestras se hirvieron durante 10 minutos. Después de 5 minutos en hielo, se añadió PGNase-F y las muestras se incubaron a 37° C durante diversos periodos de tiempo.

Tratamiento con Endo-H: se realizó como lo indicado para el tratamiento con PGNase-F, pero el pH de las muestras se ajustó en primer lugar a 5.5-6, y el SDS y el β-mercaptoetanol se disolvieron en tampón imidazol 3 mM, pH 5.5.

IV. Resultados

Preámbulo:

A continuación presentamos los resultados en relación a los objetivos planteados, en la forma de las publicaciones a que han dado lugar y añadiendo otro resultado no incluído en uno de los artículos publicados.

Aunque cada artículo contiene su propia discusión, hemos incluído una discusión final conjunta con el propósito de dar una idea global del significado de nuestro estudio.

- **OBJETIVO 1:** Estudiar los cambios de expresión y dinámica de las PTPs con dominios SH2: SHP-1 y SHP-2, en la PA inducida por ceruleína.

Available online at www.sciencedirect.com
ScienceDirect
Biochimica et Biophysica Acta 1782 (2008) 271–279
Biochimica et Biophysica Acta BBA
www.elsevier.com/locate/bbadis

Changes in the expression and dynamics of SHP-1 and SHP-2 during cerulein-induced acute pancreatitis in rats

Nancy Sarmiento [a], Carmen Sánchez-Bernal [a], Manuel Ayra [a], Nieves Pérez [a], Angel Hernández-Hernández [a], José J. Calvo [b], Jesús Sánchez-Yagüe [a,*]

[a] *Department of Biochemistry and Molecular Biology, University of Salamanca, Spain*
[b] *Department of Physiology and Pharmacology, University of Salamanca, Spain*

Received 11 October 2007; received in revised form 23 January 2008; accepted 23 January 2008
Available online 9 February 2008

Abstract

Protein tyrosine phosphatases (PTPs) are important regulators of cell functions but data on different PTP expression and dynamics in acute pancreatitis (AP) are very scarce. Additionally, both *c-Jun* N-terminal kinases (JNK) and extracellular signal-regulated kinases (ERK1/2), together with intracellular cAMP levels in inflammatory cells, play an essential role in AP. In this study we have detected an increase in PTP SHP-1 and SHP-2 in the pancreas at the level of both protein and mRNA as an early event during the development of Cerulein (Cer)-induced AP in rats. Nevertheless, while SHP-2 protein returned to baseline levels in the intermediate or later phases of AP, SHP-1 protein expression remained increased throughout the development of the disease. The increase in SHP-2 protein expression was associated with changes in its subcellular distribution, with higher percentages located in the fractions enriched in lysosomes+mitochondria or microsomes. Furthermore, while the increase in SHP-2 protein was also observed in sodium-taurocholate duct infusion or bile-pancreatic duct obstruction AP, that of SHP-1 was specific to the Cer-induced model. Neutrophil infiltration did not affect the increase in SHP-1 protein, but favoured the return of SHP-2 protein to control levels, as indicated when rats were rendered neutropenic by the administration of vinblastine sulfate. Inhibition of JNK and ERK1/2 with SP600125 pre-treatment further increased the expression of both SHP-1 and SHP-2 proteins in the early phase of Cer-induced AP, while the inhibition of type IV phosphodiesterase with rolipram only suppressed the increase in SHP-2 protein expression during the same phase. Our results show that AP is associated with increases in the expression of SHP-1 and SHP-2 and changes in the dynamics of SHP-2 subcellular distribution in the early phase of Cer-induced AP. Finally, both JNK and ERK1/2 and intracellular cAMP levels are able to modulate the expression of these PTPs.

Keywords: SHP-1; SHP-2; Acute pancreatitis; Cerulein; SP600125; Rolipram

1. Introduction

In the pathogenesis of acute pancreatitis (AP) many factors, including activated pancreatic enzymes, cytokines, chemokines, free radicals, blood flow, and neurogenic factors, have been reported. Nevertheless, the pathophysiology of the disease remains incompletely understood, especially the early acinar events. It has been suggested that it would be important to detect rapid early events and signalling mechanisms in AP because these events would probably be translated into long-term responses that would determine the development of pancreatitis [1].

One of the animal models of AP is that induced by supramaximal secretagogue stimulation. Usually, the trophic agent cerulein [Cer, an analogue of cholecystokinin (CCK)] is used in this model. Different doses of Cer (ranging from 5 to even 100 μg/Kg) have been used to induce AP in rats. Under the conditions used here [20 μg/Kg subcutaneous (s.c.) injection] the manifestations of pancreatitis include hyperamylasemia, interstitial edema, increase pancreatic cell size, increased pancreatic weight, histological damages, including increased vacuolization

* Corresponding author. Departamento de Bioquímica y Biología Molecular, Edificio Departamental. Lab. 106, Plaza Doctores de la Reina s/n, 37007 Salamanca, Spain.
E-mail address: sanyaj@usal.es (J. Sánchez-Yagüe).

0925-4439/$ - see front matter © 2008 Elsevier B.V. All rights reserved.
doi:10.1016/j.bbadis.2008.01.005

and other morphological derangements, and neutrophil infiltration [2–5]. With current ongoing research, the intracellular mechanisms by which CCK or Cer regulate pancreatic acinar function appear to be increasingly complex. Through Gq proteins, CCK and Cer lead to an increase in cytosolic free Ca^{2+}. Ca^{2+}, diacylglycerol and cAMP activate exocytosis processes. Moreover, it is known that both CCK and Cer activate pancreatic protein tyrosine kinases (PTK) [6,7] and that tyrosine phosphorylation plays important roles in the regulation of many cell functions. Cer-induced AP also activates the mitogen-activated protein kinase (MAPKs) cascade, especially extracellular signal-regulated kinase (ERK1/2) and *c-Jun* N-terminal kinase (JNK), whose activation requires the phosphorylation of both tyrosine and threonine residues [8,9]. p38MAPK is also activated by CCK and Cer. Other signalling pathways are also activated in AP, e.g. the adenosine A1-receptor pathway [10], which decreases intracellular cAMP levels. In this regard, it is known that type IV phosphodiesterase inhibitors ameliorate Cer-induced AP [11]. It is also clear that pancreatitis requires the dissociation of cell–cell contacts [12] and adherens junctions [13], and that tyrosine phosphorylation is important for the maintenance of an intact cell adhesion complex [14].

The discovery of the role of PTK in the regulation of the levels of tyrosine phosphorylation has led phosphotyrosine phosphatases (PTP) to become better appreciated as important regulators of cell functions. The structurally very similar SH2-domain containing PTPs SHP-1 and SHP-2 have been proposed to have different roles in signal transduction: SHP-1 is expressed highly in hematopoietic cells and at a moderate level in many other types of cells and plays a largely negative signalling role in hematopoietic cells. SHP-2 is more widely expressed and plays a largely positive role in the cell signalling leading to cell activation. Nevertheless, it seems that the functional nature of SHP-1 and SHP-2 depends on the systems involved. SHP-1 has been implicated in the Jak-Stat and MAPK pathways [15]. SHP-2 has compound signalling functions and it appears to be involved in a variety of signal transduction processes, such as the Ras-Raf-MAPK, Jak-Stat, PI3 kinase and NF-κB pathways [16]. Even within a single signalling pathway, SHP-2 may act at multiple sites to participate in signal transduction. All the above SHP-1 and SHP-2 signalling pathways have been implicated in the development of AP.

Data on PTP in AP are very scarce although it is well documented that these signalling enzymes are inactivated by reactive oxygen species (ROS) [17] or secondary products of oxidation [18,19] that may form during AP development [20,21]. Essentially, only one function of SHP-1 and PTPκ in the regulation of cell adhesion in the pancreas after mild experimental Cer-induced pancreatitis in rats has been described [12]. No data are available about changes in the expression of SH_2-domain PTPs either at the level of RNA or protein, and neither is the dynamics of their subcellular location along the development of pancreatitis known. Considering the importance of determining molecules or genes whose expression changes in the early phase of AP development, together with the signalling mechanisms that may modulate such expression, here we studied the expression and dynamics of the subcellular location of SHP-1 and SHP-2 in the development of Cer-induced AP, as well as the effect of SP600125 (anthrax[1,9cd]pyrazol-6(2H)-one 1,9 pyrazoloanthrone), a new JNK and ERK 1/2 inhibitor, and rolipram, a type IV phosphodiesterase inhibitor, on SHP-1 and SHP-2 expression levels in the early phase of AP development.

2. Materials and methods

2.1. Reagents

Bovine serum albumin (BSA), Cer, dithiothreitol (DTT), Percoll, phenylmethylsulfonyl fluoride (PMSF), Protein Inhibitor Cocktail, rolipram, sodium-taurocholate, soybean trypsin inhibitor, SP600125, Trizol Reagent, vinblastine sulfate were purchased from Sigma Chemical Co. (St. Louis, MO, USA). Polyvinylidene difluoride (PVDF) membranes were obtained from Amersham Biosciences, Spain. Monoclonal antibody anti-PTP-1 (D-11) was obtained from Santa Cruz Biotechnology, Inc, CA, USA. Monoclonal antibody anti-PTP-2 was obtained from BD Biosciences Pharmingen, San Diego, CA, USA. Reverse Transcriptase (RevertAid M-MULV), Taq polymerase, dNTP's and the Ribolock Ribonuclease inhibitor used in the reverse transcriptase-polymerase chain reaction (RT-PCR) were purchased from Fermentas Life Sciences, Germany. Oligonucleotides were obtained from Isogen life Sciences, The Netherlands. Isopropanol was purchased from Panreac, Spain. The Myeloperoxidase (MPO) Fluorimetric Detection Kit was purchased from Assay Desigs, Inc, USA.

2.2. Animals

Male Wistar rats weighing 250–280 g were used. The animals were given a standard rat chow diet and were fasted overnight before experiments with free access to water. Care was provided in accordance with the procedures outlined in European Community guidelines on ethical animal research (86/609/EEC), and protocols were approved by the Animal Care Committee of the University of Salamanca.

2.3. Induction of AP and preparation of samples

Rats received 4 s.c. injections of 20 μg Cer/kg body weight or its vehicle (0.9% NaCl) at hourly intervals. At 2, 4 or 9 h after the first injection, the animals were killed by cervical dislocation. The pancreases were rapidly harvested and immediately used for experiments. Serum samples were stored at −80°C until amylase determination. In some cases, AP was also induced by sodium-taurocholate duct infusion or bile-pancreatic duct obstruction (BPDO) [22,23, respectively]. Pancreases were dissected out from the surrounding fat tissue and then homogeneized with a Potter Elvehjem device in 10 volumes (v/w) of homogenization buffer (3 mM imidazole buffer, pH 7.4 containing 0.25 M sucrose, 1 mM EDTA, 1 mM PMSF, 100 μg/ml trypsin inhibitor and 2 μl/ml Protease Inhibitor Cocktail). The subcellular fractionation was done in a postnuclear homogenate from 4 pancreases as described before [21]. Four subcellular fractions were obtained: the zymogen (Z), lysosomes plus mitochondria (L+M), microsomes (Mic) and soluble (S) fractions.

Serum amylase was measured in the Roche Modular Analyzer by the method of Lorentz [24]. In brief, the oligosaccharide 4,6-ethylidene-(G7) *p*-nitrophenyl-(G1)-α, D-maltoheptaoside (ethylidene-G_7PNP) was cleaved under the catalytic action of α-amylases. The G2PNP, G3PNP γG4PNP fragments so formed were then completely hydrolysed to *p*-nitrophenol and glucose by α-glucosidase. The color intensity of the *p*-nitrophenol formed is directly proportional to the α-amylase activity and was measured photometrically. Protein concentrations were assayed by the method of Bradford [25], using BSA as standard.

2.4. Induction of neutropenia

Vinblastine sulfate was dissolved in 10 mM sodium phosphate buffer, 147 mM NaCl, 2.7 mM KCl (pH 7.4) and administered to rats intravenously (i.v.) at a dose of 0.75 mg/kg on day 1, as previously described [26]. At this dose, animals become neutropenic between days 4 and 6 [26]. On day 5 following

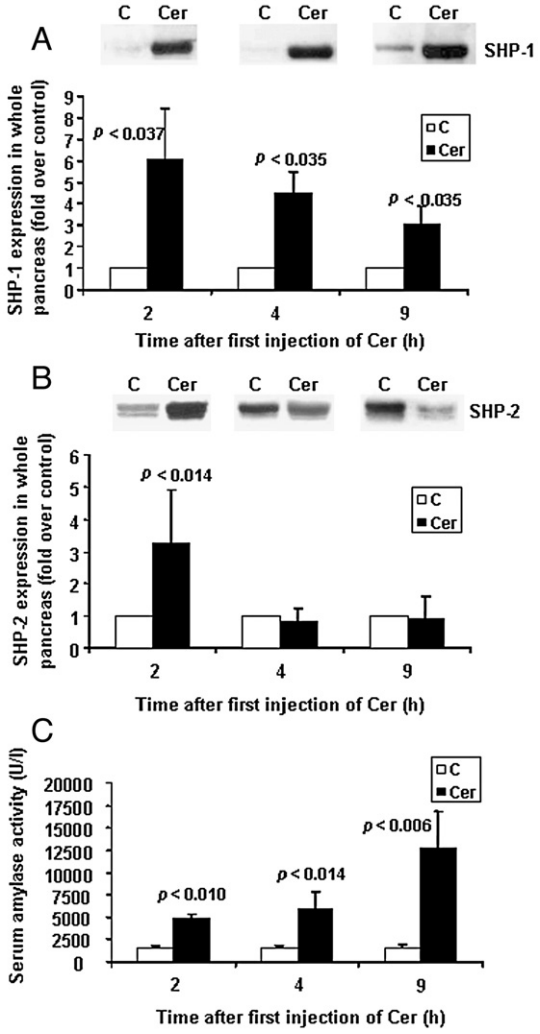

Fig. 1. Expression of SHP-1 (A) and SHP-2 (B) proteins and serum amylase activity (C) during the development of Cer-induced AP. Rats were either administered saline (0.9% NaCl) (control, C) or treated with Cer, as indicated in Materials and methods, and then killed 2, 4 or 9 h after the first injection of Cer. In (A) and (B), quantification (graphic) of expression (Western blots in whole postnuclear pancreatic homogenates — a representative for each time is shown) was carried out considering the whole pancreas. Each lane in the blots contained 30 μg of proteins. Data are means±S.D. of 5 animals.

vinblastine sulfate or saline administration, the animals were treated with 2 doses of Cer (20 μg Cer/kg, administered at hourly intervals) to induce AP.

2.5. Inhibition of JNK- and ERK1/2 by SP600125 in Cer-induced AP

Rats received intraperitoneal (i.p.) injections of SP600125 (15 mg/kg) or its vehicle (1 ml/kg of a 10% DMSO/NaCl solution) both 2 h before and 30 min after the first Cer injection [9]. Two hours after the first injection of SP600125, the rats were injected subcutaneously with Cer (20 μg Cer/kg) or its vehicle (0.9% NaCl) at hourly intervals. The animals were sacrificed 2 h after the first Cer injection (early phase of Cer-induced AP).

2.6. Inhibition of type IV phosphodiesterase by rolipram in Cer-induced AP

Rats received i.p. injections of rolipram (5 mg/kg) or its vehicle (1 ml/kg of a 10% DMSO/NaCl solution) both 30 min before and 30 min after the first Cer injection [27]. Thirty minutes after the first injection of rolipram, the rats were injected subcutaneously with Cer (20 μg Cer/kg) or its vehicle (0.9% NaCl) at hourly intervals. The animals were sacrificed 2 h after the first Cer injection (early phase of Cer-induced AP).

2.7. RNA preparation and RT-PCR

Total RNA was isolated from the pancreas and brain of the same rat by immediate solubilization in Trizol Reagent and isopropanol purification. RNA concentrations were determined by absorbance, and RNA integrity was checked by agarose electrophoresis. Reverse transcription was completed by incubating 2 μg of total RNA with 0.5 μg of a 18-mer oligo(dT) primer at 42 °C for 1 h, using 200 U of RevertAid M-MuLV Reverse Transcriptase in a solution containing 50 mM Tris–HCl, pH 8.3, 50 mM KCl, 4 mM $MgCl_2$, 10 mM DTT, 1 mM individual dNTPs and 20 U of Ribolock Ribonuclease inhibitor in a final volume of 20 μl. The reaction was stopped by heating at 70 °C for 10 min. Four microliters of this reaction was then used as a template for the polymerase chain reaction, which was performed with 1 U of Taq polymerase in a final volume of 40 μl with specific oligos at a 0.4 μM final concentration. The annealing temperature was 54 °C. Five microliters samples were taken at 25, 29, 32 and 35 cycles to ensure that we were working within the semi-quantitative range. The oligonucleotide sequences were as follows: SHP-1: forward oligo: AGGCCGGCTTCTGGGAGGAGTT; reverse oligo: CCAGTGGGGA-GATCTGCAATGTTC. SHP-2: forward oligo: TGACCTCTATGGCGGG-GAAAAGTT; reverse oligo: TCAGCGGCATTAATACGAGTTGTG. Product lengths were 400 and 486 pb for SHP-1 and SHP-2, respectively.

2.8. Myeloperoxidase (MPO) assay

Excised pancreatic tissue samples were rinsed with saline, blotted dry, snap-frozen in liquid nitrogen, and stored at −80 °C. MPO activity was detected by using the MPO Fluorimetric Detection Kit following the manufacturer's instructions.

2.9. Sodium dodecyl sulphate-polyacrylamide gel electrophoresis (SDS-PAGE) and Western blotting

SHP-1 and SHP-2 were analysed by SDS-PAGE using 10% gels [28]. The proteins present in the gels were transferred to PVDF membranes. After blocking non-specific binding with 5% non-fat dry milk (dissolved in buffer 10 mM Tris–HCl, 100 mM NaCl, 0.1% Tween 20, pH 7.5), Western blots were probed with anti-SHP-1 or anti-SHP-2 monoclonal antibodies diluted 1:150 and 1:2500, respectively, in the blocking solution. Blots were visualized by chemiluminescence. To analyse the spots on all the blots, film images were scanned using the

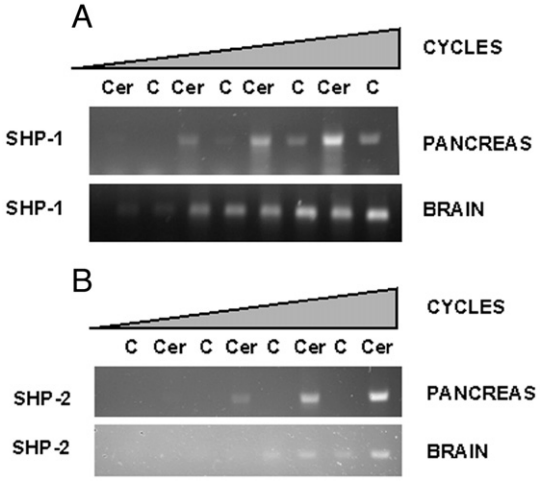

Fig. 2. SHP-1 (A) and SHP-2 (B) mRNA expression in the early phase of Cer-induced AP. Rats were either administered saline (0.9% NaCl) (control, C) or treated with Cer (P), as indicated in Materials and methods, and then killed 2 h after the first injection of Cer. mRNA expression was analysed in pancreas or brain by RT-PCR. A representative RT-PCR is shown.

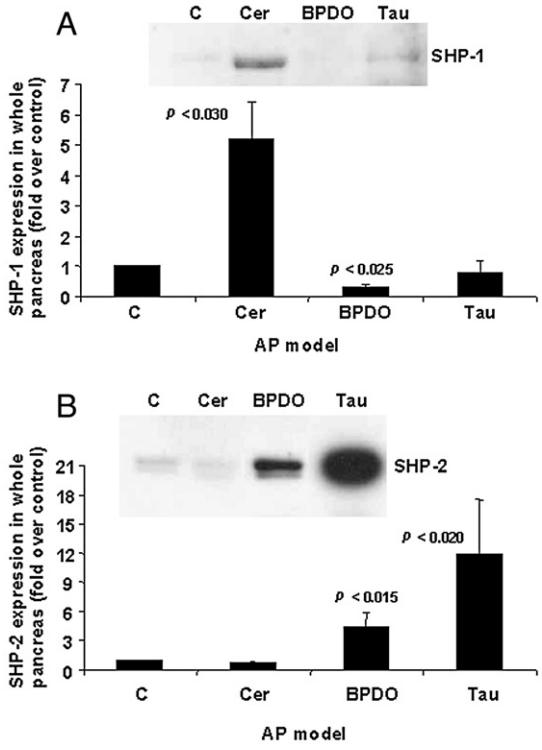

Fig. 3. Expression of SHP-1 (A) and SHP-2 (B) proteins in different models of AP. Three different AP models were used: Cer-induced (Cer), sodium-taurocholate duct infusion (Tau) or bile-pancreatic duct obstruction (BPDO) pancreatitis. Saline (0.9% NaCl)- injected rats are also shown (control, C). Cer represents 9 h treatment with Cer, as indicated in Materials and methods. Quantification (graphic) of expression (Western blots in whole postnuclear pancreatic homogenates — a representative is shown) was carried out considering the whole pancreas. Each lane in the blots contained 30 μg of proteins. Data are means±S.D. of 3 animals.

Adobe Photoshop program (version 2.5.1.), and the images were then analysed with the MacBas v 2.5. program, as described previously [29]. The images shown in the figures are from blots whose films were exposed for optimal reproduction rather than for the linearity of band densities.

2.10. Statistical analysis

Data are expressed as means±SD. They were analysed using the non-parametric Mann–Whitney U test. Statistical significance was considered for a p value <0.05. Analyses were implemented using the SPSS program for MS Windows (version 15.0).

3. Results

3.1. SHP-1 and SHP-2 expression during the development of AP

The upper parts of Fig. 1A and B show representative Western blot analyses indicating both SHP-1 and SHP-2 proteins in whole postnuclear pancreatic homogenates obtained from control or pancreatitic rats at different times after the first injection of Cer. The lower parts of Fig. 1A and B indicate quantitative data related to the whole pancreas. We considered it more appropriate to express the data in relation to the whole pancreas because pancreatitis is associated with the neutrophil infiltration and cell death that make the cell composition of the pancreases of control or pancreatitic rats different. We observed an increase in the expression of both SHP-1 and SHP-2 in the early phase of AP (2 h after the first injection of Cer) (6.1±2.4- and 3.3±1.6-fold that of controls for SHP-1 and SHP-2, respectively). For SHP-1, this early increase in expression remained in the intermediate and later phases of

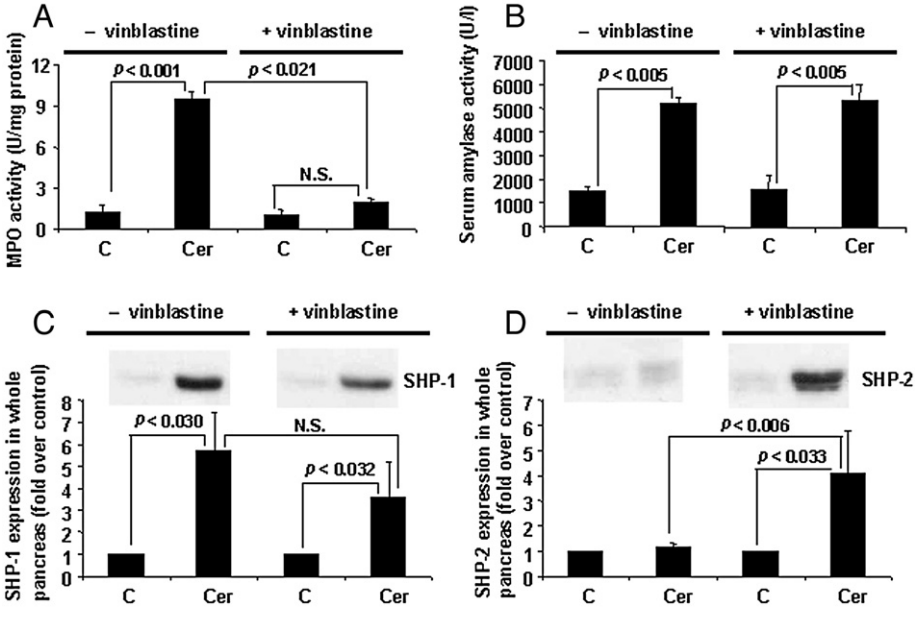

Fig. 4. Effect of neutropenia on MPO (A) and serum amylase (B) activities, and SHP-1 (C) and SHP-2 (D) protein expression during the development of Cer-induced AP. Rats were given 0.75 mg/kg i.v. vinblastine sulfate to induce neutropenia. Four days after vinblastine administration, these neutropenic rats were given 4 injections of saline (0.9% NaCl) or Cer hourly over 4 h (representing the intermediate phase of AP) as indicated in Materials and methods. The same treatments were given to control animals (C) (saline instead of vinblastine pre-treatment on day 1). In (C) and (D), quantification (graphic) of expression (Western blots in whole postnuclear pancreatic homogenates — a representative is shown) was carried out considering the whole pancreas. Each lane in the blots contained 30 μg of proteins. Data are means±S.D. of 3 animals. N.S., not significant.

AP, although to a lower extent (i.e., 3.0±0.8-fold that of the control at 9 h). By contrast, SHP-2 expression fell to levels similar to those of the controls from 4 h onwards. Fig. 2A and B depict representative gels highlighting mRNA expression for both SHP-1 and SHP-2 in the early phase of AP (2 h). It may be observed that the induction of AP by Cer resulted in an increase in SHP-1 and SHP-2 mRNAs in pancreas but not in a control organ with Cer receptors (brain), in which the expression of SHP-1 and SHP-2 proteins remained constant (data not shown). Cer-induced AP is thus associated with increases in pancreatic SHP-1 and SHP-2 at the level of both protein and mRNA. Additionally, as proof of the establishment of AP, a significant increase in serum amylase activity was observed along the development of AP, Fig. 1C).

To analyse whether the increase in SHP-1 and SHP-2 protein expression was specific to the Cer AP model, we next assayed the taurocholate and BPDO models of AP. For this, the pancreases were studied once AP was fully developed. As depicted in Fig. 3B, an increase in the expression of SHP-2 was also observed in the other two models of AP, mainly in the BPDO model (4.5±1.4- and 11.9±5.6-fold that of controls for the taurocholate and BPDO models, respectively). By contrast, an increase in SHP-1 protein expression was not detected either in the taurocholate or in the BPDO model of AP; instead, a decrease was observed, especially in the BPDO model. (Fig. 3A).

3.2. Influence of neutrophil infiltration

Neutrophil infiltration is an important component in the development of both inflammation and cell death in pancreatitis. Thus, in an attempt to see whether infiltrating neutrophils were responsible for, or could somehow influence, the increase in the protein expression of both PTPs in Cer-induced AP, rats were rendered neutropenic with vinblastine sulfate before treatment. The rats were administered vinblastine on day 1, and the experiment with Cer was conducted on day 5, at which point it has been reported that animals have no remaining neutrophils [26]. As expected, a differential count of leukocytes in the blood of the rats used in our experiments afforded zero percent of neutrophils (39±5 and 0% neutrophils in blood from Cer-induced AP (4 h) rats non-pretreated or pretreated with vinblastine sulfate, respectively, $n=3$: data not shown). Furthermore, leukocyte accumulation in the pancreas was investigated by measuring MPO activity. We chose to study the intermediate phase of AP (4 h) because it has been reported that at this time the inflammatory cell infiltration has already taken place [30]. In Fig. 4A it may be seen that while Cer treatment (4 h) caused leukocyte accumulation in the pancreas, the administration of vinblastine resulted in blunted pancreatic MPO levels. With respect to serum amylase, vinblastine treatment alone did not affect its activity, and Cer treatment in vinblastine-treated rats did not decrease serum amylase levels (Fig. 4B), in agreement with previously reported data [26]. Fig. 4C shows that the depletion of neutrophils in the rats did not significantly affect the increase in SHP-1 protein expression at 4 h after Cer treatment (5.7±1.8- and 3.6±1.6-fold above the controls in pancreatitic rats non-pretreated or pretreated with vinblastine sulfate, respectively). In the case of SHP-2 (Fig. 4D), neutrophil depletion prevented the decrease in PTP expression down to basal levels at 2 h after Cer treatment, because in the intermediate phase of AP (4 h) SHP-2 protein expression was still significantly increased (1.1±0.1- and 4.1±1.7-fold that of controls in pancreatitic rats non-pretreated or pretreated with vinblastine sulfate, respectively).

3.3. Effect of JNK and ERK1/2 kinase inhibition by SP600125

It has been proposed that MAP kinases play a pivotal role in the development of hyperstimulation-induced pancreatitis, in part due to an amelioration of the severity of Cer-induced AP after the inhibition of JNK and ERK1/2 kinases [9]. To check whether these two MAP kinases might play a role in the increase of the expression of both PTPs in the early phase (2 h) of AP, we next investigated the effect of SP600125, a new inhibitor of JNK and ERK1/2, on SHP-1 and SHP-2 protein expression. In Fig. 5, it can be observed that SP600125 pre-treatment did not reduce the increase in the expression of either

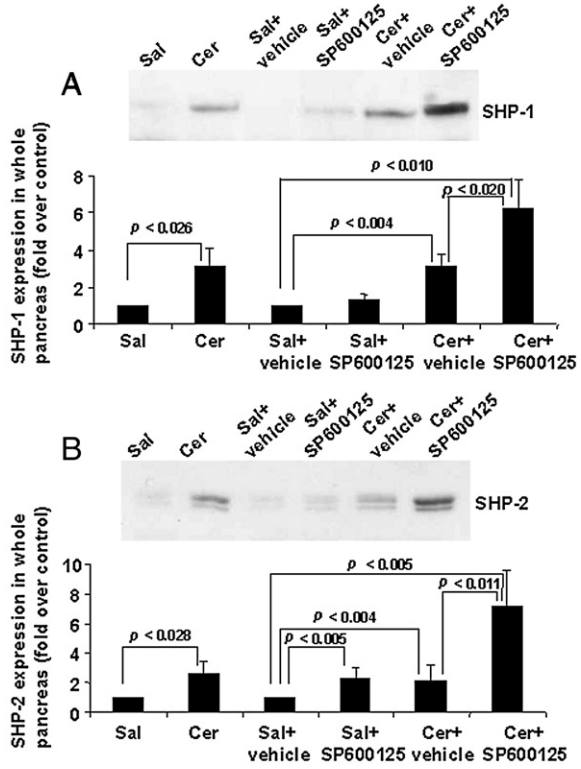

Fig. 5. Effect of SP600125 pre-treatment on SHP-1 (A) and SHP-2 (B) protein expression in the early phase of Cer-induced AP. Rats were pretreated with SP600125 or its vehicle (15 mg/kg or 1 ml/kg of 10% DMSO/NaCl solution i.p. administered 2 h before and 30 min after the first injection of Cer, respectively). Then, the animals were injected subcutaneously with either Cer or its vehicle [20 mg/kg or saline (0.9% NaCl, Sal) for each of two injections at hourly intervals, respectively]. As a positive control of the experiment, non-pretreated rats (Sal and Cer) were also included. Quantification (graphics) of expression (Western blots in whole postnuclear pancreatic homogenates — a representative is shown) was carried out considering the whole pancreas. Each lane in the blots contained 30 μg of proteins. Data are means±S.D. of 2 experiments with 3 rats per group in each.

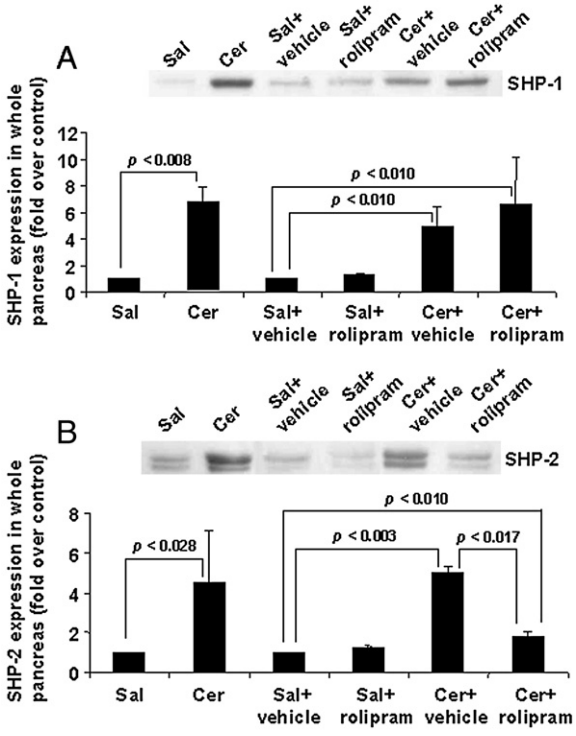

Fig. 6. Effect of rolipram pre-treatment on SHP-1 (A) and SHP-2 (B) protein expression in the early phase of Cer-induced AP. Rats were pretreated with rolipram or its vehicle (5 mg/kg or 1 ml/kg of 10% DMSO/NaCl solution i.p. administered 30 min before and 30 min after the first injection of Cer, respectively). Then, the animals were injected subcutaneously with either Cer or its vehicle [20 mg/kg or saline (0.9% NaCl, Sal) for each of two injections at hourly intervals, respectively]. As a positive control of the experiment, non-pretreated rats (Sal and Cer) were also included. Quantification (graphics) of expression (Western blots in whole postnuclear pancreatic homogenates -a representative is shown) was carried out considering the whole pancreas. Each lane in the blots contained 30 μg of proteins. Data are means±S.D. of 2 experiments with 3 rats per group in each.

PTP after Cer treatment. By contrast, the expression of both SHP-1 (Fig. 5A) and SHP-2 (Fig. 5B) was significantly increased in the pancreases of Cer-injected rats pretreated with SP600125 in comparison with the non-pretreated animals (6.2±1.6- and 3.1±0.7-fold, and 7.1±2.5- and 2.1±1.1-fold as compared with control rats for SHP-1 and SHP-2, respectively). Moreover, JNK and ERK1/2 inhibition in the absence of Cer stimulation was also able to increase SHP2 protein expression to a similar extent to Cer (2.6±0.8- and 2.1±1.1-, 2.3±0.7-fold that of control rats injected with saline or saline+vehicle (DMSO), for Cer and Cer+vehicle (DMSO) or saline+SP600125 injected rats, respectively). This latter effect was not observed for SHP-1. Regarding serum amylase activity in the early phase (2 h) of AP, SP600125 was not able to reduce the significant increase observed in the animals given Cer alone (1603±10, 1710±56, 4800±300, 5500±400 U/l, $n=3$, for rats given saline+DMSO, saline+SP600125, Cer+DMSO and Cer+SP600125, respectively, data not shown).

3.4. Effect of type IV phosphodiesterase inhibition by rolipram

We next decided to analyse the role of cAMP levels in the increase in the expression of both PTPs in the early phase (2 h) of AP, since it has recently been proposed that intracellular cAMP levels in inflammatory cells might also play an essential role in the pathogenesis of AP [27]. In Fig. 6A it can be observed that rolipram, an inhibitor of type IV phosphodiesterase, did not affect the increase in SHP-1 protein expression due to Cer, since in comparison with the non-pretreated animals PTP protein expression was not modified in the pancreases obtained from Cer-injected rats pretreated with rolipram (4.9±1.5- vs 6.6±3.5-fold above control rats, respectively). Unlike SHP-1, the increase in SHP-2 protein expression due to Cer was significantly suppressed in rolipram-pretreated rats (Fig. 6B) (1.3±0.3- vs 5.0±0.3-fold above control rats (injected with saline+vehicle) for Cer+rolipram and Cer+vehicle rats, respectively). Rolipram did not change SHP-2 protein expression in the absence of Cer stimulation [1.2±0.1-fold in saline+rolipram-injected rats as compared with saline+vehicle-injected rats]. Regarding serum amylase activity in the early phase (2 h) of AP, rolipram showed a tendency (although not significant) to reduce such activity in rats given Cer+rolipram (1450±30, 1600±50, 5500±250 and 4700±400 U/l, $n=3$, for rats given saline+DMSO, saline+rolipram, Cer+DMSO and Cer+rolipram, respectively, data not shown).

Table 1
Percentage distribution of SHP-2 protein in subcellular fractions from pancreas in control or pancreatitic rats

Time after first injection of saline or Cae (h)						
Subcellular fraction (%)	2		4		9	
	C	P	C	P	C	P
L + M	1.8±0.8	8.1±5.8[a]	0.7±0.2	4.4±1.2	3.1±2.8	4.0±3.0
Mic	3.3±1.0	21.8±8.2[b]	1.9±1.0	7.1±0.4	2.7±2.6	3.0±1.9
Z	1.0±0.7	2.6±2.5	0.4±0.06	0.6±0.2	0.7±0.9	1.5±1.1
S	93.9±1.4	67.5±5.4[a]	97.1±1.3	87.9±0.6	93.5±5.6	91.5±5.4

Subcellular fractions: L+M, lysosomes+mitochondria; Mic, microsomes; Z, zymogens; S, soluble (cytosolic fraction). Rats: C, control (saline-injected); P, pancreatitic (Cer-injected).
Values were obtained from quantification of Western blots as indicated in Materials and methods, and are expressed as relative percentages considering the sum of the integrated densities for all subcellular fractions in the whole pancreases as 100%. Data are means±S.D. of 3 experiments with 4 rats in each.
[a] $p<0.021$, [b] $p<0.020$ with respect to C at 2 h.

3.5. SHP-1 and SHP-2 subcellular distribution during the development of AP

Finally we analysed the subcellular distribution and dynamics of both PTPs. As expected, both PTPs were completely (SHP-1, data not shown) or mainly cytosolic (located in the S fraction, Table 1). SHP-1 remained as a cytosolic enzyme along the development of pancreatitis development and was never seen to become associated with any subcellular membrane-fraction (data not shown). By contrast, we observed that in the early phase of AP (2 h), the increase in the expression of SHP-2 protein was associated with significant increases in its location in the L+M fraction, but mainly in the Mic subcellular fraction. This redistribution was less marked at 4 h after the first injection of Cer, and it disappeared at 9 h.

4. Discussion

AP involves a complex cascade of local and systemic events that are initiated as a response to stress by the pancreatic acinar cell, but the cellular and molecular mechanisms responsible of the initiation of pancreatitis are not well understood. Acinar cell responses in AP include not only rapid protein activation by posttranslational modifications, but also alterations in gene and/or protein expression that may convert the rapid activation of signalling mechanisms in acinar cells into long-term responses [1]. All these events, as a whole, will determine the ultimate severity of AP.

It has been proposed that alterations in gene expression within the initiation phase of AP play an important role in its development [1]. Taking this into account, in this study we report an increase in SHP-1 and SHP-2 in the pancreas at the level of both protein and mRNA as an early event during the development of Cer-induced AP. Especially significant was the increase in the expression of SHP-2 protein, because it was observed commonly in all three different in vivo models of AP. This highlights the general importance of the increase in the expression of this PTP in AP. By contrast, the specificity of the increase in SHP-1 protein in the Cer-induced AP model could reflect a specific response to a specific insult.

It is known that both SHP-1 and SHP-2 are expressed in the rat exocrine pancreas [12] and that both PTPs are scarcely detectable in human neutrophils [31], which, together with the data obtained here with vinblastine sulfate, indicates that the increase in the expression of both PTPs most likely arises from pancreatic acinar cells. Nevertheless, it is still possible that other minor pancreatic cell types could account for some of the observed changes. In this context, further studies are currently being designed to fully determine the cellular origins of these PTPs.

It has been reported that there is a common set of genes expressed in at least Cer- and taurocholate-induced AP [1], which suggests the possibility of a common set of upstream signalling mechanisms. From previous studies, it is known that the different AP models used here induce the activation of stress kinases, including JNK [32]. Both JNK and ERK1/2 have been proposed to be important mediators during the early phase (first 1–1.5 h) of AP [9,26,33]. Many of the transcription factors (TFs) induced early on in the onset of AP are known to be regulated by the activation of stress kinase pathways [1]. Thus, the activation of stress kinases provides a potential link between the earliest known signalling events in AP and the long-term consequences that stem from changes in gene expression. Furthermore, stress kinases also regulate protein translation [34]. Since these enzymes have been reported to promote gene and protein expression early on in the development of Cer-induced AP [9,26], we decided to analyse their potential influence in the observed increase of both SHP-1 and SHP-2 proteins. We used SP600125, a new MAPK inhibitor that, under the conditions used here, has been described to almost totally inhibit Cer-induced pancreatic JNK activation and partially inhibit ERK1/2 activation [9]. Our results demonstrated that SP600125 pre-treatment was able to positively modulate both SHP-1 and SHP-2 protein expression in the early phase of Cer-induced AP. Currently it is difficult to envisage the mechanism by which the inhibition of MAPK would afford further increases in both PTP proteins. It is possible that the observed effect could be mediated through an effect on the half-life of early-activated TFs. It has been proposed that the activation of TFs also facilitates their immediate degradation, thus ensuring the end of translation activation [35]. It is possible that an inhibition of the MAPK pathway that activates specific TFs might influence the concomitant degradation rate of such TFs, thus modifying their half-life. Another possibility would be an effect of JNK and/or ERK1/2 on the half-life of both SHP-1 or SHP-2 proteins or messages. Further specific research would be necessary to analyse this surprising effect. Considering that MAPKs have also been shown to up-regulate the expression of inflammatory cytokines, such as TNF-α [9], which also primes cell infiltration in the pancreas, and that SP600125 pre-treatment results in a blunted leukocyte accumulation in the pancreases of Cer-induced AP rats [9], the positive effects of SP600125 and the data on neutropenic rats seem to be in good agreement. We believe that analyses of infiltration as a regulator of at least SHP-2 protein expression merit further investigation. The lack of a significant reduction in amylase activity after SP600125 pre-treatment seems to be in disagreement with previous results [9]. Nevertheless, it is important to recall that we were analysing the early phase of Cer-induced AP and that those previous results [9] were found in rats with fully developed AP. Therefore, the reduction in amylase activity after JNK and ERK1/2 inhibition would occur later on in the development of AP.

Excessive ATP catabolism has been reported to occur during AP [20] and increases in cAMP levels in inflammatory cells by rolipram have been reported to attenuate some inflammatory diseases, including AP [27]. Rolipram is a specific and strong inhibitor of type IV phosphodiesterase, a key enzyme in the metabolism of intracellular cAMP that is abundantly expressed in inflammatory cells such as neutrophils and that also exerts anti-inflammatory effects by increasing the level of intracellular cAMP by blocking its catalysis. Thus, rolipram has a similar action to that of adenosine A2a receptors, a receptor type mainly expressed in inflammatory cells [10]. Increases in intracellular

cAMP levels enhance the activity of cAMP-dependent protein kinase A and reduce the production of proinflammatory cytokines such as TNF-α [36]. Importantly, acinar cells can behave as true inflammatory cells, which also produce such proinflammatory cytokines [37]. Accordingly, although we are not aware of any report describing the presence of type IV phosphodiesterase in acinar cells, rolipram could be a useful tool for investigating the role of intracellular cAMP levels in cell infiltration, and probably also in acinar cells, during the development of AP. Accordingly, analysis of the putative influence of rolipram not only on infiltrating neutrophils but also on acinar cells as a cause of the specific sensitivity of SHP-2 expression to rolipram deserves further investigation. Future in vitro experiments with isolated acinar cells in the presence or absence of neutrophils will be necessary to further increase our understanding of the in vivo effect of rolipram on SHP-2 protein expression in Cer-induced AP rats.

SHP-1 remained as a cytosolic enzyme during Cer-induced AP development (this work), which is in agreement with previous results [12]. By contrast, the increase in SHP-2 in the early phase of Cer-induced AP was associated with a redistribution of its subcellular location. Preliminary data with three different lysosomal populations obtained by centrifugation of the pancreatic L+M subcellular fraction in Percoll density gradients revealed that SHP-2 significantly increases its location by more than 100% (reaching up to 50% of total SHP-2 protein in the L+M fraction) in the two densest populations (unpublished results). Electron microscopic observations of these reveal that they are composed of vesicles enclosing membrane fragments and amorphous membrane-bound material of varying sizes and shapes (unpublished results). Data on the intracellular proteolytic systems used for PTP degradation are very scarce, although it is generally accepted that most regulatory molecules involved in highly regulated cellular processes such as signal transduction are substrates of the proteasome. Thus, the meaning of the association of SHP-2 with lysosomes in AP is unknown. Despite this, it should be noted that the lysosomal/vacuolar system is a discontinuous and heterogeneous digestive system that also includes structures that are devoid of hydrolases and that carry out processes of heterophagy and autophagy [38], and that autophagy has been reported to occur in AP [39]. It is possible that as a result of autophagy, membranous and/or non-membranous material carrying SHP-2 protein could reach the densest lysosomal populations. Moreover, SHP-2 protein was also increased in the Mic subcellular fraction. At this point it is not possible to know what this would be due to. One possibility is the recruitment of SHP-2 to the plasma membrane by activated receptor protein tyrosine kinases or other phosphotyrosine-containing ligands that occur early on in the development of AP [40]. It should be noticed that most of the plasma membrane would be present in the Mic fraction in our fractionation method. Finally, it is known that AP is associated with the disassembly of the acinar cell cytoskeleton [41] and several lines of in vitro and in vivo evidence suggest that SHP-2 might be involved in the control of cytoskeletal architecture [40].

In sum, in this study we have detected an increase in SHP-1 and SHP-2 in the pancreas at the level of both protein and mARN as an early event during the development of Cer-induced AP. The increase in SHP-2 protein (which was associated with changes in its subcellular distribution) in two other different in vivo pancreatitic models points towards the general importance of this phosphatase in AP. The inhibition of JNK and ERK1/2 further increased the expression of both SHP-1 and SHP-2 proteins, while the inhibition of type IV phosphodiesterase only suppressed the increase in SHP-2 protein expression in the early phase of AP.

Acknowledgements

This work has been supported in part by MCYT (BFU2006-10362/BMC) and Junta de Castilla y León (SA033A05 and SA126A07). The authors wish to thank Drs. M. Manso and JM González de Buitrago (University of Salamanca) for their help with the BPDO model and amylase determination, respectively.

References

[1] B. Ji, X. Chen, D.E. Misek, R. Kuick, S. Hanash, S. Ernst, R. Najarian, C.D. Logsdon, Pancreatic gene expression during the initiation of acute pancreatitis: identification of EGR-1 as a key regulator, Physiol. Genomics. 14 (2003) 59–72.

[2] R. Alonso, A. Montero, M. Arévalo, L.J. García, C. Sánchez-Vicente, F. Rodríguez-Nodal, J.M. López-Novoa, J.J. Calvo, Platelet-activating factor mediates pancreatic function derangement in caerulein-induced pancreatitis in rats, Clin. Sci. 87 (1994) 85–90.

[3] R. Pescador, M.A. Manso, A.J. Revollo, I. De Dios, Effect of chronic administration of hydrocortisone on the induction and evolution of acute pancreatitis induced by cerulein, Pancreas 11 (1995) 165–172.

[4] N. Yönetçi, N. Oruç, A.O. Ozütemiz, H.A. Celik, G. Yüce, Effects of mast-cell stabilization in caerulein-induced acute pancreatitis in rats, Int. J. Pancreatol. 29 (2001) 163–171.

[5] M. Zhao, D.B. Xue, B. Zheng, W.H. Zhang, S.H. Pan, B. Sun, Induction of apoptosis by artemisin relieving the severity of inflammation in caerulein-induced acute pancreatitis, World J. Gastroenterol. 14 (2007) 5612–5617.

[6] N. Rivard, G. Rydzewska, J.-S. Lods, J. Martinez, J. Morisset, Pancreas growth, tyrosine kinase, PtdIns 3-kinase, and PLD involve high-affinity CCK-receptor occupation, Am. J. Physiol. 266 (1994) G62–G70.

[7] N. Rivard, G. Rydzewska, J.S. Lods, J. Morisset, Novel model of integration of signalling pathways in rat pancreatic acinar cells, Am. J. Physiol. 269 (1995) G352–G362.

[8] C. Widmann, S. Gibson, M.B. Jarpe, G.L. Johnson, Mitogen activated protein kinases: conservation of a three kinase module from yeast to human, Physiol. Rev. 79 (1999) 143–180.

[9] L. Minutoli, D. Altavilla, H. Marini, M. Passaniti, A. Bitto, P. Seminara, F.S. Venuti, C. Famulari, A. Macri, A. Versaci, F. Squadrito, Protective effects of SP600125 a new inhibitor of *c-Jun* N-terminal kinase (JNK) and extracellular-regulated kinase (ERK1/2) in an experimental model of cerulein-induced pancreatitis, Life Sci. 75 (2004) 2853–2866.

[10] A. Satoh, T. Shimosegawa, K. Satoh, H. Ito, Y. Kohno, A. Masamune, M. Fujita, T. Toyota, Activation of A1-receptor pathway induces edema formation in the pancreas of rats, Gastroenterology 119 (2000) 829–836.

[11] T. Sato, M. Otaka, M. Odashima, S. Kato, M. Jin, N. Konishi, T. Matsuhashi, S. Watanabe, Specific type IV phosphodiesterase inhibitor ameliorates cerulein-induced pancreatitis in rats, Biochem. Biophys. Res. Commun. 346 (2006) 339–344.

[12] J. Schnekenburger, J. Mayerle, B. Krüger, I. Buchwalow, F.U. Weiss, E. Albrecht, V.E. Samoilova, W. Domschke, M.M. Lerch, Protein tyrosine phosphatase k and SHP-1 are involved in the regulation of cell–cell contacts at adherent junctions in the exocrine pancreas, Gut 54 (2005) 1445–1455.

[13] M.M. Lerch, M.P. Lutz, H. Weidenbach, F. Muller-Pillasch, T.M. Gress, J. Leser, G. Adler, Dissociation and reassembly of adherent junctions during experimental acute pancreatitis, Gastroenterology 113 (1997) 1355–1366.
[14] T. Muller, A. Choidas, E. Reichmann, A. Ullrich, Phosphorylation and free pool of beta-catenin are regulated by tyrosine kinases and tyrosine phosphatases during epithelial cell migration, J. Biol. Chem. 274 (1999) 10173–10183.
[15] M. You, Z. Zhao, Positive effects of SH2 domain-containing tyrosine phosphatase SHP-1 on epidermal growth factor- and interferon-g-stimulated activation of STAT transcription factors in HeLa cells, J. Biol. Chem. 272 (1997) 23376–23381.
[16] C.-K. Qu, Role of the SHP-2 tyrosine phosphatase in cytokine-induced signalling cellular response, Biochim. Biophys. Acta 1592 (2002) 297–301.
[17] J. Den Hertog, A. Grogen, T. Van Der Wijk, Redox regulation of protein-tyrosine phosphatases, Arch. Biochem. Biophys. 434 (2005) 11–15.
[18] A. Hernández-Hernández, J. Sánchez-Yagüe, E.M. Martín-Valmaseda, M. Llanillo, Oxidative inactivation of human and sheep platelet membrane-associated phosphotyrosine phosphatase activity, Free Radical Bio. Med. 26 (1999) 1218–1230.
[19] A. Hernández-Hernández, M.N. Garabatos, M.C. Rodríguez, M.L. Vidal, A. López-Revuelta, J.I. Sánchez-Gallego, M. Llanillo, J. Sánchez-Yagüe, Structural characteristics of a lipid peroxidation product, trans-2-nonenal, that favour inhibition of membrane associated phosphotyrosine phosphatase activity, Biochim. Biophys. Acta 1726 (2005) 317–325.
[20] R. Lüthen, C. Niedereau, J.H. Grendell, Intrapancreatic zymogen activation and levels of ATP and glutathione during cerulein pancreatitis in rats, Am. J. Physiol. 268 (1995) G592–G604.
[21] C. Sánchez-Bernal, O.H. García-Morales, C. Domínguez, P. Martín-Gallán, J.J. Calvo, L. Ferreira, N. Pérez-González, Nitric oxide protects against pancreatic subcellular damage in acute pancreatitis, Pancreas 28 (2004) e9–e15.
[22] H.J. Aho, S.M. Koskensalo, T.J. Nevalainen, Experimental pancreatitis in the rat. Sodium-taurocholate-induced acute haemorrhagic pancreatitis, Scand. J. Gastroenterol. 15 (1980) 411–416.
[23] A. de la Mano, L.S. Sevillano, I. De Dios, S. Vicente, M. Manso, Low enzyme content in the pancreas does not reduce the severity of acute pancreatitis induced by bile-pancreatic duct obstruction, Moll. Cell. Biochem. 240 (2002) 75–81.
[24] K. Lorentz, Approved recommendation of IFCC methods for the measurement of catalytic concentration of enzymes. Part 9. IFCC method for a-amylase (1,4-a-D-Glucan 4-Glucanohydrolase, EC 3.2.1.1), Clin. Chem. Lab. Med. 36 (1998) 185–203.
[25] M.M. Bradford, A rapid and sensitive method for the quantitation of microgram quantities of protein utilizing the principle of protein-dye binding, Anal. Biochem. 72 (1976) 248–254.
[26] A.P. Clemons, D.M. Holstein, A. Galli, C. Saunders, Cerulein-induced acute pancreatitis in the rat is significantly ameliorated by treatment with MEK1/2 inhibitors U0126 and PD98059, Pancreas 25 (2002) 251–259.
[27] T. Sato, M. Otaka, M. Odashima, S. Kato, M. Jin, N. Konishi, T. Matsuhashi, S. Watanabe, Specific type IV phosphodiesterase inhibitor ameliorates cerulein-induced pancreatitis in rats, Biochem. Biophys. Res. Commun. 346 (2006) 339–344.
[28] A. Hernández-Hernández, M. Llanillo, M.C. Rodríguez, F. Gómez, J. Sánchez-Yagüe, Amphiphilic and hydrophilic nature of sheep and human platelet phosphotyrosine phosphatase forms, Biochim. Biophys. Acta 1419 (1999) 195–206.
[29] A. Hernández-Hernández, M.C. Rodríguez, A. López-Revuelta, J.I. Sánchez-Gallego, V. Shnyrov, M. Llanillo, J. Sánchez-Yagüe, Alterations in erythrocyte membrane protein composition in advanced non-small cell lung cancer, Blood Cell Mol. Dis. 36 (2006) 355–363.
[30] J. Mayerle, J. Schnekenburger, B. Kruger, J. Kellermann, M. Ruthenburger, F.U. Weiss, A. Nalli, W. Domschke, M.M. Lerch, Extracellular cleavage of E-cadherin by leukocyte elastase during acute experimental pancreatitis in rats, Gastroenterology 129 (2005) 1251–1267.
[31] N. Tidow, B. Kasper, K. Welte, SH2-containing protein tyrosine phosphatases SHP-1 and SHP-2 are dramatically increased at the protein level in neutrophils from patients with severe congenital neutropenia (Kostmann's syndrome), Exp. Hematol. 27 (1999) 1038–1045.
[32] M.L. Steer, A.K. Saluja, Experimental acute pancreatitis studies of the early events that lead to cell injury, in: V.L.W. Go, E.P. Di Magno, J.D. Gardner, E. Lebenthal, H.A. Rebar, G.A. Scheele (Eds.), The Pancreas: Biology, pathophysiology and Diseases, Raven, New York, 1993, pp. 489–499.
[33] T. Hofken, N. Keller, F. Fleischer, B. Goke, A.C. Wagner, Map Kinase Phosphatases (MKP's) are early responsive genes during induction of cerulein hyperstimulation pancreatitis, Biochem. Biophys. Res. Commun. 276 (2000) 680–685.
[34] J.A. Williams, Intracellular signalling mechanisms activated by cholecystokinin-regulating synthesis and secretion of digestive enzymes in pancreatic acinar cells, Ann. Rev. Physiol. 63 (2001) 77–97.
[35] A. Hernández-Hernández, P. Ray, G. Litos, M. Ciro, S. Ottolenghi, H. Beug, J. Boyes, Acetylation and phosphorylation co-operate to target transcriptionally active GATA-1 for degradation, EMBO J. 25 (2006) 3264–3274.
[36] J. Semmler, H. Wachtel, S. Endres, The specific type IV phosphodiesterase inhibitor rolipram suppresses tumor necrosis factor-a production by human mononuclear cells, Int. J. Immunopharmacol. 15 (1993) 409–413.
[37] A.S. Gukovskaya, I. Gukovsky, V. Zaninovic, M. Song, D. Sandoval, S. Gukovsky, S.J. Pandol, Pancreatic acinar cells produce, release, and respond to tumor necrosis factor-alpha. Role in regulating cell death and pancreatitis, J. Clin. Invest. 100 (1997) 1853–1862.
[38] A. Ciechanover, Intracellular protein degradation: from a vague idea thru the lysosome and the ubiquitin-proteasome system and onto human diseases and drug targeting, Hematology Am. Soc. Hematol. Educ. Program (2006) 1–12.
[39] J.M. Grönroos, H.J. Aho, A.J. Hietaranta, T.J. Nevalainen, Early acinar cell changes in Cerulein-induced interstitial acute pancreatitis in the rat, Exp. Pathol. 41 (1991) 21–30.
[40] G.S. Feng, Shp-2 tyrosine phosphatase: signalling one cell or many, Exp. Cell. Res. 253 (1999) 47–54.
[41] J. Jungermann, M.M. Lerch, H. Weidenbach, M.P. Lutz, B. Krüger, G. Adler, Disassembly of rat pancreatic acinar cell cytoskeleton during supramaximal secretagogue stimulation, Am. J. Physiol. 268 (1995) G328–G338.

- **OBJETIVO 2:** Investigar los cambios de expresión de la PTP PTP1B durante el desarrollo de la PA inducida por ceruleína.

ORIGINAL ARTICLE

Rolipram and SP600125 Suppress the Early Increase in PTP1B Expression During Cerulein-Induced Pancreatitis in Rats

Nancy Sarmiento, BSc, Carmen Sánchez-Bernal, PhD,* Nieves Pérez, PhD,* José L. Sardina, BSc,* Arturo Mangas, PhD,† José J. Calvo, PhD,‡ and Jesús Sánchez-Yagüe, PhD**

Objectives: To analyze the expression modulation of pancreatic protein tyrosine phosphatase (PTP)1B during the development of cerulein (Cer)-induced acute pancreatitis (AP) and the effect of inhibition of type 4 phosphodiesterase and c-*Jun N*-terminal kinase and extracellular signal-regulated kinase 1/2 on its expression levels.

Methods: Acute pancreatitis was induced in rats by subcutaneous injections of 20 μg Cer per kilogram body weight at hourly intervals, and the animals were killed at 2, 4, or 9 hours after the first injection. Neutropenia was induced with vinblastine sulfate. Phosphodiesterase and the mitogen-activated protein kinases were inhibited with rolipram and SP600125, respectively, before the induction of AP.

Results: Protein tyrosine phosphatase 1B increases its expression at the levels of both protein and messenger RNA during the early phase of Cer-induced AP. The increase in protein expression persisted along the development of the disease, and neutrophil infiltration seemed to play a central role. Rolipram and SP600125 pretreatments mostly suppressed the increase in the expression of PTP1B during the early phase of AP.

Conclusions: Cerulein-induced AP is associated with an increase in the expression of PTP1B in its early phase. An increase in cyclic adenosine monophosphate levels in inflammatory cells and the inhibition of c-*Jun N*-terminal kinase and extracellular signal-regulated kinase 1/2 are able to suppress the increase in PTP1B protein level.

Key Words: PTP1B, acute pancreatitis, cerulein, SP600125, rolipram

(*Pancreas* 2010;39: 639–645)

One of the animal models of human edematous pancreatitis is that induced in the rat by cerulein (Cer), an analog of cholecystokinin (CCK). The subcutaneous injection of 20 μg Cer per kilogram body weight, the treatment used for the induction of acute pancreatitis (AP) in the present studies, results in the manifestations of pancreatitis, including different indicators of morphological and histological damage to the pancreas, interstitial edema, and hyperamylasemia as well as neutrophil infiltration.[1–4] It is reasonable to assume that the development of pancreatitis would be based on rapid early events and the activation of primary signaling pathways, whose unmasking would be important for the study of AP at the molecular level.[5] With respect to the Cer-induced AP model, the intracellular mechanisms by which CCK or Cer regulates pancreatic acinar function are complex. Within the signaling mechanisms that play important roles in the regulation of many cellular functions, those that are controlled by tyrosine phosphorylation are particularly important. It is well known that in Cer-induced AP, different signaling routes that modulate the phosphorylation state of proteins are activated: (1) pancreatic protein tyrosine kinases (PTKs),[6,7] (2) the mitogen-activated protein kinase (MAPK) cascade, especially extracellular signal-regulated kinase (ERK1/2) and c-*Jun N*-terminal kinase (JNK),[8,9] (3) p38MAPK, (4) the adenosine A1 receptor pathway,[10] which decreases intracellular cyclic adenosine monophosphate (cAMP) levels. It is also known that type 4 phosphodiesterase inhibitors ameliorate Cer-induced AP.[11]

Unlike the case of PTKs, data on protein tyrosine phosphatases (PTPs) in AP are very scarce despite (1) their roles in the regulation of the levels of tyrosine phosphorylation in exocytotic processes in exocrine pancreatic acinar cells[12] and in different inflammatory diseases and (2) their inactivation by reactive oxygen species or secondary products of oxidation[13] that may form during the development of AP.[14] This association between PTPs and diseases calls for an examination of PTP expression modulation and their corresponding function, and, in the case of AP, it is strengthened by the demonstration of PTP1B as a key controller of several cytokine signaling pathways through their negative action on specific members of the Janus kinases/signal transducers and activators of transcription (JAK/STAT) pathway.[15] JAK2/STAT3 inflammatory signaling has been implicated in AP,[16] and JAK2 is a target of PTP1B.[16] PTP1B also plays important roles in cells with a high endoplasmic reticulum (ER) content,[15] such as pancreatic acinar cells, which have the highest rate of protein synthesis among all human tissues.[17] In fact, acinar cells seem to be susceptible to ER homeostasis, and all major ER stress-sensing and signaling mechanisms have been shown to be activated in AP.[5,18,19] In addition, we have recently demonstrated that the Src homology 2 (SH2)-domain PTPs, SHP-1 and SHP-2, are early responsive elements in AP and that their expression increases in the early phase of Cer-induced AP.[20]

The goal of the present work was to study the expression response of a member of the subfamily of intracellular PTPs, the PTP1B, during the development of Cer-induced AP as well as the effect of rolipram, a type 4 phosphodiesterase inhibitor, and SP600125 (anthrax[1,9cd]pyrazol-6(2H)-one 1,9 pyrazoloanthrone), a JNK and ERK 1/2 inhibitor, on PTP1B expression levels in the early phase of AP development. We developed this research in view of the importance of unmasking the molecules or genes whose expression changes in the early phase of AP development, together with the signaling mechanisms that may modulate such expression.

From the Departments of *Biochemistry and Molecular Biology, †Cell Biology and Pathology, and ‡Physiology and Pharmacology, University of Salamanca, Salamanca, Spain.

Received for publication April 3, 2009; accepted September 25, 2009.

Reprints: Jesús Sánchez-Yagüe, PhD, Department of Biochemistry and Molecular Biology, University of Salamanca, Edificio Departamental, Lab. 102, Plaza Doctores de la Reina s/n. 37007, Salamanca, Spain (e-mail: sanyaj@usal.es).

This study was supported in part by Junta de Castilla y León (Biomedicina SAN673/SA10/08, SA033A05, and SA126A07) and FIS (PS09/01075), Spain.

MATERIALS AND METHODS

Reagents

Bovine serum albumin (BSA), Cer, dithiothreitol, phenylmethylsulfonyl fluoride, protein inhibitor cocktail, rolipram, soybean trypsin inhibitor, SP600125, Trizol reagent, and vinblastine sulfate were purchased from Sigma Chemical Co. (St. Louis, Mo). Polyvinylidene difluoride membranes were obtained from Amersham Biosciences, Barcelona Spain. Polyclonal antibody anti-PTP1B (H-135) was obtained from Santa Cruz Biotechnology, Inc., Santa Cruz, Calif. Monoclonal antibody anti–β-tubulin was obtained from Sigma Chemical Co. Reverse transcriptase (RevertAid M-MULV), *Taq* polymerase, deoxynucleoside triphosphates, and the RiboLock ribonuclease inhibitor used in the reverse transcriptase polymerase chain reaction (RT-PCR) were purchased from Fermentas Life Sciences (St. Leon-Rot, Germany); Isogen Life Science (De Meern, The Netherlands); Panreac (Barcelona, Spain). Oligonucleotides were obtained from Isogen Life Science, the Netherlands. Isopropanol was purchased from Panreac, Spain.

Animals

Experiments were performed in male Wistar rats weighing 250 to 280 g, obtained from the University of Salamanca breeding colony. Rats were housed in rooms maintained at 22°C ± 1°C using a 12-hour light/dark cycle. Animals were fasted overnight before the experiment but had free access to water. Care was provided in accordance with the procedures outlined in the European Community guidelines on ethical animal research (86/609/EEC), and protocols were approved by the Animal Care Committee of the University of Salamanca.

Induction of AP and Preparation of Samples

Acute pancreatitis was induced as described previously.[20] Briefly, rats received 4 subcutaneous injections of 20 μg Cer per kilogram body weight or its vehicle (0.9% NaCl) at hourly intervals. At 2, 4, or 9 hours after the first injection, the animals were killed by cervical dislocation. The pancreata were rapidly harvested and used immediately for experiments. After dissection and homogenization of the pancreata,[20] postnuclear homogenates were obtained[20] to minimize the putative cross-reactivity of the PTP1B antibody with T cell protein tyrosine phosphatases (TC-PTP), the other member of the non-transmembrane 1 subfamily of intracellular PTPs. Although TC-PTP has not been reported to be present in rat pancreas, it has been described to be expressed in many organs of the mouse as a nuclear 45-kd form. In cell lines derived from a hamster glucagonoma, no TC-PTP protein or messenger RNA (mRNA) was detected.[21]

Serum amylase was measured in a Roche modular analyzer (Roche Diagnostics España, Barcelona, Spain) as reported previously.[20] Protein concentrations were assayed by the method of Bradford[22] using bovine serum albumin as the standard. Special care was taken with this assay to minimize deviations in the amount of proteins loaded into each lane of the sodium dodecyl sulfate polyacrylamide gel electrophoresis gels. Quality control of the assays was ensured by repeating them at least 3 times with 5 different volumes of 3 to 5 different sample dilutions.

Histological Assessment of Pancreatitis

For light microscopy, small pieces of the pancreas were rapidly removed at different times (2, 4, and 9 hours) after the induction of AP and fixed in 4% paraformaldehyde in 0.15-mol/L phosphate-buffered saline (pH 7.2) for 48 hours at 4°C. Subsequently, they were dehydrated in ascending concentrations of ethanol (50%–100%), rinsed in xylene, and then embedded in paraffin. Sections (10 μm thick) were mounted on gelatin-coated slides, deparaffinized, hydrated, and stained with hematoxylin and eosin (H & E).

Induction of Neutropenia

Neutropenia was induced in rats by an intravenous injection of vinblastine sulfate at a dose of 0.75 mg/kg on day 1, as previously described.[20,23] At this dose, the animals become neutropenic between days 4 and 6.[23] Five days after the induction of neutropenia, the animals were treated with 2 hourly injected doses of Cer (20 μg Cer per kilogram) to induce AP.

Inhibition of Type 4 Phosphodiesterase by Rolipram or of JNK and ERK1/2 by SP600125 in Cer-Induced AP

Rats received intraperitoneal injections of rolipram (5 mg/kg), SP600125 (15 mg/kg) or its vehicle (1 mL/kg of a 10% dimethyl sulphoxide/NaCl solution) both 30 minutes before and 30 minutes after, or both 2 hours before and 30 minutes after, the first Cer injections of rolipram[11,20] and SP600125,[9,20] respectively. Thirty minutes or 2 hours after the first injection of rolipram or SP600125, respectively, the rats were injected subcutaneously with Cer (20 μg Cer per kilogram) or its vehicle (0.9% NaCl) at hourly intervals. The animals were killed 2 hours after the first Cer injection (early phase of Cer-induced AP).

RT-PCR Assays

Total RNA was isolated from the pancreas and the brain of the same rat by immediate solubilization in Trizol reagent and isopropanol purification. Reverse transcriptase polymerase chain reaction was performed in a total volume of 20 μL containing 2 μg complementary DNA, 50-mmol/L Tris-HCl, pH 8.3, 50-mmol/L KCl, 4-mmol/L $MgCl_2$, 10-mmol/L dithiothreitol, 1-mmol/L deoxynucleoside triphosphates, 0.5 μmol/L of each primer, 20 units of Ribolock ribonuclease inhibitor, and 200 U RevertAid M-MuLV reverse transcriptase. The PTP1B oligonucleotide sequences were as follows: forward oligo, 5′-CTCACCCAGGGCCCTTTACCAA-3′; reverse oligo, 5′-TGGATGAGCCCCATGCGGAACC-3′. The product length was 539 bp. Oligonucleotide primers for β-actin were used as an internal control (forward oligo, 5′-TCTGTGTGGATTGGTGGCTCTA-3′; reverse oligo, 5′-CTGCTTGCTGATCCACATCTG-3′). Cycle steps were performed as previously described.[20]

SDS-PAGE and Western Blotting

Proteins were analyzed by sodium dodecyl sulfate polyacrylamide gel electrophoresis using 10% gels[24] and then transferred to polyvinylidene difluoride membranes. Western blots were probed with anti-PTP1B polyclonal or anti–β-tubulin monoclonal antibodies diluted 1:1000 and 1:4000, respectively. Blots were visualized by chemiluminescence. Analyses of the spots on all the blots were performed as described previously.[25] The densities of the β-tubulin bands were used to ascertain that an approximately equal amount of proteins had been loaded in each lane, although the densities corresponding to the PTP1B bands in the different treatments were not normalized to the β-tubulin band densities mainly because our samples were heterogeneous systems that did not always contain the same set of cellular proteins (ie, samples from pancreatitic pancreas included the proteins from the infiltrates and reflected all the histological damages associated with AP). This feature makes it impossible to guarantee that the same amount of loading protein/mg protein will be present in all the samples. Nevertheless, a significant influence (if any) of the loading in our results can be ruled out because of the magnitude of the differences

observed for PTP1B expression among the different conditions tested. The images shown in the figures are from blots whose films were exposed for optimal reproduction rather than for the linearity of band densities.

Statistical Analyses

Data (means ± SD) were analyzed (version 15.0 of the SPSS program for MS Windows, SPSS, Chicago, Ill) using the nonparametric Mann-Whitney *U* test. Statistical significance was considered for a $P < 0.05$.

RESULTS

Increases in the Expression of PTP1B in AP

In Figure 1A, it can be observed that the expression of PTP1B protein in whole postnuclear pancreatic homogenates increased during the development of AP. The bar diagram indicates quantitative data related to the whole pancreas. We considered it more appropriate or even necessary to express the data in relation to the whole pancreas because pancreatitis is associated with the neutrophil infiltration and cell death that render the cell composition of the pancreata of the rats in the

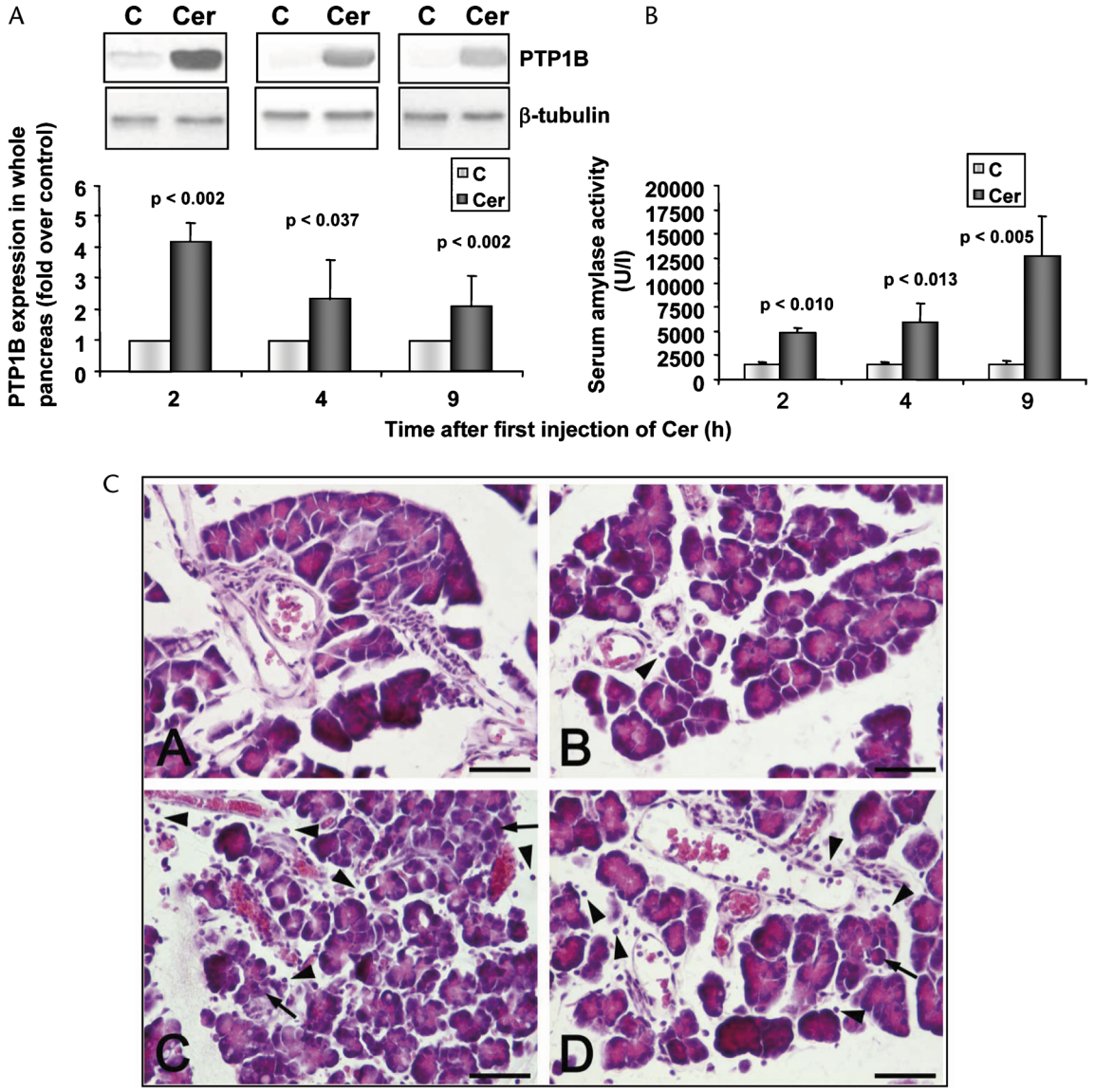

FIGURE 1. Expression of PTP1B protein (A) and serum amylase activity (B) and light microscopy of the rat pancreas stained with H & E (C) during the development of Cer-induced AP. Rats were either administered saline (0.9% NaCl; control, C) or treated with Cer, as indicated in the ''Materials and Methods'' section, and then killed 2, 4, or 9 hours after the first injection of Cer. A, Quantification (graphic) of expression (Western blots—1 representative for each time point is shown) was carried out considering the whole pancreas. Anti–β-tubulin antibody was used as an approximate loading control. Each lane in the blots contained 30 μg of proteins. Data are means ± SD of 5 animals. In the histological pancreatic sections: control animal (photomicrograph A), low magnification of the pancreas showing a normal morphology; 2-hour (photomicrograph B), 4-hour (photomicrograph C), and 9-hour (photomicrograph D) pancreatitic rats. Compare the morphology of normal acini with other acini showing altered morphology (arrows). Note also the different and increasing degree of leukocyte infiltration (arrowheads) through 2, 4, and 9 hours. Scale bar: 50 μm.

control group or the pancreatitic rats different. Accordingly, the total amount of proteins per pancreas changes with treatment, and the exact amount of any protein, including PTP1B, should be calculated in the whole organ rather than in a fixed amount of proteins. We observed an increase in the expression of PTP1B in the early phase of AP (2 hours after the first injection of Cer; 4.1 ± 0.8–fold that of the controls) that remained in the intermediate and later phases of AP, although to a lower extent (ie, 2.3 ± 0.7–fold that of the control at 9 hours). The establishment of AP was monitored by serum amylase determination and the histological assessment as follows: (1) a significant increase in the serum amylase activity was observed along with the development of AP (Fig. 1B), and (2) histological sections of the pancreata from the control and the 2-, 4-, and 9-hour pancreatitic rats showed clear differences concerning tissue architecture and the degree of leukocyte infiltration. In the control animals (Fig. 1C, photomicrograph A), the pancreatic tissue showed normal acini, and no infiltration was observed. In the 2-hour pancreatitic rats (Fig. 1C, photomicrograph B), small numbers of unstructured acini and scarce lymphocytes were observed outside the vessels. In the 4-hour pancreatitic rats (Fig 1C, photomicrograph C), a higher degree of leukocyte infiltration was visualized, and higher numbers of unstructured acini were also found. In addition, neutrophils were detected. Finally, in the 9-hour pancreatitic rats (Fig. 1C, photomicrograph D), a higher degree of tissue disorganization was seen, and numerous leukocytes were observed outside the vessels surrounding the acini and also adhering to the vascular endothelium. All these features are consistent with those described previously.[1,3,4] Moreover, in the early phase of AP (2 hours), PTP1B mRNA increased in pancreas but not in a control organ with Cer receptors (brain; Fig. 2) in which the expression of the PTP1B protein remained constant (data not shown). A similar type of behavior has been reported for SHP-1 and SHP-2, the SH2 domain–containing PTPs.[20] The edematous Cer-induced AP is thus associated with increases in pancreatic PTP1B at the level of both protein and mRNA.

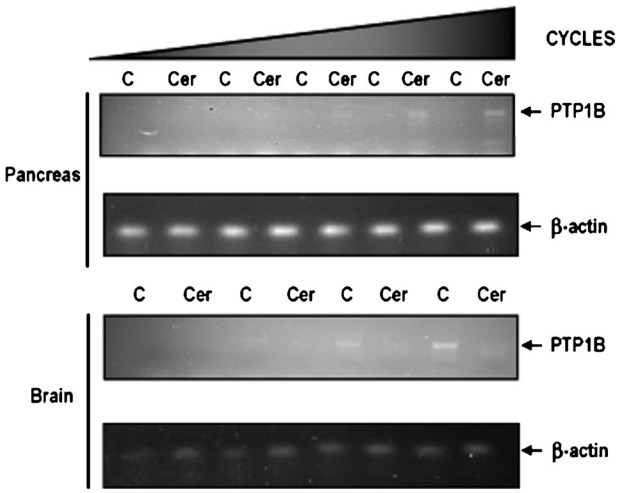

FIGURE 2. PTP1B mRNA expression in the early phase of Cer-induced AP. Rats were either administered saline (0.9% NaCl; control, C) or treated with Cer (P), as indicated in the ''Materials and Methods'' section, and then killed 2 hours after the first injection of Cer. Messenger RNA expression was analyzed in pancreas or brain by RT-PCR. β-actin was used as loading control. A representative RT-PCR is shown. Experiments were repeated in 4 different animals with similar results.

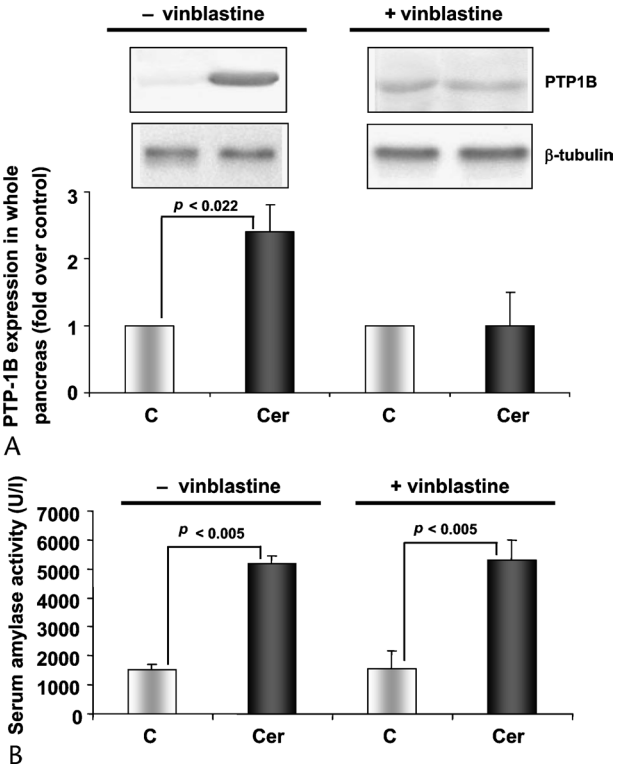

FIGURE 3. Effect of neutropenia on PTP1B protein expression during the development of Cer-induced AP. Rats were given 0.75 mg/kg i.v. vinblastine sulfate to induce neutropenia. After 4 days, these neutropenic rats were given 4 injections of saline (0.9% NaCl) or Cer hourly over 4 hours (representing the intermediate phase of AP) as indicated in the ''Materials and Methods'' section. The same treatments were given to control animals (C; saline instead of vinblastine pretreatment on day 1). Quantification (graphic) of expression (Western blots—a representative is shown) was carried out considering the whole pancreas. Anti–β-tubulin antibody was used as an approximate loading control. Each lane in the blots contained 30 μg of proteins. Data are means ± SD of 4 animals.

Influence of Neutrophil Infiltration

Neutrophil infiltration is an important component in the development of both inflammation and cell death in pancreatitis. We chose to study the intermediate phase of AP (4 hours) because it has been reported that at this time, inflammatory cell infiltration has already started or taken place,[26] as shown in our AP model (Fig. 1C). As expected, neutropenia was associated with the disappearance of neutrophils from the blood: 39% ± 5% and 0% neutrophils in a differential leukocyte count in the blood from Cer-induced AP (4 hours) rats not pretreated or pretreated with vinblastine sulfate, respectively; n = 3 (data not shown). We have previously reported that under the same conditions described here, the Cer treatment (4 hours) caused leukocyte accumulation in the pancreas,[20] whereas the administration of vinblastine resulted in blunted pancreatic myeloperoxidase levels,[20] pointing to the subsequent depletion in situ of neutrophil infiltration after the vinblastine treatment. Figure 3A shows that the depletion of neutrophils in the rats suppressed the increase in PTP1B protein expression at 4 hours after the Cer treatment. In Figure 3B, it may be seen that the vinblastine treatment alone did not affect the serum amylase activity and

that the Cer treatment in the vinblastine-treated rats did not decrease its levels, in agreement with previously reported data.[20,23]

Effect of Rolipram Pretreatment on PTP1B Expression

Based on the aforementioned data obtained on the neutropenic rats, we next analyzed the role of cAMP levels in the increase in the expression of PTP1B in the early phase (2 hours) of AP. This was because it has recently been proposed that intracellular cAMP levels in neutrophils might play an essential role in the pathogenesis of AP because increases in such levels due to rolipram administration attenuate inflammatory diseases including AP.[11] Figure 4A shows that the increase in the PTP1B protein expression due to Cer was suppressed in the rolipram-pretreated rats: 1.0 ± 0.2–fold versus 2.8 ± 0.5–fold higher than that of the control rats (injected with saline+vehicle) for the Cer+ rolipram and Cer+vehicle rats, respectively. Rolipram did not change the PTP1B protein expression in the absence of Cer stimulation (1.1 ± 0.3–fold in the saline+rolipram–injected rats compared with the saline+vehicle–injected rats). On the other hand, rolipram showed a tendency (although not significant) to reduce the serum amylase activity in the rats given Cer+rolipram (Fig. 4B) as reported previously.[23]

Effect of SP600125 Pretreatment on PTP1B Expression

The observation that the severity of the Cer-induced AP was ameliorated after the inhibition of the JNK and ERK1/2 kinases[9] points toward the major role of MAPKs in the development of hyperstimulation-induced pancreatitis. Accordingly, we next investigated whether these 2 MAPKs might play a role in the increase of the expression of PTP1B in the early phase (2 hours) of AP by using SP600125. In Figure 4C, it can be observed that SP600125 pretreatment reduced the increase in the expression of PTP1B after the Cer treatment: 2.9 ± 0.8– and 1.5 ± 0.3–fold compared with control rats (the sal+ vehicle–injected rats) for the Cer+vehicle (dimethyl sulphoxide)– or Cer+ SP600125–injected rats, respectively. There was no significant effect on the expression of PTP1B in the absence of Cer stimulation (0.9 ± 0.3–fold for Sal+SP600125–injected

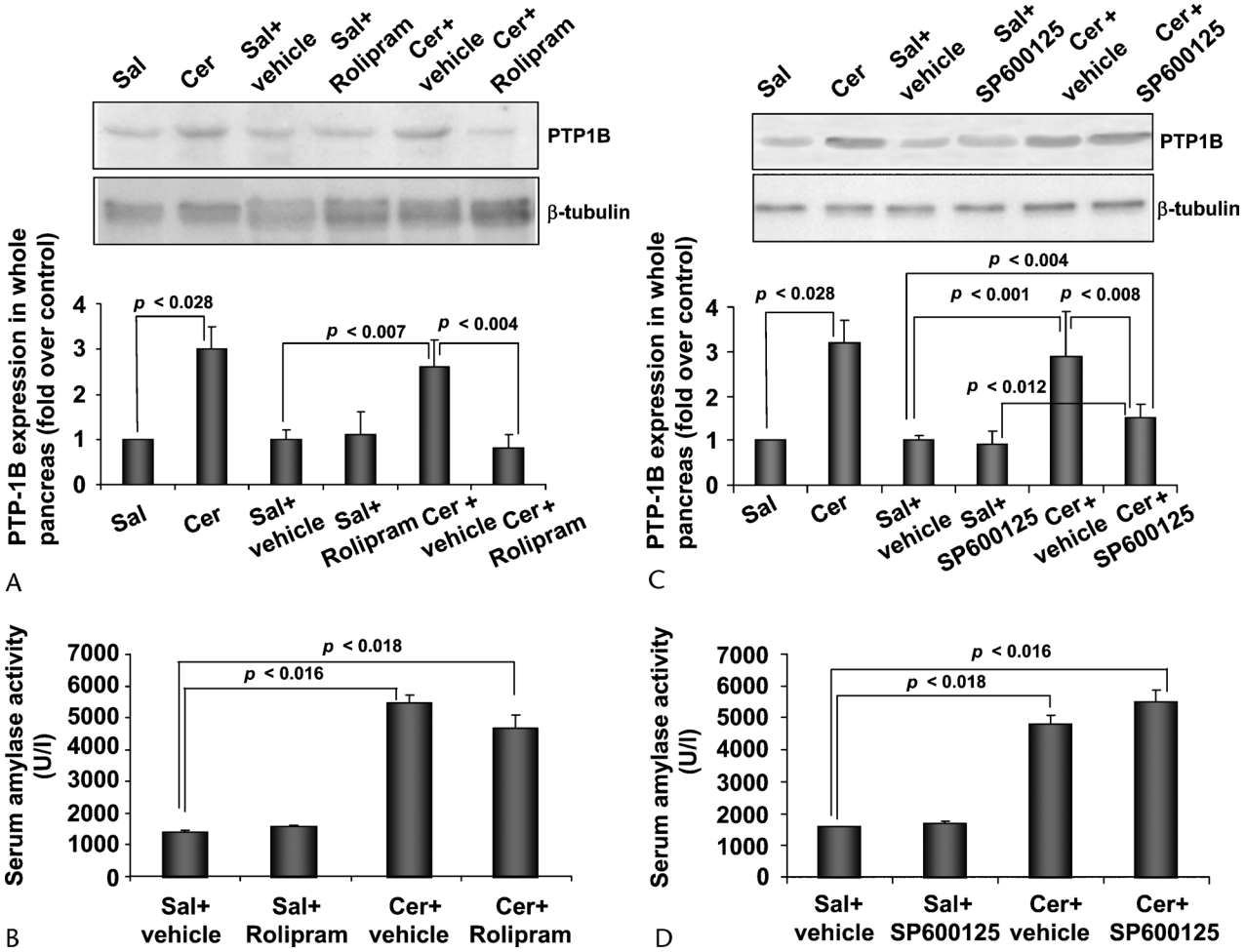

FIGURE 4. Effect of rolipram or SP600125 pretreatment on PTP1B protein expression in the early phase of Cer-induced AP. Rats were pretreated with rolipram or its vehicle (A and B), or with SP600125 or its vehicle (C and D), as indicated in the ''Materials and Methods'' section. Then, the animals were injected subcutaneously with either Cer or its vehicle (20 mg/kg or saline [0.9% NaCl, Sal] in 2 injections at hourly intervals, respectively). As a positive control of the experiments, non-pretreated rats (Sal and Cer) were also included. Quantification (graphics) of expression (Western blots—a representative is shown) was carried out considering the whole pancreas. Anti–β-tubulin antibody was used as an approximate loading control. Each lane in the blots contained 30 μg of proteins. Data are means ± SD of 3 experiments with 3 rats per group in each.

rats compared with control rats). In addition, SP600125 was not able to reduce the significant increase in the serum amylase activity observed in the animals given Cer alone (Fig. 4D), as reported elsewhere.[20]

DISCUSSION

It has been proposed that alterations in gene and/or protein expression within the initiation phase of AP play an important role in its development because such changes might convert the rapid activation of signaling pathways in acinar cells into long-term responses.[1] Taking this into account, in this study, we report an increase in PTP1B in the pancreas at the levels of both protein and mRNA as an early event during the development of the Cer-induced AP, a model that closely mimics clinically relevant AP reflecting a relatively mild edematous pancreatitis.

The data obtained on the neutropenic rats seem to indicate a central role of neutrophil infiltration as a regulator of the PTP1B protein expression because the increase in the expression of PTP1B was not detected in the rats treated with vinblastine sulfate. To further investigate the role of infiltration, we treated rats with rolipram, a strong specific inhibitor of type 4 phosphodiesterase, which is a key enzyme in the metabolism of intracellular cAMP that is abundantly expressed in inflammatory cells such as neutrophils and that also exerts anti-inflammatory effects, probably mediated by the inhibition of diverse leukocyte functions, ie, the production/secretion of proinflammatory cytokines such as tumor necrosis factor–α.[27] Our data support a role for the neutrophil cAMP signaling pathway as a regulator of the PTP1B protein expression in the Cer-induced AP. They are also in accordance with a previous work describing a suppression of inflammatory cell infiltration in the pancreas of rats pretreated with rolipram before Cer administration.[11] A more complex scenario could be considered if acinar cells can behave as true inflammatory cells, also producing proinflammatory cytokines.[28] Accordingly, rolipram might also have an effect in acinar cells. This possibility deserves further investigation, and steps are currently being taken in our laboratory to check whether type 4 phosphodiesterase is present also in acinar cells.

The activation of stress kinases, including JNK and ERK1/2, regulates transcription factors and promotes gene and protein expressions during the early phase (the first 0.5–3 hours) of the Cer-induced AP,[1,9,23,29] thus providing a potential link between the earliest known signaling events in AP and the long-term consequences that stem from changes in gene expression. Therefore, we used the stress kinase inhibitor SP600125 to analyze their potential influence in the observed increase in PTP1B protein. SP600125, under the conditions used here, has been described to almost totally inhibit Cer-induced pancreatic JNK activation and partially inhibit ERK1/2 activation.[9] The underlying mechanism must be complex because SP600125 could target not only pancreatic kinases but also the JNK and ERK1/2 of the infiltrating netrophils, similar to the mitogen-activated protein kinase/extracellular signal-regulated kinase kinase inhibition by U0126 and PD98059 in the Cer-induced AP described previously.[23] Considering that MAPKs have also been shown to up-regulate the expression of inflammatory cytokines such as tumor necrosis factor–α,[9] which also primes cell infiltration in the pancreas, and that SP600125 pretreatment results in a blunted leukocyte accumulation in the pancreata of the Cer-induced AP rats,[9] the effects of SP600125 together with the data on neutropenic rats on PTP1B protein expression in the Cer-induced AP seem to be in good agreement. A link between cAMP and MAPK can be suggested from studies addressing the role of cAMP signaling in the regulation of cell cycle survival of human pancreatic cells. In this system, it has been demonstrated that increasing cAMP levels inhibits ERK cascade.[30] It can therefore be proposed that regardless of whether rolipram and SP600125 target acinar cells, neutrophils, or both cell types, the results obtained with both inhibitors should probably be similar as indeed shown in the present work. Regarding the amylase activity, the findings of this work and those of a previous one[20] support the notion that the observed reduction in such activity after JNK and ERK1/2 inhibition[9] would not occur during the early phase of AP but later in its development.

In summary, in this study, we have detected for the first time an increase in PTP1B in the pancreas, at the level of both protein and mRNA, as an early event during the development of Cer-induced AP in which neutrophil infiltration seems to play an important role. The increase in PTP1B protein expression in the early phase of AP was mostly prevented by type 4 phosphodiesterase and JNK and ERK1/2 inhibition.

ACKNOWLEDGMENTS

The authors thank Dr J. M. González de Buitrago (University of Salamanca) for his help with the amylase determinations and N. Skinner for his assistance in the preparation of the manuscript. β-actin primers were kindly provided by Dr Serrano (University of Salamanca).

REFERENCES

1. Alonso R, Montero A, Arévalo M, et al. Platelet-activating factor mediates pancreatic function derangement in caerulein-induced pancreatitis in rats. *Clin Sci*. 1994;87:85–90.
2. Pescador R, Manso MA, Revollo AJ, et al. Effect of chronic administration of hydrocortisone on the induction and evolution of acute pancreatitis induced by cerulean. *Pancreas*. 1995;11:165–172.
3. Yönetçi N, Oruç N, Ozütemiz AO, et al. Effects of mast-cell stabilization in caerulein-induced acute pancreatitis in rats. *Int J Pancreatol*. 2001; 29:163–171.
4. Zhao M, Xue DB, Zheng B, et al. Induction of apoptosis by artemisin relieving the severity of inflammation in caerulein-induced acute pancreatitis. *World J Gastroenterol*. 2007;14:5612–5617.
5. Ji B, Chen X, Misek DE, et al. Pancreatic gene expression during the initiation of acute pancreatitis: identification of EGR-1 as a key regulator. *Physiol Genomics*. 2003;14:59–72.
6. Rivard N, Rydzewska G, Lods J-S, et al. Pancreas growth, tyrosine kinase, PtdIns 3-kinase, and PLD involve high-affinity CCK-receptor occupation. *Am J Physiol*. 1994;266:G62–G70.
7. Rivard N, Rydzewska G, Lods JS, et al. Novel model of integration of signalling pathways in rat pancreatic acinar cells. *Am J Physiol*. 1995;269:G352–G362.
8. Widmann C, Gibson S, Jarpe MB, et al. Mitogen activated protein kinases: conservation of a three kinase module from yeast to human. *Physiol Rev.* 1999;79:143–180.
9. Minutoli L, Altavilla D, Marini H, et al. Protective effects of SP600125 a new inhibitor of c-*Jun N*-terminal kinase (JNK) and extracellular-regulated kinase (ERK1/2) in an experimental model of cerulein-induced pancreatitis. *Life Sci*. 2004;75:2853–2866.
10. Satoh A, Shimosegawa T, Satoh K, et al. Activation of A1-receptor pathway induces edema formation in the pancreas of rats. *Gastroenterology.* 2000;119:829–836.
11. Sato T, Otaka M, Odashima M, et al. Specific type IV phosphodiesterase inhibitor ameliorates cerulein-induced pancreatitis in rats. *Biochem Biophys Res Commun*. 2006;346:339–344.
12. Feick P, Gilhaus S, Blum IR, et al. Inhibition of amylase secretion from differentiated AR4-2J pancreatic acinar cells by an actin cytoskeleton controlled protein tyrosine phosphatase activity. *FEBS Lett*. 1999;451:269–274.
13. Hernández-Hernández A, Garabatos MN, Rodríguez MC, et al. Structural characteristics of a lipid peroxidation product,

trans-2-nonenal, that favour inhibition of membrane associated phosphotyrosine phosphatase activity. *Biochim Biophys Acta*. 2005;1726:317–325.
14. Sánchez-Bernal C, García-Morales OH, Domínguez C, et al. Nitric oxide protects against pancreatic subcellular damage in acute pancreatitis. *Pancreas*. 2004;28:e9–e15.
15. Bourdeau A, Dubé N, Tremblay ML. Cytoplasmic protein tyrosine phosphatases, regulation and function: the roles of PTP1B and TC-PTP. *Curr Opin Cell Biol*. 2005;17:203–209.
16. Yu J-H, Kim K-H, Kim H. SOCS 3 and PPAR-γ ligands inhibit the expression of IL-6 and TGF-β1 by regulating JAK2/STAT3 signalling in pancreas. *Int J Biochem Cell Biol*. 2008;40:677–688.
17. Case RM. Synthesis, intracellular transport and discharge of exportable proteins in the pancreatic acinar cell and other cells. *Biol Rev Camb Philos Soc*. 1978;53:211–354.
18. Kubish CH, Sans MD, Arumugan T, et al. Early activation of endoplasmic reticulum stress is associated with arginine-induced acute pancreatitis. *Am J Physiol Gastrointest Liver Physiol*. 2006;291: G238–G245.
19. Suyama K, Ohmuraya M, Hirota M, et al. C/EBP homologous protein is crucial for the acceleration of experimental pancreatitis. *Biochem Biophys Res Commun*. 2008;267:176–182.
20. Sarmiento N, Sánchez-Bernal C, Ayra M, et al. Changes in the expression and dynamics of SHP-1 and SHP-2 during cerulein-induced acute pancreatitis in rats. *Biochim Biophys Acta*. 2008;1782:271–279.
21. Wimmer M, Tag C, Schreimer D, et al. Protein tyrosine phosphatase 1B is located with glucagon vesicles, and its concentration is inversely correlated with the rate of glucagon secretion of INR1G9 cells. *J Endocrinol*. 2004;181:437–447.
22. Bradford MM. A rapid and sensitive method for the quantitation of microgram quantities of protein utilizing the principle of protein-dye binding. *Anal Biochem*. 1976;72:248–254.
23. Clemons AP, Holstein DM, Galli A, et al. Cerulein-induced acute pancreatitis in the rat is significantly ameliorated by treatment with MEK1/2 inhibitors U0126 and PD98059. *Pancreas*. 2002;25:251–259.
24. Hernández-Hernández A, Llanillo M, Rodríguez MC, et al. Amphiphilic and hydrophilic nature of sheep and human platelet phosphotyrosine phosphatase forms. *Biochim Biophys Acta*. 1999; 1419:195–206.
25. Hernández-Hernández A, Rodríguez MC, López-Revuelta A, et al. Alterations in erythrocyte membrane protein composition in advanced non-small cell lung cancer. *Blood Cell Mol Dis*. 2006;36:355–363.
26. Mayerle J, Schnekenburger J, Kruger B, et al. Extracellular cleavage of E-cadherin by leukocyte elastase during acute experimental pancreatitis in rats. *Gastroenterology*. 2005;129:1251–1267.
27. Semmler J, Wachtel H, Endres S. The specific type IV phosphodiesterase inhibitor rolipram suppresses tumor necrosis factor-α production by human mononuclear cells. *Int J Immunopharmacol*. 1993;15:409–413.
28. Gukovskaya AS, Gukovsky I, Zaninovic V, et al. Pancreatic acinar cells produce, release, and respond to tumor necrosis factor-alpha. Role in regulating cell death and pancreatitis. *J Clin Invest*. 1997;100: 1853–1862.
29. Hofken T, Keller N, Fleischer F, et al. Map kinase phosphatases (MKPs) are early responsive genes during induction of cerulein hyperstimulation pancreatitis. *Biochem Biophys Res Commun*. 2000; 276:680–685.
30. Boucher MJ, Duchesne C, Lainé J, et al. cAMP protection of pancreatic cancer cells against apoptosis induced by ERK inhibition. *Biochem Biophys Res Commun*. 2001;285:207–216.

RESULTADOS NO PUBLICADOS:

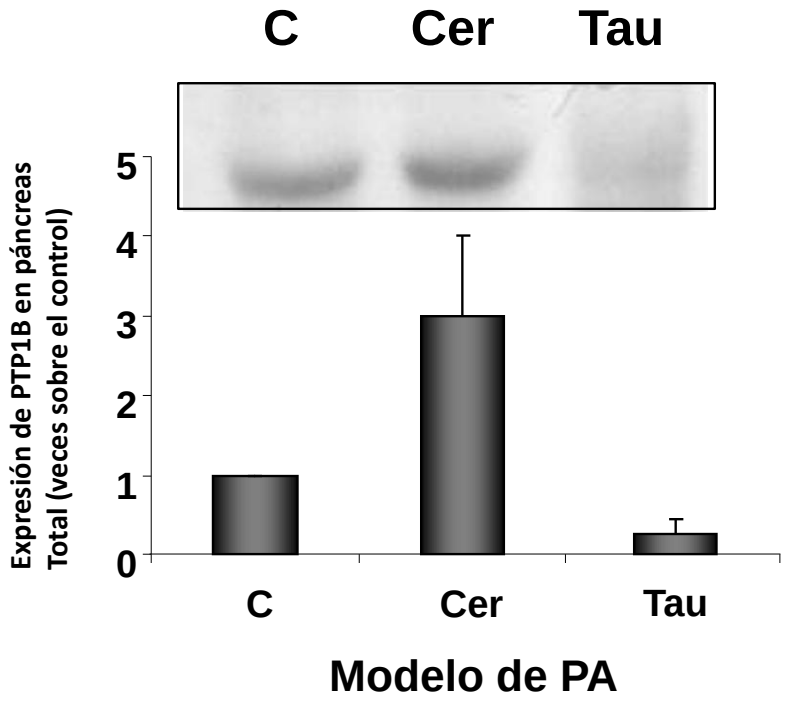

Figura 8. Expresión de PTP1B en diferentes modelos de PA. Se usaron dos modelos distintos de PA, en producido por ceruleína (Cer) y el debido a infusión de taurocolato (Tau). También se muestran las ratas inyectadas con solución salina (0,9% NaCl) (Control, C). Cer representa 9 horas de tratamiento con ceruleína, como se indica en Materiales y Métodos. La cuantificación (gráfico) de la expresión (transferencias de Western, se muestra una representativa) se llevó a cabo considerando el páncreas total. Cada carril en el blot contenía 30 μg de proteínas. Los datos son la media ± DS de 3 animales.

Interpretación. La especificidad del aumento de la proteína PTP1B en el modelo de pancreatitis aguda inducido por ceruleína puede explicarse de dos modos distintos: (1) como una respuesta específica a un insulto específico, de modo similar a la inducción de otros genes por ceruleína o taurocolato (Ref 5 del paper); (2) como resultado de la severidad del modelo de PA, porque mientras que el de ceruleína semeja una pancreatitis aguda edematosa, el modelo del taurocolato representa una pancreatitis hemorrágica. Esta gravedad podría afectar de algún modo a la integridad y/o al intercambio de diferentes proteínas, lo que originaría niveles menores de tales proteínas una vez que la pancreatitis se desarrolle completamente.

- **OBJETIVO 3:** Desarrollar un método para el aislamiento de subpoblaciones de lisosomas de páncreas de rata que nos permita el estudio futuro de las proteínas lisosómicas

Digestive and Liver Disease 43 (2011) 132–138

Contents lists available at ScienceDirect

Digestive and Liver Disease

journal homepage: www.elsevier.com/locate/dld

Liver, Pancreas and Biliary Tract

Changes in the morphology and lability of lysosomal subpopulations in caerulein-induced acute pancreatitis☆

Nancy Sarmiento[a], Jesús Sánchez-Yagüe[a], Pedro P. Juanes[a], Nieves Pérez[a], Laura Ferreira[b], Violeta García-Hernández[a], Arturo Mangas[c], José J. Calvo[d], Carmen Sánchez-Bernal[a,*]

[a] Department of Biochemistry and Molecular Biology, University of Salamanca, Salamanca 37007, Spain
[b] Unit of Research, University Hospital, Salamanca 37007, Spain
[c] Department of Cell Biology and Pathology, University of Salamanca, Salamanca 37007, Spain
[d] Department of Physiology and Pharmacology, University of Salamanca, Salamanca 37007, Spain

ARTICLE INFO

Article history:
Received 11 February 2010
Accepted 21 August 2010
Available online 8 October 2010

Keywords:
Lysosomes
Acute pancreatitis
N-acetyl-β-D-glucosaminidase
Caerulein

ABSTRACT

Background and aims: Lysosomes play an important role in acute pancreatitis (AP). Here we developed a method for the isolation of lysosome subpopulations from rat pancreas and assessed the stability of lysosomal membranes.
Methods: AP was induced by four subcutaneous injections of 20 μg caerulein/kg body weight at hourly intervals. The animals were killed 9 h after the first injection. Marker enzymes [N-acetyl-β-D-glucosaminidase (NAG), cathepsin B and succinate dehydrogenase (SDH)] were assayed in subcellular fractions from control pancreas and in pancreatitis. Lysosomal subpopulations were separated by Percoll density gradient centrifugation and observed by electron microscopy. NAG molecular forms were determined by DEAE-cellulose chromatography.
Results: AP was associated with: (i) increases in the specific activity of lysosomal enzymes in the soluble fraction, (ii) changes in the size and alterations in the morphology of the organelles from the lysosomal subpopulations, (iii) the appearance of large vacuoles in the primary and secondary lysosome subpopulations, (iv) the increase in the amount of the NAG form associated with the pancreatic lysosomal membrane as well as its release towards the soluble fraction.
Conclusions: Lysosome subpopulations are separated by a combination of differential and Percoll density gradient centrifugations. Primary lysosome membrane stability decreases in AP.

1. Introduction

Acute pancreatitis (AP) is an inflammatory disorder of the pancreas that can sometimes be lethal and that has a steadily increasing incidence [1]. In the caerulein (Cer)-induced model of mild pancreatitis intra-acinar zymogen activation plays an essential role [2]. Early on in the course of AP, lysosomal hydrolases colocalize with digestive zymogens, activating them [3–7] and causing acinar cell injury and necrosis [4,8]. However, it has not been totally elucidated how hydrolases and zymogen meet each other. Lysosomes are the site of degradation of both the extracellular macromolecules introduced by endocytosis and phagocytosis, and intracellular material by autophagy mechanisms [9–11]. In fact, autophagy accelerates trypsinogen activation by lysosomal hydrolases under acidic conditions, thus triggering AP in its early stage [12]. A decrease in the stability of the lysosomes in AP has also been proposed [4,13–15].

N-acetyl-β-D-glucosaminidase (NAG, EC 3.2.1.30) is a lysosomal hydrolase that exists in two major isoforms: A and B. These enzyme forms were first described by Robinson and Stirling [16] and are characterized by their acidic optimum pH, their different p*I* and their thermostability. NAG is a marker enzyme for lysosomes, but while the B form is bound to the lysosomal membrane, the A form remains soluble inside the organelle. Although variations in total NAG activity in the pancreas have been described previously in different experimental models of AP [14,15,17], the molecular forms of this enzyme have not been analyzed, and neither have the isolation and analysis of the pancreatic lysosome (sub)population(s) been carried out in AP, in spite of their role in the disease. Accordingly, the purpose of the present study was: (1) to develop a procedure for the separation of different subpopulations of rat pancreatic lysosomes, checking their changes in AP by electron microscopy; (2) to assess, by ion-exchange chromatography of the molecular forms of NAG, the stability of the pancreatic lysosomal membranes in AP.

☆ *Supported by*: FIS (PS09/01075) and Junta de Castilla y León (Biomedicina SAN673/SA10/08, SA033A05, and SA126A07) of Spain.
* Corresponding author. Tel.: +34 923 294526; fax: +34 923 294576.
E-mail address: csabe@usal.es (C. Sánchez-Bernal).

1590-8658/$36.00
doi:10.1016/j.dld.2010.08.009

The procedure of lysosome isolation should provide information for future investigations addressing pancreatitis.

2. Materials and methods

2.1. Animals

Male Wistar rats (weighing 250–280 g) were housed in rooms maintained at 22 ± 1 °C using a 12-h light/dark cycle. Animals were fasted 24 h before the experiment but had free access to water. Care was provided in accordance with the procedures outlined in European Community guidelines on ethical animal research (86/609/EEC), and the protocols were approved by the Animal Care Committee of the University of Salamanca.

2.2. Induction and histological assessment of AP, and sample preparation

AP was induced as previously described [18,19]. Briefly, rats received four subcutaneous injections of 20 μg of Cer/kg body weight at hourly intervals. Nine hours after the first injection, the animals were killed by cervical dislocation. Control rats were injected with equivalent volumes of saline. AP was assessed by light microscopy (haematoxylin and eosin staining) as reported previously [19].

Whole pancreata were obtained immediately after the rats had been killed. Pancreata were dissected from the surrounding fat tissue and a small portion of them was used for haematoxylin and eosin staining [19]. The remaining parts of the pancreata were homogenized with a Potter Elvehjem device in 10 volumes (w/v) of homogenization buffer (3 mM imidazole buffer, pH 7.4 containing 0.25 M sucrose, 1 mM EDTA and 100 μg/ml trypsin inhibitor). In order to have enough material to achieve each aims of the research, 4 pancreata corresponding to 4 control or 4 pancreatitic animals, respectively, were homogenized together in each experiment. Then, subcellular fractionation was carried out in the postnuclear homogenate following a method in which lysosomes were coprecipitated with mitochondria at 20,000 × *g* after separation of the zymogen fraction at 1300 × *g*, as described previously by us [18,20]. Four subcellular fractions were obtained: the zymogen (Z), the lysosome plus mitochondria (L + M), the microsome (Mic) and the soluble (S) fractions. NAG, cathepsin B and succinate dehydrogenase (SDH) were determined in all four subcellular fractions isolated. Data from 7 independent experiments ($n = 7$) were used for the characterization of the subcellular fractions from pancreas and the lysosomal subpopulations, electron microscopy and ionic exchange chromatography, respectively. Detergent analysis and the determination of NAG thermal stability was performed in 5 independent experiments ($n = 5$).

2.3. Biochemical assays

NAG was assayed by mixing 50 μl of a suitably diluted sample with 100 μl of the appropriate 3 mM 4-methylumbelliferyl substrate in 0.1 M sodium citrate buffer, pH 4.5. After 30 min at 37 °C, the reaction was stopped and fluorescence was developed by the addition of 2 ml of 0.5 M glycine–NaOH buffer, pH 10.4. The 4-methylumbelliferone fluorescence released was measured using a spectrofluorimeter at 465 nm (excitation at 340 nm). The spectrofluorimeter was calibrated with freshly prepared 4-methylumbelliferone in 0.5 M glycine–NaOH buffer, pH 10.4. One unit of enzyme activity (U) was defined as nmol of methylumbelliferone released/h under the assay conditions. Cathepsin B (EC 3.4.22.1) was assayed according to Mc Donald and Ellis [21], with CB-ala-arg-arg-4-methoxy-β-naphthylamide as a substrate at 20 °C. SDH (EC 1.3.99.1) was determined spectrophotometrically, following the method described by Pennington [22]. Serum amylase was measured as reported previously [18,19]. Protein concentrations were assayed according to Marxwell et al. [23], using bovine serum albumin as the standard.

2.4. Percoll gradient

Aliquots (0.5 ml) of the L + M fractions diluted three times with homogenization buffer were layered on top of discontinuous gradients consisting of three layers of isotonic 17%, 10% and 5% Percoll solutions (3.8 ml each) prepared in homogenization buffer and placed from the bottom of the tube upwards, respectively. The density partial-gradients were then formed by centrifugation at 50,500 × *g* for 30 min in a Beckman SW40 rotor. Aliquots of 0.5 ml were collected from the top of the gradient tube with a Pasteur pipette and assayed for NAG and SDH activities. The aliquots showing the peak of the major NAG activity of the gradient (band 1 in Fig. 2) were pooled, dialyzed and used for DEAE-cellulose chromatography. For the calibration of the Percoll density gradients, density marker beads were used, following the manufacturer's instructions.

For electron microscopy, three bands of organelles were recovered close to the interfaces of the density gradients. Each band was collected with a Pasteur pipette, diluted with homogenization buffer and washed by centrifugation at 50,000 × *g* for 15 min to remove the Percoll reagent. The organelles, which were located above the Percoll pellet, were finally transferred to Eppendorf tubes and used immediately for electron microscopy.

2.5. Electron microscopy

The organelles were washed in ice-cold 0.1 M sodium phosphate buffer, pH 7.4, containing 6.8% sucrose and 1% $CaCl_2$ (buffer A) and were then fixed in 5% glutaraldehyde in buffer A. Following this, the samples were suspended in agar and slices containing the organelles were fixed again in 3% glutaraldehyde in buffer A. After washing in buffer A, the pellets were post-fixed in 1% OsO_4 in buffer A. Finally, the samples were dehydrated in a series of acetone and propylene oxide and were embedded in Durcupan resin, sectioned, and post-stained with 2% uranyl acetate and 2% Pb-citrate. Sections were cut on an Ultracut E (Reichert-Jung) ultramicrotome and examined under a Zeiss EM 900 electron microscope.

Estimates for the size of the organelles in each band were obtained by randomly evaluating the fields (25–30 for first and second bands, eight for third band), at a magnification of 50,000×, with a total of about seven hundred organelles assessed, for each control or pancreatitic sample. Results are expressed both in control and pancreatitic groups in terms of percent relative abundance within the populations of vesicle sizes analyzed.

2.6. Separation of pancreatic NAG isoenzyme by DEAE-cellulose ion-exchange chromatography

Percoll-separated lightest (primary) lysosome or soluble fraction samples were dialysed at 4 °C against elution buffer (10 mM sodium phosphate buffer, pH 7.0: buffer B). Dialyzed samples were loaded on to the top of a 2 ml disposable syringe packed with 2 ml of DEAE-cellulose and the elution buffer was applied to obtain the unadsorbed proteins. Bound proteins were then eluted in a linear gradient (0–0.3 M sodium chloride) in 20 ml of elution buffer. Fractions of 0.4 ml were collected, and NAG activity was determined as indicated above. Protein contents were monitored by measuring absorbance at 280 nm. The activity present in each peak was expressed as a percentage of the activity recovered in the total peaks.

Table 1
Specific activities of marker lysosomal and mitochondrial enzymes in subcellular fractions from rat pancreas.

Enzyme	Homogenate		Zymogens		Lysosomes + mitochondria		Microsomes		Soluble	
	C	P	C	P	C	P	C	P	C	P
NAG	3.70 ± 0.29	4.07 ± 0.33	6.40 ± 0.57	9.75 ± 1.15	4.90 ± 0.29	6.90 ± 0.78	3.43 ± 0.39	3.20 ± 0.40	2.50 ± 0.26	2.22 ± 0.25
Cathepsin B	0.40 ± 0.03	0.41 ± 0.04	0.64 ± 0.03	0.56 ± 0.04	0.72 ± 0.05	0.61 ± 0.04	0.02 ± 0.01	0.04 ± 0.01	0.37 ± 0.02	0.50 ± 0.02
SDH	0.90 ± 0.06	0.53 ± 0.03	1.96 ± 0.17	1.13 ± 0.09	1.85 ± 0.15	1.64 ± 0.11	0.19 ± 0.02	0.13 ± 0.02	0.30 ± 0.01	0.14 ± 0.01

Values are means ± S.D. of specific activity expressed as nmol product released/h per mg protein.

2.7. Detergent analysis

L + M samples were solubilised with 0.5% of the non-ionic detergent IGEPAL CA-630 for 30 min, dialyzed against buffer B, and finally applied to DEAE-cellulose as indicated above. The percentages of the NAG forms were compared to those from samples not treated with the detergent.

2.8. Thermal stability

Diluted primary lysosome samples were incubated at 45 °C. Samples were removed at different times and assayed for NAG activity under standard conditions.

2.9. Statistical analyses

Data are expressed as means ± S.D. They were analyzed using the Mann–Whitney *U* non-parametric test. Statistical significance was considered for a *P*-value <0.05. The confidence interval was 95%. Analyses were implemented using the SPSS program for MS Windows (version 18.0).

3. Results

One of the animal models of human oedematous pancreatitis is that induced in the rat by Cer. Here, the establishment of AP was monitored by light microscopy and serum amylase determination (data not shown): (1) histological sections of the pancreata showed normal acini and no infiltration in the control animals, but tissue disorganization and numerous leukocytes adhering to the vascular endothelium and also outside the vessels surrounding the acini were observed in the pancreatitic animals; (2) serum amylase activity increased significantly in AP (1220 ± 70 U/l vs 12,450 ± 3850 U/l, $P < 0.006$, in control and pancreatitic rats, respectively). All these features are consistent with those described previously [18,19,24–26].

3.1. Marker enzyme activities in the subcellular fractions from pancreas

Table 1 shows the distribution of the marker enzymes in the different subcellular fractions. With respect to the homogenates, the L + M fraction was enriched: (i) 1.3-fold ($P < 0.05$) and 1.7-fold ($P < 0.01$), and 1.8-fold ($P < 0.001$) and 1.5-fold ($P < 0.05$), in NAG and cathepsin B activities (marker enzymes for lysosomes), (ii) 2-fold ($P < 0.001$) and 3.1-fold ($P < 0.001$) in SDH activity (a marker enzyme for mitochondria) in control and pancreatitic samples, respectively. By contrast, the degree of enrichment of the Mic and S fractions in the three marker enzymes was lower than in the homogenates. These data support the notion that the L + M fraction was enriched in lysosomes and mitochondria. Additionally, NAG specific activity increased significantly in both the Zymogen and L + M fractions from pancreatitic rats when compared with the control group ($P < 0.05$). At least for the L + M fraction, this is probably due to the decrease in the amount of proteins from this fraction (see below). As shown in Fig. 1, 50% of both the total NAG (Fig. 1A) and cathepsin B (Fig. 1B) activity was located in the L + M fraction from control pancreas. This value decreased to 38% and 22% in the case of the pancreatitic samples ($P < 0.01$), and this was accompanied by a concomitant increase in the marker enzyme activities of the S fraction ($P < 0.01$). Regarding total SDH activity (Fig. 1C), almost

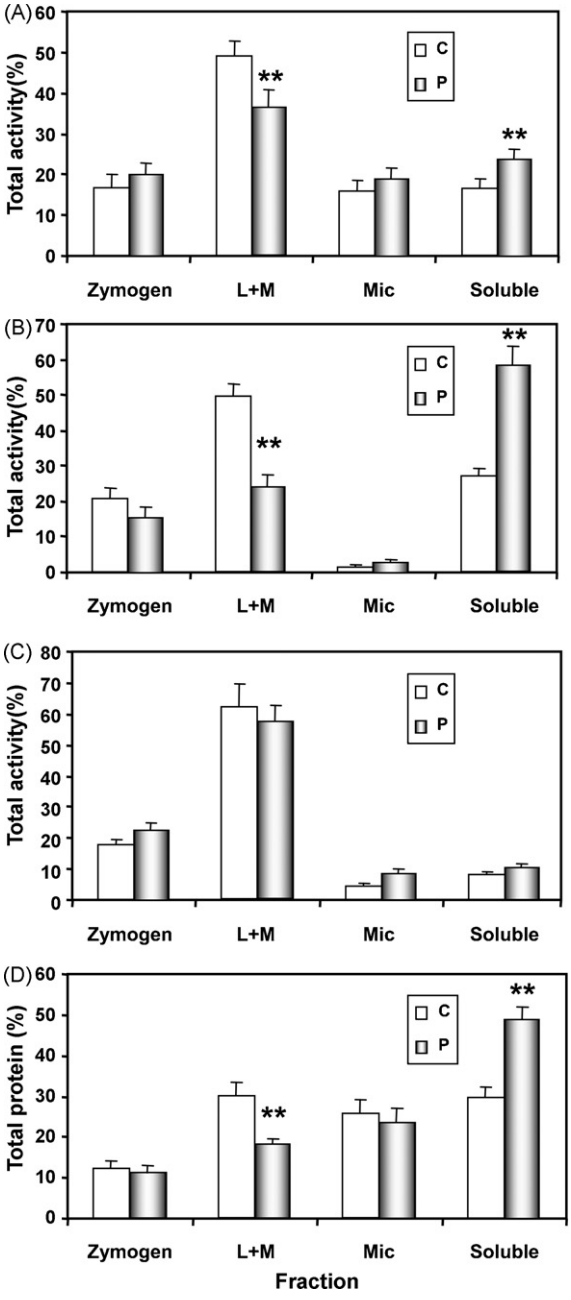

Fig. 1. Percentage distribution of NAG (panel A), Cathepsin B (panel B), SDH (panel C) and total proteins (panel D) in subcellular fractions from pancreas of control (C) and pancreatitic (P) rats. $^{**}P < 0.01$.

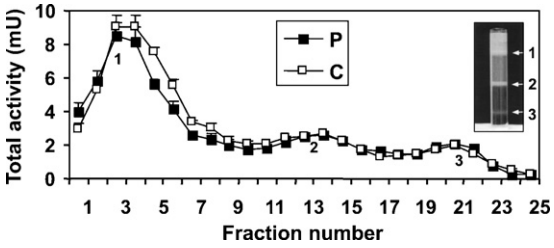

Fig. 2. Total NAG activity in each Percoll gradient fraction in pancreatic L + M subcellular fraction from control (C) and pancreatitic (P) rats. The photograph represents a density gradient tube showing the position of the three bands.

60% was located in the L + M fraction in both control and pancreatitic pancreas. Moreover, AP was associated with a decrease in the amount of total proteins from the L + M fraction ($P < 0.01$) that was closely paralleled by an increase in the S fraction ($P < 0.01$) (Fig. 1D). The recovery of all the above-mentioned marker enzymes, calculated with respect to the homogenates, was close to 100% (range 88–104%, data not shown). Accordingly, leakage of the lysosomal enzymes was clearly accelerated in the pancreatitic group as compared with the control group.

3.2. Isolation of lysosomes from rat pancreas

The L + M fraction was subjected to a discontinuous Percoll gradient. In both control and pancreatitic pancreas NAG activity was distributed in three peaks along the gradient, such peaks coinciding with three bands of organelles (Fig. 2A, photography). Accordingly, these three bands included the lysosome populations. SDH activity was only distributed in the two peaks corresponding to the densest bands of organelles, although such activity was low. Often, the highest SDH activity was obtained at the bottom of the tube (data not shown).

Considering the sum of total proteins present in the lysosome subpopulations as 100%, band 1 represented more than 80% ($86.5 \pm 5.0\%$ and $80.8 \pm 7.0\%$ in the control and pancreatitic pancreata, respectively). A tendency, although not significant, towards an increase in the amount of proteins included in band 2, probably at the expense of band 1, was observed in pancreatic pancreata ($12.1 \pm 5.9\%$ vs $17.8 \pm 6.5\%$ in control and pancreatitic pancreata, respectively). Finally, band 3 represented only 2% of total proteins ($2.1 \pm 1.2\%$ and $2.0 \pm 0.4\%$ in control and pancreatitic pancreata, respectively).

3.3. Electron microscopy studies of lysosome subpopulations

In order to collect structural information about the bands obtained in the Percoll gradient, electron microscopy observations were performed. Each band was seen to have an essentially different morphology, indicating a good separation from the other bands.

The first band contained the less dense (1.030 g/ml) organelles, which in the case of the control samples had a uniform appearance with little material (Fig. 3, 1C). This population was devoid of mitochondria, as indicated above. Accordingly, this band must include primary lysosomes and endosomes. It was observed that the single lysosomal membrane had a characteristic electron-lucent halo on its luminal side. The sizes of the vesicles (data not shown) ranged between 0.05–0.2 and 0.05–0.55 μm for the control and pancreatitic pancreata, respectively (see Fig. 3, 1P, arrow for a 0.55 μm vacuole). Accordingly, pancreatitis is associated with the presence of larger vesicles in this first band (25% of the total). The second band contained slightly denser vesicles (1.037 g/ml) with internal membrane fragments and even smaller vesicles inside. Thus, this band must include late endosomes (secondary lysosomes, arrowhead) (Fig. 3, 2C), although smaller vesicles were observed, with a size ranging between 0.05–0.45 and 0.05–0.70 μm for the control and pancreatitic samples, respectively (data not shown). The third band had the densest organelles (1.043 g/ml), including multivesicular bodies which contained large numbers of internal vesicles and material inside (i.e. Fig. 3C shows a double-membrane vesicle – autophagosome). This band contained the largest organelles, although their dimensions varied considerably (0.1–1.6 and 0.05–0.75 μm for the control and pancreatitic pancreata respectively, data not shown), and sometimes, in control samples, vacuoles as large as 1.6 μm with smaller vesicles inside were observed. It should be noted that the amount of material in this population was scant, hindering its morphological analysis.

3.4. Patterns of pancreatic NAG isoenzymes

Since primary lysosomes corresponded mainly to the upper band of the Percoll gradient, the remaining experiments were carried out with this lysosome-enriched subpopulation. Two peaks of glucosaminidase activity (Fig. 4) were observed with ion-exchange chromatography. The first peak (form I) eluted with the equilibration buffer from a DEAE-cellulose column equilibrated at pH 7.0. When a KCl gradient was applied to the column, an additional major peak (form II) was detected. In control pancreas, the I and II forms represented 3.7% and 96.3% of the total enzyme activity, respectively (Fig. 4A). In pancreatitic pancreas, a 4.4-fold increase in form I (16.5% and 83.5% of the total enzyme activity for forms I and II, respectively) was observed (Fig. 4B).

In the S fraction from control pancreas, the relative percentages of enzyme activity were 2.1% and 97.9% for forms I and II, respectively (Fig. 4C). A 5.4-fold increase was detected in the percentage of form I in pancreatitic pancreas (Fig. 4D).

When a L + M sample from control pancreas was treated with the non-ionic detergent IGEPAL CA-630, dialyzed, and finally subjected to DEAE-cellulose, a 3.7-fold increase in the percentage of form I (10.8% vs. 2.9% in detergent treated vs. non treated sample) was observed (data not shown).

3.5. Thermal stability

The two NAG forms from the primary lysosomes showed a different degree of stability when they were heated. Form II proved to be more labile than form I (Fig. 5), since after 60 min at 45 °C the remaining enzyme activity was 70% and 25% for forms I and II, respectively.

4. Discussion

The excess of Cer, a cholecystokinin analogue, stimulation leads to abnormally high secretion of digestive enzymes, resulting in AP. The pancreas of this model is histologically quite similar to the early phase of acute pancreatitis in humans [27]. The main goal of this study was to develop a procedure to isolate primary lysosomes from rat pancreas in order to assess the stability of lysosomal membranes in Cer-induced AP.

Pancreatic lysosomal enzymes were not only present in the fraction enriched in lysosomes. They also appeared in: (i) the zymogen fraction, probably because they are normal components of granule contents, since the segregation of lysosomal and digestive enzymes seems to be incomplete in normal acinar cells [17,28,29]; (ii) the soluble fraction, since some lysosomal hydrolases, even under physiological conditions, undergo regulated secretion from pancreatic acinar cells [6,30]. These processes have mostly been attributed to a secretagogue-dependent diversion of the enzymes into zymogen granules [31] and secretory lysosomes [32,33], which

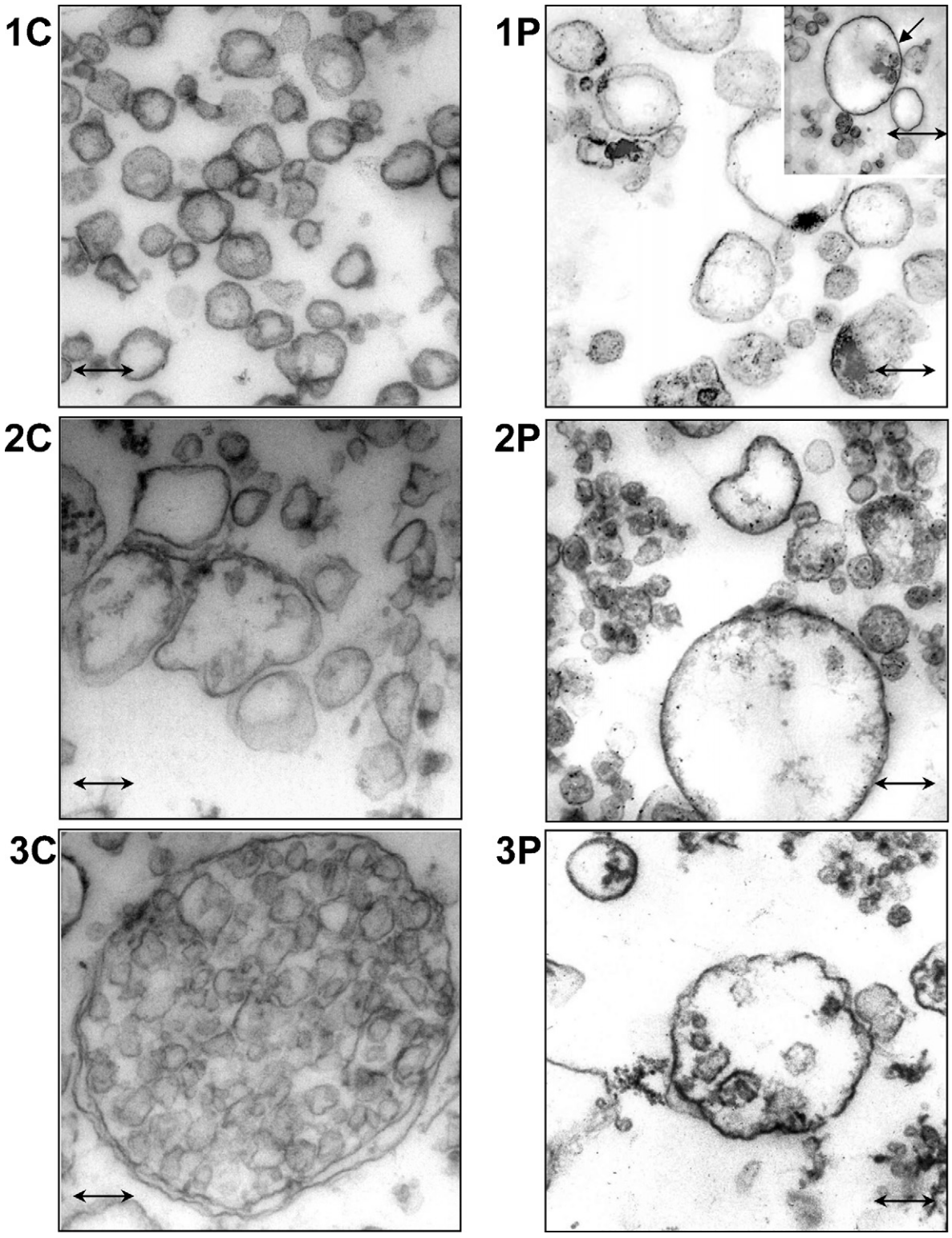

Fig. 3. Electron micrographs of isolated rat pancreas lysosomal subpopulations. 1–3: Percoll bands. C: control rat; P: pancreatitic rat. Insert micrograph in 1P: the arrow indicates a 0.55 μm vacuole (↔: 0.18 μm; insert micrograph in 1P, ↔: 0.59 μm) (50,000×).

could explain how lysosomal hydrolases can emerge from cells. Thus, the enzymes will appear in the soluble fraction after a differential centrifugation of a pancreatic homogenate.

The increase in cathepsin B and total NAG activities in the soluble fraction from pancreatitic animals reflects an alteration in pancreatic lysosomal stability, and is consistent with previously reported data [3,4,13–15,34–38]. Also, supramaximal Cer stimulation has been associated with increases in cathepsin B gene expression [39]. The slight increase in NAG activity in the zymogen fraction after the induction of the pancreatitis could be due to a redistribution of the lysosomal and digestive enzymes, as reported by other authors [4,17].

Regarding the Percoll-separated lysosomal populations, in non-pancreatitic samples electron microscopy confirmed the

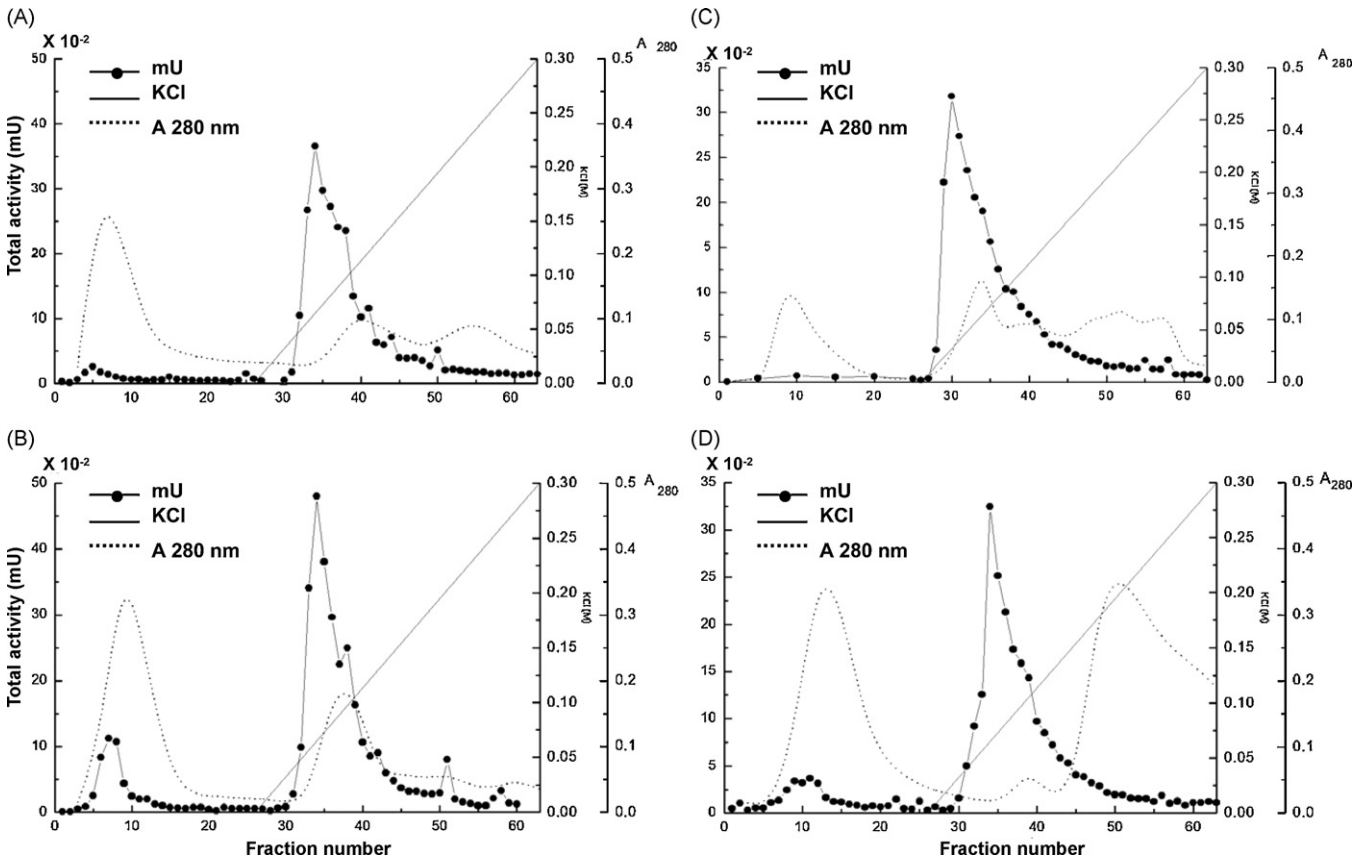

Fig. 4. DEAE-cellulose elution profiles of pancreatic NAG from lysosomal Percoll light (panels A and B) or soluble (panels C and D) fractions from control (panels A and C) and pancreatitic (panels B and D) rats. (●): NAG activity, (. . .): absorbance at 280 nm. A representative experiment is shown.

homogeneity of the light fraction in which the primary lysosomes are located. The observed luminal halo would probably be due to the highly glycosylated luminal domains of lysosomal membrane proteins. Moreover, the NAG activity would be due to both the acid hydrolases already contained in the primary lysosomes and to the newly synthesized lysosomal enzymes that are introduced into the endocytic pathway through early endosomes, and even via the plasma membrane [40–42]. The secondary lysosomes were mainly located in the intermediate band. The larger cytoplasmic vacuoles observed for this population in the pancreatitic samples would probably correspond to vesicles with increased lysosomal enzyme activities, as has been proposed previously [36].

Finally, most of the organelles present in the densest lysosome population might be formed by multiple fusion and fission cycles between multivesicular bodies and lysosomes [43–45]. The presence of the smallest (<0.05) free vesicles detected especially in the second and third fractions from the pancreatitic samples might be due not only to a higher density of such vesicles, but also, at least in part, to their release from larger organelles, whose membranes would be more fragile, probably due to changes in their composition [46]. Additionally, it has been reported that during infusion with supramaximal doses of Cer, cathepsin B-containing organelles become progressively more fragile [4]. Also, a close relationship between the fragility of subcellular organelles and the pathogenesis of AP has been suggested by other authors [47]. Although the first (light) Percoll-separated lysosomal population exhibited the highest glucosaminidase activity, the other two lysosomal populations also displayed NAG activity due to condensing vacuoles, in which lysosomal enzymes are normally present. Thus, the gradient was able to resolve the primary and secondary lysosomes (bands 1 and 2).

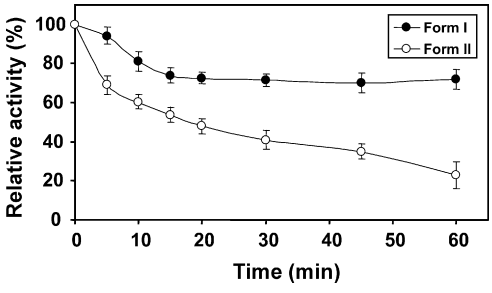

Fig. 5. Thermal stability of the NAG I (●) and II (○) forms at 45 °C.

Since the integrity of endosomes and lysosomes is fundamental for a suitable separation of digestive proteins [48], the greater fragility of the organelles described here could be fatal for pancreatic tissue and would lead to the release of enzymes, with the consequent danger for acinar cells.

Regarding the NAG molecular forms, since form I was less electronegative and thermosensitive than form II and was essentially located in the lysosomal membrane, the NAG I and II forms reported here could correspond to the previously described B and A forms, respectively [16]. Our data also support the notion that putative lysosomal damage occurring during pancreatitis would lead to an increase in both the total and form I NAG in the pancreatic soluble fraction. Such an increase could be indicative of the intensity of lysosomal alterations, as previously proposed [49]. Alternatively, it has also been proposed that an increase in lysosomal fragility might also occur during stimulated pancreatic secretion [13].

In conclusion, we have developed a method for the separation of different subpopulations of pancreatic lysosomes by using a combination of differential centrifugation and a discontinuous Percoll

density gradient. The organelles isolated are suitable for the investigation of lysosomal proteins. Moreover, changes in the morphology and size of such organelles and an alteration of membrane integrity of primary lysosomes during AP have been demonstrated. Finally, the altered dynamics of the NAG molecular forms observed in AP provides additional information as an indicator of lysosomal membrane damage.

Conflict of interest statement

No potential conflicts of interest were disclosed.

References

[1] Frossard JL, Steer ML, Pastor CM. Acute pancreatitis. Lancet 2008;371:143–52.
[2] Saluja AK, Lerch MM, Phillips PA, et al. Why does pancreatic overstimulation cause pancreatitis? Ann Rev Physiol 2007;69:249–69.
[3] Watanabe O, Baccino FM, Steer ML, et al. Supramaximal caerulein stimulation and ultrastructure of rat pancreatic acinar cell: early morphological changes during development of experimental pancreatitis. Am J Physiol 1984;246:G457–67.
[4] Saluja AK, Hashimoto S, Saluja M, et al. Subcellular redistribution of lysosomal enzymes during caerulein-induced pancreatitis. Am J Physiol 1987;253:G508–16.
[5] Halangk W, Lerch MM. Early events in acute pancreatitis. Clin Lab Med 2005;25:1–15.
[6] van Acker GJD, Perides G, Steer ML. Co-localization hypothesis: a mechanism for the intrapancreatic activation of digestive enzymes during the early phases of acute pancreatitis. World J Gastroenterol 2006;12:1985–90.
[7] Cosen-Binker LI, Gaisano HY. Recent insights into the cellular mechanisms of acute pancreatitis. Can J Gastroenterol 2007;21:19–24.
[8] Dlugosz JW, Triebling AT, Brzozowski J. The role of lysosomal alterations in the damage to the pancreas and liver in acute experimental pancreatitis in dogs. Mater Med Pol 1993;25:119–25.
[9] De Duve C. Lysosomes revisited. Eur J Biochem 1983;137:391–7.
[10] Kornfeld S, Mellman I. The biogenesis of lysosomes. Annu Rev Cell Biol 1989;5:483–525.
[11] Kunziker W, Geuze HJ. Intracellular trafficking of lysosomal membrane proteins. BioEssays 1996;118:379–89.
[12] Ohmura M, Yamamura KI. Autophagy and acute pancreatitis: a novel autophagy theory for trypsinogen activation. Autophagy 2008;4:1060–2.
[13] Wilson JS, Korsten MA, Apte MV, et al. Both ethanol consumption and protein deficiency increase the fragility of pancreatic lysosomes. J Lab Clin Med 1990;115:749–55.
[14] Baniukiewicz AA, Dlugosz JW, Gabryelewicz A. The lysosomal hydrolases in the rat pancreas after maximal or supramaximal stimulation with cerulein. Int J Pancreatol 1994;16:71–9.
[15] Guillaumes S, Blanco I, Villanueva A, et al. Activity and subcellular distribution of lysosomal enzymes in acute pancreatitis induced by CDE diet in mice. Gastroenterol Hepatol 1996;19:146–52.
[16] Robinson D, Stirling J. N-acetyl-β-glucosaminidases in human spleen. Biochem J 1968;107:321–7.
[17] Willemer S, Bialek R, Adler G. Localization of lysosomal and digestive enzymes in cytoplasmic vacuoles in caerulein-pancreatitis. Histochemistry 1990;94:161–70.
[18] Sarmiento N, Sánchez-Bernal MC, Ayra M, et al. Changes in the expression and dynamics of SHP-1 and SHP-2 during caerulein-induced acute pancreatitis in rats. Biochim Biophys Acta 2008;1782:271–9.
[19] Sarmiento N, Sánchez-Bernal MC, Pérez-González MN, et al. Rolipram and SP600125 suppress the early increase in PTP1B expression during caerulein-induced pancreatitis in rats. Pancreas 2009;39:639–45.
[20] Sánchez-Bernal C, García-Morales OH, Domínguez C, et al. Nitric oxide protects against pancreatic subcellular damage in acute pancreatitis. Pancreas 2004;28:e9–15.
[21] Mc Donald JK, Ellis S. On the substrate specificity of cathepsin B_1 and B_2 including a new fluorogenic for cathepsin B_1. Life Sci 1975;17:1269–76.
[22] Pennington RJ. Biochemistry of distrophic muscle, mitochondrial succinatetrazolium reductase adenosine triphosphatase. Biochem J 1961;80:649–54.
[23] Marxwell MAK, Haas SM, Bieber LL, et al. A modification of the Lowry procedure to simplify protein determination in the membrane and lipoprotein samples. Anal Biochem 1978;87:206–10.
[24] Alonso R, Montero A, Arévalo M, et al. Platelet-activating factor mediates pancreatic function derangement in caerulein-induced pancreatitis in rats. Clin Sci 1994;87:85–90.
[25] Yönetçi N, Oruç N, Ozütemiz AO, et al. Effects of mast-cell stabilization in caerulein-induced acute pancreatitis in rats. Int J Pancreatol 2001;29:163–71.
[26] Zhao M, Xue DB, Zheng B, et al. Induction of apoptosis by artemisin relieving the severity of inflammation in caerulein-induced acute pancreatitis. World J Gastroenterol 2007;14:5612–7.
[27] Cheung YC, Leung PS. Acute pancreatitis: animal models and recent advances in basic research. Pancreas 2007;34:1–14.
[28] Hirano T, Saluja A, Ramarao P, et al. Effects of chloroquine and methylamine on lysosomal enzyme secretion by rat pancreas. Am J Physiol 1992;262:G344–439.
[29] Hirano T. Lysosomal enzyme secretion into pancreatic juice in rats injected with pancreatic secretagogues and augmented secretion after short-term pancreatic duct obstruction. Nippon Geka Hokan 1994;63:21–35.
[30] Rinderknecht H, Renner IG, Koyama HH. Lysosomal enzymes in pure pancreatic juice from normal healthy volunteers and chronic alcoholic. Dig Dis Sci 1979;24:180–6.
[31] Hirano T, Manabe T, Saluja AK, et al. Pancreatic secretion of lysosomal enzymes stimulated by intraduodenal instillation of a liquid meal in rabbits. Clin Sci (Lond) 1992;83:277–80.
[32] Grondin G, Beaudoin AR. Immunocytochemical and cytochemical demonstration of a novel selective lysosomal pathway (SLP) of secretion in the exocrine pancreas. J Histochem Cytochem 1996;44:357–68.
[33] Andrews NW. Regulated secretion of conventional lysosomes. Trends Cell Biol 2000;10:316–21.
[34] Lampel M, Kerrn HF. Acute interstitial pancreatitis in the rat induced by excessive doses of a pancreatic secretagogue. Virchows Arch A Pathol Anat Histol 1977;373:97–117.
[35] Adler G, Rohr G, Kern HF. Alteration of membrane fusion as a cause of acute pancreatitis in the rat. Dig Dis Sci 1982;27:993–1002.
[36] Adler G, Hahn C, Kern HF, et al. Cerulein-induced pancreatitis in rats: increased lysosomal enzyme activity and autophagocytosis. Digestion 1985;32:10–8.
[37] Saluja AK, Saito I, Saluja M, et al. In vivo rat pancreatic acinar cell function during supramaximal stimulation with caerulein. Am J Physiol 1985;249:G702–10.
[38] Saito I, Hashimoto S, Saluja A, et al. Intracellular transport of pancreatic zymogens during caerulein supramaximal stimulation. Am J Physiol 1987;253:G517–26.
[39] Yuan S, Rosenberg L, Ilieva A, et al. Early changes of gene expression during cerulein supramaximal stimulation. Pancreas 1999;19:45–50.
[40] Peters C, Braun M, Weber B, et al. Targeting of a lysosomal membrane protein: a tyrosine-containing endocytosis signal in the cytoplasmic tail of lysosomal acid phosphatase is necessary and sufficient for targeting to lysosomes. EMBO J 1990;9:3497–506.
[41] Ludwig T, Griffiths G, Hoflack B. Distribution of newly synthesized lysosomal enzymes in the endocytic pathway of normal rat kidney cells. J Cell Biol 1991;115:1561–72.
[42] Tjelle TE, Brech A, Juvet LK, et al. Isolation and characterization of early endosomes, late endosomes and terminal lysosomes: their role in protein degradation. J Cell Sci 1996;109:2905–14.
[43] Futter CE, Pearse A, Hewlett LJ, et al. Multivesicular endosomes containing internalized EGF-EGF receptor complexes mature and then fuse directly with lysosomes. J Cell Biol 1996;132:1011–23.
[44] Luzio JP, Pryor PR, Bright NA. Lysosomes: fusion and function. Nat Rev Mol Cell Biol 2007;8:622–32.
[45] van Meel E, Klumperman J. Imaging and imagination: understanding the endolysosomal system. Histochem Cell Biol 2008;129:253–66.
[46] Ferreira-Redondo L, Pérez-González N, Llanillo M, et al. Acute pancreatitis decreases pancreas phospholipid levels and increases susceptibility to lipid peroxidation in rat pancreas. Lipids 2002;37:167–71.
[47] Hirano T, Manabe T, Yotsumoto F, et al. Effect of prostaglandin E on the redistribution of lysosomal enzymes in caerulein-induced pancreatitis. Hepatogastroenterology 1993;40:155–8.
[48] Scheele GA. Biosynthesis, segregation, and secretion of exportable proteins by the exocrine pancreas. Am J Physiol 1980;238:G467–77.
[49] Brzozowski J, Dlugosz J, Gabryelewicz A. Pancreatic lysosomal hydrolases in acute experimental pancreatitis in dogs. Z Exp Chir Transplant Kunstliche Organe 1984;17:350–9.

- **OBJETIVO 4:** Investigar los cambios de expresión y dinámica de la proteína lisosómica LAMP-2 durante el desarrollo de la PA inducida por ceruleína.

Increase and missorting of LAMP-2 during cerulein-induced pancreatitis in rats

Nancy Sarmiento[a], Carmen Sánchez-Bernal[a], Violeta García-Hernández[a], Arturo Mangas[b], Angel Hernández-Hernández [a], José J. Calvo[c], Jesús Sánchez-Yagüe[a,*]

[a]*Department of Biochemistry and Molecular Biology, University of Salamanca, Spain*

[b]*Department of Cell Biology and Pathology, University of Salamanca, Salamanca, Spain,*

[c]*Department of Physiology and Pharmacology, University of Salamanca, Spain*

*Corresponding author. Departamento de Bioquímica y Biología Molecular, Edificio Departamental. Lab. 106, Plaza Doctores de la Reina s/n, 37007 Salamanca, Spain. Fax: +34 923 294579

E-mail address: sanyaj@usal.es (J. Sánchez-Yagüe)

Abstract

Lysosomal LAMP-2 plays an important role in the cytoplasmic vacuolization of acinar cells in pancreatitis. We report increases in pancreatic LAMP-2 protein and mRNA levels as early events during the development of cerulein (Cer)-induced acute pancreatitis (AP), which returned to below baseline levels in its later phase. The increase in protein levels was due to a soluble-type form with a higher molecular weight (≈120 kDa) than LAMP-2 in control pancreata. Nevertheless, in a lysosome-enriched fraction LAMP-2 expression decreased along the development of Cer-induced AP, as well as in three density-separated lysosomal subpopulations. Immunostaining revealed that the cellular source of LAMP-2 following Cer administration was mainly acinar and islet cells. Neutrophil infiltration was not the main cause of the increased LAMP-2 protein levels, as observed when rats were rendered neutropenic with vinblastine sulfate. The endoglycosidase-H resistance of the 120 kDa LAMP-2 form indicated that it was not a high-mannose precursor. Additionally, its higher molecular weight was not due to an association with a small protein but to a change in its glycosylation pattern (not related to a difference in its sialic acid level), accompanied by resistance to its complete deglycosylation with peptide *N*-glycosidase treatment. Together, these results indicate that the pancreatic expression of LAMP-2 increases during the early phase of Cer-induced AP, while a different post-translational processing in its carbohydrate content, accompanied by cellular missorting, would finally lead to a decrease in its expression in the lysosome.

Keywords: LAMP-2; Cerulein; Acute pancreatitis

1. Introduction

Pancreatitis is an auto-digestive disease that damages acinar cells and causes severe inflammation [1]. One of the animal models of human edematous pancreatitis is that induced in the rat by cerulein (Cer). The treatment used in the model of acute pancreatitis (AP) of the present studies, results in several manifestations of pancreatitis, including interstitial edema and hyperamylasemia, different indicators of morphological and histological damage to the pancreas, and neutrophil infiltration [2-6]. It is reasonable to assume that the development of pancreatitis would be based on rapid early events. It is known that early on in the course of secretagogue-induced pancreatitis, lysosomal hydrolases colocalize with digestive zymogens and activate them [7,8], which is believed to be essential in the development of pancreatitis [9]. Furthermore, an inhibition of the release of secretory proteins as well as an alteration of protein trafficking occurs in Cer-induced pancreatitis [10]. In fact, in AP this altered vesicular traffic in the secretory pathway is involved in vacuole formation and the activation of intracellular zymogens [11]. It is also known that in AP glycoprotein processing is inhibited in the Golgi complex [10]. Membrane glycoproteins in the secretory pathway are believed to exert protective effects, especially for compartments with active enzymes such as the lysosome. Thus, changes in the processing of glycoproteins in pancreatitis may significantly alter lysosome membrane stability, which could finally affect vacuole disruption and the release of active proteases into the cytosol [10].

LAMP-2 (lysosomal-associated membrane protein 2), also called lgp96 in the rat, is an ubiquitous major type-I transmembrane protein of the lysosome that is extensively glycosylated in its large luminal/extracellular domain. It is highly expressed in normal pancreatic tissue [12]. The molecular mass of the polypeptide backbone is around 40 kDa, but after glycosylation its mass increases up to almost 100-120 kDa [13], depending on the cell type and organism. Several mRNAs arising from alternative splicing of a single transcript encode three LAMP-2 molecules that differ in their single transmembrane and short cytoplasmic tail [14]. LAMP-2, as well as

other LAMPs, can follow two different pathways to reach the lysosome [15]: (1) from the *trans*-Golgi to late endosomes or to lysosomes, (2) another different and complex pathway, involving movement to early endosomes and the cell surface, before delivery to lysosomes after several rounds of exocytosis and endocytosis. However, the distribution and sorting events responsible for the transfer of lysosomal membrane glycoproteins to their final destination may differ among cells [16]. Thus, the enrichment of different proteins in the lysosome is a dynamic condition resulting from complex trafficking among several cellular compartments. Although the levels of LAMPs at the cell surface are usually low at steady-state, the regulated movement of LAMPs between the plasma membrane and the endocytic pathway may play important roles in the maintenance of cell-cell interactions due to their complex saccharide chains [14]. In this sense, the changes in LAMP distribution are often accompanied by alterations in the glycosylation pattern of LAMPs.

It has been proposed that lysosomal LAMP-2 would have several functions: (1) a specific function in chaperone-mediated autophagy, (2) a role as a receptor on the lysosomal membrane, designed to mediate the binding and transport of substrate cytosolic proteins into lysosomes for degradation [17], (3) it is required for the proper fusion of lysosomes with autophagosomes in the late stage of the autophagic process [18]. Autophagy is a cytoprotective mechanism through which cells maintain homeostatic functions such as protein and organelle turnover. LAMP-2 depletion results in the inhibition of cytoprotective autophagy signaling secondary to the failure of fusion between lysosomes and autophagosomes [19]. In humans, Danon disease is a consequence of mutations in the gene encoding LAMP-2. This pathology is characterized by the accumulation of late autophagic vacuoles in the heart and skeletal muscle [20]. Additionally, mice deficient in Lamp-2 exhibit an accumulation of autophagic vacuoles in several tissues, including pancreatic acinar cells [21]. Cytoplasmic vacuolization is also one of the early signs of cellular and tissue damage in pancreatitis, although its precise mechanism is not fully understood.

Recently, based on an alcoholic model of pancreatitis it has been proposed that pancreatitic acinar cell vacuolization is mediated by an inhibition of the late stage of autophagy, in which the depletion of lysosomal proteins, including LAMP-2, would play a critical role [22]. Nevertheless, the reasons for such depletion and the dynamics of LAMP-2 during the course of pancreatitis has not been addressed previously.

Bearing in mind the importance of unmasking the molecules or genes whose expression changes along the development of AP, the goal of the present work was to study the expression and cell dynamics of LAMP-2 as from the early phase of Cer-induced AP.

2. Materials and methods

2.1. Reagents

Agarose-conjugated lectin from *Triticum vulgaris* (wheat germ agglutinin, WGA), cerulein, concanavalin A-sepharose 4B (Con A) from *Canavalia ensiformis*, monoclonal antibody anti-β-Tubulin, Protease Inhibitor Cocktail, sodium taurocholate, Trizol Reagent, trypsin inhibitor, and vinblastine sulfate were purchased from Sigma Chemical Co. (St. Louis, MO, USA). Density marker beads were purchased from Pharmacia (Uppsala, Sweden). The Oxyblot protein oxidation detection kit was obtained from Intergen (Purchase, NY, USA). The 2-D Clean-Up Kit was obtained from GE Healthcare (GE Healthcare Europe, Barcelona, Spain). Anti-LAMP-2 polyclonal antibody was obtained from Zymed Laboratories Inc (Invitrogen, Carlsband, CA, USA). Biotinylated anti-rabbit immunogammaglobulin and avidin–biotin–peroxidase complex were purchased from Vector (Burlingame, CA, USA).

2.2. Animals

Male Wistar rats weighing 250-280 g were used. Care was provided in accordance with the procedures outlined in European Community guidelines on ethical animal research (86/609/EEC), and the protocols were approved by the Animal Care Committee of the University of Salamanca.

2.3. Induction of AP and preparation of samples

AP was induced as described previously [6,23,24]. Briefly, rats received up to 4 s.c. injections of 20 μg Cer/kg body weight or its vehicle (0.9% NaCl) at hourly intervals. At 2, 4 or 9 h after the first injection, the animals were killed by cervical dislocation. The pancreata were rapidly harvested and used immediately for experiments. In some cases, AP was also induced by sodium-taurocholate duct infusion or bile-pancreatic duct obstruction (BPDO), as indicated previously [23]. After dissection and homogenization of the pancreata [23], postnuclear homogenates were obtained [23]. Subcellular fractionation was carried out in the homogenates following a method in which lysosomes were coprecipitated with mitochondria at 20,000 $\times g$ after separation of the zymogen fraction at 1300 $\times g$, as described previously by us [23,24]. Four subcellular fractions were obtained: the zymogen (Z), the lysosome *plus* mitochondria (L+M), the microsome (Mic) and the soluble (S) fractions.

Serum amylase was measured as reported previously [6,23]. Protein concentrations were assayed according to the method of Bradford [25].

2.4. Induction of neutropenia

Neutropenia was induced in rats by intravenous (i.v.) injection of vinblastine sulfate at a dose of 0.75 mg/kg on day 1, as previously described [6,23]. At this dose, the animals become

neutropenic between days 4 and 6 [26]. On day 5 following vinblastine sulfate or saline administration, the animals were treated with 4 doses of Cer (20 μg Cer/kg, administered at hourly intervals), and killed 4 h after the first injection of Cer (intermediate phase of AP).

2.5. Percoll gradient centrifugation

Aliquots (0.5 ml) of the L+M fractions diluted three times in 3 mM imidazole buffer, pH 7.4 containing 0.25 M sucrose, 1 mM EDTA, 1mM PMSF, 100 μg/ml trypsin inhibitor and 2 μl/ml Protease Inhibitor Cocktail (buffer A [6]) were layered on top of discontinuous gradients (performed in ultraclear centrifuge tubes) consisting of three layers of isotonic 17%, 10% and 5% Percoll solutions (3.8 ml each) prepared in buffer A and placed from the bottom of the tube upwards, respectively. The density partial-gradients were then formed by centrifugation at 50,500 $\times g$ for 30 min in a Beckman SW40 rotor. For the calibration of the Percoll density gradients, density marker beads were used, following the manufacturer's instructions. Three bands of organelles were recovered close to the interfaces of the density gradients. Each band was collected with a Pasteur pipette, diluted with buffer A, and washed by centrifugation at 50,000 x g for 15 min to remove the Percoll reagent. The organelles, which were located above the Percoll pellet, were finally transferred to Eppendorf tubes for their use in sodium dodecyl sulphate-polyacrylamide gel electrophoresis (SDS-PAGE) and Western blotting. The morphologic characterization of these bands has been described elsewhere (Sarmiento at al., 2009).

2.6. RNA preparation and RT-PCR

Total RNA was isolated from the pancreas and brain of the same rat by immediate solubilization in Trizol Reagent and isopropanol purification. RT-PCR was performed as

Previously described [6, 23]. The oligonucleotide sequences were as follows: LAMP2: forward oligo: 5´-CCACCGCTATGGGCACAAGGAAGTT-3´

reverse oligo: 5´-CAGCTGAACATCACCGAGGAGAAGG-3´.

Product length was 427 pb. Oligonucleotide primers for β-actin were used as an internal control : forward oligo: 5´-TCTGTGTGGATTGGTGGCTCTA-3´

reverse oligo: 5´-CTGCTTGCTGATCCACATCTG-3´.

2.7. Light microscopy and immunohistochemistry

Paraffin-embedded tissue sections (8-to 10-μm thick) were stained with hematoxylin and eosin (H&E staining), as indicated previously [6], or subjected to immunostaining using the streptavidin peroxidase technique. For the latter, the sections were incubated for 30 min at room temperature in phosphate-buffered saline (0.15 M, pH 7.2) containing 1% normal horse serum and 0.3% Triton X-100 (buffer A) before overnight incubation at 4 ºC with anti-LAMP2 polyclonal antibody diluted 1:50. Bound antibody was detected with a biotinylated anti-rabbit immunoglobulin (Ig) G (1 h, 1:200 dilution in buffer A at room temperature) and an avidin–biotin–peroxidase complex (1 h, 1:100 dilution in buffer A at room temperature). The tissue-bound peroxidase was developed with H_2O_2, using 3,3-diaminobenzidine as chromogen. To ensure the specificity of the primary antibody, we incubated sections in either the absence of the primary antibody or with a non-immunized rabbit IgG antibody. In these cases, no immunostaining was detected. For estimation of the intensity of immunostaining, random film images were scanned, using the Adobe Photoshop program (version CS2), and the images were then analysed with the MacBas v 2.5. program. At least 8-10 fields were evaluated at a magnification of × 4 in both the control and Cer-treated groups. In each image, small rectangles (50-60) of equal surface area were analyzed, which altogether basically represented all the acini

observed in each image. The results are expressed as arbitrary units (AU) per equivalent area (500 px2).

2.8. SDS-PAGE and Western blotting

In experiments addressing LAMP-2 expression, proteins were analysed by dodecyl sulfate polyacrylamide gel electrophoresis（SDS-PAGE) using 8% or 10% gels, after which they were transferred to polyvinylidene difluoride membranes. Western blots were probed with anti-LAMP2 polyclonal or the approximate loading-control: anti-β-Tubulin monoclonal antibodies diluted 1:1000 and 1:4000, respectively. Blots were visualized by chemiluminescence. Analyses of the spots on all the blots were performed as described previously [6,23]. Some samples were pretreated with 2-D Clean-Up kit to precipitate proteins, leaving behind non-protein impurities and allowing the rehydratation buffer to be changed. For this, the manufacturer´s instructions were followed.

Protein carbonyl contents and profiles were measured by immunoblot detection using the Oxyblot protein oxidation detection kit, as indicated elsewhere [27,28]. Briefly, 15 mg of protein from each sample was incubated with DNPH for 15 min at room temperature. Samples were neutralized, reduced by the addition of 2-mercaptoethanol, and loaded into 6% SDS-PAGE gels. After electroblotting , oxidized proteins were revealed with an anti-DNP antibody, and visualized by chemiluminescence.

In studies addressing the carbohydrate content of LAMP-2, samples were first incubated with no additions for different times; with 100 mU/ml neuraminidase for up to 24 h; with 10 U/ml peptide *N*-glycosidase-F (PGNase-F) for 8 or 24 h, or with 100 mU/ml endoglycosidase-H (Endo-H) for 24 h in the presence of 2 μl/ml Protease Inhibitor Cocktail, at 37 ºC and under gentle shaking. Neuraminidase treatment: samples were first dialyzed against 50 mM sodium

acetate buffer, pH 5.5 or 6, containing 134 mM NaCl and 9 mM $CaCl_2$, after which 2.5% NP-40 (final concentration) was added before neuraminidase incubation. Aliquots were collected at different times and used for blotting. PGNase-F treatment: 1% NP-40 (final concentration) was added and the samples were kept on ice for 1 h with occasional shaking. Then, 0.1% SDS and 10mM β-mercaptoethanol (final concentration, dissolved in 3 mM imidazole buffer, pH 7.4 [25]) were added, and samples were boiled for 10 min After 5 min on ice, PGNase-F was added and the samples were incubated at 37 ºC. Endo-H treatment: as for PGNase-F treatment, but the pH of samples was first adjusted to 5.5-6, and SDS and β-mercaptoethanol were dissolved in 3 mM imidazole buffer, pH 5.5.

2.9. Treatment of solubilized LAMP-2 with lectins

Pancreatic samples were first solubilized at 4 ºC with 0.5-1% NP-40 for 60 min under continuous rotation. Fixed amounts of solubilized proteins were mixed in Eppendorf tubes with 200 μl of immobilized lectins resuspended in 3 mM imidazole buffer, pH 7.4 containing 0.5% NP-40. The mixtures were rotated for 4 h at 4 ºC and then centrifuged in a table centrifuge at full speed for 10 min These conditions were chosen for convenience and did not represent the optimal ones for maximal lectin binding. The supernatants represented the lectin-unbound proteins (supernatant 1, Sp 1 in Fig. 7B) Then, the gels were washed twice with imidazole buffer, centrifuged again, and finally the lectin-bound proteins were eluted from the lectins with 0.5 M *N*-acetyl-glucosamine (WGA) or 1M methyl α-mannopyranoside (Con A) overnight at 4 ºC under rotation. Centrifugation of the mixtures afforded the lectin-bound proteins (supernatant 2, Sp 2 in Fig. 7B).

2.10. Statistical analyses

Data are expressed as means ± S.D. They were analysed using the non-parametric Mann-Whitney U test. Statistical significance was considered for a p value <0.05. Analyses were implemented using the SPSS program for MS Windows (version 15.0).

3. Results

3.1. Changes in the expression of LAMP-2 during the development of AP

The upper part of Fig. 1A shows representative Western blot analyses indicating LAMP-2 protein in whole postnuclear pancreatic homogenates obtained from control or pancreatitic rats at different times after the first injection of Cer. The lower part of Fig. 1A indicates quantitative data relative to the whole pancreas. As we have reported previously [6,23], the expression of data with respect to the whole pancreas would be more appropriate because pancreatitis is associated with cell death and neutrophil infiltration. These features imply that the pancreata of control and pancreatitic rats will have different cell compositions. Accordingly, the exact amount of any protein, including LAMP-2, should be calculated in the whole organ rather than in a fixed amount of proteins. Here, we observed an increase in the expression of LAMP-2 in the early phase of AP (2 h after the first injection of Cer)(3,4± 0.7- fold that of controls), which persisted in the intermediate phase (4.5 ± 1.6-fold that of controls). In the later phase, once Cer-induced AP had fully developed, LAMP-2 expression fell to levels even lower than those of the controls (0.8 ± 0.1-fold that of the controls). Nevertheless, LAMP-2 from pancreatitic pancreata showed a higher molecular weight (≈120 kDa) than the well established molecular weight of LAMP-2 in control pancreata (≈96 kDa). The establishment of AP was tested by checking that serum amylase activity did indeed increase significantly along the development of pancreatitis (Fig. 1B). Also,

using histological sections of pancreata, we have previously demonstrated [6] that our model of pancreatitis shows tissue architecture and leukocyte infiltration consistent with parameters described previously for AP [1,3,4] [some photomicrographs of H&E staining at 2 and 4 h after the first injection of Cer are also shown here (see Fig. 3A)]. Moreover, in the early phase of AP (2 h), LAMP-2 mRNA levels were increased in pancreata but hardly not at all in a control organ with Cer receptors (brain) (Fig. 2A), in which the expression of LAMP-2 protein remained constant (data not shown). Since it has been described that oxidative stress transcriptionally regulates at least LAMP-2A expression [29], we wondered if we could detect such stress in the early phase of AP by analyzing the carbonyl content of the proteins from different subcelular fractions as well as the pancreatic homogenate. As shown in Fig. 2B, this was indeed the case, since different proteins clearly became carbonylated, or their levels of carbonylation were increased. Previous results did not reveal individual, selectively modified proteins in Cer-induced AP [30]. This difference seems to be due to the fact that most of the newly modified proteins were mainly visible with 6% rather than with 10% gels. To examine the cellular source of LAMP-2 following Cer administration, we performed immunohistochemical studies (Fig. 3). In the control pancreata, a moderate to strong degree of immunoreactivity was present in islet cells, and a faint immunostaining was observed in acinar cells. The ductal cells of the normal pancreata were mostly negative for LAMP-2, as reported previously for normal human pancreas [31], although some of them were very slightly immunostained. Blood vessel endothelial cells were completely negative for LAMP-2. During the early and intermediate phase of Cer-induced AP, an increase in the immunoreactivity of both acinar and islet cells was detected (Fig. 3B). In fact, the image analysis used here revealed significant increases (≈ 45% and 28%, 2 h and 4 h after the first Cer injection, respectively) in the mean intensity of acinar cell immunostaining: 799 ± 519, 1157 ± 522 and 1029 ± 558 AU/500 (px2), $p \leq 0.001$, for control, 2 h and 4 h Cer-treated rats, respectively, similar to the values observed for islet cells (data not shown). Also, in comparison

with the control pancreata an increase in the number of ductal cells showing a weak immunostaining was found, although again most of these cells were negative for LAMP-2.

3.2. LAMP-2 subcellular distribution during the development of AP

We next analyzed the subcellular distribution and dynamics of LAMP-2 (Fig. 4). Fig. 4A shows the results corresponding to the early phase of Cer-induced AP (2 h after the first injection of Cer). In total control pancreata, LAMP-2 was located in the four subcellular fractions analyzed, although almost 50% was present in the L+M fraction. In the Cer-injected animals, almost 94% of LAMP-2 was associated with the soluble fraction and, as expected, it corresponded to the 120 kDa form. Notably, this LAMP-2 form was also detected in the microsome fraction in significant amounts (Fig. 4A). Fig. 4B shows that the amount of LAMP-2 in the L+M fraction decreased significantly along the development of Cer-induced AP (60-90% of the LAMP-2 expressed in total control pancreata). Additionally, in the intermediate and later phases of Cer-induced AP (4 and 9 h after the first injection of Cer, respectively), the 120 kDa LAMP-2 form was also detected in the L+M subcellular fraction (Fig. 4B, see Western blots), although it was not always detectable. Finally, the decrease in LAMP-2 expression after Cer-induced AP was also observed in three density-separated lysosomal subpopulations obtained after Percoll-centrifugation of the L+M fraction (Fig. 4C). These subpopulations were mostly devoid of succinate dehidrogenase activity, a marker of mitochondria, which were mainly located at the bottom of the tube (Sarmiento at al., 2011). The 120 kDa LAMP-2 form was also detected in another two models of AP: the BPDO and taurocholate models, although it was mainly expressed in the BPDO model, also as a soluble-type form (data not shown).

The presence of LAMP-2 in the soluble fraction is intriguing because LAMP-2 is an integral protein. To analyze this feature, we then submitted the soluble fraction of both control and pancreatitic pancreata to centrifugation at 400,000 × *g*. Fig. 5 shows that most of the 96 kDa LAMP-2 form present in control pancreata was in fact a membrane-associated protein, because after centrifugation it was mainly located in the precipitate (70-80%). By contrast, the 120 kDa LAMP-2 form was mainly located in the supernatant (≈ 98%). This result suggests that the 120 kDa LAMP-2 form is soluble or, if membrane-associated, that the amount of lipids surrounding the enzyme would be insufficient to allow the enzyme to reach the precipitate.

3.3. Influence of neutrophil infiltration

In pancreatitis, neutrophil infiltration is an important component in the development of both inflammation and cell death. It has been reported that during the intermediate phase of AP inflammatory cell infiltration has already started or taken place [32], as we observed in our AP model by light microscopy analysis [6]. Therefore, we decided to perform the study 4 h after the first injection of Cer. As expected, neutropenia was associated with the disappearance of neutrophils from the blood: 40 ± 6% and 0% neutrophils in a differential leukocyte count in the blood from Cer-induced AP (4 hours) rats not-pretreated or pretreated with vinblastine sulfate, respectively, $n = 3$ (data not shown). Moreover, as seen in Fig. 6A, vinblastine treatment resulted in blunted pancreatic MPO levels, pointing to an in situ depletion of neutrophil infiltration, as described elsewere [23]. We have previously reported that under the same conditions described here vinblastine treatment alone did not affect serum amylase activity and that vinblastine treatment in Cer-treated rats did not decrease serum amylase levels [6,23]. Fig. 6B shows that although the depletion of neutrophils in the rats slightly suppressed (≈ 20%) the increase in LAMP-2 protein expression at 4 h after Cer treatment, neutrophil infiltration did not seem to be the main cause of that increase, and neither did it prevent the expression of the 120 kDa LAMP-2

form. Furthermore, it is clear that the 120 kDa LAMP-2 form is not the LAMP-2 protein expressed in rat lymphocytes.

3.4. Studies addressing the nature and carbohydrate content of the 120 kDa LAMP-2

In Fig. 7A we show that the higher molecular weight of the 120 kDa LAMP-2 does not seem to be due to an association with a small protein, because its size did not change even after rehydration in a buffer containing 7M urea; i.e., the buffer solution usually employed in two-dimensional electrophoresis. Accordingly, we attempted to demonstrate that the 120 kDa LAMP-2 was, as expected, a glycoprotein. In Fig. 7B we show that this protein was bound by two different lectins. Although the experiments were not designed to be quantitative, WGA seemed to bind the 120 kDa LAMP-2 more efficiently than Con A, possibly reflecting a better recognition of β-*N*-acetylglucosamine by WGA than of α-linked mannose residues by Con A. Finally, we performed experiments to address the carbohydrate content of the 120 kDa LAMP-2. For this, the most appropriate conditions for the functioning of the different enzymes used were employed.
First, Fig. 7C shows that neuraminidase treatment did not significantly change the molecular size of either the 96 kDa or the 120kDa LAMP-2 located in the soluble fraction of the control and pancreatitic pancreata. This result suggests the absence, or very low levels, of terminal sialic acids, whose elimination would not change the electrophoretic mobility of LAMP-2. In the left panel of Fig. 7D we show that the complete deglycosylation of the LAMP-2 located in the L+M fraction from control pancreata after treatment with PGNase F resulted in a decrease in the molecular size of the protein down to 40-45 kDa, which is the molecular weight of its backbone. Despite this, PGNase treatment of the soluble fraction from pancreatitic pancreata did not afford the same result. In fact, the molecular weight of the120 kDa LAMP-2 was only very slightly reduced, and did not even reach the regular 96 kDa of LAMP-2. Finally, treatment with Endo-H, an endoglycosidase that breaks down high-mannose-content carbohydrates, did not change the

molecular weight of the 120 kDa LAMP-2. This Endo-H resistance indicated that it was not a high-mannose precursor of LAMP-2. Taken together, these results indicate that the higher molecular weight of LAMP-2 seen in pancreatitic pancreata is probably due to a change in its glycosylation pattern, accompanied by resistance to its complete deglycosylation with PGNase treatment.

4. Discussion

It has been proposed that alterations in gene and/or protein expression within the initiation phase of AP play an important role in its development [33]. It has also been suggested that the final step of autophagy signalling is inhibited, presumably due to the depletion of lysosomal proteins, which is associated with the acinar cell vacuolization observed in pancreatitis [22].
Based on these features, here we show that the pancreatic expression of LAMP-2, an integral protein of lysosomes directly involved in autophagy, is increased at the level of both protein and mRNA as from the early phase of Cer-induced AP. Nevertheless, it seems to have a different post-translational processing in its carbohydrate content, which is accompanied by cellular missorting, and hence it behaves as a soluble-type protein. As a consequence, its level of expression decreases dramatically in the lysosome.

Previous studies of both the Cer-induced and the taurocholate models of pancreatitis have revealed increased oxidative stress, and oxidative protein modification as an early event [30, 34]. Here we show that in fact oxidative stress, detected as the appearance or an increase in the level of oxidized proteins in different subcelular fractions or whole pancreas homogenates, occurs during the early phase of Cer-induced AP. This oxidative stress might be the cause of the increased LAMP-2 mRNA level detected here. In fact, in rat liver it has been described that oxidative stress increases chaperone-mediated autophagy (CMA), the mechanism responsible for the selective degradation of cytosolic proteins in lysosomes during stress conditions. In this case,

one of the LAMP-2 members, LAMP-2A, is overexpressed due to transcriptional regulation, its mRNA level being increased [29]. LAMP-2 has been found to occur as spliced-variant molecules (LAMP-2A, -2B and -2C), which are encoded by different transcripts in chicken, mouse and human cells [19]. The differences in the amino acid sequences of the three variants are confined to the transmembrane region and cytosolic tail [17]. In the mouse, it has been reported that the LAMP-2A transcript is the most prevalent one in the pancreas during morphogenesis [35]. The primers used in our RT-PCR analysis allowed us to follow all the LAMP-2 mRNA types. Thus, the issue that it is indeed the LAMP-2 variant that affords the increase in LAMP-2 gene expression detected in Cer-induced AP remains to be resolved, although the data concerning the stress-mediated transcriptional regulation of LAMP-2A in rat liver, as indicated above, suggest that it would be the LAMP-2 form that is involved. Additionally, there is a tissue-dependent expression of the different forms of LAMP-2 [12], suggesting that they might have different cellular functions. It has previously been reported that in the normal human pancreas LAMP-2 mRNA is present in islet and acinar cells, but absent in ductal cells, and that LAMP-2 protein immunoreactivity is detected only in islet cells, macrophages, and acinar cells [31]. The immunostaining procedure performed here revealed that in the rat LAMP-2 was also present, mainly but not exclusively, in islet and acinar cells, and that, importantly, during its early phase, Cer-induced AP was associated with a similar increase in LAMP-2 expression in both types of cell. Nevertheless, the much greater numbers of acinar *vs* islet cells in whole pancreas means that most of the increase observed here would reflect the increase associated with acinar cells. The meaning of LAMP-2 overexpression in islet cells from Cer-induced AP is unknown and deserves further investigation, although it is out of the scope of this work. Also, the overexpression of LAMP-2 is a feature associated with a high proportion of pancreatic carcinomas, although in our hands, it was located mainly in ductal carcinoma cells [31].

One of the early signs of cell and tissue damage in pancreatitis is cytoplasmic vacuolization, a common feature in pathological alterations of acinar cells that, however, is not completely understood [36]. Such vacuoles are linked to an alteration of autophagy, a cytoprotective mechanism through which cells deliver autophagosomes (carrying cytosolic components and organelles) to lysosomes, thus forming autophagolysosomes or autolysosomes, which are devoted to the degradation of the autophagic cargo. In fact, autophagy is one of the cell responses to stress, [33], and endoplasmic reticulum stress occurs during AP, pancreatic acinar cells being particularly susceptible to ER perturbations [37]. It is also known that the formation of autophagolysosome is a LAMP-2-dependent process, since LAMP-2 depletion results in the failure of lysosomes and autophagosomes to fuse [19]. Accordingly, vacuolization in Cer-induced AP might be explained in terms of an accumulation of autophagosomes, as has been proposed in alcoholic pancreatitis [22]. The decreased-LAMP-2 expression in lysosomes detected in this work, as a consequence of the missorting of the protein, might be physiologically relevant because it could be directly related to such an accumulation, although at present it is not possible to distinguish between a specific role of LAMP-2 and a general exhaustion of the lysosomal system as being responsible for the inhibition of autophagy observed in AP, as has been pointed out previously [22]. In retinal pigment epithelium, a mistargeting of cathepsin D (the main lysosomal protease) into the extracellular space has been shown to occur, probably due to an accumulation of the products of lipid peroxidation (oxidatively damaged lipid-protein complexes) [38]. Lipid peroxidation processes and the covalent binding of 4-hydroxyalkenals to the sulfhydryl groups of pancreatic tissue proteins also occur in Cer-induced AP [39,40]. Notably, LAMP proteins contain different conserved cysteine residues that, under normal conditions, form the four disulfide loops present in the intralysosomal portion [41]. By contrast, apparently an increase in 4-hydroxynonenal bound to pancreatic protein histidines does not occur in the taurocholate model of pancreatitis [34], although it does occur in the lung [42]. The implications

of the accumulation of oxidized lipid-protein cross-links in the missorting of lysosomal proteins in pancreatitis remain to be explored. In any case, the inhibition of secretion that occurs in pancreatitis would lead any mistargeted lysosomal protein to remain longer inside the pancreatic cells, which might have important physiological consequences. Additionally, it is known that in Cer-induced AP a perturbation of protein trafficking occurs, and the altered vesicular traffic in the secretory pathway is involved in vacuole formation [11]. Also, the carbohydrate composition of glycoproteins in the secretory pathway and vacuoles is altered in experimental pancreatitis, indicating that glycoproteins passing through the Golgi complex are not processed normally [10,11]. This might have important cellular implications, since highly glycosylated LAMP proteins coat the inner face of lysosomes, probably protecting this organelle from self-destruction, although this aspect remains unclear [43]. Accordingly, changes in the carbohydrate content of LAMPs might also produce changes in their effectiveness regarding the protection of the lysosomal membrane and/or their role in vacuole disruption and the release of active proteases into the cytosol.

Interestingly, LAMP-2 is one of the major carriers of poly-N-acetyllactosamines in cells [41], and its molecular weight increases along with the increase in its polylactosamine glycosylation, a feature that has been observed to be correlated with a longer LAMP-2 residence time in the Golgi complex, irrespective of Golgi integrity [44]. The extension of polylactosamine glycosylation requires the repeated action of two transferases, a glycosyltransferase and a galactosyl transferase, presumably within the same Golgi cisterna [45]. Galactosyl transferase has been localized in trans Golgi cisternae and the overlapping distribution of glycosyltransferases in Golgi cisternae has been already described [45]. All these data might be relevant with respect to the structure of LAMP-2 in our model of Cer-induced AP since, as we have reported above, glycoprotein processing is altered in the Golgi compartment in pancreatitis [10]. Moreover, microtubule disorganization occurs in Cer-induced AP [46], and although the depolymerisation of

the microtubule cytoskeleton results in the dispersion of numerous small Golgi clusters, LAMP-2 polylactosamine glycosylation still occurs in these clusters [10].

An intriguing issue is the fact that the 120 kDa LAMP-2 behaves as a soluble-type protein. In this regard, at least in the rat liver it is known that one portion of LAMP-2 is also located in the lysosomal matrix [47,48], whose origin is unclear. Both a direct deinsertion from the lysosomal membrane after conformational change as well as a release by proteolytic cleavage of the short transmembrane and cytosolic tail have been proposed [47]. Furthermore, lipids associated with at least LAMP-2A may also play an important role in lysosomal membrane deinsertion or reinsertion [47]. Several other membrane protein insertions/deinsertions have been described for other type I membrane proteins, sometimes probably driven only by hydrophobic interactions with lipids [49]. Cleavage has also been described for other lysosomal membrane proteins [50]. The origin of the solubility of our 120kDa LAMP-2 form remains to be resolved.

In conclusion, this study shows that the pancreatic expression of LAMP-2 is increased during the early phase of Cer-induced AP, although a different post-translational processing in its carbohydrate content, accompanied by cellular missorting, would finally afford a decrease in its expression level in the lysosome. The latter feature links our work to others addressing the relevance of the depletion of lysosomal proteins in pancreatitic acinar cell vacuolization. Our results also appear to offer a starting point for further investigations regarding the biology of the synthesis and post-translational processing of LAMP-2 in experimental pancreatitis, and in Cer-induced AP in particular.

Acknowledgements

This work has been supported in part by FIS (PS09/01075), MCINN (BFU2009-10568) and Regional Government of Castilla y León (Biomedicina SAN673/SA10/08, SA033A05, and SA126A07), Spain. The authors wish to thank Dr. J.M. González de Buitrago (University of

Salamanca) for his help with the amylase determinations. The β-actin primers were kindly provided by Dr. Serrano (University of Salamanca).

References

[1] A.K. Saluja , L. Bhagat, H.S. Lee, M. Bhatia, J.L. Frossard, M.L. Steer, Secretagogue-induced digestive enzyme activation and cell injury in rat pancreatic acini, Am. J. Physiol. Gastrointest. Liver Physiol. 279 (1999) G835-G842.

[2] R. Alonso, A. Montero, M. Arévalo, L.J. García, C. Sánchez-Vicente, F. Rodríguez-Nodal, J.M. López-Novoa, J.J. Calvo, Platelet-activating factor mediates pancreatic function derangement in caerulein-induced pancreatitis in rats, Clin. Sci. 87 (1994) 85-90.

[3] R. Pescador, M.A. Manso, A.J. Revollo, I. De Dios, Effect of chronic administration of hydrocortisone on the induction and evolution of acute pancreatitis induced by cerulein, Pancreas 11 (1995) 165-172.

[4] N. Yönetçi, N. Oruç, A.O. Ozütemiz, H.A. Celik, G, Yüce, Effects of mast-cell stabilization in caerulein-induced acute pancreatitis in rats, Int. J. Pancreatol. 29 (2001) 163-171.

[5] M. Zhao, D.B. Xue, B. Zheng, W.H. Zhang, S.H. Pan, B. Sun, Induction of apoptosis by artemisin relieving the severity of inflammation in caerulein-induced acute pancreatitis, World J. Gastroenterol. 14 (2007) 5612-5617.

[6] N. Sarmiento, M.C. Sánchez-Bernal, M.N. Pérez-González, A. Mangas, J.L. Sardina, J.J. Calvo, J. Sánchez-Yagüe, Rolipram and SP600125 suppress the early increase in PTP1B expression during cerulein-induced pancreatitis in rats, Pancreas 39 (2010) 639-645.

[7] W. Halangk, M.M. Lerch, Early events in acute pancreatitis, Clin. Lab. Med. 25 (2005) 1-15.

[8] G.J.D. van Acker, G. Perides, M.L. Steer, Co-localization hypothesis: A mechanism for the intrapancreatic activation of digestive enzymes during the early phases of acute pancreatitis, World J. Gastroenterol. 12 (2006) 1985-1990.

[9] A.K. Saluja, M.M. Lerch, P.A. Phillips, V. Dudeja, Why does pancreatic overstimulation cause pancreatitis?, Ann. Rev. Physiol. 69 (2007) 249-269.

[10] R.C. de Lisle, Altered posttranslational processing of glycoproteins in cerulein-induced pancreatitis, Exp. Cell Res. 308 (2005) 101-113.

[11] I. Saito, S. Hashimoto, A. Saluja, M.L. Steer, J. Meldolesi, Intracellular transport of pancreatic zymogens during cerulein supramaximal stimulation, Am. J. Physiol. 253 (1987) G517-G526.

[12] K. Furuta, X.L. Yang, J.S. Chen, R. Hamilton, J.T. August, Differential expression of the lysosome-associated membrane proteins in normal tissues, Arch. Biochem. Biophys. 365 (1999) 75-82.

[13] Y. Cha, S.M. Holland, J.T. August, The cDNA sequence of mouse LAMP-2. Evidence for two classes of lysosomal membrane glycoproteins, J. Biol. Chem. 265 (1990) 5008-5013.

[14] N.R. Gough, D.M. Fambrough, Different steady state subcelular distributions of the three splice variants of lysosome-associated membrane protein LAMP-2 are determined largely by the COOH-terminal amino acid residue, J. Cell Biol. 137 (1997) 1161-1169.

[15] T. Braulke, J.S. Bonifacino, Sorting of lysosomal proteins, Biochim. Biophys. Acta. 1793 (2009) 605-614.

[16] H. Maeda, K. Akasaki, Y. Yoshimine, A. Akamine, K. Yamamoto, Limited and selective localization of the lysosomal membrane glycoproteins LGP85 and LGP96 in rat osteoclasts, Histochem. Cell Biol. 111 (1999) 245–251.

[17] E.L. Eskelinen , A.M. Cuervo, M.R. Taylor, I. Nishino, J.S. Blum, J.F. Dice, I.V. Sandoval, J. Lippincott-Schwartz, J.T. August, P. Saftig, Unifying nomenclature for the isoforms of the lysosomal membrane protein LAMP-2, Traffic 6 (2005) 1058-1061.

[18] B. Levine, G. Kroemer, Autophagy in the pathogenesis of disease, Cell 132 (2008) 27-42.

[19] E.L. Eskelinen, A.L. Illert, Y. Tanaka, G. Schwarzmann, J. Blanz, K. von Figura, P. Saftig, Role of Lamp-2 in lysosome biogenesis and autophagy, Mol. Biol. Cell. 13 (2002) 3355-3368.

[20] I. Nishino, Autophagic vacuolar myopathies, Curr. Neurol. Neurosci. Rep. 3 (2003) 64-69.

[21] Y. Tanaka, G. Guhde, A. Suter, E.L. Eskelinen, D. Hartmann, R. Lüllmann-Rauch, P.M. Janssen, J. Blanz, K. von Figura, P. Saktig, Accumulation of autophagic vacuoles and cardiomyopathy in Lamp-2-deficient mice, Nature 406 (2000) 902-906.

[22] F. Fortunato, H. Bürgers, F. Bergmann, P. Rieger, M.W. Büchler, G. Kroemer, J. Werner, Impaired autolysosome formation correlates with Lamp-2 depletion: role of apoptosis, autophagy, and necrosis in pancreatitis, Gastroenterology 137 (2009) 350-360.

[23] N. Sarmiento, C. Sánchez-Bernal, M. Ayra, N. Pérez, A. Hernández-Hernández, J.J. Calvo, J. Sánchez-Yagüe, Changes in the expression and dynamics of SHP-1 and SHP-2 during cerulein-induced acute pancreatitis in rats, Biochim. Biophys. Acta. 1782 (2008) 271-279.

[24] C. Sánchez-Bernal, O.H. García-Morales, C. Domínguez, P. Martín Gallán, J.J. Calvo, L. Ferreira, N. Pérez-González, Nitric oxide protects against pancreatic subcellular damage in acute pancreatitis, Pancreas 28 (2004) e9-e15.

[25] M.M. Bradford, A rapid and sensitive method for the quantitation of microgram quantities of protein utilizing the principle of protein-dye binding, Anal. Biochem. 72 (1976) 248-254.

[26] A.P. Clemons, D.M. Holstein, A. Galli, C. Saunders C, Cerulein-induced acute pancreatitis in the rat is significantly ameliorated by treatment with MEK1/2 inhibitors U0126 and PD98059, Pancreas 25 (2002) 251-259.

[27] A. Hernández-Hernández, M.N. Garabatos, M.C. Rodríguez, M.L. Vidal, A. López-Revuelta, J.I. Sánchez-Gallego, M. Llanillo, J. Sánchez-Yagüe, Structural characteristics of a lipid peroxidation product, trans-2-nonenal, that favour inhibition of membrane associated phosphotyrosine phosphatase activity, Biochim. Biophys. Acta. 1726 (2005) 317-325.

[28] J. de Castro, A. Hernández-Hernández, M.C. Rodríguez, M. Llanillo, J. Sánchez-Yagüe, Comparison of changes in erythrocyte and platelet fatty acid composition and protein oxidation in advanzed non-small cell lung cancer, Cancer Invest. 24 (2006) 339-345.

[29] J.F. Dice, Chaperone-mediated autophagy, Autophagy 3 (2007) 295-299.

[30] T. Reinheckel, J. Prause, B. Nedelev, W. Augustin, H.-U. Schulz, H. Lippert, W. Halangh, Oxidative stress affects pancreatic proteins during the early pathogenesis of rat cerulein pancreatitis, Digestion 60 (1999) 56-62.

[31] B. Künzli, P.O. Berberat, Z.W. Zhu, M. Martignoni, J. Kleeff, A. Tempia-Caliera, M. Fukuda, A. Zimmermann, H. Friess, M.W. Büchler, Influences of the lysosomal associated membrane proteins (Lamp-1, Lamp-2) and Mac-2 binding protein (Mac-2-BP) on the prognosis of pancreatic carcinoma, Cancer 94 (2002) 228-239.

[32] J. Mayerle, J. Schnekenburger, B. Kruger, J. Kellermann, M. Ruthenburger, F.U. Weiss, A. Nalli, W. Domschke, M.M. Lerch, Extracellular cleavage of E-cadherin by leukocyte elastase during acute experimental pancreatitis in rats, Gastroenterology 129 (2005) 1251-1267.

[33] B. Ji, X. Chen, D.E. Misek, R. Kuick, S. Hanash, S. Ernst, R. Najarian, C.D. Logsdon, Pancreatic gene expression during the initiation of acute pancreatitis: identification of EGR-1 as a key regulator, Physiol. Genomics 14 (2003) 59-72.

[34] T. Reinheckel, B. Nedelev, J. Prause, W. Augustin, H.-U. Schulz, H. Lippert, W. Halangh, Occurrence of oxidatively modified proteins: an early event in experimental acute pancreatitis, Free Radic. Biol. Med. 24 (1998) 393-400.

[35] U. Lichter-Konecki, S.E. Moter, B.R. Krawisz, M. Schlotter, C. Hipke, D.S. Konecki, Expression patterns of murine lysosome-associated membrane protein 2 (Lamp-2) transcripts during morphogenesis. Differentiation 1999; 65: 43-58.

[36] J.E. Oertel, The pancreas. Nonneoplastic alterations, Am. J. Surg. Pathol. 13(Suppl 1) (1989) 50-65.

[37] C.H. Kubisch CH, C.D. Logsdon, Endoplasmic reticulum stress and the pancreatic acinar cell, Expert Rev. Gastroenterol. Hepatol. 2 (2008) 249-260.

[38] G. Hoppe G, J. O´Neil J, H.F. Hoff HF, J. Sears, Products of lipid peroxidation induce missorting of the principal lysosomal protease in retinal pigment epithelium, Biochim. Biophys. Acta. 1689 (2004) 33-41.

[39] A. Dabrowski, S.J. Konturek, J.W. Konturek, A. Gabryelewicz, Role of oxidative stress in the pathogenesis of caerulein-induced acute pancreatitis, Eur. J. Pharmacol. 377 (1999) 1-11.

[40] A. Dabrowski, A. Gabryelewicz, M. Chwiecko, Products of lipid peroxidation and changes in sulfhydryl compounds in pancreatic tissue of rats with caerulein-induced acute pancreatitis, Biochem. Med. Metab. Biol. 46 (1991) 10-16.

[41] M. Fukuda, Lysosomal membrane glycoproteins. Structure, biosynthesis and intracelular trafficking, J. Biol. Chem. 266 (199) 21327-21330.

[42] O. Gilgenast, B. Brandt-Nedelev, I. Wiswedel, H. Lippert, W. Halangk, T. Reinheckel, Differential oxidative injury in extrapancreatic tissues during experimental pancreatitis: modification of lung proteins by 4-hydroxynonenal, Dig. Dis. Sci. 46 (2001) 932-937.

[43] N. Andrejewski, E.L. Punnonen, G. Guhde, Y. Tanaka, R. Lullmann-Rauch, D. Hartman, K. von Figura, P. Saftig, Normal lysosomal morphology and function in LAMP-1-deficient mice, J. Biol. Chem. 274 (1999) 12692-12701.

[44] I.R. Nabi, E. Rodriguez-Boulan, Increased LAMP-2 polylactosamine glycosylation is associated with its slower Golgi transit during establishment of a polarized MDCK epitelial monolayer, Mol. Biol. Cell. 4 (1993) 627-635.

[45] I.R. Nabi, J.W. Dennis, The extent of polylactosamine glycosylation of MDCK LAMP-2 is determined by its Golgi residence time, Glycobiology 8 (1998) 947-953.

[46] T. Ueda, Y. Takeyama, M. Adachi, A. Toyokawa, S. Kishida, M. Yamamoto, Y. Saitoh, Effect of the microtubule-disrupting drug colchicine on rat cerulein-induced pancreatitis in comparison with the microtubule stabilizer taxol, Pancreas 11 (1995) 294-302.

[47] M. Jadot M, R. Wattiaux R, F. Mainferme F, F. Dubois F, A. Claessens A, S. Wattiaux-De Coninck, Soluble form of Lamp II in purified rat liver lysosomes, Biochim. Biophys. Res. Commun. 223 (1996) 353-359.

[48] A.M. Cuervo, J.F. Dice, Regulation of Lamp2a levels in the lysosomal membrane, Traffic 1 (2000) 570-583.

[49] S.L. Rusch, D.A. Kendall, Oligomeric states of the SecA and SecYEG core components of the bacterial Sec translocon, Biochim. Biophys. Acta. 1768 (2007) 5-12.

[50] A.M. Cuervo, J.F. Dice, Unique properties of lamp2a compared to other lamp2 isoforms, J. Cell Sci. 113 (2000) 4441-4450.

FIGURE LEGENDS

Fig. 1. Expression of LAMP-2 (A) and serum amylase activity (B) during the development of Cer-induced AP. Rats were either administered saline (0.9% NaCl) (control, C) or treated with Cer, as indicated in Materials and methods, and then killed 2, 4 or 9 h after the first injection of Cer. In (A), the quantification (graphic) of expression (Western blots in whole postnuclear pancreatic homogenates- one representative for each time-point is shown) was carried out considering the whole pancreas. Anti-β-tubulin antibody was used as an approximate loading control. Each lane in the blots contained 30 μg of protein. Data are mean ± S.D. of 5 animals.

Fig. 2. LAMP-2 mRNA expression (A) and Western blot analysis of oxidized proteins (B) in the early phase of Cer-induced AP. Rats were either administered saline (0.9% NaCl) (control, C) or treated with Cer, as indicated in Materials and methods, and then killed 2 h after the first injection of Cer. (A) mRNA expression was analysed in pancreas or brain by RT-PCR. β-actin was used as a loading control. (B) Western blot analysis from different subcelular fractions as well as from postnuclear pancreatic homogenates was performed using the Oxyblot Protein Oxidation Detection Kit, in the presence of β-mercaptoethanol, as indicated in Materials and methods. Some of the proteins with increased contents of carbonyl groups are indicated by arrows. Each lane contained 8 μg of protein. Experiments were repeated in four different animals with similar results. A representative is shown.

Fig. 3. Light microscopy of the rat pancreas stained with H&E (A, C, E) and immunostaining of LAMP-2 (B, D, F) in normal pancreas (A, B) and during the early (C, D) and intermediate (E, F) phases of Cer-induced AP. Rats were either administered saline (0.9% NaCl) or treated with Cer,

as indicated in Materials and methods, and then killed 2 or 4 h after the first injection of Cer. In the histologic pancreatic sections: control animal (A) showing a normal morphology; 2 h (C), 4 h (E) pancreatitic rats. Compare the morphology of normal acini with other acini showing an altered morphology (arrows). Note also the different and increasing degree of leukocyte infiltration (arrowheads) from 2 to 4 h. In the immunohistochemistry, note the increased immunoreactivity in the acinar and islet cells as from 2 h (D) and 4 h (F) pancreatitc rats compared with control animals (B).

Fig. 4. Subcellular distribution and dynamics of LAMP-2. Rats were either administered saline (0.9% NaCl) (control, C) or treated with Cer, as indicated in Materials and methods, and then killed 2, 4 or 9 h after the first injection of Cer. (A) Distribution of LAMP-2 in different subcellular fractions from pancreas 2 h after the first injection of Cer (early phase of Cer-induced AP). The quantification (graphic) of expression (Western blots- one representative for each subcelular fraction) is shown as relative percentages considering the sum of the integrated densities for all subcellular fractions in the whole pancreas as 100%. (B) Distribution of LAMP-2 in the Lysosome+Mitochondria subcellular fraction during the development of Cer-induced AP. The quantification (graphic) of expression (Western blots- one representative for each time) is shown as relative percentages considering that of controls in the whole pancreas as 100%. (C) Presence of LAMP-2 in 3 lysosomal subpopulations separated by Percoll density gradient centrifugation. A representative Western blot is shown. In (A) and (B), the data are means ± S.D. of 3 experiments with 4 rats in each. Each lane in all blots contained 30 μg of protein.

Fig. 5. Membrane-association of LAMP-2 from the pancreatic soluble fraction. Equal volumes of the soluble fractions of both control and pancreatitic pancreata [2 h (A), 4 h (B) or 9 h (C) after the first injection of Cer] were subjected to centrifugation at 400,000 $\times g$. Then, Western blots of

the supernatant (Sp) and the precipitate (Pp) were developed. The quantification (graphics) of expression is depicted as relative percentages considering the sum of the integrated densities of the whole volume of Sp and the whole Pp as 100%. The LAMP-2 shown in the control and pancreatitic pancreata represent the 96 and 120 kDa form, respectively. Data are means ± S.D. of 3 samples from different experiments.

Fig. 6. Effect of neutropenia on MPO (A) and LAMP-2 protein expression (B) during the development of Cer-induced AP. Rats were given 0.75 mg/kg i.v. vinblastine sulfate to induce neutropenia. Four days after vinblastine administration, these neutropenic rats were given 4 injections of saline (0.9% NaCl) or Cer hourly over 4 h (representing the intermediate phase of AP), as indicated in Materials and methods. The same treatments were given to control animals (C) (saline instead of vinblastine pre-treatment on day 1). In (B) the quantification (graphic) of expression (Western blots in whole postnuclear pancreatic homogenates- a representative is shown) was carried out considering the whole pancreas. Samples from rat lymphocytes and 4-h pancreatitic pancreas were also included for comparison of LAMP-2 protein molecular weight and expression levels. Anti-β-tubulin antibody was used as an approximate loading control. The lanes in the blots contained: 100, 60 and 30 μg of protein (lymphocytes, C and the last three lanes, respectively). Data are means ± S.D. of 4 animals.

Fig. 7. Nature and carbohydrate content of the 120 kDa LAMP-2. (A) Urea does not change the molecular weight of LAMP-2. From the left, lanes 1 to 3 correspond to samples from the soluble fraction from pancreatitic pancreata (Cer, 2 h after the first injection of Cer) and the soluble and L+M fractions from control pancreata (C), respectively. The sample in lane 4 is the same as that of lane 1, but it was treated previously with the 2-D Clean-Up kit and finally rehydrated in sample buffer containing urea 7M, 2M thiourea and 50 mM DTT, and boiled for 5 min Each lane

in the blot contained 100 μg of proteins. (B) The 120 kDa LAMP-2 associated with the soluble fraction from pancreatitic rats (Cer, 2 h after the first injection of Cer) is a glycoprotein that is bound by two different lectins: Con A and WGA. Microsomes from control pancreas (C) expressing the normal 96 kDa LAMP-2 were also assayed for comparison. None, Sp1 and Sp2 represent non-lectin-treated samples and the lectin-unbound and -bound proteins, respectively, as indicated in Materials and methods. Each lane in the blots contained approximately 40 or 4 μg of protein for the microsomes or soluble fractions, respectively. (C) Increased LAMP-2 molecular weight is not due to a different sialic acid content. Soluble fractions from control (C) or pancreatitic rats (Cer, 2 h after the first injection of Cer) were digested with neuraminidase for different times. (D) the increased LAMP-2 molecular weight is due to a different glycosylation pattern. The L+M fraction from control pancreata (left panel) or the soluble fraction from pancreatitic pancreata (right panel, 2 h after the first injection of Cer) were left undigested (none) or were digested with PGNase or Endo H, as indicated in Materials and methods. The Cer and L+M lanes in right panel represent untreated samples and were included in the Western blot analyses only as internal controls for the assesment of the correct molecular weight of the 120 and 96 kDa LAMP-2 forms, respectively. All blots are representative of three experiments.

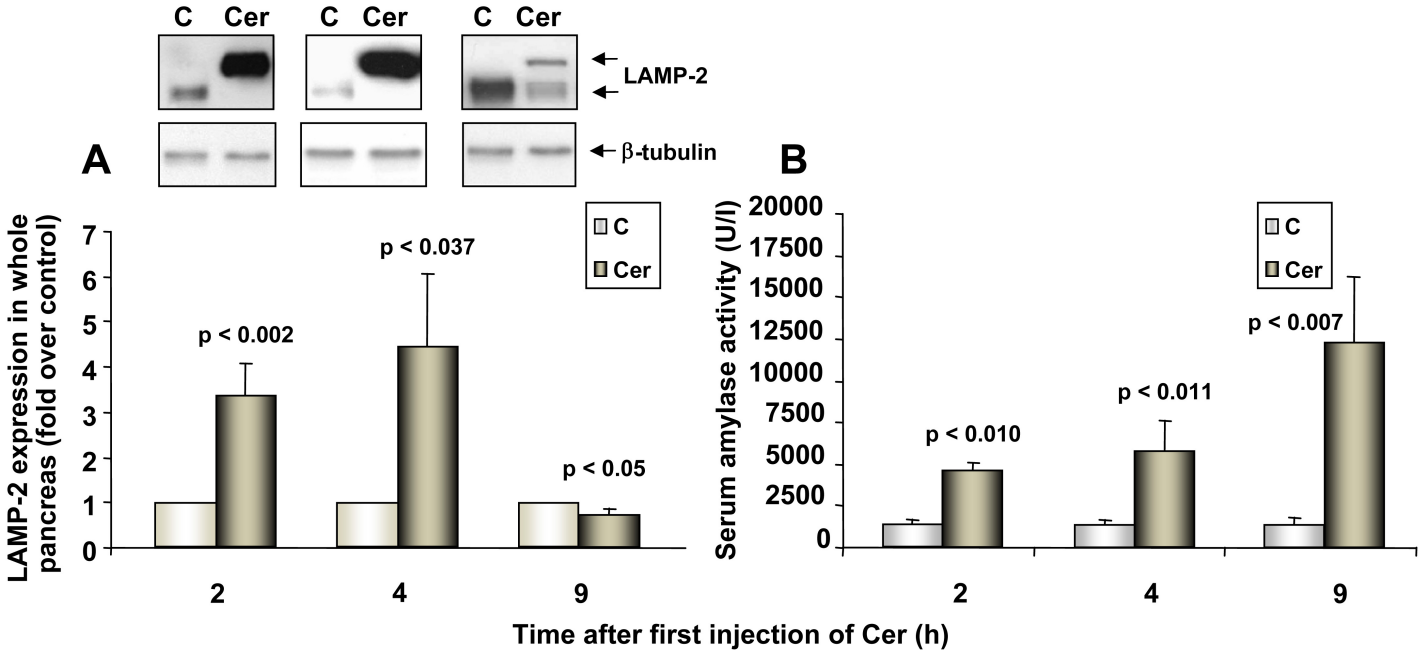
C
Cer
C
Cer
C
Cer
LAMP-2
β-tubulin
A
B
LAMP-2 expression in whole pancreas (fold over control)
7
6
5
4
3
2
1
0
p < 0.002
p < 0.037
p < 0.05
C
Cer
2
4
9
Serum amylase activity (U/l)
20000
17500
15000
12500
10000
7500
5000
2500
0
p < 0.010
p < 0.011
p < 0.007
C
Cer
2
4
9
Time after first injection of Cer (h)

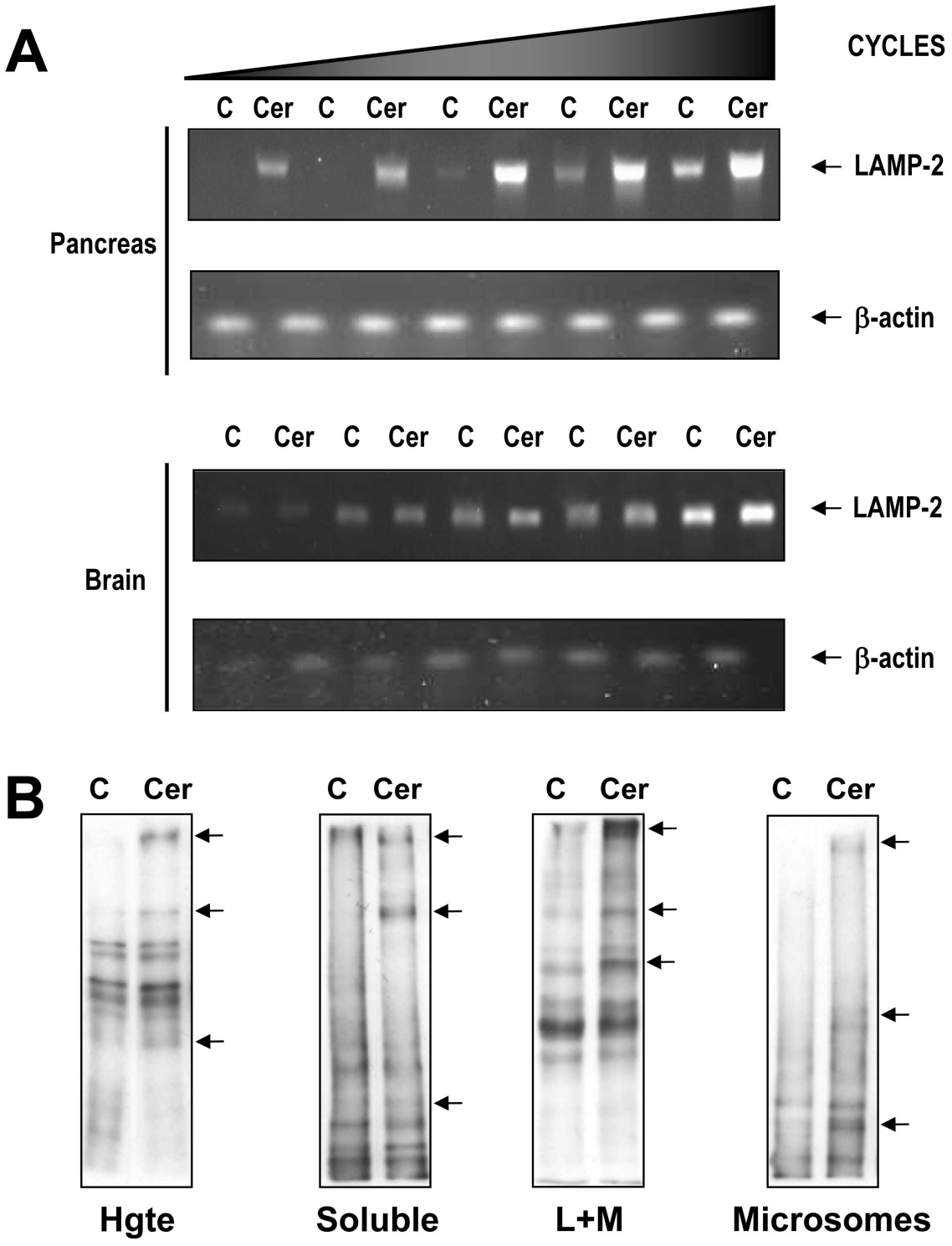
A
CYCLES
C Cer C Cer C Cer C Cer C Cer
Pancreas
LAMP-2
β-actin
C Cer C Cer C Cer C Cer C Cer
Brain
LAMP-2
β-actin
B
C Cer
C Cer
C Cer
C Cer
Hgte
Soluble
L+M
Microsomes

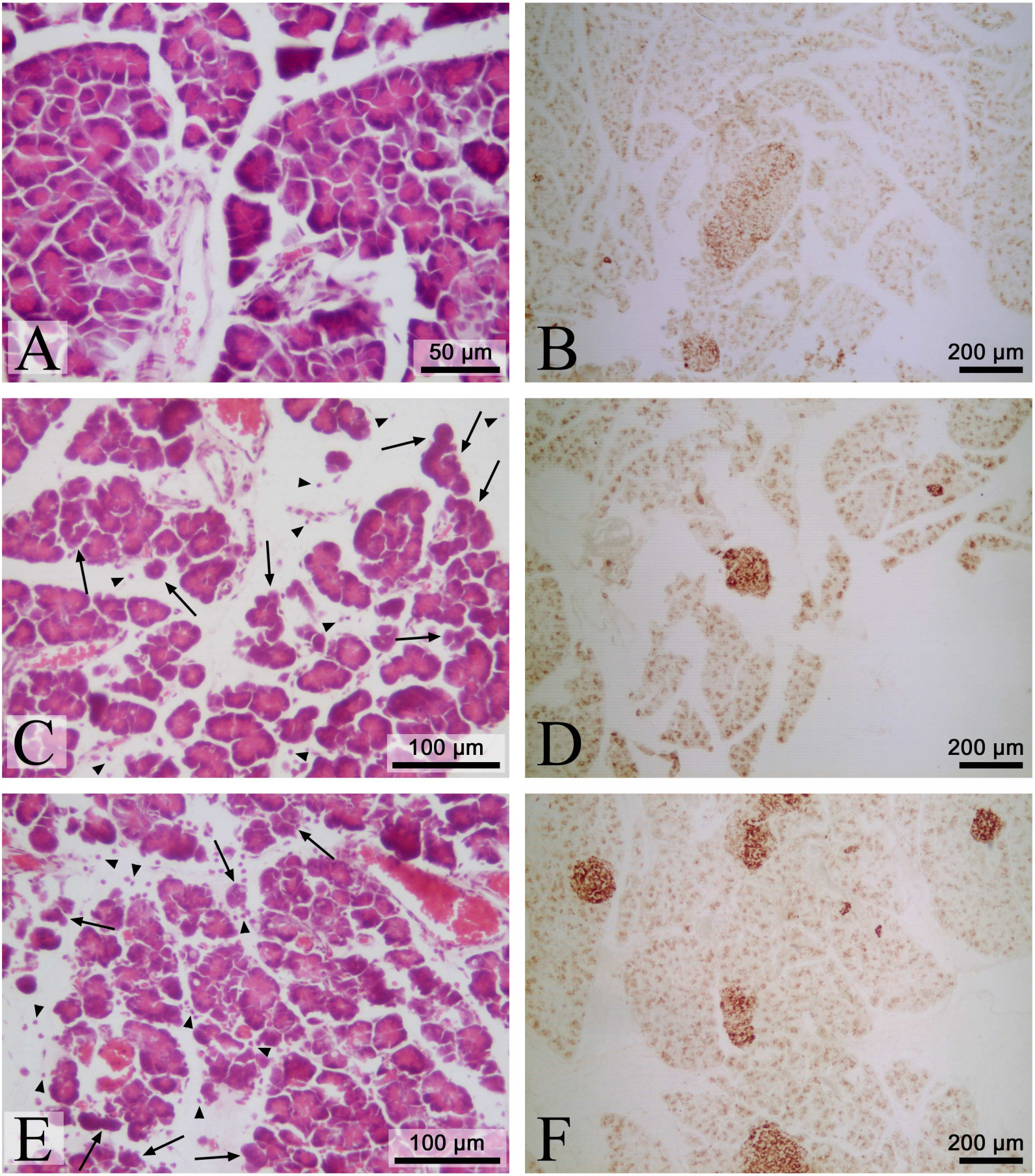
A
50 µm
B
200 µm
C
100 µm
D
200 µm
E
100 µm
F
200 µm

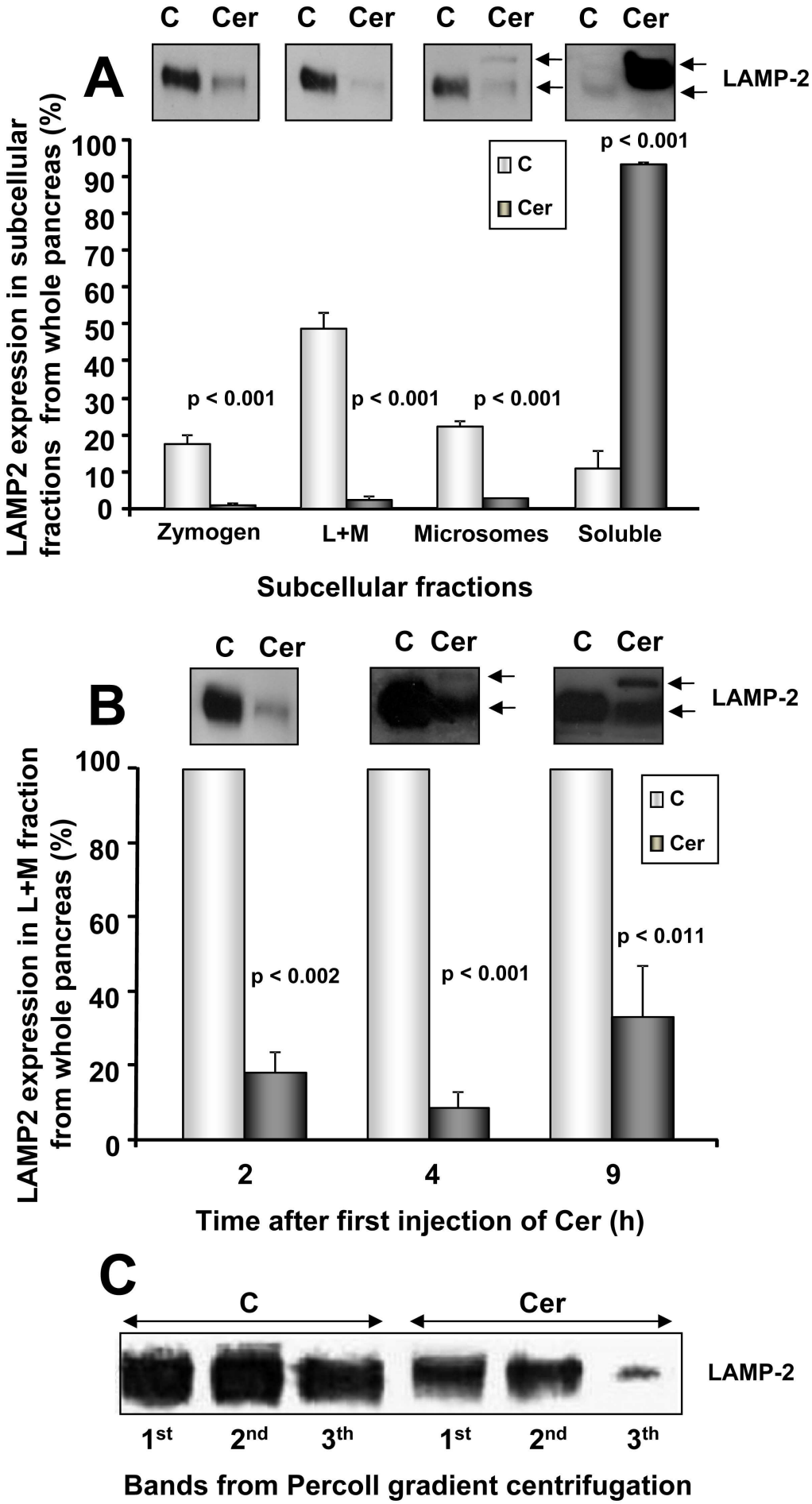
A
C
Cer
C
Cer
C
Cer
C
Cer
LAMP-2
LAMP2 expression in subcellular fractions from whole pancreas (%)
100
90
80
70
60
50
40
30
20
10
0
C
Cer
p < 0.001
p < 0.001
p < 0.001
p < 0.001
Zymogen
L+M
Microsomes
Soluble
Subcellular fractions
B
C
Cer
C
Cer
C
Cer
LAMP-2
LAMP2 expression in L+M fraction from whole pancreas (%)
100
80
60
40
20
0
C
Cer
p < 0.002
p < 0.001
p < 0.011
2
4
9
Time after first injection of Cer (h)
C
C
Cer
LAMP-2
1st
2nd
3th
1st
2nd
3th
Bands from Percoll gradient centrifugation

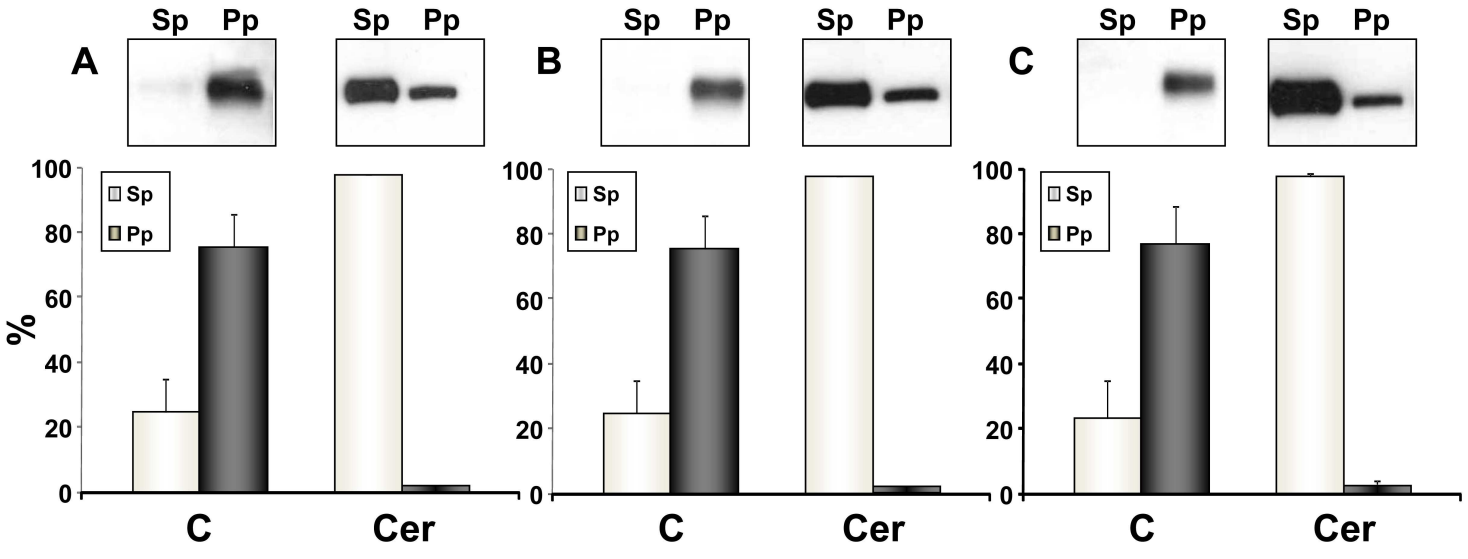
A
B
C
Sp
Pp
Sp
Pp
Sp
Pp
Sp
Pp
Sp
Pp
Sp
Pp
100
80
60
40
20
0
%
Sp
Pp
C
Cer

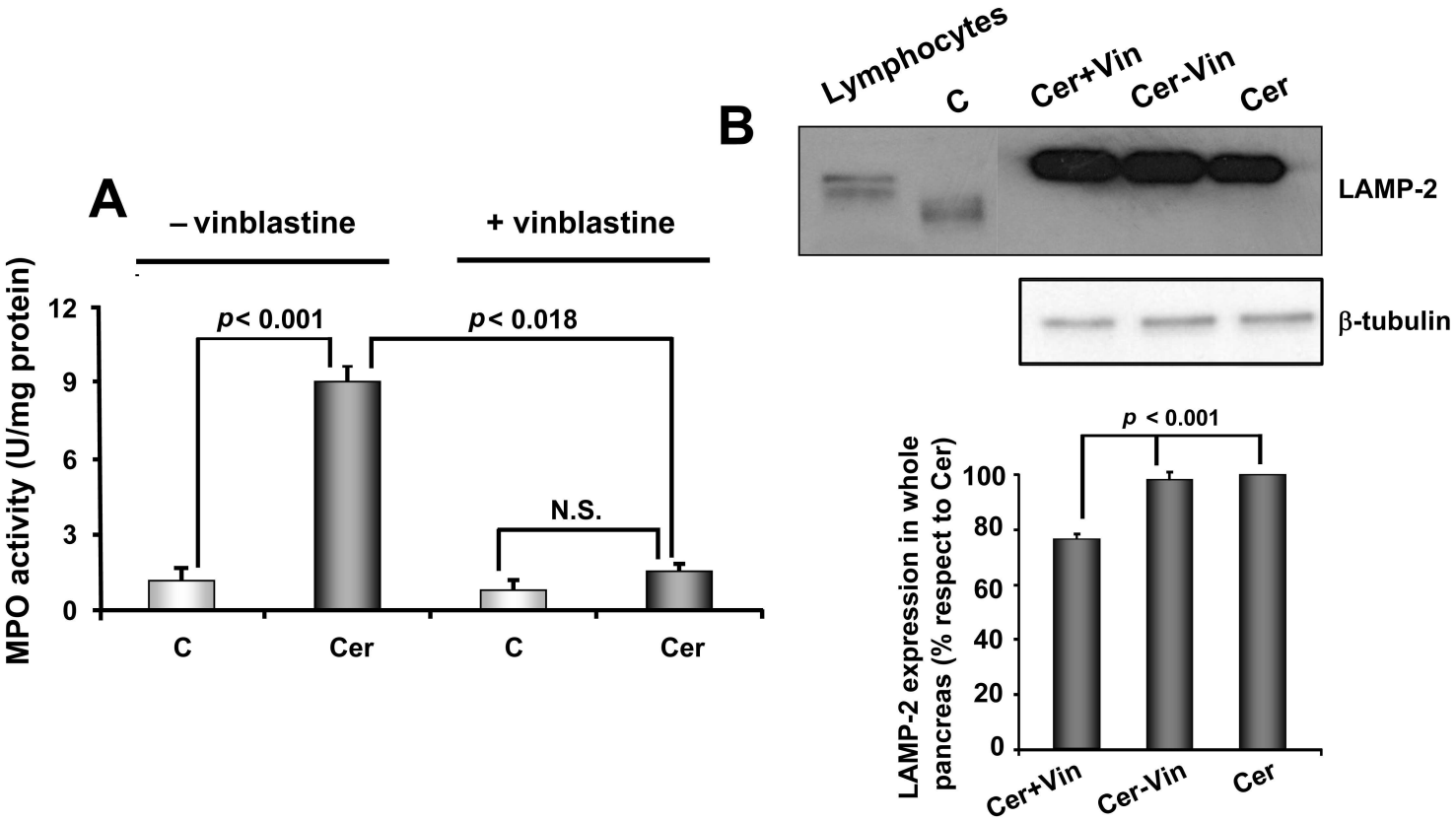
A
– vinblastine
+ vinblastine
MPO activity (U/mg protein)
12
9
6
3
0
p< 0.001
p< 0.018
N.S.
C
Cer
C
Cer
B
Lymphocytes
C
Cer+Vin
Cer-Vin
Cer
LAMP-2
β-tubulin
p < 0.001
LAMP-2 expression in whole pancreas (% respect to Cer)
100
80
60
40
20
0
Cer+Vin
Cer-Vin
Cer

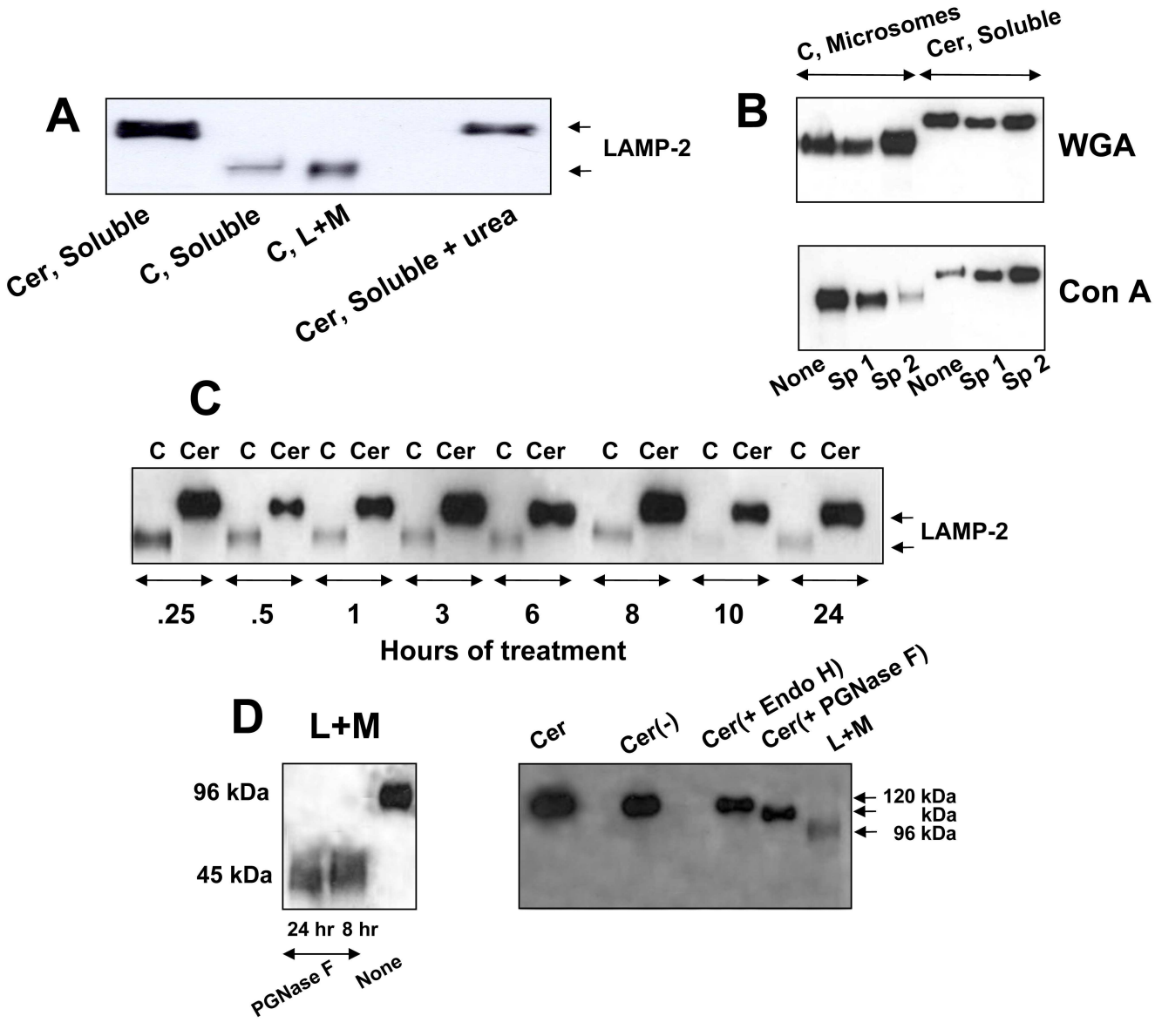
A
LAMP-2
Cer, Soluble
C, Soluble
C, L+M
Cer, Soluble + urea
B
C, Microsomes
Cer, Soluble
WGA
Con A
None
Sp 1
Sp 2
None
Sp 1
Sp 2
C
C Cer C Cer C Cer C Cer C Cer C Cer C Cer C Cer
LAMP-2
.25
.5
1
3
6
8
10
24
Hours of treatment
D
L+M
96 kDa
45 kDa
24 hr 8 hr
PGNase F
None
Cer
Cer(-)
Cer(+ Endo H)
Cer(+ PGNase F)
L+M
120 kDa
kDa
96 kDa

V. Discusión

SOBRE EL DISEÑO EXPERIMENTAL

Debido a la inaccesibilidad al páncreas humano en vida, lo fundamental del conocimiento de la fisiopatología de la PA está basado en modelos animales. Uno de los modelos animales de PA es el inducido en la rata por estimulación supramáxima con secretagogos, y normalmente, el agente trófico utilizado es la ceruleína [un análogo de la colescistoquinina (CCK)]. El modelo, que es histológicamente muy similar a la fase temprana de la pancreatitis aguda de humanos (*Cheung y Leung, 2007*), simula una PA moderada y edematosa, siendo fácilmente reproducible, por lo que es muy adecuado para el estudio de los fenómenos bioquímicos que se desencadenan durante el desarrollo de la enfermedad. Para inducir PA en ratas se han utilizado dosis diferentes de Cer (desde 5 hasta 100 μg/Kg). En las condiciones que describimos en esta Memoria [inyecciones s.c. de 20 μg/Kg], las manifestaciones de la PA incluyen hiperamilasemia, edema intersticial, aumento del tamaño de las células acinares, aumento del peso pancreático, daños histológicos (vacuolización y otras alteraciones morfológicas), e infiltración por leucocitos (*Alonso y cols., 1994; Pescador et al., 1995; Yönetçi et al., 2001; Zhao et al., 2007*). También hemos utilizado en distintos momentos otros dos modelos adicionales de PA: (1) la obstrucción biliopancreática en rata, como otro modelo de PA de tipo edematoso, que simula la etiología más frecuente de la PA humana (*Pandol et al., 2007*), (2) la perfusión retrógrada de taurocolato sódico (TcNa) en el conducto biliopancreático, un modelo descrito por Aho y colaboradores (*Aho et al., 1984*) y bien estandarizado experimentalmente como modelo de PA necrotizante. Aunque se han utilizado diferentes concentraciones de TcNa (3-5%) en distintas especies animales (*Poch et al., 1999; Vaquero et al., 2001; Liu et al., 2003; Shi et al., 2006*), el Dr. Manso, quien nos ayudó en la realización de este modelo, nos indicó que una concentración al 3,5% de TcNa permite estudiar las alteraciones que progresivamente se desarrollan en los primeros estadios de la PA, ya que concentraciones de TcNa del 5% resultan muy lesivas para las células pancreáticas desde el momento de su perfusión.

SOBRE LA DINÁMICA DE LAS PROTEÍNA TIROSINA FOSFATASAS (PTP)

Muchas y diversas rutas intracelulares de señalización regulan la función de las células acinares pancreáticas tras estimulación del páncreas con CCK o ceruleína. Ambas moléculas aumentan los niveles de calcio citosólico libre a través de proteínas Gq. El Ca^{2+}, el diacilglicerol y el AMPc activan los procesos de exocitosis. Además, se conoce que tanto CCK como ceruleína activan proteína tirosina quinasas (PTKs) pancreáticas (*Rivard et al., 1995*), y que la fosforilación en tirosinas desempeña funciones importantes en la regulación de muchas funciones celulares. También se sabe que la pancreatitis cursa con una disociación de los contactos célula-célula (*Schnekenburger et al., 2005*) y de las uniones adherentes, y que la fosforilación en tirosina juega un papel central en el mantenimiento de un complejo de adhesión celular intacto (*Muller et al., 1999*). Otra ruta de señalización que se activa tras estimulación del páncreas con CCK o ceruleína, es la activación de la cascada de las proteínas quinasas activadas por mitógeno (MAPKs), de hecho, la activación de MAPKs es uno de los mecanismos patogénicos centrales no sólo en la pancreatitis, sino en enfermedades inflamatorias en general (*Kyriakys et al., 2001*), incluyendo a la quinasa regulada por señales extracelulares (ERK1/2) y a la quinasa N-terminal *c-Jun* (JNK) (*Widmann et al., 1999; Minutoli et al., 2004*), cuyas activaciones requieren la fosforilación de residuos de tirosina y treonina (*Widmann et al., 1999; Minutoli et al., 2004*). Los datos acerca de la activación de p38MAPK como respuesta a la estimulación con Cer son contradictorios. Así, se ha descrito tanto su activación (*Namkung et al., 2008*) como su no activación (*Fleischer et al., 2001*). En nuestras condiciones experimentales, nuestro grupo investigador demostró recientemente que p38MAPK no se activa (*García-Hernández et al., 2014*). Otra ruta de transducción de señales que también se activa en la PA es la ruta del receptor de adenosina A1 (*Satoh et al., 2000*), que disminuye los niveles de AMPc intracelular. La importancia de la activación de estas rutas de señalización en la PA se pone de manifiesto porque: (1) se activan en su fase más temprana, y (2) al menos en el caso de ERK1/2, JNK y receptor de adenosina A1, su inhibición disminuye la gravedad de la PA inducida por Cer (*Minutoli et al., 2004; Satoh et al., 2000*).

El descubrimiento del papel de las PTKs en la regulación de los niveles de fosforilación en tirosina ha hecho que las PTPs sean consideradas como reguladores fundamentales de las funciones celulares. Las PTPs con dominios SH2: SHP-1 y SHP-2, que son estructuralmente muy similares, tienen diferentes funciones en la transducción de señales. SHP-1 se expresa abundantemente en las células hematopoyéticas y a menor nivel en muchos otros tipos celulares, y juega un papel señalizador negativo en las células hematopoyéticas. SHP-2 se expresa más ampliamente y desempeña un papel básicamente positivo en la transducción de señales que conduce a la activación celular. No obstante, parece que la naturaleza funcional de SHP-1 y SHP-2 depende de los sistemas analizados. Se ha implicado a SHP-1 en las rutas Jak-Stat y MAPK (*You et al., 1997*). SHP-2 tiene funciones señalizadoras mezcladas, y parece implicada en una variedad de procesos de transducción de señales tales como las rutas Ras-Raf-MAPK, JAK-STAT, quinasa PI3 y NF-κB (*Qu et al., 2002*). Precisamente, NF-κB es uno de los factores de transcripción al que se le está otorgando un papel preponderante en la iniciación de la cascada inflamatoria que ocurre en la PA (*Liu et al., 2003; Huang et al., 2012*). SHP-2 puede actuar en múltiples lugares incluso dentro de una misma ruta de señalización. Respecto a PTP1B, esta PTP juega un papel central de control en la señalización por diversas citoquinas, debido a su acción negativa en miembros específicos de la ruta JAK/STAT (*Bourdeau et al., 2005*). La señalización inflamatoria por JAK2/Factor de transcripción STAT3 está implicada en la PA (*Bourdeau et al., 2005*) y JAK2 es una diana de PTP1B (*Yu et al., 2008*). Aunque todas las rutas de señalización descritas anteriormente, y en las que, en algún momento, interviene SHP-1, SHP-2 y/o PTP1B, se han implicado en el desarrollo de la PA, los datos acerca de las PTPs en la PA son muy escasos. Esta falta de datos también es llamativa cuando se considera que estas enzimas señalizadoras se inactivan por especies reactivas del oxígeno (ROS) (*Den Hertog et al., 2005*), cuya influencia en la cascada inflamatoria es más importante de lo que se predijo en un principio (*Escobar et al., 2012*). Estos ROS se producirían en la PA, principalmente vía la NADPH oxidasa, tanto de células inflamatorias infiltrantes como de las propias células acinares (*Leung y Chan, 2009*). Las PTPs también se inactivan por productos secundarios de oxidación (*Hernández-Hernández et al., 2005*) que se producen

durante el desarrollo de la PA (*Sánchez-Bernal et al., 2004*). Esencialmente, sólo se ha descrito la función de SHP-1 y PTPκ en la regulación de la adhesión celular del páncreas de rata en la PA moderada inducida por Cer (*Schnekenburger et al., 2005*). Por otro lado, se sabe que PTP1B desempeña importantes funciones en células con alto contenido en retículo endoplasmático (RE) (*Bourdeau et al., 2005*), como es el caso de las células acinares del páncreas, que tienen el mayor nivel de síntesis proteica de todos los tejidos humanos (*Case et al., 1978*). De hecho, las células acinares son susceptibles a la homeostasis del RE, y se conoce que los principales mecanismos de señalización de respuesta al estrés se activan en la PA (*Kubish et al., 2006; Suyama et al., 2008; Ji et al., 2003*).

Tanto JNK como ERK1/2 son mediadores importantes en la fase temprana de la PA (horas 1-1,5) (*Minutoli et al., 2004; Clemons et al., 2002; Hofken et al., 2000*). Muchos de los factores de transcripción que se inducen de modo temprano en el desarrollo de la PA están regulados por la activación de MAPKs (*Ji et al., 2003*), de modo que la activación de estas enzimas representa el lazo de unión entre los sucesos de señalización más tempranos conocidos en la PA, y las consecuencias a más largo plazo derivadas de los cambios en la expresión génica. Además, se sabe que las quinasas de estrés también regulan la traducción proteica (*Williams et al., 2001*). Por otro lado, se ha descrito que la PA cursa con un excesivo catabolismo del ATP (*Lüthen et al., 1995*), y que el aumento de los niveles de AMPc intracelular en las células inflamatorias atenúa la gravedad de numerosos procesos inflamatorios, incluida la PA, por lo que el AMPc podría jugar un papel relevante en la patogénesis de la PA (*Sato et al., 2006*).

Como indicamos antes, la observación fundamental que relaciona a las rutas de señalización mediadas por MAPKs y por AMPc con la fisiopatología de la PA es que la inhibición de las MAPKs y el aumento de los niveles de AMPc intracelular disminuyen su gravedad. Desde un punto de vista más bioquímico, una relación entre AMPc y MAPKs la sugieren diversos trabajos donde se analiza el papel de la señalización por AMPc y la regulación del ciclo celular en células pancreáticas humanas; sistema en el que se ha demostrado que el aumento de los niveles de AMPc inhibe la cascada de señalización mediada

por ERK (*Boucher et al., 2001*). La disminución en la gravedad de la PA se ha demostrado mediante el uso de inhibidores; así, el tratamiento con SP600125, o con U0126 o PD98059, bloquea fundamentalmente la activación, mediada por ceruleína, de JNK o de ERK1/2, respectivamente, y disminuye la severidad de la PA (*Minutoli et al., 2004; Namkung et al., 2008*), al menos porque dicho bloqueo impide la sobreexpresión de citoquinas inflamatorias (p. e. TNF-α) (*Minutoli et al., 2004*), lo que dificulta el proceso de infiltración del páncreas. De hecho, el pre-tratamiento con SP600125 resulta en una disminución de la acumulación de leucocitos en el páncreas de ratas pancreatíticas mediante Cer (*Minutoli y cols., 2004*). Respecto a la modulación con inhibidores de la ruta del AMPc intracelular en la PA, se ha empleado el rolipram, un fuerte y específico inhibidor de la fosfodiesterasa tipo IV (PDE4, enzima clave en el metabolismo del AMPc intracelular que se expresa de modo abundante en células inflamatorias tales como los neutrófilos). El rolipram ejerce efectos anti-inflamatorios ya que facilita el aumento de los niveles de AMPc intracelular al bloquear su catabolismo. De este modo, el rolipram tiene una acción similar a la del receptor de adenosina A2a, un tipo de receptor que se expresa principalmente en las células inflamatorias (*Satoh et al., 2000*). El aumento de los niveles de AMPc intracelular activa a la proteína quinasa dependiente de AMPc, la cual también reduce la producción de citoquinas proinflamatorias tales como TNF-α (*Semmler et al., 1993*). Este hecho relaciona la ruta de las MAPKs con la del AMPc en la PA, y podría explicar, al menos en parte, por qué SP600125 y rolipram disminuyen la gravedad de la PA inducida por Cer. Se ha propuesto incluso el uso del rolipram en clínica para tratar los efectos de la PA (*Sato et al., 2006*).

La complejidad de las interacciones entre las diferentes vías de señalización implicadas en la PA (descritas arriba) hace que los sucesos bioquímicos que ocurren a nivel de la célula acinar en la fase más temprana de la PA no estén totalmente esclarecidos. Teniendo esto en cuenta, se ha sugerido que sería muy importante detectar eventos bioquímicos, mecanismos de señalización y alteraciones en la expresión de genes y/o de proteínas que ocurriesen de modo rápido y temprano en la PA, porque dichos sucesos moleculares conducirían hacia, o influirían en, las respuestas a más largo

término que finalmente determinarían el desarrollo de la pancreatitis (*Ji et al., 2003*). Directamente relacionado con la necesidad de encontrar mecanismos de señalización y alteraciones en la expresión de genes y/o de proteínas que ocurriesen de modo rápido y temprano en la PA, en esta memoria describimos por primera vez (usando ratas como modelo experimental) que en la PA inducida por ceruleína se producen aumentos en los niveles de expresión de SHP-1, SHP-2 y PTP1B, tanto a nivel proteico como a nivel génico. Dicho aumento parece ocurrir mayoritariamente en las células acinares, y cursa con cambios en la dinámica de localización subcelular de, específicamente, SHP-2. Todos estos cambios suceden en las fases tempranas de la PA, lo que potencialmente tiene un importante significado funcional en el desarrollo de la enfermedad. El aumento de expresión de SHP- 2 ocerre también en otros modelos de PA, como son los producidos por perfusión retrógrada de TcNa en el conducto biliopancreático, o el modelo de la ligadura del conducto bilio-pancreático. Además, la infiltración por neutrófilos modula los niveles de expresión proteica de SHP-2 y determina el incremento en expresión de PTP1B.

La implicación de la infiltración en la expresión proteica de dichas PTPs es muy interesante dado el papel central de la infiltración en el desarrollo de la PA. De hecho, la infiltración por neutrófilos es el suceso universal de los procesos inflamatorios agudos o crónicos, y la evidencia de activación celular. Por tanto, nuestros resultados indicarían un potencial entendimiento *in vivo* entre mecanismos de señalización de la célula acinar pancreática con las células sanguíneas infiltrantes, que operaría en la fase temprana del desarrollo de la enfermedad para modular los niveles de expresión de determinadas PTPs. Asimismo, es significativo, como ya indicamos antes, que para el fenómeno de la diapédesis leucocitaria y linfocitaria que ocurre en la PA se necesita que las uniones adherentes de la membrana basolateral celular se disocien, permitiendo así una acumulación de fluido intersticial y de células inflamatorias. En este fenómeno se ha implicado al menos a SHP-1 (*Schnekenburger et al., 2005*).

Una inhibición de JNK y ERK1/2, así como los niveles de AMPc intracelular también son capaces, por un lado, de modular la expresión proteica

de SHP-1 y SHP-2 y, por otro, de suprimir el incremento en expresión de PTP1B**.** Esta modulación de la expresión de PTPs intracelulares por rutas de señalización que jugarían un papel relevante en el desarrollo de la PA (MAPKs y AMPc) indica que la regulación de los fenómenos de fosforilación en tirosinas también desempeñaría un papel importante en su desarrollo.

SOBRE LA DINÁMICA DE LA PROTEINA LISOSÓMICA LAMP-2

Por otro lado, se ha sugerido que el paso final de la señalización en la autofagia se inhibe, probablemente, por una disminución de las proteínas lisosómicas, lo cual está asociado con la vacuolización de la célula acinar que se observa en la pancreatitis (*Fortunato et al., 2009*). En esta memoria mostramos que LAMP-2, una proteína integral de los lisosomas que juega un papel directo en la autofagia, incrementa su expresión tanto a nivel proteico como de ARNm, desde la fase temprana de la pancreatitis aguda inducida por ceruleína. No obstante, parece sufrir un diferente procesamiento post-traduccional en su contenido en glúcidos, lo que se acompaña de una deslocalización celular, de modo que pasa a comportarse como una proteína de tipo soluble. Como consecuencia, su presencia disminuye de modo muy acusado en el lisosoma.

Se conoce que varios modelos de pancreatitis, como los inducidos por ceruleína o por perfusión retrógrada de TauNa, cursan con un aumento del estrés oxidativo y oxidación proteica desde sus fases tempranas (*Reinheckel et al., 1998; Reinheckel et al., 1999*). En esta memoria demostramos que, efectivamente, el estrés oxidativo, detectado como la aparición o el aumento del nivel de proteínas oxidadas en diferentes fracciones subcelulares o en homogenados de páncreas, ya sucede durante la fase temprana de la pancreatitis aguda inducida por ceruleína. Dicho estrés podría ser la causa del aumento de los niveles del ARNm de LAMP-2 que hemos detectado. De hecho, en hígado de rata se ha descrito que el estrés oxidativo aumenta la autofagia mediada por chaperones moleculares (CMA), el mecanismo responsable de la degradación selectiva de proteínas citosólicas en los lisosomas durante las condiciones de estrés. En este caso, uno de los miembros LAMP-2: LAMP-2A,

se sobreexpresa debido a regulación transcripcional y concomitante incremento de su ARNm (*Dice, 2007*).

Existen tres variantes de LAMP-2 producidas por empalme alternativo: LAMP-2A, LAMP-2B y LAMP-2C. En células de pollo, ratón y humanas, estas tres variantes están codificadas por diferentes tránscritos (*Eskelinen et al., 2002*). Las diferencias en la estructura primaria de las tres variantes se localizan exclusivamente en la región que atraviesa la membrana y en la cola citoplasmática (*Eskelinen et al., 2005*). En el ratón, se ha descrito que el tránscrito para LAMP-2 es el prevalente en el páncreas durante su morfogénesis (*Lichter-Konecki et al., 1999*). Los cebadores utilizados en nuestros análisis de RT-PCR nos permiten seguir todos los tipos de ARNm de LAMP-2. Por lo tanto, no podemos concluir cual de las tres variantes es la responsable del aumento en la expresión génica detectada en la PA inducida por ceruleína, aunque los datos descritos antes, acerca de la regulación transcripcional de LAMP-2A dependiente de estrés, en el hígado de rata, podrían sugerir que ésta sería la variante implicada.

La expresión de las distintas variantes de LAMP-2 es dependiente de tejido (*Furuta et al., 1999*), lo que sugiere diferentes funciones celulares. Se ha descrito que en el páncreas humano no patológico, el ARNm para LAMP-2 se localiza en las células acinares y en las células de los islotes, pero no en las células ductales, mientras que la inmunorreactividad frente a la proteína LAMP-2, se detecta únicamente en las células endocrinas, los macrófagos y las células acinares (*Künzli et al., 2002*). Nuestro inmunomarcado revela que, en la rata, LAMP-2 también está presente principalmente, aunque no de modo exclusivo, en las células de los islotes y en las acinares, y que, de modo importante, durante su fase temprana, la PA inducida por ceruleína cursa con un incremento similar en la expresión de LAMP-2 en ambos tipos celulares. No obstante, en el páncreas total, el número mucho mayor de células acinares frente al de células de islotes, refleja que la mayor parte del aumento de expresión de LAMP-2 observado corresponde a las células acinares. Desconocemos el significado funcional de la sobreexpresión de LAMP-2 en los islotes en la PA inducida por ceruleína. Asimismo, la sobreexpresión de LAMP-2

es una característica asociada con una elevada proporción de carcinomas pancreáticos (*Künzli et al., 2002*).

Uno de los signos más tempranos del daño celular y tisular en la pancreatitis es la vacuolización citoplasmática, una característica común en las alteraciones patológicas de las células acinares cuyas causas, no obstante, no se conocen con exactitud (*Oertel, 1989*). Dichas vacuolas se asocian a una alteración de la autofagia, un mecanismo citoprotector por el cual las células llevan autofagosomas (que transportan componentes citoplasmáticos y orgánulos) hacia los lisosomas, formándose autofagolisosomas ó autolisosomas, cuya misión es la degradación de la carga autofágica. De hecho, la autofagia es una de las respuestas celulares al estrés (*Ji et al., 2003*), y el estrés en el retículo endoplasmático (RE) es importante en el desarrollo de la PA, siendo las células acinares particularmente susceptibles a las perturbaciones del RE (*Kubisch y Logsdon, 1998*). También se sabe que la formación de los autofagolisosomas es un proceso dependiente de LAMP-2, ya que la disminución de los niveles de expresión de esta proteína conduce a fallos en la fusión de los lisosomas y los autofagosomas (*Eskelinen et al., 2002*). Asimismo, se ha descrito recientemente un deterioro en los procesos autofágicos, dependientes de LAMP-2, en la PA inducida por L-arginina (*Zhu et al., 2015*). Por consiguiente, la vacuolización en la PA inducida por ceruleína podría explicarse en términos de una acumulación de autofagosomas, como ya ha sido propuesto en la pancreatitis alcohólica (*Fortunato et al., 2009, Fortunato y Kroemer, 2009*).

La disminución de LAMP-2 en los lisosomas, que describimos en esta memoria, podría tener relevancia fisiológica porque podría estar directamente relacionada con la acumulación citada anteriormente, aunque se desconoce si en el mecanismo responsable de la inhibición de la autofagia que se observa en la PA, LAMP-2 tendría un papel específico, o más bien se debería a un agotamiento general del sistema lisosómico (*Fortunato et al., 2009*). En el epitelio pigmentario retiniano, la catepsina D (la principal proteasa lisosomal) se deslocaliza hacia el espacio extracelular, probablemente por la acumulación de productos de peroxidación lipídica (complejos lípido-proteína dañados oxidativemente) (*Hoppe et al., 2004*). Se sabe que en la PA inducida por

ceruleína, ocurren procesos de peroxidación lipídica y unión covalente de 4-hidroxialquenales a los grupos sulfhidrilo de las proteínas del tejido pancreático (*Dabrowski et al., 1999, Dabrowski et al., 1991*). Las proteínas LAMP contienen diferentes residuos conservados de cisteína que, en condiciones normales, forman los cuatro puentes disulfuro presentes en la parte intralisosomal (*Fukuda, 1991*). El modelo de la perfusión retrógrada de TcNa perece que no cursa con incrementos de 4-hidroxialquenales unidos a residuos de histidina de las proteínas pancreáticas (*Reinheckel et al., 1998*), aunque sí lo hace a nivel pulmonar (*Gilgenast et al., 2001*), un órgano que comúnmente puede sufrir daño agudo de modo asociado a la pancreatitis (*Elder et al., 2012; Akbarshahi et al., 2012*).

Se desconoce la implicación de la acumulación de agregados lípidoproteicos en la deslocalización de proteínas lisosómicas en la pancreatitis. En cualquier caso, la inhibición de la secreción que ocurre en la pancreatitis haría que cualquier proteína lisosómica deslocalizada permaneciese más tiempo en el interior de las células pancreáticas, lo que podría tener importantes consecuencias fisiológicas. También se conoce que en la PA inducida por ceruleína el tráfico proteico está alterado, y que el tráfico vesicular modificado de la ruta de secreción juega un papel en la formación de las vacuolas (*Saito et al., 1987*). La composición de glúcidos de las glicoproteínas en la ruta de la secreción y en las vacuolas está alterada en la pancreatitis experimental, lo que sugiere que las glicoproteínas que se transportan a través del complejo del aparato de Golgi no se procesan de modo correcto (*Saito et al., 1987; de Lisle, 2005*). Esto podría tener implicaciones celulares importantes, ya que las proteínas LAMP, muy glicosiladas, y que recubren la cara interna de los lisosomas, probablemente protegen a este orgánulo de la auto destrucción, aunque este aspecto no está completamente aclarado (*Andrejewski et al., 1993*). Por consiguiente, los cambios en el contenido en glúcidos de las proteínas LAMP también podrían alterar la efectividad proteica para proteger la membrana del lisosoma y/o su papel en la rotura vacuolar y eliminación activa de proteasas al citoplasma.

LAMP-2 es uno de los principales transportadores de poli-N-acetilgalactosaminas en las células (*Fukuda, 1991*), y su peso molecular

se incrementa de acuerdo al aumento de su glicosilación con polilactosaminas, un proceso que está correlacionado con un mayor tiempo de localización de LAMP-2 en el complejo de Golgi (*Nabi et al., 1993*). El aumento de la glicosilación con polilactosaminas requiere la acción repetida de dos transferasas, una glicosiltransferasa y una galactosiltransferasa, probablemente en las mismas cisternas del Golgi (*Nabi et al., 1998*). La galactosiltransferasa se ha localizado en las cisternas del *trans*-Golgi, y se ha descrito que las glicosiltransferasas pueden distribuirse de modo solapado en las cisternas del Golgi (*Nabi et al., 1998*). Todos estos datos podrían ser relevantes respecto a la estructura de LAMP-2 en nuestro modelo de PA inducido por ceruleína, ya que, como hemos dicho antes, en la pancreatitis, el procesamiento glicoproteico está alterado a nivel del aparato de Golgi (*de Lisle, 2005*). Además, se sabe que la PA inducida por ceruleína cursa con desorganización microtubular (*Ueda et al., 1995*), y aunque la despolimerización del citoesqueleto microtubular produce la dispersión de muchos grupos pequeños de complejo de Golgi, la glicosilación con polilactosamina de LAMP-2 aún ocurre en dichos grupos (*de Lisle, 2005*).

El aspecto más controvertido de nuestros resultados es que la proteína tipo-LAMP-2 de 120 kDa se comporta como una proteína de tipo soluble. A este respecto, se sabe que, al menos en el hígado de rata, una parte de LAMP-2 también se localiza en la matriz lisosómica (*Jadot et al., 1996, Cuervo y Dice, 2000a*), siendo desconocido su origen. Se han propuesto tanto una desinserción directa desde la membrana lisosómica después de un cambio conformacional, como una liberación por rotura proteolítica de los cortos dominios transmembrana y citoplasmáticos (*Jadot et al., 1996*). Además, los lípidos asociados con al menos LAMP-2A, podrían jugar un papel importante en la desinserción o reinserción en la membrana lisosómica (*Jadot et al., 1996*). Se han descrito otras inserciones/desinserciones de proteínas de membrana de tipo I (LAMP-2 también es una proteína de membrana tipo I), a veces probablemente dirigidas por interacciones de tipo hidrofóbico con los lípidos de su entorno (*Rusch y Kendall, 2007*). La rotura proteolítica también se ha descrito para otras proteínas lisosómicas (*Cuervo y Dice, 2000b*), y se ha propuesto que en pancreatitis, las proteínas LAMP se degradan por catepsinas

(*Gukovsky et al., 2012*). El origen de la solubilidad de la proteína tipo-LAMP-2 de 120 kDa que describimos en esta memoria deberá ser resuelta en un futuro.

En resumen, nuestro estudio muestra que la expresión pancreática de LAMP-2 está aumentada durante la fase temprana de la PA inducida por ceruleína, aunque un diferente procesamiento traduccional de su contenido en glúcidos, junto a una deslocalización subcelular, finalmente conduciría a la disminución de su nivel de expresión en el lisosoma. Este último aspecto relaciona nuestro trabajo con otros donde se aborda la relevancia de la disminución de diversas proteínas lisosómicas en la vacuolización de las células acinares pancreáticas.

Los lisosomas son, junto con las mitocondrias, los orgánulos subcelulares que sufren una profunda disfunción en diversos modelos tanto *in vivo* como *ex vivo* de pancreatitis (*Gukovsky et al., 2012*). Del mismo modo, como explicamos anteriormente, también sufre gran alteración la principal ruta degradativa celular: la autofagia (por extensión disfunción lisosómica/autofágica) (*Gukovskaya y Gokovsky, 2012*). Para poder realizar futuras investigaciones sobre las glicoproteínas principales residentes del lisosoma, hemos desarrollado un procedimiento para aislar lisosomas primarios del páncreas de rata control y pancreatíticas. Las diferentes poblaciones lisosómicas se obtienen por centrifugación de un homogenado pancreático en un gradiente de Percoll. Los estudios a microscopía electrónica confirmaron la homogeneidad de la fracción ligera, en la cual se localizan los lisosomas primarios, los cuales presentan un halo luminal que probablemente corresponda a los dominios altamente glicosilados de las proteínas de su membrana. La actividad NAG correspondería tanto a las hidrolasas ácidas de los lisosomas primarios como a las enzimas de nueva síntesis que son dirigidas a la ruta endocítica vía endosomas tempranos, e incluso vía la membrana plasmática (*Peters et al., 1990; Ludwig et al., 1991; Tjelle et al., 1996*). Los lisosomas secundarios se localizarían principalmente en la banda de densidad intermedia, que en el caso de las ratas pancreatíticas, se asocian a vacuolas citoplasmáticas mayores, probablemente vesículas donde la actividad de las enzimas lisosómicas estaría aumentada (*Adler et al., 1985*). En la población lisosómica más densa se encuentran orgánulos formados por

cuerpos multivesiculares y lisosomas que han sufrido múltiples ciclos de fusión-fisión (*Futter et al., 1996; Luzio et al., 2007; van Meel y Klumperman, 2008*). Las vesículas libres más pequeñas (< 0,05 μm), que se localizan sobre todo en las bandas segunda y tercera de las muestras pancreatíticas, podrían deberse no sólo a una mayor densidad, sino, al menos en parte, a un proceso de liberación desde orgánulos mayores, cuyas membranas serían más frágiles, probablemente por cambios en su composición química (*Ferreira-Redondo et al., 2002*).

Se ha descrito que el tratamiento con dosis supramáximas de ceruleína produce orgánulos, que contienen catepsina B, cuya fragilidad está incrementada (*Saluja et al., 1987*). También se ha sugerido que hay una estrecha relación entre la fragilidad de los orgánulos subcelulares y la patogénesis de la PA (*Hirano et al., 1993*). Aunque la población menos densa de lisosomas tiene la actividad NAG más elevada, las otras dos poblaciones lisosómicas también la presentan debido a condensación vacuolar, ya que también se localizan enzimas lisosómicas en las vacuolas. Por consiguiente, el gradiente permite resolver satisfactoriamente poblaciones de lisosomas primarios y secundarios.

Ya que la integridad de los endosomas y de los lisosomas es fundamental para la correcta separación de las proteínas digestivas (*Scheele et al., 1980*), la mayor fragilidad de los orgánulos que describimos en esta memoria, podría resultar perjudicial para el tejido pancrático, ya que permitiría la liberación de las enzimas, dañándose, por consiguiente, las células acinares.

VI. Conclusiones

1.- La obtención de un método para la separación de diferentes poblaciones de lisosomas pancreáticos usando una combinación de centrifugación diferencial y un gradiente discontinuo de Percoll, ha permitido demostrar que la pancreatitis aguda inducida por ceruleína está asociada a cambios en la morfología y tamaño de los orgánulos de dichas poblaciones.

2.- La dinámica de las formas moleculares de la N-acetilglucosaminidasa revela una alteración de la integridad de la membrana de los lisosomas primarios y es un indicador adicional del daño en dicha membrana, asociado a la pancreatitis aguda.

3.- El incremento en la expresión de SHP-1 y SHP-2, así como los cambios en la distribución subcelular de SHP-2, son sucesos tempranos en el desarrollo de la pancreatitis aguda inducida por ceruleína.

4.- El aumento en la expresión de SHP-2 en tres modelos diferentes de pancreatitis in vivo, indica una importancia general de esta fosfatasa en la pancreatitis aguda.

5.- Las MAPKs JNK y ERK ½, así como los niveles de AMPc intracelular modulan de diferentes modos la expresión de SHP-1 y SHP-2.

6.- El incremento en la expresión de PTP1B es un suceso temprano en el desarrollo de la pancreatitis aguda inducida por ceruleína, en el cual, la infiltración por neutrófilos parece jugar un papel relevante.

7.- En la fase temprana de la pancreatitis aguda inducida por ceruleína, el aumento en los niveles de AMPc intracelular en las células inflamatorias, así como la inhibición de JNK y ERK ½, previenen, principalmente, el incremento en la expresión de PTP1B.

8.- Expresión de LAMP-2 aumenta durante la fase temprana de la pancreatitis aguda inducida por ceruleína, aunque un diferente procesado post-transcripcional de su contenido en glúcidos, acompañado de una deslocalización subcelular de la proteína en la patología, finalmente conduciría a su disminución en el lisosoma.

VII. Bibliografía

Abela JE, Carter CR. (2010). Acute pancreatitis. Hepatob Surg II, 28: 5.

Adler G, Hahn C, Kern HF, Rao KN. (1985). Cerulein-induced pancreatitis in rats: increased lysosomal enzyme activity and autophagocytosis. Digestion, 32: 10-8.

Aho, H.J, Koskensalo, S.M.; Nevalainen, T.J. (1980).Experimental pancreatitis in the rat.Sodium taurocholate-induced acute haemorrhagic pancreatitis. Scan J Gastroenterol, 15: 411-416.

Aho HJ, Suonpää K, Ahola RA, Nevalainen TJ. (1984). Experimental pancreatitis in the rat. Ductal factors in sodium taurocholate-induced acute pancreatitis. Exp Pathol, 25: 73-79.

Akbarshahi H, Rosendahl AH, Westergren-Thorsson G, Andersson R. (2012). Acute lung injury in acute pancreatitis-awaiting the big leap. Respir Med , 106: (2012) 1199-210.

Alonso A, Sasin J, Bottini N, Friedberg I, Osterman A, Godzik A, Hunter T, Dixon J, Mustelin T. (2004). Protein tyrosine phosphatases in the human genome. Cell, 117: 699-711.

Alonso R, Montero A, Arévalo M, García LJ, Sánchez-Vicente C, Rodríguez-Nodal F, López-Novoa JM, Calvo JJ. (1994). Platelet-activating factor mediates pancreatic function derangement in caerulein-induced pancreatitis in rats. Clin Sci, 87: 85-90.

Andrejewski N, Punnonen EL, Guhde G, Tanaka Y, Lullmann-Rauch R, Hartman D, von Figura K, Saftig P. (1999). Normal lysosomal morphology and function in LAMP-1-deficient mice. J Biol Chem, 274 : 12692-12701.

Baddeley RNB, Skipworth JRA, Pereira SP. (2010). Acute pancreatitis. Medicine, 39:2.

Barriocanal JG, Bonifacio JS, Juan L, Sandoval IV. (1986). Biosynthesis, glycosylation movement through the Golgi system, and transport to lysosomes by an N-linked carbohydrate –independent mechanism of three lysosomal integral membrane proteins. J Biol Chem, 261: 16755-16763

Bockman, DE "Histology and fine structure of the pancreas". (1998). The pancreas. Oxford Blackwell Science Ltd: 19-26.

Boucher MJ, Duchesne C, Lainé J, Morisset J, Rivard N. (2001). cAMP protection of pancreatic cancer cells against apotosis induced by ERK inhibition. Biochim Biophys Res Commun, 285:207-216.

Bourdeau A, Dubé N, Tremblay ML. (2005). Cytoplasmic protein tyrosine phosphatases, regulation and function : the roles of PTP1B and TC-PTP. Current Opinion in Cell Biology, 17: 203-209.

Boya P, Reggiori F and Codogno P. (2013). Emerging regulation and functions of autofagy. Nat Cell Biol 15: 713-720.

Bragado, MJ, Sánchez-Bernal C, García LJ, López, MA, San Román JI, Calvo JJ. (1998). Effect of high fiber intake on pancreatic lysosomal stability in ethanol-fed rats. *Nutritional Biochem,* 9: 164-169.

Bright NA, Reaves BJ, Mullock BM, Luzio JP. (1997). Dense core lysosomes can fuse with late endosomes and are re-formed from the resultant hybrid organelles. J Cell Sci, 110: 2027-2040.

Carlsson SR, Lycksell PO, Fukuda M. (1993). Assignment of O-glycan attachment sites to the hinge-like regions of human lysosomal membrane glycoproteins lamp-1 and lamp-2. Arch Biochem Biophys, 304**:** 65-73.

Case RM. (1978). Synthesis, intracellular transport and discharge of exportable proteins in the pancreatic acinar cell and other cells. Biol Rev Camb Philos Soc, 53: 211-354.

Chen J W, Murphy TL, Willingham MC, Pastan I, August JT. (1985). Identification of two lysosomal membrane glycoproteins. J Cell Biol, 101: 85-95.

Cheung YC, Leung PS. (2007). Acute pancreatitis: animal models and recent advances in basic research. Pancreas 34: 1-14.

Clemons AP, Holstein DM, Galli A, Saunders C. (2002). Cerulein-induced acute pancreatitis in the rat is significantly ameliorated by treatment with MEK1/2 Inhibitors U0126 and PD98059. Pancreas 25: 251–259.

Cuervo AM and Dice JF. (1998). Lysosomes, a meeting point of proteins, chaperons, and proteases. J Mol Med Berl, 76: 6-12.

Cuervo AM, Dice JF. (2000a). Regulation of Lamp2a levels in the lysosomal membrane. Traffic 1: 570-583.

Cuervo AM, Dice JF. (2000b). Unique properties of lamp2a compared to other lamp2 isoforms. J Cell Sci, 113: 4441-4450.

Dabrowski A, Gabryelewicz A, Chwiecko M. (1991). Products of lipid peroxidation and changes in sulfhydryl compounds in pancreatic tissue of rats with caerulein-induced acute pancreatitis. Biochem. Med Metab Biol, 46: 10-16.

Dabrowski A, Konturek JW, Konturek JW, Gabryelewicz A. (1999). Role of oxidative stress in the pathogenesis of caerulein-induced acute pancreatitis. Eur J Pharmacol, 377: 1-11.

De Duve C. and EWattiaux R. (1966) Functions of lysosomes. Annu Rev Physiol 28: 435-492. **Faouzi M and Penner R. 2014**. Trpm2. Handb Exp Pharmacol, 222: 403-426.

de Lisle RC. (2005). Altered posttranslational processing of glycoproteins in cerulein-induced pancreatitis. Exp Cell Res, 308: 101-113.

den Hertog J, Groen A, van der Wijk T. (2005). Redox regulation of protein-tyrosine phosphatises. Arch Biochem Biophys, 434: 11-15.

de Duve C. (1983). Lysosomes revised. Eur J Biochem, 137: 391-397.

Dice JF. (2007). Chaperone-mediated autophagy. Autophagy, 3: 295-299.

Elder AS, Saccone GT, Dixon DL. (2012). Lung injury in acute pancreatitis: mechanisms underlying augmented secondary injury. Pancreatology, 12: 49-56.

Elchebly M, Payette P, Michaliszyn E, Cromlish W, Collins S. (1999). Increased insulin sensitivity and obesity resistance in mice lacking the protein tyrosine phosphatase-1B gene. Science, 283: 1544–1548.

Ëlsaser HP, Adler G, Kern HF. (1986). Time course and cellular source of pancreatic regeneration following acute pancreatitis in the rat. Pancreas, 5: 421-429.

Eskelinen EL, AL Illert AL, Y Tanaka YG, Schwarzmann GJ, Blanz JK, von Figura KP, Saftig P. (2002). Role of Lamp-2 in lysosome biogenesis and autophagy. Mol Biol Cell, 13: 3355-3368.

Eskelinen EL, Tanaka, Y, Saftig P. (2003). At the acidic edge: emerging functions for lysosomal membrane proteins. Trends Cell Biol, 13: 137-145.

Eskelinen EL, Cuervo AM, Taylor MR, Nishino I, Blum JS, Dice JF, Sandoval IV, Lippincott-Schwartz J, August JT, Saftig P. (2005). Unifying nomenclature for the isoforms of the lysosomal membrane protein LAMP-2. Traffic, 6: 1058-1061.

Eskelinen EL. (2006). Roles of LAMP-1 and LAMP-2 in lysosome biogenesis and autophagy. Elsevier, 27: 495-502

Ferreira L, Pérez-González N, Llanillo M, Calvo JJ, Sánchez-Bernal C. (2002). Acute pancreatitis decreases pancreas phospholipid levels and increases susceptibility to lipid peroxidation in rat pancreas. Lipids, 372: 167-171.

Fleischer R, Dabew R, Ke BG, Wagner ACC. (2001). Stress kinase inhibition modulates acute experimental pancreatitis. World J. Gastroenterol. 7: 259–265.

Foitzik T, Hotz HG, Eibl G, Buhr HJ. (2000). Experimental models of acute pancreatitis: are they suitable for evaluating therapy? Int J Colorectal Dis, 15: 127-135.

Fortunato F, Bürgers H, Bergmann F, Rieger P, Büchler MW, Kroemer G, Werner J. (2009). Impaired autolysosome formation correlates with Lamp-2 depletion: role of apoptosis, autophagy, and necrosis in pancreatitis. Gastroenterolog, 137(1): 350-360.

Fortunato F, Kroemer G. (2009). Impaired autophagosome-lysosome fusion in the pathogenesis of Pancreatitis. Autophagy, 5: 850-853.

Frangioni JV, Oda A, Smith M, Salzman EW, Neel BG. (1993). **Calpain catalyzed** cleavage and subcellular relocation of protein phosphotirosine phosphatase 1B (PTP-1B) in human platelets. EMBO J, 12: 4843-4856.

Frossard JL, Steer ML, Pastor CM. (2008). Acute pancreatitis. Lancet, 371: 143-152.

Fukuda M. (1991). Lysosomal membrane glycoproteins. Structure, biosynthesis, and intracellular trafficking. J Biol Chem, 266: 21327-21330.

Furuta K, Yang XL, Chen JS, Hamilton R, August JT. (1999). Differential expression of the lysosome-associated membrane proteins in normal tissues. Arch Biochem Biophys, 365: 75-82.

Futter CE, Pearse A, Hewlett LJ, Hopkins CR. (1996). Multivesicular endosomes containing internalized EGF-EGF receptor complexes mature and then fuse directly with lysosomes. *J Cell Biol*, 132: 1011-1023.

García-Hernández V, Sarmiento N, Sánchez-Bernal C, Matellán L, Calvo JJ, Sánchez-Yagüe J. (2014). Modulation in the expression of SHP-1, SHP-2 and PTP1B due to the inhibition of MAPKs, cAMP and neutrophils early on in the development of cerulein-induced acute pancreatitis in rats. Biochim Biophys Acta, 1842(2): 192-201.

Geneser, F. (2000). "*Histología*". Ed. Panamericana (3) pp: 510-513.

Gilgenast O, Brandt-Nedelev B, Wiswedel I, Lippert H, Halangk W, Reinheckel T. (2001). Differential oxidative injury in extrapancreatic tissues during experimental pancreatitis: modification of lung proteins by 4-hydroxynonenal. Dig Dis Sci, 46: 932-937.

Grady T, Saluja A, Kaiser A, Steer M. (1996). Edema and intrapancreatic trypsinogen activation precede glutathione depletion during caerulein pancreatitis. J Gastroenterol Hepatol, 271: 20-26.

Groen A, Lemeer S, van der Wijk T, Overvoorde J, Heck AJ, Ostman A, Barford D, Slijper M, den Hertog J. (2005). Differential oxidation of protein-tyrosine phosphatases. J Biol chem, 280: 10298-10304.

Guillaumes S, Blanco I, Sans MD, Clavé P, Farré A, Lluís F. (1996). Physiopathology of acute pancreatitis. Gastroenterología y Hepatología, 19 (4): 224-230.

Gukovsky I, Pandol SJ, Gukovskaya AS. (2011). Organellar dysfunction in the pathogenesis of pancreatitis. Antioxid redox signal, 15: 2699-2710.

Gukovskaya AS, Gukovsky I. (2012). Autophagy and Pancreatitis. Am J Physiol Gastrointest Liver Physiol, 303(9): 999-1003.

Gukovsky I, Pandol SJ, Gukovskaya AS. (2011). Organellar dysfunction in the pathogenesis of pancreatitis. Antioxid redox signal, 15: 2699-2710.

Gukovsky I, Pandol SJ, Mareninova OA, Shalbueva N, Jia W, Gukovskaya AS. (2012). Impaired autophagy and organellar dysfunction in pancreatitis. J Gastroenterol Hepatol, 27(2): 27–32.

Hernandez-Hernandez A, J Sanchez-Yague, EM Martin-Valmaseda, M Llanillo. (1999). Oxidative inactivation of human and sheep platelet membrane-associated phosphotyrosine phosphatase activity. Free Radic Biol Med, 26: 1218-1230.

Hernández-Hernández A, Garabatos MN, Rodríguez MC, Vidal ML, López-Revuelta A, Sánchez-Gallego JI, Llanillo M, Sánchez-Yagüe J. (2005). Structural characteristics of a lipid peroxidation product, trans-2-nonenal, that favour inhibition of membrane associated phosphotyrosine phosphatase activity. Biochim Biophys Acta, 1726: 317-325.

Hendriks WJ, Elson A, Harroch S, Pulido R, Stoker A, den Hertog J. (2013). Protein tyrosine phosphatases in health and disease. FEBS J, 280: 708–30.

Hashimoto D, Ohmuraya M, Hirota M, Yamamoto A, Suyama K, Ida S, Okumura Y, Takahashi E, Kido H, Araki K, Baba H, Mizushima N, Yamamura K. (2008). Involvement of autophagy in trypsinogen activation within the pancreatic acinar cells. J Cell Biol, 181: 1065-1072.

Helin H, Mero M, Markkula H, Helin M. (1980). Pancreatic acinar ultrastructure in human acute pancreatitis. Virchows Arch A Pathol Anat Histol, 387:259-270.

Hirano T, Manabe T, Yotsumoto F, Ando K, Imanishi K, Tobe T. (1993). Effect of prostaglandin E on the redistribution of lysosomal enzymes in caerulein-induced pancreatitis. Hepatogastroenterology, 40(2): 155-8.

Hofbauer B, Saluja AK, Lerch MM, Bhagat L, Bhatia M, Lee HS, Frossard JL, Adler G, Steer ML. (1998). Intra-acinar cell activation of trypsinogen during caerulein-induced pancreatitis in rats. Am J Physiol, 275: 352-62.

Hofken T, Keller N, Fleischer F, Goke B, Wagner AC. (2000). Map Kinase Phosphatases (MKP´s) are early responsive genes during induction of cerulein hyperstimulation pancreatitis. Biochem Biophys Res Commun, 276: 680-685.

Hoppe G, O´Neil J, Hoff HF, Sears J. (2004). Products of lipid peroxidation induce missorting of the principal lysosomal protease in retinal pigment epithelium. Biochim Biophys Acta, 1689: 33-41.

Huang H, Liu Y, Daniluk J, Gaiser S, Chu J, Wang H, Logsdon C, Ji B. (2012) Activation of nuclear Factor-κB in acinar cells increases the severity of pancreatitis in mice. Gastroenterology, 144(1): 202-210.

Hunziker W and Geuze HJ. (1996). Intracellular trafficking of lysosomal membrane proteins. Bioessays, 18: 379-389.

Jadot M, Wattiaux R, Mainferme F, Dubois F, Claessens A, Wattiaux-De Coninck S. (1996). Soluble form of Lamp II in purified rat liver lysosomes. Biochim Biophys Res Commun, 223: 353-359.

Jha RK, Ma Q, Sha H, Palikhe M. (2009). Acute pancreatitis: a literature review. Med Sci Monit, 15(7): 147-156.

Ji B, Chen X, Misek DE, Kuick R, Hanash S, Ernst S, Najarian R, Logsdon CD. (2003). Pancreatic gene expression during the initiation of acute pancreatitis: identification of EGR-1 as a key regulator. Physiol Genomics, 14: 59-72.

Klaman LD, Boss O, Peroni OD, Kim JK, Martino JL. (2000). Increased energy expenditure, decreased adiposity, and tissue-specific insulin sensitivity in protein-tyrosine phosphatase 1B-deficient mice. Mol Cell Biol, 20: 5479–5489.

Kontaridis MI, S Eminaga, M Fornaro, CI Zito, R Sordella, J Settleman, AM Bennett. (2004). SHP-2 positively regulates myogenesis by coupling to the Rho GTPase signaling pathway. Mol Cell Biol, 24: 5340-5352.

Klein AS, Lillemoe KD, Yeo ChJ, Pitt HA. (1996). Liver, biliary tract and pancreas. The physiologic basis of surgery. Williams & Wilkins, (2): 441-478.

Kroemer G, Levine B. (2008). Autophagic cell death: the story of a misnomer. *Nat Rev,* 9: 1004-1010.

Kubish CH, Sans MD, Arumugan T, Ernst SA, Williams JA, Longsdon CD. (2006). Early activation of endoplasmic reticulum stress is associated with arginine-induced acute pancreatitis. Am J Physiol Gastrointest Liver Physiol, 291: G238-G245.

Kubisch CH, Logsdon CD. (2008). Endoplasmic reticulum stress and the pancreatic acinar cell. (2008). Expert Rev Gastroenterol Hepatol, 2: 249-260.

Künzli B, Berberat PO, Zhu ZW, Martignoni M, Kleeff J, Tempia-Caliera A, Fukuda M, Zimmermann A, Friess H, Büchler MW. (2002). Influences of the lysosomal associated membrane proteins (Lamp-1, Lamp-2) and Mac-2 binding protein (Mac-2-BP) on the prognosis of pancreatic carcinoma. Cancer, 94: 228-239.

Kyriakys JM, Avruch J. (2001). Mammalian mitogen-activated protein kinase signal transduction pathways activated by stress and inflammation. Physiol Rev, 81: 807-869.

Lampel M, Kern HF. (1977). Acute interstitial pancreatitis in the rat induced by excessive doses of a pancreatic secretagogue. Virchows Arch A, 373: 97-117.

Lankisch P G, Apte M, Banks PA. (1988). Acute pancreatitis. Lancet, 386: 85-96.

Le Borgne R, Alconada A, Bauer U, Hoflack B. (1998). The mammalian AP-3 adaptor-like complex mediates the intracellular trasnport of lysosomal membrana glycoproteins. J Biol Chem, 273: 29451-29461.

Leung PS, Chan YC. (2009) Role of oxidative stress in pancreatic inflammation. Antioxid Redox Signal, 11: 135-165.

Levine B. and Kroemer G. (2008). Autophagy in the pathogenesis of disease. Cell, 132: 27-42.

Lewis V, Green SA, Marsh M, Vihco P, Helenius A, Mellman I. (1985). Glycoproteins of the lysosomal membrane. J Cell Biol, 100: 1839-1847.

Lichter-Konecki U, Moter SE, Krawisz BR, Schlotter M, Hipke C, Konecki DS. (1999). Expression patterns of murine lysosome-associated membrane protein 2 (Lamp-2) transcripts during morphogenesis. Differentiation, 65: 43-58.

Lippincott-Schwartz Fambrough. (1986**)**. Lysosomal membrane dynamics: structure and interorganellar movement of a major Lysosomal membrane glycoprotein. J Cell Biol, 102: 1593-1605.

Liu H-S, Pan C-E, Liu Q-G, Yang W, Liu X-M. (2003). Effect of NF-kB and p38MAPK in activated monocytes/macrophages on pro-inflammatory cytokines of rats with acute pancreatitis. World J. Gastroenterol, 9: 2513-2518.

Longnecker D. (2014). Anatomy and Histology of the Pancreas. The Pancreapedia: exocrine pancreas knowledge base.

Ludwig T, Griffiths G, Hoflack B. (1991). Distribution of newly synthesized lysosomal enzymes in the endocytic pathway of normal rat kidney cells. J Cell Biol, 115: 1561-72.

Lüthen R, Niedereau C, Grendell JH. (1995). Intrapancreatic zymogen activation and levels of ATP and glutathione during cerulein pancreatitis in rats. Am J Physiol, 268: G592-G604.

Luzio J, Rous BA, Bright N A, Pryor PR, Mollock BM, Piper RC. (2000). Lysosome-endosome fusion and lysosome biogenesis. J Cell Sci, 113: 1515-1524.

Luzio JP, Pryor PR, Bright NA. (2007). Lysosomes: fusion and function. Nat Rev Mol Cell Biol, 8: 622-32.

Mansfield C. (2012). "Pathophysiology of Acute Pancreatitis: Potential Application from Experimental Models and Human Medicine to Dogs. J Vet Intern Med, 26: 875-887.

Mareninova OA, Hermann K, French SW. (2009). Impaired autophagic flux mediates acinar cell vacuole formation and trypsinogen activation in rodent models of acute pancreatitis. J Clin Invest, 119: 3340-3355.

Mareninova OA, Yakubov I, Jia W, Gukovsky I, Gukovskaya AS. (2010a). Experimental acute pancreatitis causes pathologic changes in lysosomal membrane protein and lipid composititon. Gastroenterology, 138: 125-126.

Mareninova OA, Yakubov I, Pandol SJ, Gorelick FS, Gukovsky I, Gukovskaya AS. (2010b). Disordering of lysosomal and autophagic pathways in nonalcoholic and alcoholic experimental pancreatitis. Pancreas, 39: 1332.

Marschner K et al., (2011). A key enzyme in the biogénesis of lysosomes is a protease that regulates colesterol metabolism. Science, 333: 87-90.

Mayerle J, Schnekenburger J, Kruger B, Kellermann J, Ruthenburger M, Weiss FU, Nalli A, Domschke W, Lerch MM. (2005). "Extracellular cleavage of E-cadherin by leukocyte during acute experimental pancreatitis in rat. Gastroenterology, 129: 1251-1267.

Mindell JA. (2012). Lysosomal acidification mechanisms. Annu Rev Physiol, 74: 69-86.

Minutoli L, Altavilla D, Marini H, Passaniti M, Bitto A, Seminara P, Venuti FS, Famulari C, Macri A, Versaci A, Squadrito F. (2004) Protective effects of SP600125 a new inhibitor of c-jun N-terminal kinase (JNK) and extracellular-regulated kinase (ERK1/2) in an experimental model of cerulein-induced pancreatitis. Life Sci, 75: 2853-2866.

Muller T, Choidas A, Reichmann E, Ullrich A. (1999). Phosphorylation and free pool of beta-catenin are regulated by tyrosine kinases and tyrosine phosphatases during epithelial cell migration. J Biol Chem, 274: 10173-10183.

Nabi IR, Rodriguez-Boulan E. (1993). Increased LAMP-2 polylactosamine glycosylation is associated with its slower Golgi transit during establishment of a polarized MDCK epitelial monolayer. Mol Biol Cell, 4: 627-635.

Nabi IR, Dennis JW. (1998). The extent of polylactosamine glycosylation of MDCK LAMP-2 is determined by its Golgi residence time. Glycobiology, 8: 947-953.

Namkung W, Yoon JS, Kim KH, Lee MG. PAR2 exerts local protection against acute pancreatitis via modulation of MAP kinase and MAP kinase phosphatase signaling. Am J Physiol Gastrointest Liver Physiol, 295: G886-G894.

Neel BG, H Gu, L Pao. (2003). The 'Shp'ing news: SH2 domain-containing tyrosine phosphatases in cell signaling. Trends Biochem Sci, 28: 284-293.

Niederau C, Niederau M, Lüthen R, Strohmeyer G, Ferrel LD, Grendell JH. (1990). Pancreatic exocrine secretion in acute experimental pancreatitis. Gastroenterology, 99: 1120-1127.

Oertel JE. The pancreas. (1989). Nonneoplastic alterations. Am J Surg Pathol, 13(1): 50-65.

Pao LI, K Badour, KA Siminovitch, BG Neel. (2007). Nonreceptor protein-tyrosine phosphatases in immune cell signaling. Annu Rev Immunol, 25: 473-523.

Perera RM et al., (2015). Transcriptional control of autophagy-lysosome function drives pancreatic cancer metabolism. Nature, 524: 361-365.

Persson C, Savenhed C, Bourdeau A, Tremblay M L, Markova B, Bohmer F D, Haj F G, Neel B G, Elson A, Heldin C H, Ronstrand LO, Ostman A, Hellberg C. (2004). Site-selective regulation of platelet- derived wroght factor beta receptor tyrosine phosphorylation by T-cell protein tyrosine phosphatise. Mol Cell Biol, 24: 2190-2201.

Pescador R, Manso MA, Revollo AJ. (1995). De Dios I. Effect of chronic administration of hydrocortisone on the induction and evolution of acute pancreatitis induced by cerulean. Pancreas. 11: 165-72.

Peters C, Braun M, Weber B, Wendland M, Schmidt B, Pohlmann R, Waheed A, von Figura K. (1990). Targeting of a lysosomal membrane protein: a tyrosine-containing endocytosis signal in the cytoplasmic tail of lysosomal acid phosphatase is necessary and sufficient for targeting to lysosomes. EMBO J, 9: 3497-506.

Peters C. and von Figura K. (1994). Biogenesis of lysosomal membranes. FEBS Lett, 346: 146-150.

Poch B, Gansauge F, Rau B, Wittel U, Gansauge S, Nüsslern AK, Schoenberg M, Beger HG. (1999). The role of polimorphonuclear leukocytes and oxygen-derived free radicals in experimental acute pancreatitis: mediators of local destruction and activators of inflammation. FEBS Lett, 461: 268-272.

Qu CK, Nguyen, Chen J, Feng GS. (2001). Requirement of Shp-2 tyrosine phosphatase in lymphoid and hematopoietic cell development. Blood, 97: 911-914.

Qu CK. (2002). Role of the SHP-2 tyrosine phosphatase in cytokine-induced signalling cellular response. Biochim Biophys Acta, 1592: 297-301.

Reinheckel T, Nedelev B, Prause J, Augustin W, Schulz H-U, Lippert H, Halangh W. (1998). Occurrence of oxidatively modified proteins: an early event in experimental acute pancreatitis. Free Radic Biol Med, 24: 393-400.

Reinheckel T, Prause J, Nedelev B, Augustin W, Schulz H-U, Lippert H, Halangh W. (1999). Oxidative stress affects pancreatic proteins during the early pathogenesis of rat cerulein pancreatitis. Digestion, 60: 56-62.

Repnik U, Hatner Cesen M and Turk B. (2014). Lysosomal membrane permeabilization in cell death: concepts and challenges. Mitocondrion, 19: 49-57.

Rivard N, Rydzewska G, Lods JS, Morisset J. (1995). Novel model of integration of signalling pathways in rat pancreatic acinar cells. Am J Physiol, 269: 352-362.

Rusch SL, Kendall DA. (2007). Oligomeric states of the SecA and SecYEG core components of the bacterial Sec translocon. Biochim Biophys Acta, 1768: 5-12.

Sah RP, Garg P, Saluja A. (2012). Pathogenic mechanisms of acute pancreatitis. Curr Opin Gastroenterol, 28: 507–515.

Saluja A, Hashimoto S, Saluja M, Powers RE, Meldolesi J. (1987). Subcellular redistribution of lysosomal enzymes during caerulein-induced pancreatitis. Am J Physiol, 253: 508-516.

Sánchez-Bernal C, García-Morales OH, Domínguez C, Martín-Gallán P, Calvo JJ, Ferreira L, Pérez-González N. (2004). Nitric oxide protects against pancreatic subcellular damage in acute pancreatitis. Pancreas, 28: 9-15.

Sardiello M et al., (2009). A gene network regulating lysosomal biogenesis and function. Science, 325: 473-477.

Sarmiento N, Sánchez-Bernal C, Pérez N, Sardina JL, Mangas A, Calvo JJ, Sánchez-Yagüe J. (2010). Rolipram and SP600125 supress the early increase in PTP1B expression during cerulein-induced pancreatitis in rats. Pancreas, 39(5): 639-645.

Sarmiento N, Sánchez-Yagüe, J Juanes PP, Pérez N, Ferreira L, García-Hernández V, Mangas A, Calvo JJ, Sánchez-Bernal C. (2011). Changes in the morphology and lability of lysosomal subpopulations in caerulein-induced acute pancreatitis. Dig Liver Dis, 43(2): 132-138.

Sastre J, Sabater L, Aparisi L. (2005). Fisiología de la secreción pancreática. Gastroenterol Hepatol, 28(2): 3-9.

Sato T, Otaka M, Odashima M, Kato S, Jin M, Konishi N, Matsuhashi T, Watanabe S. (2006). Specific type IV phosphodiesterase inhibitor ameliorates cerulein-induced pancreatitis in rats. Biochem Biophys Res Commun, 346: 339-344.

Satoh A, Shimosegawa T, Satoh K, Ito H, Kohno Y, Masamune A, Fujita M, Toyota T. (2000). Activation of A1-receptor pathway induces edema formation in the pancreas of rats. Gastroenterology, 119: 829-836.

Scheele GA. (1980). Biosynthesis, segregation, and secretion of exportable proteins by the exocrine pancreas. Am J Physiol, 1980: 238: 467-77.

Schnekenburger J, Mayerle J, Krüger B, Buchwalow I, Weiss FU, Albrecht E, Samoilova VE, Domschke W, Lerch MM. (2005). Protein tyrosine phosphatase and SHP-1 are involved in the regulation of cell-cell contacts at adherent junctions in the exocrine pancreas. Gut, 54: 1445-1455.

Semmler J, Wachtel H, Endres S. (1993). The specific type IV phosphodiesterase inhibitor rolipram suppresses tumor necrosis factor-production by human mononuclear cells. Int J Immunopharmacol, 15: 409-413.

Segarra, E. (2006). "Fisiología de los aparatos y sistemas". Pp: 91-98.

Senis YA. (2013). Protein-tyrosine phosphatases: a new frontier in platelet signal transduction. J Thromb Haemost, 11: 1800-1813.

Serrano-Puebla A and Boya P. (2015). Lysosomal membrane permeabilization in cell death:new evidence and implications for healt and disease. Ann N Y Acad Sci 1-15. Doi: 10.1111/nyas.12966.

Zhang F & Li PL. (2007). Reconstitution and characterization of a nicotinic acid adenine dinucleotide phsphate (NAADP)-sensitive Ca2+ release cannel from liver lysosomes of rats J Biol Chem, 282: 25259-25269.

Shen HM & Mizushima N. (2014). At the end of the autophagic road: an emerging understanding of lysosomal functions in autophagy. Trends Biochem Sci, 39: 61-71.

Shi C, Zhao X, Lagergren A, Sigvardsson M, Wang X, Andersson R. (2006). Immune status and inflammatory response differ locally and systemically in severe acute pancreatitis. Scan J Gastroenterol, 41: 472-480.

Steer ML. (1992). Pathobiology of Expermintal Acute Pancreatitis. Yale J Biol Med, 65: 421-430.

Stypmann J, Janssen PM, Prestle J, Engelen MA, Kogler H, Lullmann-Rauch R, Eckardt L, von Figura K, Landgrebe J, Mleczko A. (2006). LAMP-2 deficient mice show depressed cardiac contractile function without significant changes in calcium handling. Basic Res Cardiol, 101: 281-291.

Suyama K, Ohmuraya M, Hirota M, Ozaki N, Ida S, Endo M, Araki K, Gotoh T, Baba H, Yamamura K. (2008). C/EBP homologous protein is crucial for the acceleration of experimental pancreatitis. Bochem Biophys Res Commun, 267: 176-182.

Tanaka Y, Guhde G, Suter A, Eskelinen EL, Hartmann D, Lullmann-Rauch R, Janssen PML, Blanz J, von Figura K, Saftig P. (2000). Accumulation of autophagic vacuoles and cardiomyopathy in LAMP-2 deficient mice. Nature, 406: 902-906.

Tjelle TE, Brech A, Juvet LK, Griffiths G, Berg T. (1996). Isolation and characterization of early endosomes, late endosomes and terminal lysosomes: their role in protein degradation. J Cell Sci, 109: 2905-14.

Tenev T, H Keilhack, S Tomic, B Stoyanov, M Stein-Gerlach, R Lammers, AV Krivtsov, A Ullrich, FD Bohmer. (1997). Both SH2 domains are involved in interaction of SHP-1 with the epidermal growth factor receptor but cannot confer receptor-directed activity to SHP-1/SHP-2 chimera. J Biol Chem, 272: 5966-5973.

Tonks NK. Protein tyrosine phosphatases: from genes, to function, to disease. (2006). Nat Rev Mol Cell Biol, 7: 833–46.

Tonks NK. Protein tyrosine phosphatases--from housekeeping enzymes to master regulators of signal transduction. FEBS J, 280: 346-378.

Ueda T, Takeyama Y, Adachi M, Toyokawa A, Kishida S, Yamamoto M, Saitoh Y. (1995). Effect of the microtubule-disrupting drug colchicine on rat cerulein-induced pancreatitis in comparison with the microtubule stabilizer taxol. Pancreas 11: 294-302.

Van Acker GJD, Perides G, Steer ML. (2006). Co-localization hypothesis: A mechanism for the intrapancreatic activation of digestive enzymes during the early phases of acute pancreatitis. World J Gastroenteorol, 12: 1985-1990.

Van Acker GJD, Weiss E, Steer ML, Perides G. (2007). Cause-effect relationships between zymogen activation another early events in secretagogue-induced acute pancreatitis. Am J Physiol Gastrointest Liver Physiol, 292: G1738-G1746.

van Meel E, Klumperman J. (2008). Imaging and imagination: understanding the endo-lysosomal system. Histochem Cell Biol, 129(3): 253–66.

Vaquero E, Gukovsky I Zaninovic V, Gukovskaya A, Pandol SJ. (2001). Localized pancreatic NK-kB activation and inflammatory response in taurocholate-induced pancreatitis. Am J Physiol, 280: 1197-1208.

Wang GJ, Gao CF, Wei D, Wang C, Ding SQ. (2009). Acute pancreatitis: Etiology and common pathogenesis. World J Gastroenterol, 15(12): 1427-1430.

Weidberg H, Shvets E, Elazar Z. (2011). Biogenesis and cargo selectivity of autophagosomes. Ann Rev Biochem, 80: 125-156.

Widmann C, Gibson S, Jarpe MB, Johnson GJ. (1999). Mitogen activated protein kinases: conservation of a three kinase module from yeast to human. Physiol Rev, 79: 143-180.

Willemer S, Elsasser HP, Adler G. (1992). Hormone-induced pancreatitis. Eur Surg Res, 24(1): 29-39.

Williams JA. (2001). Intracellular signalling mechanisms activated by cholecystokinin-regulating synthesis and secretion of digestive enzymes in pancreatic acinar cells. Ann Rev Physiol, 63: 77-97.

Yönetçi N, Oruç N, Ozütemiz AO, Celik HA, Yüce G. (2001). Effects of mast-cell stabilization in caerulein-induced acute pancreatitis in rats. Int J Pancreatol, 29: 163-171.

You M, Zhao Z. (1997). Positive effects of SH2 domain-containing tyrosine phosphatase SHP-1 on epidermal growth factor- and interferon-stimulated activation of STAT transcription factors in HeLa cells. J Biol Chem 272: 23376-23381.

Yu J-H, Kim K-H, Kim H. (2008). SOCS 3 and PPAR-ligands inhibit the expression of IL-6 and TGF-1 by regulating JAK2/STAT3 signalling in pancreas. Int J Biochem Cell Biol, 40: 677-688.

Zhao M, Xue DB, Zheng B, Zhang WH, Pan SH, Sun B. (2007). Induction of apoptosis by artemisin relieving the severity of inflammation in caerulein-induced acute pancreatitis. World J Gastroenterol, 14: 5612-5617.

Zhao JB, Liao DH, Nissen TD. (2013). Animal models of pancreatitis: Can it be translated to human pain study? World J Gastroenterol, 19(42): 7222-7230.